FIFTH INTERNATIONAL CONFERENCE ON STABILITY
OF
SHIPS AND OCEAN VEHICLES

NOVEMBER 7-11, 1994

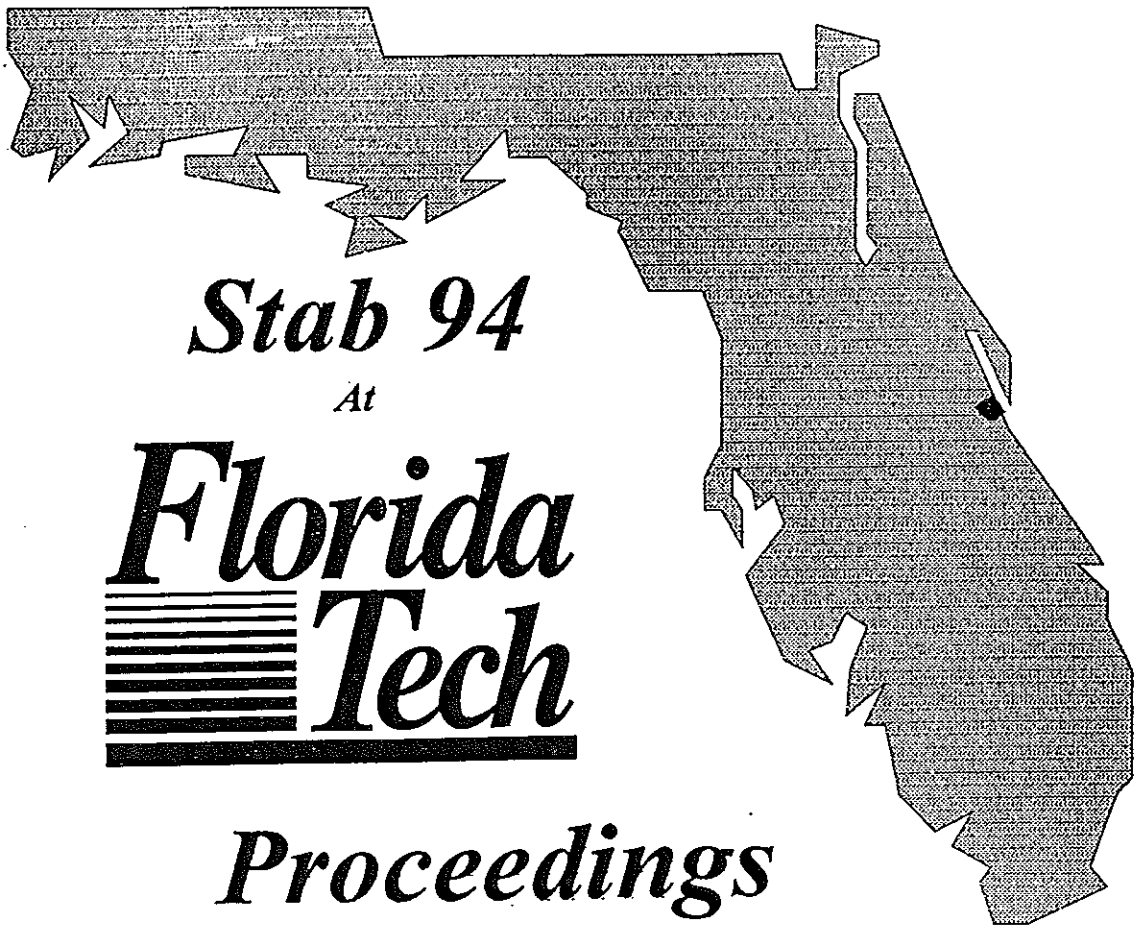

Stab 94

At

Florida Tech

Proceedings

Volume 4

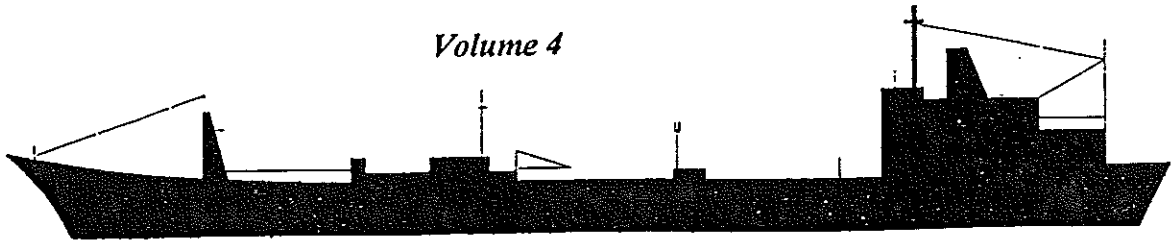

150 W. UNIVERSITY BLVD.
MELBOURNE, FL 32901-6988

FLORIDA INSTITUTE OF TECHNOLOGY

LYNN E. WEAVER, Ph.D. - PRESIDENT

COLLEGE OF ENGINEERING
ROBERT L. SULLIVAN, Ph.D. - DEAN

DIVISION OF MARINE AND ENVIRONMENTAL SYSTEMS
GEORGE A. MAUL, Ph.D. - DIRECTOR

OCEAN ENGINEERING PROGRAM
ANDREW ZBOROWSKI, Ph.D. - CHAIRMAN

WILLIAM R. DALLY, Ph.D.

GRAEME RAE, Ph.D.

GEOFFREY W. J. SWAIN, Ph.D.

LEE HARRIS - ASSOCIATE PROFESSOR

W. A. CLEARY, JR. - ADJUNCT PROFESSOR

PURPOSE OF STAB 94

STAB 94 had been offered to promote a full exchange of ideas and methodologies regarding STABILITY OF SHIPS AND OCEAN VEHICLES and to provide an opportunity to professional naval architects, capsize prevention researcher, regulatory agencies, inspection and certifying authorities, ship owners, consultants and ship operators to present, discuss and listen to improvements in capsize prevention for all types and sizes of ships.

SPONSORS
The Society of Naval Architects and Marine Engineers
The Royal Institution of Naval Architects

STAB 94

TABLE OF CONTENTS

THURSDAY 10 NOVEMBER

GLEASON AUDITORIUM

PAPERS SESSION 13

Moderator: R. SONNENSCHEIN
U. S. Maritime Administration

0900-0925
The Practical Implications of Fitting Devices to Attain SOLAS '90 on Existing RoRo Passenger Ships
Author: T. Allen

0930-0955
Broaching To - 30 Years On
Authors: D. Vassalos A. Maimun

1000-1025
Mechanism of Broaching-To of Ships from the Perspective of Nonlinear Dynamics
Authors: B. Bandyopadhyay C. Helung

A. M. BREAK

PAPERS SESSION 14

Moderator: Prof. A. TROESCH
University of Michigan

1035-1100
Capsize Criteria for Nonlinear Coupled Heave and Roll Oscillations in a Beam Sea
Authors: P. Donescu L. Virgin

1105-1130
The Probability Distribution of Rolling Amplitude of a Ship in High Waves
Authors: H. Xiangiu G. Xiechong B. Weiguang

1135-1200
Transverse Stability of Ships in Waves in Consideration of Ship Generated Waves
Authors: Z. Huang C. Helung

LUNCH - DELEGATES LOUNGE

PAPERS SESSION 15

Moderator: Dr. S. GROCHOWALSKI
National Research Council, Canada

1330-1355
The Correlation of Ship Hull Form and her Static Stability Diagram
Authors: Y. Vorobyov V. Sizov

1400-1425
On the Statistical Properties of the Metacentric Height of Ships in Following Seas
Author: M. Palmquist

1430-1455
On the Rolling Motion Instability Induced by Sail Action
Authors: G. Boccodamo E. Tortora S. deRosa, L. Lecce

P. M. BREAK

PAPERS SESSION 16

Moderator: Dr. H. UMEDA Japan
National Research Institute of Fisheries Engineering

1515-1540
Operational Factors in Stability Safety of ships in Heavy Seas
Authors: S. Grochowalski J.B. Archibald F. J. Connally C. K. Lee

1545-1610
Dynamic Stability of a Ship in Quartering Seas
Authors: M. Hamamoto M. Fujino Y. Kim

1615-1640
Ships Stability Safety in Resonance Case
Author: W. Blocki

CENTRAL BAPTIST AUDITORIUM

WORKSHOP / PANEL

Moderator: Dr. J. O. deKAT
MARIN, Wageningin, Netherlands

MANUEVERING & SURVIVAL IN STORM SEAWAYS

A. M. BREAK

MANUEVERING & SURVIVAL IN STORM SEAWAYS
(continued)

and

(concluded)

LUNCH - DELEGATES LOUNGE

WORKSHOP / PANEL

Moderator: Dr. S. ALLEN
USCG R & D Center

HUMAN FACTORS IN STABILITY

P. M. BREAK

HUMAN FACTORS IN STABILITY
(continued)

and

(concluded)

THE PRACTICAL IMPLICATION OF FITTING DEVICES TO ATTAIN SOLAS '90 ON EXISTING RO-RO PASSENGER SHIPS

By Tom Allan Bsc, C.ENG, FRINA,
Chief Surveyor (Ship Construction),
United Kingdom Marine Safety Agency

PREAMBLE

This paper primarily considers the practical implication of the proposed SOLAS '90 survivability requirements on existing ro-ro passenger ships and the modifying of such ships to meet the new requirements. The paper addresses the "devices" investigated in both Phases I and II of the United Kingdom ro-ro passenger ship research programme to improve the survivability standards of existing ferries. The term "device" refers to any means whereby the risk of capsize or sinking of a Ro-Ro ferry following a flooding incident can be reduced or eliminated.

INTRODUCTION

Shortly after the issue of the official report[1] of the Formal Inquiry into the loss of the "HERALD", the United Kingdom Secretary of State for Transport initiated a comprehensive research programme, with a view to establishing ways in which the stability of ro-ro passenger ships could be enhanced.

In considering the research, it was concluded that the most likely cause of capsize would be side damage resulting from a collision either with another vessel or with a fixed object. Cross channel ferries operate in a high risk environment as, of necessity, they have to cross main shipping lanes. In general, they have a very good record of collision free voyages but the risk of collision is always present and the consequences can be disastrous.

Accordingly, it was made clear within the specification for the research programme that the primary objective was to determine the "standard of residual stability which would be necessary to enable a ro-ro passenger ferry to survive flooding (caused by a side-collision with another ship or fixed object), and avoid rapid capsize in realistic sea-going conditions.

It must be recognised that the margin of residual stability of ro-ro ferries, in the damaged condition, was never very great. There are many different ways that slender margins could be reduced to nothing - whether through uncertainty about the draughts, the weight of cargo carried or its distribution, or because of growth in the lightship weight, permeability - or indeed the trim of the ship.

The Secretary of State, in agreeing to the research proposals, appointed a Steering Committee made up of naval architects, operators and the trade unions. The research was to be carried out in two phases; the first phase indicated that the residual stability standards introduced by IMO in April 1990 (SOLAS '90) should provide an adequate standard of protection against rapid capsize in seas up to sea state 3. This was a very important finding and one which appeared to validate SOLAS '90 as a standard that should enable ro-ro ferries to avoid capsize the effects of damage of the prescribed extent in such seas. The research also showed that a typical ferry built to the stability standards prior to SOLAS '90 would be unlikely to survive "worst case" collision in slight seas.

AIMS AND OBJECTIVES OF THE RESEARCH.

There were two aspects of the official report of the formal investigation into the loss of the "HERALD". The first identified means of stopping a similar accident happening in the future. The second was more fundamental, it was to take a more long term view of the survivability standards of ro-ro passenger ferries. This was to address the very serious concerns, on the existing survivability standards of ro-ro ferries in general, being expressed at that time by many prominent naval architects.

The second part proposed the following recommendations:-

1. Detailed investigations and model tests with a view to:

   .1 increasing the stability of ro-ro passenger ferries;

   .2 examining the implications of the provision of bulkheads on the vehicle deck; and

   .3 increasing the required distance from the margin line to the bulkhead deck in new designs of ro-ro passenger ferries to perhaps 1 metre;

2. A feasibility study be carried out to investigate the transverse subdivision of the vehicle space, to investigate the practical details of such divisions and their effect upon commercial operations. The thrust of any analysis to be decided towards operational practicability; and

3. To investigate either permanent or activated buoyancy external to the hull proper.

PHASE I OF THE RESEARCH

The agreed specification on the proposed research consisted of six distinct parts and an overview study:

Part I A Risk Analysis Study.[2]

Part II A Study of Collision Resistance.[3]

Part III A Study Of Hull Form and Superstructure.[4]

Part IV An Assessment of Internal Arrangements and Devices.[5]

Part V Ship Model Testing.[6]

Part VI An Assessment of the Residual Stability Standards as proposed by IMO, (completed in 1988).[7]

With respect to "devices":

1. The study of hull form and superstructure concluded that:

.1 a naval architect could design a 'high-stability' hull form by various means: stern wedge shaped appendages; flare in the region of the waterplane; or V-shaped hull sections. However none of the ways to increase waterplane inertia were particularly effective, unless combined with an adequate residual freeboard;

.2 the fitting of structural sponsons, provided they were of reasonable width and extend well above the waterline, could improve survivability significantly. They were recommended as a retro-fit measure on existing ferries only; and

.3 the use of inflatable sponsons, (if they were successfully deployed an emergency), may improve survivability to such an extent that a ship might survive a damage even greater than the minimum prescribed extent for a two-compartment ship, and in quite severe sea conditions.

2. The assessment of internal arrangements concluded that:

.1 the choice of 'device' depended primarily on a ferry's service pattern, (short- or long-haul), and whether a new design or an 'existing' ferry is involved.

.2 consideration of one proposed passive 'device', based upon the principle of 'water-dumping' and another with controlled washports capable of discharging floodwater quickly from the vehicle deck led to the conclusion that such 'devices', could not be recommended. The practical difficulties as regards structural and mechanical means for the discharge of the vast amount of water involved were extensive;

.3 the fitting of transverse barriers on the vehicle deck was reasonably effective; however, a short-haul ferry fitted with such 'devices' could incur a significant penalty in operating costs;

.4 the presence of buoyant wing spaces on the bulkhead deck could improve the survivability of a ferry to above the SOLAS '90 standard, provided that the damage did not extend to the central vehicle space. Even for damage which extended inboard to the central space, the residual stability characteristics would remain quite good;

.5 fitting wing spaces below the bulkhead deck also improved survivability to some extent. However, if this arrangement was combined with an absence of transverse subdivision inside of the B/5 line, the chances of a disastrous flooding/capsize appeared extremely likely; in other words the practice of allowing long central spaces beyond B/5 bulkheads should be dis-continued;

.6 the combination of watertight wing spaces together with a 'perforated' vehicle deck would provide good residual stability characteristics even under extended damage scenarios and greatly reduce the probability of capsize. However, there were doubts about the practicalities of such a 'device'; there were problems associated with fire hazards, fire protection measures, accessibility to spaces and ventilation arrangements. Until those attendant problems were resolved satisfactorily, this 'device' should be considered as still in the development stage; and,

.7 the research showed quite clearly that the 'human factor' was involved, to a varying degree, in the majority of casualty incidents. Therefore, when 'devices' are considered, preference should always be given to those which are 'passive' (rather than 'active') in nature.

3. The test results from the damaged models indicated that the SOLAS '90 standard should provide an adequate standard of protection against rapid capsize, up to sea state 3, (ie. waves of significant height up to 1.5 metres).

4. The computer study into the SOLAS '90 residual stability standards concluded that there was no easy option when deciding what measures should be used to improve the residual stability characteristics of existing ro-ro passenger ferries. To increase depth to the bulkhead deck, reduce the draught or the distance of the margin line below the bulkhead deck, all required significant changes in internal/external geometry and/or a revision in trading pattern. It also concluded that most 'existing' designs of ro-ro passenger ferry did not meet the residual stability standards of SOLAS '90.

OVERVIEW STUDY OF PHASE I

To comply with the SOLAS '74 Convention, passenger ships should have "sufficient stability for all sea conditions so as to enable the ship to withstand the final stage of flooding". The UK believes the research showed beyond any doubt that the prescribed stability criteria for ships built before April 1990 were not "sufficient".

Having established that a higher standard of survivability was necessary, a thorough study of the research led to the conclusion that the standard should be that recently introduced for new passenger ships; the **SOLAS '90** standard. The Research Steering Committee in considering this took the view that **all** existing ro-ro passenger ferries which operated in and out of UK ports should be required to comply with a higher standard of damage stability. To achieve international application these proposals were then forwarded to the IMO Maritime Safety Committee (MSC).

The Overview Report[8] comments in detail on the various measures proposed for enhancing survivability. The means of modifying existing ferries to meet this higher standard of survivability included:

1. Enhanced structural sponsons;
2. Retractable transverse barriers;
3. Inflatable sponsons;
4. Buoyant wing spaces;
5. High stability hull form with increased freeboard; and
6. Buoyant lifebelt with perforated decks.

The UK investigated[9] the effects the higher standard would have on a total of 15 typical ro-ro ferries and the modifications needed for compliance. The primary aim was to identify the modifications best suited to bring the ships up to the **SOLAS '90** standard. In deciding upon such modifications account was taken of:

1 cost;

2 the effect on operation; ie:
.1 turn around time, and
.2 the continued use of existing berthing facilities;

3 re-siting of life saving appliances and their launching arrangements;

4 re-siting of stabilisers or increasing their capability;

5 the effect on performance, particularly sea kindliness;

6 the effect on cargo/passenger carrying capacity; and

7 any loss of speed and/or increased fuel consumption.

SUMMARY OF THE REVIEW STUDY:

Whilst the results indicated that modifications would be required in most cases, some ships would need very little modification in order to meet the **SOLAS '90** standard. On the other hand there could be a few ships which would be so difficult to modify that their replacement would be necessary.

A particular problem revealed was the difficulties which existing berthing facilities might impose, eg length and shape of link span, depth of water etc.

The principal findings from the investigation into the 15 ferries were:

1 that the modifications would, in all cases, add steel weight and could increase operating costs (extra use of fuel) and in most cases lead to a reduction in payload (also vehicle deck area) and may increase 'turn round' time. However if sponsons were designed judiciously an increase in deadweight (payload) could be achieved, which may offset some of the disadvantages. One problem with sponsons which must not be overlooked, however, is their effect on the metacentric height (GM). An excessive GM could affect the sea kindliness of the ship and in extreme cases, due to high accelerations, create a hazard to passengers and freight. The "comfortability" of these vessels could be improved by fitting either additional stabilisers and/or replacing existing stabiliser systems.

2 The initial cost for the required modifications varied from £10,000 ($15,000 US) to £2,610,000 ($3,950,000 US). The annual running costs would, in most cases, also be increased to an estimated average of £650,000 ($975,000 US), ranging from nil to an extreme of £5,000,000 ($7,500,000 US) should an additional ship be required to maintain the service.

Using these figures, for the UK ferries on international voyages an initial cost of £60 million to modify the ships was estimated, with a further £20 million per annum for running costs. Berth modification costs would be over and above those figures; and for the UK 'domestic' fleet, an initial cost of £25 million to modify the ships has been estimated, with a further £2 million per annum thereafter for running costs. Berth modification costs of £50 million have been identified.

The above costs did not include the possibility that in some cases modification may not be possible and that a replacement ship may be required.

PHASE II OF THE RESEARCH

The basic objective of the UK research programme was to determine what survivability standard would be required to enable a typical ro-ro ship, (with a completely open vehicle space), to survive in realistic sea-going conditions. Phase I of the programme supplied some of the answers. However, since the analysis of the 'damaged' model test results indicated that much higher stability standards needed to be introduced for all ro-ro passenger ferries, it was very important to obtain as much amplification and corroboration of these results as possible.

One of the principal aims in mind, therefore, when the phase II specification was drawn up was:

> "To conduct tests with the models fitted with scaled versions of the various "devices", which were investigated in Phase I, in order to establish whether the expected improvement in survivability suggested by Phase I would be achieved in reality.".

Models were tested at DMI[10], Lyngby Denmark and BMT[11], Teddington England. The models were adapted to simulate the effect of fitting the various proposed 'enhancing devices' which were considered to be the most promising. These 'devices' may be summarised as:

1 half- or full- height transverse barriers fitted in the vehicle space;

2 wing spaces, port and starboard, outboard of the central vehicle space;

3 buoyancy external to the main hull, in the form of either permanent (structural) or temporary (inflatable) air-bags; and

4 flare in the region of the waterline at the midship portion of the ship.

TESTS CARRIED OUT AT DMI

The DMI model was exposed to waves with a midship, and later, with a forward side damage open to the sea. Systematic observations were made to investigate possible ways of improving damage stability by means of the various devices and the results assessed in relation to the SOLAS '90 stability requirements

The extensive model tests were divided into two parts. Their main objective in phase I of the research programme was to evaluate the importance of the three parameters:

- KG
- Sea State
- Damaged Freeboard

in respect to the model's ability to survive a midship damage.

The main goal of the Phase II research investigations was to examine the value of various realistic suggestions for improving damage stability of existing Ro-Ro ferries exposed to rough seas. The DMI report[10] fully describes the model tests carried out in Phase II.

The effects of external devices, such as; sponsons; flare and buoyancy air bags were examined in case of midship damage only. In addition, in respect to most of the combinations, the tests were repeated involving a reduced damaged opening definition as compared to the SOLAS standard. For the majority of cases the model was placed with the damage facing the waves. Some of the tests were repeated with the damage away from the on-coming waves.

Survival characteristics were determined with a flooded freeboard of 0.57 meter and significant wave heights of 2.5 and 5.0 metres

The main aim of the investigations was to determine the effects of the devices on the survivability of the model in terms of flooded GM at the point when capsize occurs within 60 minutes (ship time). Full details of the test methods can be found in the DMI report[10].

Tank Test Results

The tank tests were the crucial part of the investigation. A true capsize will normally happen, when a ship for some reason loses its stability. In the tests true capsize occurred with only relatively small water amounts necessary to heel the model out of balance, i.e. with relatively low GM and/or small amounts of side buoyancy.

In many cases, when the model "went down", the amount of water on the vehicle deck was considerable, and the model sank with relatively limited heel. In most of the cases, there was a combination of both mechanisms. The criterion survive/capsize depended on whether the model was able to survive the damage in tested condition for at least 60 minutes.

The most important results of this investigation are shown in the Overview diagram on the following pages.

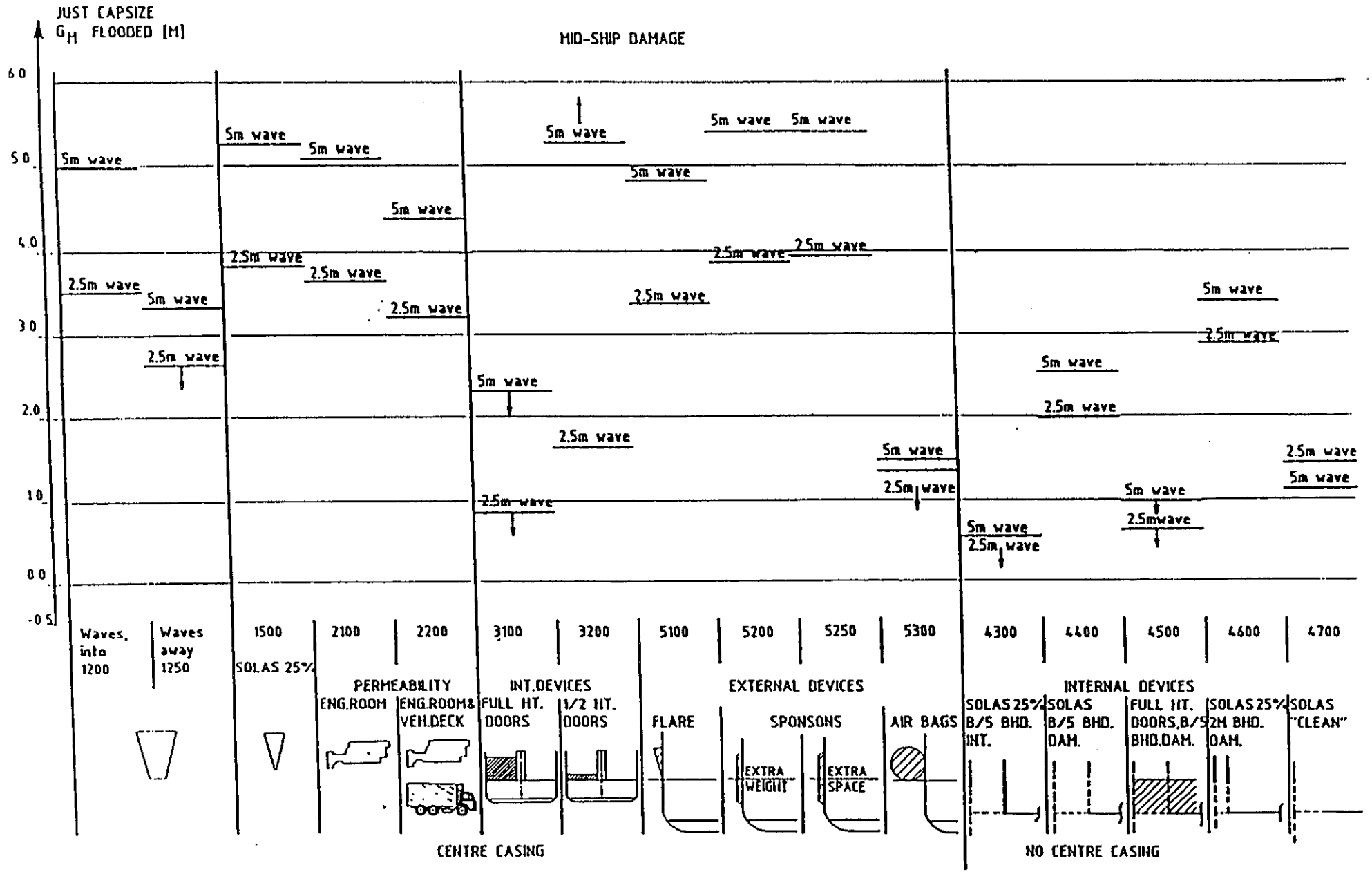
JUST CAPSIZE
G_M FLOODED [M]
MID-SHIP DAMAGE
6.0
5.0
4.0
3.0
2.0
1.0
0.0
-0.5
5m wave
2.5m wave
Waves into 1200
Waves away 1250
1500
SOLAS 25%
2100
2200
PERMEABILITY
ENG.ROOM
ENG.ROOM& VEH.DECK
3100
3200
INT.DEVICES
FULL HT. DOORS
1/2 HT. DOORS
5100
5200
5250
5300
EXTERNAL DEVICES
FLARE
SPONSONS
EXTRA WEIGHT
EXTRA SPACE
AIR BAGS
CENTRE CASING
4300
4400
4500
4600
4700
INTERNAL DEVICES
SOLAS 25% B/5 BHD. INT.
SOLAS B/5 BHD. DAM.
FULL HT. DOORS,B/5 BHD.DAM.
SOLAS 25% 2M BHD. DAM.
SOLAS "CLEAN"
NO CENTRE CASING

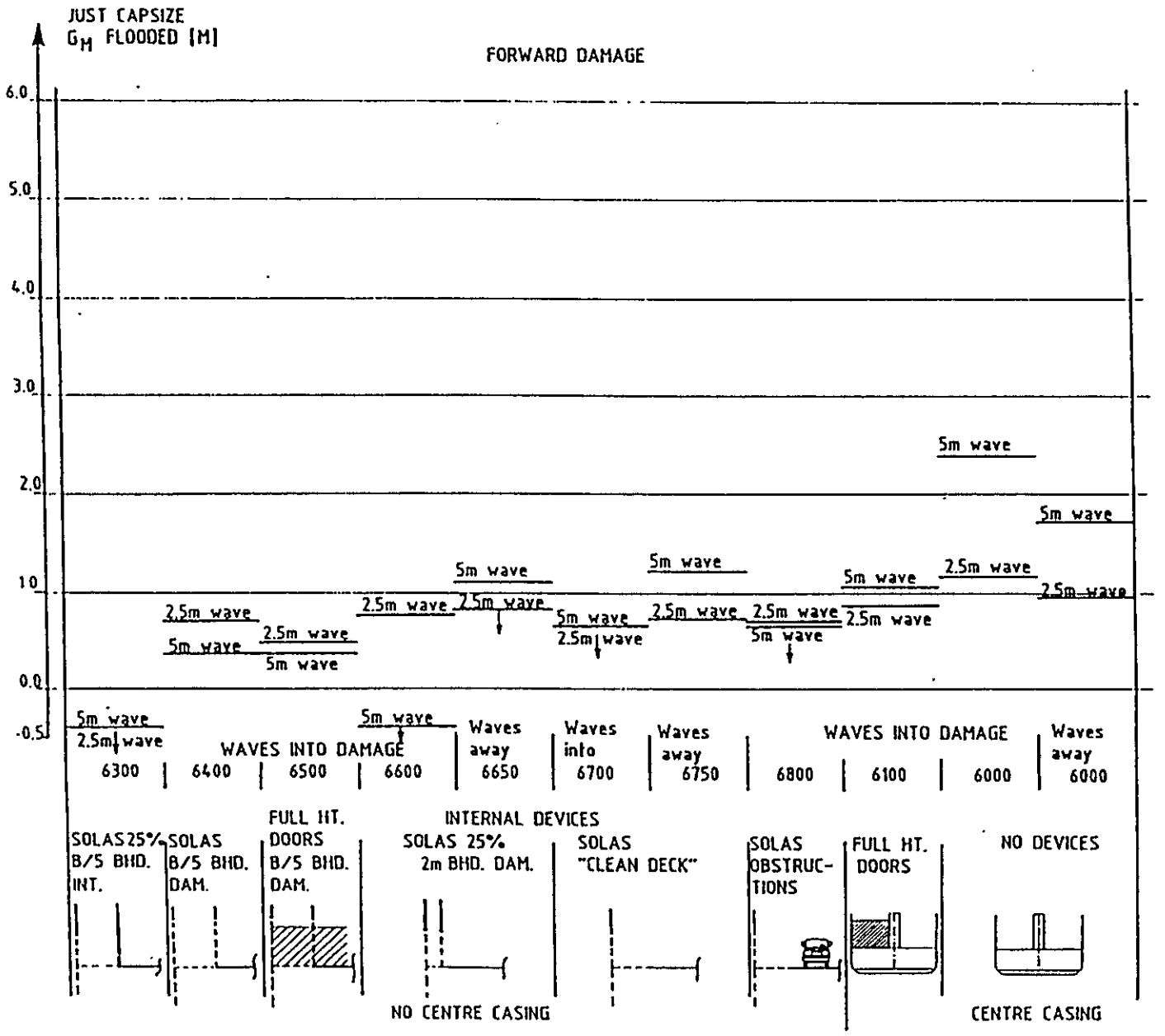
JUST CAPSIZE
G_M FLOODED (M)
FORWARD DAMAGE
6.0
5.0
4.0
3.0
2.0
1.0
0.0
-0.5
5m wave
2.5m wave
WAVES INTO DAMAGE
Waves away
Waves into
6300
6400
6500
6600
6650
6700
6750
6800
6100
6000
6000
SOLAS 25% B/S BHD. INT.
SOLAS B/S BHD. DAM.
FULL HT. DOORS B/S BHD. DAM.
INTERNAL DEVICES
SOLAS 25% 2m BHD. DAM.
SOLAS "CLEAN DECK"
SOLAS OBSTRUC-TIONS
FULL HT. DOORS
NO DEVICES
NO CENTRE CASING
CENTRE CASING

Table 2

All results reproduced in the tables were obtained from the tests at a damaged freeboard = 0.57 metre in 2.5 and 5.0 metres waves, and are presented in form of "just capsize" GM flooded. The icons symbolizing the nature of devices applied in each test group, hopefully, make the diagrams more clear.

The four-digit numbers, just above the icons are the test number series referring to a certain model configuration and/or test condition.

The Effects of Wind and Wave

The tests confirmed, what instinctively might be expected, that the situation when the damage faces the on-coming waves is more dangerous than if the damage is to the lee side. There was no doubt that if the waves and wind came from the same direction and if the damaged side faced the waves, the resulting wind forces would have a positive effect on survivability in rough sea.

Transient Moments and Permeability Effects

These effects, when applied to the damaged space below the bulkhead deck, had no measurable influence on the result. On the bulkhead deck, the reality was different. It appeared that reduced free surface effects, due to the presence of vehicles, effectively prevented water from transferring to the opposite side of the deck thus decreasing heeling moments away from the damage. The tests also showed that if the vehicles were fixed and if they remained intact after water entry, their buoyancy much improved the chances of survival.

The Test Results in Relation to the SOLAS '90 Criteria

The capsize phenomena demonstrated by the tests at DMI were mainly caused by free water trapped on the vessel's ro-ro deck. It was also demonstrated that where high values of GM, or reserve buoyancy at the level of the ro-ro deck existed, loss of the vessel was not due purely to a lack of stability, but more due to the effect of weight of trapped water. A final capsize of the ship would probably be caused by a much greater range of flooding than the original damage. The relationship between stability criteria and the model's capsize/survival stability is fully demonstrated in ref [10].

In looking back on the effects of some of the configurations tested DMI concluded that, even if concentrating only on those devices which basically do not contribute to additional reserve of buoyancy, their test experience would be at greater divergence with the SOLAS '90 formulation than indicated in their paper. This is due to important dynamic effects which were not regarded by SOLAS '90 and they recall three of them:

.1 the centre casing reflects the "high energy" water originating from the wave crests, preventing it from reaching the opposite side of the deck, considerably increasing the GM requirement for survival;

.2 the "1/2 height transverse doors" when tested in high waves, retained some of the water behind them, thus preventing it from escaping back through the damage opening. The resulting requirement for survival GM is increased considerably in high waves; and

.3 the reduced "damage opening" will to some extent hinder water from leaving the damaged side of the deck, increasing the GM requirement.

They concluded that there was a need for a better and a more flexible stability requirement for ships in the damaged condition and a way to develop this was to continue with model tests that were at least as accurate and repeatable as those tests performed for the Department of Transport Ro-Ro research programme.

BMT MODEL TESTS

BMT, in their report describe the indications and trends from the two parts of their study[11] which included physical model tests and a computer model before considering their conclusions.

Effectiveness of the Remedial Measures.

The model tests on a sudden entry of water into the flooded compartment showed that if the damage is confined below and the subdivision deck which remains intact, then the vessel is unlikely to capsize and can withstand quite severe wave motions. Furthermore, tests in Phase I[6], showed that, provided the subdivided hull and superstructure remain intact, large quantities of water on the subdivision deck can be accommodated without capsize.

In the former case the damage stability is sufficient to keep the vessel afloat if two compartments are flooded. In the latter case, the intact stability of the vessel is sufficient to withstand large quantities of loose water on the subdivision deck. Therefore damage and water on the vehicle deck when isolated from each other were not of themselves enough to cause capsize with the model as tested. But when both occurred together, capsize was a likely, but not inevitable, outcome.

They stated that remedial measures, if they were to be of any use, should be set against this background and must be able to

cope with flood water both above and below the subdivision deck. The concepts tested in the study were compared against a number of criteria in the following table:

MEASURE	EFFECT ON			
	MOTIONS	WATER ON DECK	CAPSIZE	STATIC FLOODED STABILITY
Sponsons	moderate -- more severe	moderate	beneficial	moderate increase
Air Bags	large -- more severe	large	very beneficial	large increase
Flare	small	small	small benefit	slight increase
Casing	none	moderate	can be beneficial	none

Table 3

From this it is clear that air bags had the most beneficial effect on capsize at the expense of increased severity of motions at large GM values. In the model tests air bags were fitted all round the model (except in way of the damage) and appeared to eliminate the possibility of capsize.

Casing position was included in the table in spite of the fact that it was not seen in the original study specification as having any bearing on remedial measures.

Both the physical and computer model studies showed that side or centre casings could have a noticeable effect on capsize and therefore it seemed appropriate to place them in the Table. Their position clearly made a difference to the capsize behaviour of the physical model and, from a design point of view, they could be incorporated into any internal subdivision scheme on the vehicle deck. Presence of a central casing gives increased likelihood of capsize toward the damage as results in this study repeatedly illustrated. Casing position could not be relied upon to prevent capsize in all cases (any more than sponsors or flare) but it could increase or reduce the chance of capsize.

In relation to the devices tested BMT concluded that:

1. The position of the longitudinal casing had a noticeable effect on the propensity to capsize. Side casings appeared to reduce the likelihood of capsize.

2. A static heel toward the damage greatly increased the chance of capsize; a static heel away greatly reduced it.

3. A sudden influx of water to a compartment below an undamaged subdivision deck had very little effect on both motions and the chance of capsize.

4. The effect of wind on capsize was small.

5. A reduced damage opening reduced the chance of capsize, especially if the damage faced away from the waves.

6. Obstructions in the flooded compartment slightly reduced the chance of capsize as did a reduction in deck permeability.

7. Structural sponsons and flare slightly reduced the chance of capsize.

8. Inflated air bags gave rise to a major reduction in the chance of capsize.

SUMMARY OF PHASE II RESULTS

1. Additional transverse subdivision in the vehicle space.

Not surprisingly, full height divisions were shown to improve the level of survivability in all sea states. Partial (say 'half'-height) divisions, on the other hand, were shown to be effective at low/medium sea states, but in high sea states the presence of these partial barriers can make the situation worse, since the incoming floodwater tends to be trapped beyond the barrier and therefore is unable to flow out of the "damage" opening.

2. Port and starb'd wing spaces outboard of the vehicle space.

Those tests which involved wing spaces fitted outboard of the vehicle space indicated quite clearly that there were considerable advantages in such an arrangement. Where the assumed damage penetration did not extend beyond the wing spaces, the results confirmed, that the presence of such a large amount of intact side buoyancy immediately above deck level ensured that the possibility of a capsize, even in high sea states, was extremely unlikely, (unless cargo shift occurs!).

When the assumed damage opened up the centre vehicle space, the remaining 'lifebelt' of buoyancy around the outer parts of the damaged waterplane reduced the probability of capsize significantly. Even when wing spaces were comparatively narrow, the tests showed that there was still a significant gain in survivability.

3. Additional buoyancy, (permanent and temporary), external to the main hull.

1 Structural Sponsons.

Tests indicated gains in survivability similar to that from the use of flared sections. (Again, with the proviso that the residual freeboard was adequate). Advantage could be taken of the increased waterplane inertia (and displacement) by raising the KG and/or decreasing the loaded draught.

It was also clear that the creation of a 'double-skin' improved the energy-absorbing characteristics of the side structure in way of the sponsons.

2 Inflatable Air Bags.

Tests with modelled air-bags confirmed the findings in Phase I, that there were considerable potential gains in the use of such 'devices', (provided they operated effectively in an emergency!). Whatever the sea state, capsize in such cases was extremely unlikely.

The use of both structural sponsons, (provided they extend well above the 'damage' waterline), and inflatable air-bags yielded a significant improvement in the residual stability lever curve. However "passive" means of improving survivability should always be considered first, and "active" means evaluated only after "passive" means are known to be impracticable.

4. The use of increased waterplane inertia in enhancing survivability

The effect of flared sections, (midships), was modelled by the use of temporary additions to the hull. The results confirmed the conclusions reached following Phase I - that flared sections provide sufficient improvements in survivability, provided they are linked with adequate residual freeboard.

Another means of augmenting waterplane inertia is the use of 'stern wedges' in the region of the waterline. However such 'wedges' will be ineffective if damage is sustained at the fore end. Additionally, the gain in inertia (and GM) when the wedge enters the water will be lost as the ship's heel increases.

OVERALL SUMMARY

Since the great majority of ro-ro passenger ferries were designed and built prior to the coming-into-force of the SOLAS '90 standard, it is hardly surprising that few, if any, of them comply with this standard. Enhancing the standards of such ships

to achieve compliance can only be achieved by modification using at least one of the "devices" addressed - which "device" to use can only be decided on a ship-to-ship basis.

The research indicates, quite clearly, the prime importance of adequate residual freeboard. The required enhancement in survivability of present-day ro-ro ferries, (ie. those having no subdivision in the vehicle space), cannot be achieved by increasing residual freeboard alone. The economic penalty from loss of deadweight prevents this.

"Safety", in its fullest sense, involves the entire gamut of ro-ro passenger ship operations. It is entirely possible that a marginal improvement in survivability standard could result in an effective downgrading in overall safety. For example, providing partial height transverse divisions in the vehicle space will lead to extra problems connected with vehicle space ventilation and efficient fire-patrol procedures.

The preferred solution in obtaining the necessary enhancement is to be one where total safety is not significantly impaired, whilst achieving the SOLAS '90 standard, or its equivalent.

Where longitudinal subdivision is provided as a way of enhancing survivability, it is important to minimise the risk of large heel angles developing immediately after collision has occurred.

"Passive" design features only should be included in a 'new' design of ro-ro ferry. (The exception to this being cross-flooding, provided that the counterflooding measures operate sufficiently quickly to avoid large heel angles occurring).

I trust that the information presented in this paper, together with the reports of the work carried out within the United Kingdom research programme will assist all owners/operators in their efforts in deciding which "device" is best suited to their vessels to increase their survivability to greater levels.

The views and opinions expressed in this paper are those of the author and may not necessarily be those of the Marine Safety Agency.

List of References

[1] Official Report of the Formal Investigation into the loss of the "Herald of Free Enterprise", Report of Court No 8074 - HMSO.

[2] "The Safety Record and Risk Analysis of Ro-Ro Passenger Ferries" - D.S. Alwinkle, Lloyd's Register of Shipping.

[3] "Collision Resistance" by P Sen and J A Cocks - University of Newcastle upon Tyne.

[4] "Ro-Ro Passenger Ferry Survivability Study - Hull Form and Superstructure" P.H. Judd - Yard Ltd.

[5] "Enhancing the Stability and Survivability Standards of Ro-Ro Passenger Ferries - Internal Arrangements" - C.J. Lloyd BMT Ltd.

[6] "Experiments with a Floodable model of a Ro-Ro Passenger Ferry" - I.W. Dand - BMT Ltd.

and

"Ro-Ro Passenger Ferry Safety Studies - Model Test of a Typical Ferry" - F Pucill and S. Velschon - DMI.

[7] "A Study to Compare the Residual Standards of Stability After Damage of Existing Ro-Ro Passenger Ferries" - A.J. Rogan.

[8] "Research into Enhancing the Stability and Survivability of Ro-Ro Passenger Ferries - Overview Study - C.J. Lloyd, BMT

[9] IMO paper SLF 35/INF.7.

[10] "Phase 2 Experiments with a Floodable Ferry Model" - BMT - I.W. Dand.

[11] "Ro-Ro Passenger Damage Stability Studies - A Continuation of Model Tests for a Typical Ferry" - DMI - M.Schindler and S. Velschon

BROACHING-TO: THIRTY YEARS ON

by

D. Vassalos* and A. Maimun**
* Department of Ship and Marine Technology, University of Strathclyde, UK
** Department of Naval Architecture, Universiti Technologi Malaysia

ABSTRACT

Thirty years after the monumental paper by Du Cane and Goodrich, [6], the subject of broaching is still described and discussed qualitatively in the literature. Fuelled by a recent resurgence of interest in the topic, this paper aims to review developments in the treatment of phenomena associated with broaching-to and to put forward a new mechanism which may be a dominant factor leading to vessel capsize in a broach-to situation. This derives from a strong non-linear coupling between longitudinal and transverse motions that proved to play a key role both in regard to the onset of broaching and in the ensuing extreme vessel behaviour. The approach adopted in studying extreme vessel behaviour in extreme following/quartering seas is briefly described and, with reference to a Canadian Trawler, representative results from a large scale investigation are presented and discussed.

1. INTRODUCTION

The question of ship safety, as characterised by ship stability, has been fraught with difficulties for over a hundred years. Despite an immense amount of research, a universally-acceptable solution for the problem has still not been achieved, nor is it likely to be in the foreseeable future. The reason for this is simple: complexity. One of the major modes of ship capsize, as observed in model experiments and deducible from accident statistics, is linked to the so-called broaching-to phenomenon. Capsizing by broaching-to is the most dynamic mode of ship capsize, resulting from loss of controllability in severe following/quartering seas. The vessel experiences a rapid development of forced turning that can cause it to end up almost beam-on to the wave direction despite maximum rudder action . This is frequently accompanied by large angles of heel that can cause considerable damage and may lead to capsize. Mariners have long appreciated the fact that most ships run the danger of this possibility.

However, in spite of the fact that most ships run the danger of this possibility and despite considerable research effort, a rigorous treatment of this capsize mode is still lacking. Reasons for this state of affairs include:

- In a broach the ship is in a very extreme condition which makes studies of the physics, either theoretical or experimental, difficult.
- Capsizing by broaching-to represents a single event in which are present many potentially dangerous scenarios linked in a cause-effect relationship, which are usually investigated separately.

Notwithstanding the above, stability research in the recent past has addressed a number of complementary scenarios pertaining to the behaviour of a vessel in severe following/quartering seas, such that, if the complementary expertise gained were brought together it would be possible to simulate the capsize sequence of a ship by broaching-to. Progress in this area is clearly essential in order to reduce the risk of vessel capsize.

2. BRIEF BACKGROUND

A brief account is given here of recent studies that have shed light on individual mechanisms which are likely to play a key role in the capsize scenario. These include:

a) Surf-riding [1], [2], [3], [10]

Depending on the wave conditions, a ship travelling at high speed in heavy following seas may, become "trapped" in a wave and forced to run at the wave's speed. Once this condition arose, it may be difficult to alter the ship's state by controlled action. Surf-riding, however, is not a necessary nor a sufficient condition for broaching to occur. So far, this phenomenon has been treated either through a single degree of freedom system (surge motion), [1], [2], [3] or by using the standard planar motions manoeuvring model (surge, sway, yaw), [10].

b) Directional Instability and Loss of Course Control [4], [5], [6],[7]

A head-down condition was found to be a most important factor affecting this situation. The loss of course control (and broaching) induces a dynamic yaw motion and leeward heel, which essentially constitute the same behaviour as follows the impact of a quartering wave. The only difference derives from the higher initial forward speed and acceleration (because of the following wave position) and subsequently longer yaw rate. The high yaw rate with the large forward speed creates centrifugal moments which increase the leeward angle.

c) Wave-Excited Yaw Moment [8]

When a ship travels on the down slope of a wave in a non-zero encounter angle, the cross-flow drag, which acts on the bow and stern of the ship in opposite directions, forms a couple with a tendency to turn the ship towards the crest line of the wave. Broaching-to will therefore occur when the wave-excited yaw moment exceeds the course-keeping ability of the rudder.

d) Loss of Transverse Stability and Capsize [4],[5],[9]

The exact capsize sequence once control has been lost in a wave environment is still subject to speculation. It is conjectured that the ship is brought into a beam-wave condition whilst remaining on the wave crest where, with the vessel's restoring capability reduced (pure loss of transverse stability) any heeling moments acting on the ship will cause either a large heel or a capsize. Studies of the coupling of planar motions into roll, for a non-linear system, are virtually non-existent, [4].

e) Ship Manoeuvring in Waves [14], [11]

A six-degrees-of-freedom time simulation programme has been developed with the potential of studying the dynamics of a ship manoeuvring in waves, [14]. Use is made, however, of a curious superposition between a manoeuvring and a seakeeping model. Ship manoeuvring behaviour in the presence of wind, waves and current has also been investigated in [11] using a coupled surge-sway-yaw-roll model.

f) Non-Linear Coupling Between Longitudinal and Transverse Motions [12]

Recent research has demonstrated, by means of theoretical and experimental investigations, the potential for loss of directional control leading to broaching and capsize as a result of strong non-linear coupling from heave and pitch onto roll and yaw when vessels move in low encounter periods in severe astern seas.

g) Dynamical Systems Theory [5], [10], [15]

The use of time simulations alone to study the dynamics of non-linear systems is limited by the fact that the global behaviour of the system cannot be easily investigated. Recent studies have demonstrated the potential of dynamical systems theory in overcoming this limitation. Related to broaching, the dynamical systems approach has mainly been applied to one-degree-of-freedom surge models, [1], even though some attempts involved application to more degrees-of-freedom manoeuvring models, e.g. [10]. Ship directional stability has been studied in [5] using a surge-sway-yaw-roll model whilst in [15] a global investigation of the same has been undertaken in the presence of wind.

It would appear from the foregoing that considerable expertise has been gained and experience accumulated concerning ship broaching. Broaching itself, however, is only a necessary but not a sufficient condition for a vessel to capsize. This fact has been generally overlooked with the broaching normally studied by means of a planar motions model whilst the phenomenon of actual ship capsize following a broach has hardly been tackled. At best, broaching has been studied as a roll-yaw coupling problem.

In relation to the above, on-going research at Strathclyde University in the subject of *Ship Stability and Operational Safety in Extreme Following/Quartering Seas* aims to address broaching along the following three fronts:

- Focus in studying systematically ship behaviour during broaching-to and on the phenomenon of actual ship capsize, following a broach.
- Development of a six-dgreès-of freedom mathematical model, including rudder control, to account for the non-linear coupling from heave and pitch onto roll and yaw.
- Make use of recent developments in non-linear system dynamics to gain a better insight and a global understanding of the vessel behaviour in a broaching-to situation.

Some aspects and results form this on-going research are presented in the following.

3. APPROACH ADOPTED

3.1 General

The need to understand the reasons for the capsizing of fishing vessels in steep astern seas and shallow waters provided the motivation for undertaking this research. This situation arises when small Malaysian vessels, such as fishing vessels, are entering harbours or river mouths whilst exposed to following/quartering seas. The presence of shallows in this case exacerbates the severity of the sea, thus creating an environment where the safety of the vessel is tested to its maximum.

The strong influence of non-linearities on the behaviour of the vessel necessitated the adoption of a time-domain analysis. The technique of using time-domain simulation to study capsizing in astern seas has been demonstrated previously, e.g. [16],[17],[18] and [19] and has gained much popularity. The adopted mathematical models and derived results are well discussed in the previous stability conferences.

Following ideas put forward by Bovet, [18], the present analysis focuses on the influence of the dominant hydrostatic effect of astern waves on the capsizal resistance of a vessel. A four-degrees of freedom mathematical model, comprising coupled heave, pitch, roll and yaw including an autopilot, is considered in order to address more emphatically the coupling effect between the longitudinal motions of heave and pitch and

the lateral motions of roll and yaw. This idea stems from studies into capsizing by broaching-to, the onset of which (i.e. uncontrollable yaw) is invariably linked to a vessel experiencing large amplitude heave, pitch and roll motions. Other reasons for this choice include:

- In a longitudinal seaway, the hydrostatic coupling between heave, pitch and roll have been shown to be very significant, [18], especially in steep waves and large amplitude motions. In such an environment, however, a heading deviation is unavoidable as a result of coupling from other modes of motion or "errors" in directional control. A heading of $\pm 15^{\circ}$ was, therefore allowed in the present model.

- Based on experimental evidence and computer simulation studies, Froude-Krylov forces are dominant in affecting vessel behaviour in astern seas, mainly due to the relatively low encounter frequencies. Therefore, these forces are presently computed accurately up to the instantaneous free surface. As such, the influence of shallow water and current on the wave profile is taken into account by considering second order Stokes waves.

- Sway and surge were initially omitted from the mathematical model in order to focus on the effects of coupling from pitch and heave on roll and yaw. In any case, it was assumed that in a situation where hydrostatic effects dominate, sway and surge motions are mainly affecting the planar position of the vessel relative to the wave and their influence could be independently investigated. The effect of incorporating these motions became the focus of a subsequent study.

3.2 Mathematical Model

To describe the motions and forces involved, two co-ordinate systems are utilised as shown in Figure 1; a wave co-ordinate system with its origin at the still water level amidships, for the calculation of wave excitation and a body co-ordinate system with its origin at the centre of gravity, for the computation of rigid body motions.

To describe a four-degrees-of-freedom system coupled in heave, roll, pitch and yaw, the Newtonian equations of motion are used in the following form:

$$m(\dot{w} - uq) = F_z \quad \ldots\ldots\ldots\ldots\ldots\ldots\ldots\ldots \textit{Heave}$$

$$I_{xx}\dot{p} + (I_{zz} - I_{yy})qr = K \quad \ldots\ldots\ldots\ldots\ldots \textit{Roll}$$

$$I_{yy}\dot{q} + (I_{xx} - I_{yy})rp = M \quad \ldots\ldots\ldots\ldots\ldots \textit{Pitch}$$

$$I_{zz}\dot{r} + (I_{yy} - I_{xx})pq = N \quad \ldots\ldots\ldots\ldots\ldots \textit{Yaw}$$

where,

m	:	vessel mass
u, v, w	:	rectilinear ship velocity components in X, Y, Z directions, respectively
p, q, r	:	angular ship velocity components about axes X, Y, Z, respectively
F_z, K, M, N	:	external force and moments in X, Y, Z directions, respectively
I_{xx}, I_{yy}, I_{zz}	:	principal moments of inertia about axes X, Y, Z, respectively

For large amplitude motions, the vessel orientation in relation to the fixed co-ordinate system is described by using Eulerian angles. As mentioned earlier, the dominant Froude-Krylov forces are calculated up to the instantaneous free surface whilst diffraction and radiation contributions are calculated up to the mean surface or taken from model experiments. Viscous effects are accounted for in the calculation of roll damping, [20], [21], wave-induced drag due to orbital velocities and manoeuvring forces, [22], [23], with correction for sinkage and trim in shallow waters from [24]. Finally, the vessel heading is controlled by means of a rudder in a way similar to an autopilot system with proportional angular deviation and angular velocity control.

The equations of motion are solved by numerical integration using the Runge-Kutta-Merson method.

3.3 Nature of Coupling From Longitudinal to Transverse Motions

An experimental technique based on forced oscillation has been devised to obtain zero speed hydrodynamic coupling coefficients, investigating especially large amplitude motions where coupling could be important. The method and results are described in detail in [12]. Some typical results are presented here in order to demonstrate the nature of heave and pitch coupling into roll. Figures 3 and 4 show the roll response due to heave and pitch, respectively. It is clear that there is a harmonic and a superharmonic response, the latter being characterised by larger roll amplitudes over a larger frequency range. It is interesting to mention that sudden jumps in the roll response were normally observed at the lower frequency range.

It should also be noted that this type of coupling depends critically on the amplitude of heave and pitch motions and on the roll stiffness.

4. PRESENTATION OF RESULTS AND DISCUSSION

4.1 General

Selective results from a large scale investigation are presented here with a view to demonstrate the influence of the aforementioned coupling on the onset of broaching-to as well as the ensuing vessel behaviour. In relation to the latter, the influence of diffraction forces and of surge and sway motions will also be discussed.

4.2 Choice of Vessel

A Canadian Trawler was chosen for the present study, mainly because this boat has been extensively investigated for stability in astern seas, [25]. The vessel particulars at the design waterline are given in Table 1 and the body plan in Figure 2.

TABLE 1: MAIN PARTICULARS OF THE CANADIAN VESSEL

L_{BP}	18.600 m
Beam	6.090 m
Depth	3.682 m
Draught (zero trim)	141.35 tonnes
Displacement	-0.359 m
LCG	2.660 m
KG	3.024 m
GM_T	0.533 m
T_{Roll}	6.280 secs

4.3 Ship Capsize by Broaching-to

As part of an extensive parametric investigation aiming to derive boundary stability curves that describe relationships between ship design and environmental parameters and stability related parameters, in known capsize sequences, broaching-to has been studied as a possible cause of ship capsize with the view to identify and quantify the governing factors that determine the vessel behaviour in a broach. As a result of such studies, the following characteristic sequences of vessel behaviour were identified to be directly linked to the coupling between longitudinal and lateral motions, referred to earlier.

a) Pseudo-Broaching (Cumulative Yaw Motion, [7])

Cumulative yaw motion, which might be construed as broaching, is referred to here as *pseudo-broaching* in order to distinguish it from the true broach which is the result of one wave only. This condition refers to the occurrence of persistently increasing yaw motion in the presence of a succession of steep waves rapidly overtaking the ship. In this situation, a certain combination between heave, pitch, roll and yaw motions was observed which could generally be described by using the right hand rule.

When a wave crest approaches the stern, for example, the ship will heave upwards, pitch by the bow and if she rolls to starboard a yawing motion to port will result. The yaw excitation moment depends critically on the instantaneous vessel-wave attitude and phase, as a direct result of vessel motions, the sequence of occurrence of which could lead to a persistent increase in yaw and eventual capsize in a pseudo-broach situation. Figure 5 shows some typical results describing a condition where the roll period is approximately twice the wave encounter period and the ship speed to wave speed ratio less than 0.5. On the basis of these, a number of interesting observations can be made. There appears to be a persistent heeling to starboard as the vessel yaws to starboard which coincides with bow up and heave down. The reverse is true with rolling to port. What is important, in relation to the theme presently explored, is that the yaw angle, rate and sense of rotation are influenced directly by both the heave, roll and pitch motion amplitudes as well as the direction of these motions. This is explained below.

With the wave crest having passed the stern, at a distance approximately L/4 from amidships, the vessel pitches bow down whilst heaving upwards. If the vessel at the same time rolls to port, the coupling between roll and pitch will cause a starboard yaw. As the wave crest moves forward passing amidships, rolling to starboard and pitching bow up will give rise to a port yaw. At this point, a large roll restoring develops due to a combination of a starboard roll, a downward heave and a wave trough amidships which causes the vessel to roll violently to port and yaw to starboard. With the roll restoring moment countering, the roll angle is not allowed to develop and with the wave crest re-appearing amidships, the vessel is rolling to starboard again. The yaw angle to starboard, on the other hand, becomes comparatively large due to lack of restoring forces to counteract the large inertia developed. Large yaw to starboard with the wave crest amidships, especially if the yaw rate is high, would augment roll motion, perhaps fatally.

Figure 6 depicts a similar situation. It will be noticed, however, that the persistent increase in yaw motion is now towards the port rather than the starboard side. This is primarily due to a change in the phase between the wave and roll motions. To obtain a persistent yaw to port, maximum roll to port should occur when the wave trough is near amidships. The resultant high potential energy will cause a roll to starboard whilst the coupling between roll and pitch will give rise to a large port yaw. Should the rudder be in the opposite direction when these changes take place, the yaw motion would be greatly enhanced. These events are typical of a broaching-to situation.

In the absence of surge motion in the simulated vessel behaviour, changes in the phase between wave and vessel motions could only be the result of changes in the magnitude of vessel motions, vessel heading relative to waves and vessel speed. In a real situation, however, a change in phase could be due to surf-riding. In addition, the relatively low encounter period at which cumulative yaw motion takes place, suggest that dynamic effects and hence wave diffraction forces might be important. These two aspects are further discussed next.

b) True Broaching (One Wave Broach)

In contrast to the cumulative yaw motion where the vessel speed is relatively low compared to the wave speed, in a true broach situation the vessel is travelling at a speed approximately equal to the wave speed, i.e. at very low wave encounter frequencies. To be able to simulate the vessel behaviour in this condition, the initial four-degrees-of-freedom mathematical model was extended to six degrees and a limited study has been undertaken, making use of experimental results from [25], in order to investigate the significance of including surge and sway as well as the relative importance of accounting for wave diffraction.

The Influence of Wave Diffraction

As indicated in [26], the equivalent effect of diffraction in head/following waves is a reduction of the wave amplitude. As such, wave excitation and hence vessel motions should also be reduced as shown in Figure 7. As a consequence of this, it may be claimed that ignoring the effect of diffraction could be regarded as a safeguarding measure in assessing ship safety. Heaving said this, it will be noted from Figure 7 that as the vessel heading relative to the waves increases, wave excitation also increases giving rise to a larger yaw motion. This alone could be detrimental regarding the onset of broaching, thus making necessary the consideration of the diffraction effect.

The Influence of Surge and Sway Motions

Comparing the results between the four- and six-degrees-of-freedom models, leads to the conclusion that surge motion is quite significant in affecting vessel behaviour in severe astern seas. As vessel speed increases (Fn approximately > 0.25), the vessel may be forced to travel at the speed of wave, i.e. surf-riding may occur. A similar situation, however, may arise when the vessel advances at a speed reaching near the wave speed. In both cases, the vessel motion is locked-on in a particular orientation resulting in a persistent increase in yaw motion. The key to broaching occurrence, however, lies on the vessel-wave attitude when surf-riding takes place. In this situation, as the vessel is "pushed" forward at a high speed with the wave crest near the stern, it is the coupling between longitudinal and lateral motions that sets up the initial yaw, as described earlier. If the yaw moment exceeds the rudder applied moment, the vessel will be locked-on in a rapidly increasing yaw. As the vessel turns, large roll amplitude develops that may lead to vessel capsizing. Sway motion becomes significant in quartering seas, mainly because of its influence on the roll motion.

Some simulated results are shown in Figure 8 where it may be seen that the main influence of surge and sway motions derives from the fact that their inclusion alters the phase between vessel and wave motions as postulated earlier. However, the occurrence of capsizing is primarily influenced by the variation of the roll restoring moment as affected by all ship motions on a purely hydrostatic basis.

5. CONCLUDING REMARKS

Based on the points raised in the foregoing, the following remarks are noteworthy.

- Experimental and numerical investigations have confirmed earlier findings concerning the coupling between longitudinal and lateral motions and have, for the first time, shown this to be of paramount importance in affecting both the onset of broaching and the ensuing extreme vessel behaviour.

- Numerical results have shown that a realistic simulation of a broaching-to situation, addressing the capsizal resistance of the ship, requires a six-degrees-of freedom system including an autopilot, where both hydrostatic and hydrodynamic effects are considered to the extent allowed by the state of the art.

6. ACKNOWLEDGMENTS

The support of the Malaysian Government and of the Universiti Technolologi Malaysia in undertaking part of this research is gratefully acknowledged. Special thanks are also due to the Laboratory Staff at the Department of Ship and Marine Technology of the University of Strathclyde for their valuable help in the experimental programme.

7. REFERENCES

[1] KAN, M: *A Guideline to Avoid the Dangerous Surf-riding.* STAB '90, Naples, 1990.

[2] UMEDA, N: *Probabilistic Study on Surf-riding of a Ship in Irregular Following Seas.* STAB '90, Naples, 1990.

[3] THOMAS, G A & RENILSON, M R: *Surf-riding and Loss of Control of Fishing Vessels n Severe Following Seas.* Spring Meeting, RINA. 1991.

[4] VASSALOS, D & SPYROU K: *An Investigation into the Combined Effects of Directional and Transverse Stabilities.* STAB '90, Naples, 1990

[5] VASSALOS, D & SPYROU, K: *The Effect of Trim by Bow: A Dynamical Systems Approach.* Second Kummerman Int. Conf. on Ro-Ro Safety and Vulnerability. RINA. April 1991, London.

[6] Du CANE, P & GOODRICH, G J: *The Following Sea, Broaching and Surging.* Transactions of RINA, 1962.

[7] RENILSON, M R & DRISCOLL, A: *Broaching - an Investigation into the Loss of Directional Control in Severe Following Seas.* RINA Spring Meetings 1981.

[8] MOTORA, S et al: *On the Mechanism of Broaching-to Phenomenon.* STAB' 82, Tokyo, 1982.

[9] VASSALOS, D et al: *Intact Ship Stability Criteria in Following and Quartering Seas.* IMAEM '84, Athens, 1984.

[10] UMEDA, N & RENILSON, M R: *A Dynamic Analysis of Yaw Behaviour of a Vessel in a Following Sea.* 2nd MCMC, Southampton, 1992.

[11] VASSALOS, D & DELVENAKIOTIS, C: *The Effect of the Environment on the Stability and Turning of Ships.* 2nd MCMC, Southampton, 1992.

[12] MAIMUN, A: *Stability of Fishing Vessels in an Astern Sea - Shallow Water Environment.* PhD Thesis, Dept of Ship and Marine Technology, University of Strathclyde, 1993.

[13] RUTGERSSON, O & OTTOSSON, P: *Model Tests and Computer Simulation - An Effective Combination for Investigation of Broaching Phenomena.* SNAME Annual Meeting, 1987.

[14] OTTOSSON, P & BYSTROM, L: *Simulation of the Dynamics of a Ship Manoeuvring in Waves.* Trans. SNAME, 1991.

[15] SPYROU, K & VASSALOS, D: *A Global Investigation of Directional Stability of Ships n a Wind Environment..* IMAEM '90, Athens, 1990.

[16] PAULLING, J R, OAKLEY, O H and WOOD, P D: "Ship Capsizing in Heavy Seas: The Correlation of Theory and Experiments", STAB'75, Glasgow, 1975.

[17] DE KAT, J O: "The simulation of Ship Motions and Capsizing in Severe Seas", SNAME Annual Meeting, New York, 1989.

[18] BOVET, D M: "Development of a Time Domain Simulation for Ship Capsizing in Following Waves", USCG, Report No. CG-d-28-74, Oct. 1973.

[19] HAMAMOTO, M and AKIYOSHI, T: "Study of Ship Motions and Capsizing in Following Seas - Equations of Motion for Numerical Simulation", Spring Meeting SNAJ, May 1988.

[20] HIMENO, Y: "Prediction of Ship Roll Damping - State of the Art", Naval Arch, & Marine Eng., The University of Michigan, report No. 239, Sept. 1981.

[21] IKEDA, Y, TANAKA, N and HIMENO, Y: "Effect of Hull Form and Appendage on the Roll Motion of a Small Fishing Vessel", STAB'82, Tokyo, 1982.

[22] CLARKE, D, GEDDING, P. and HINE, G.: "The Application of Manoeuvring Criteria in Hull Design Using Linear Theory", Trans. RINA, Vol. 125, 1983.

[23] FUJINO, M: "Experimental Studies on Ship Manoeuvrability in Restricted Waters", ISP, Vol. 15, 1981

[24] MILLWARD, A: "A Preliminary Design Method for the Prediction of Squat in Shallow Water", Marine Technology, Vol. 27, No. 1, Jan. 1990.

[25] GROCHOWALSKI, S: "Investigation into the Physics of Ship Capsizing by Combined Captive and Free-Running Model Tests", SNAME Annual Meeting, New York, 1989.

[26] BARRIE, D: "The Influence of Ship and Environmental Parameters on Stability Assessment", PhD Thesis, Dept. of Ship and Marine Technology, University of Strathclyde, 1986.

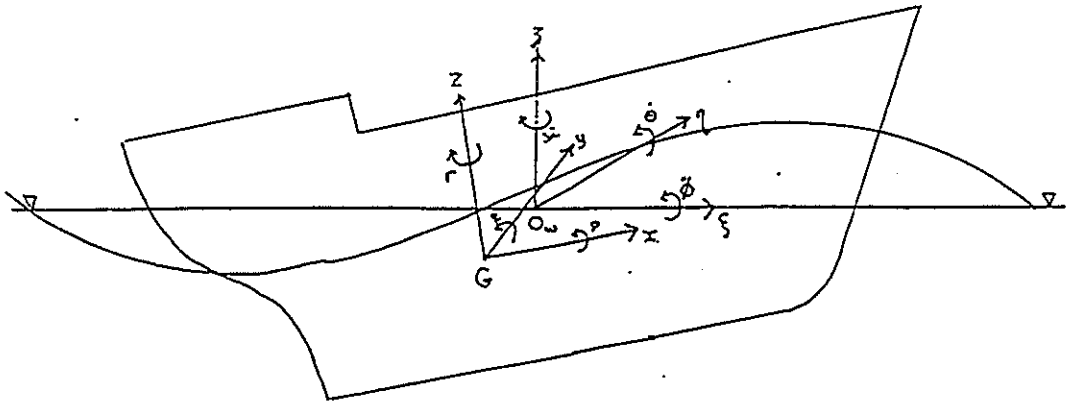

Figure 1: Co-ordinate Systems

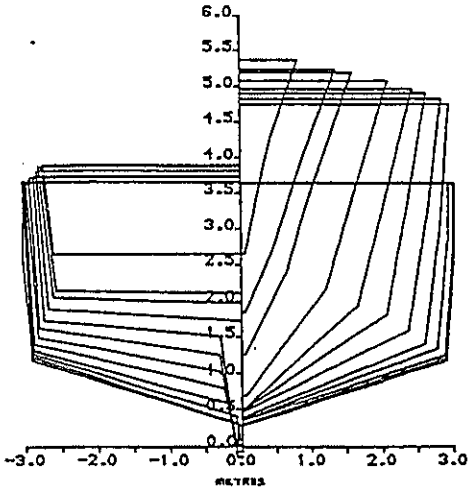

Figure 2: Canadian Fishing Vessel

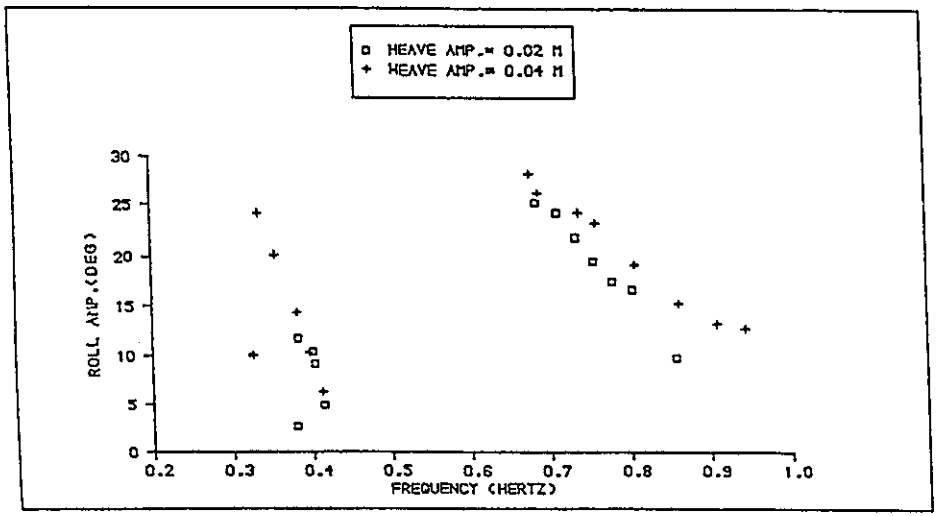

Figure 3: Roll Response - Coupling of Heave into Roll (GM=0.025m)

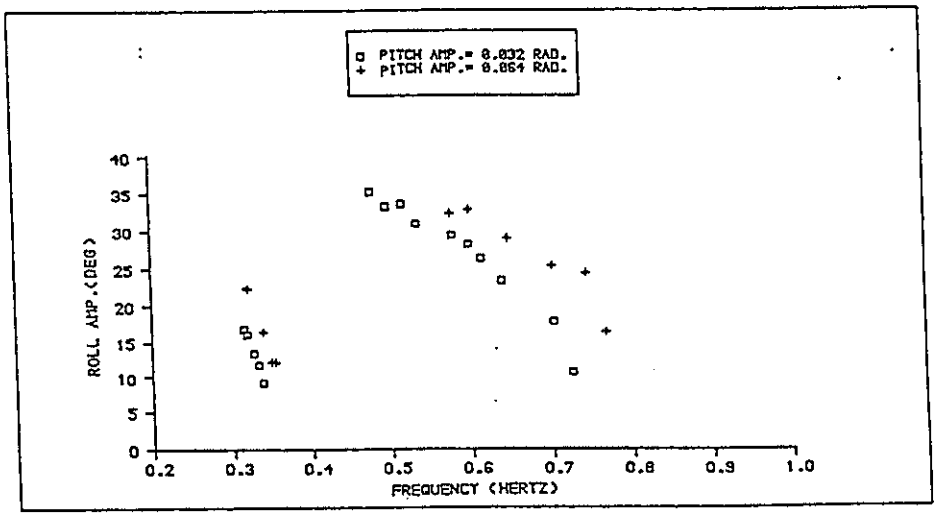

Figure 4: Roll Response - Coupling of Pitch into Roll (GM=0.025m)

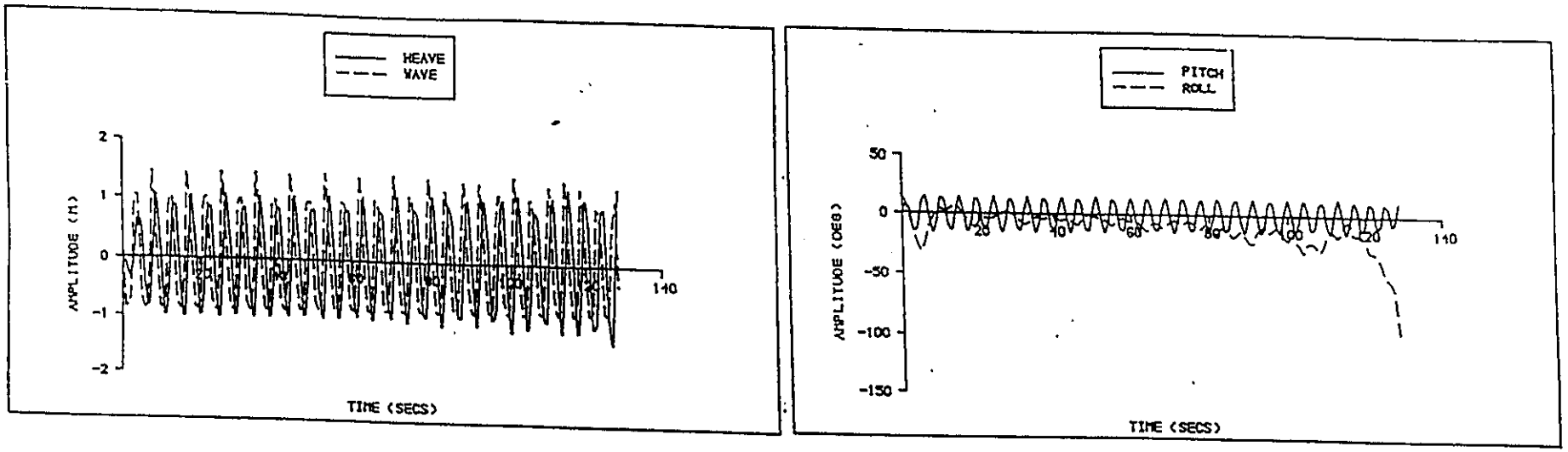

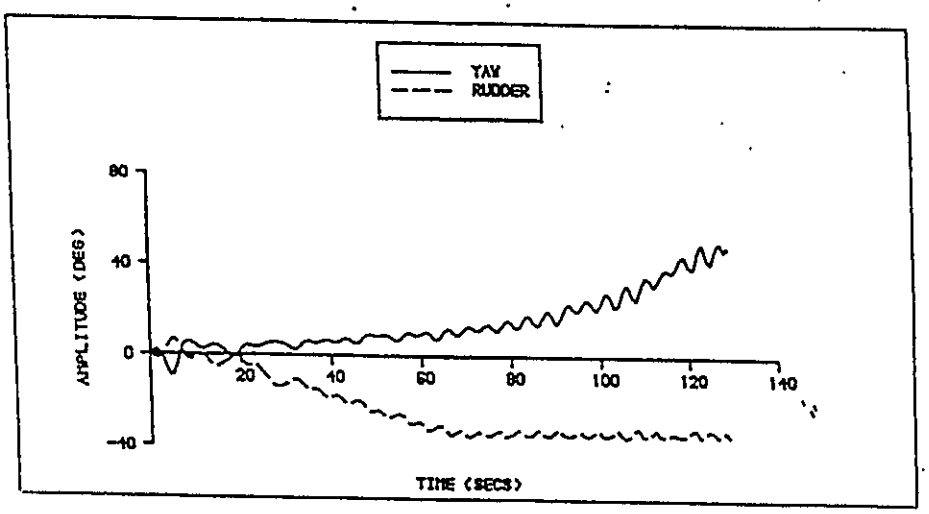

Figure 5: Pseudo-Broaching
(Vessel: V_S=1.1 m/s; KG=3.314m - Wave: L_W=18.6 m; H_W=5.32m; V_W=5.24 m/s)

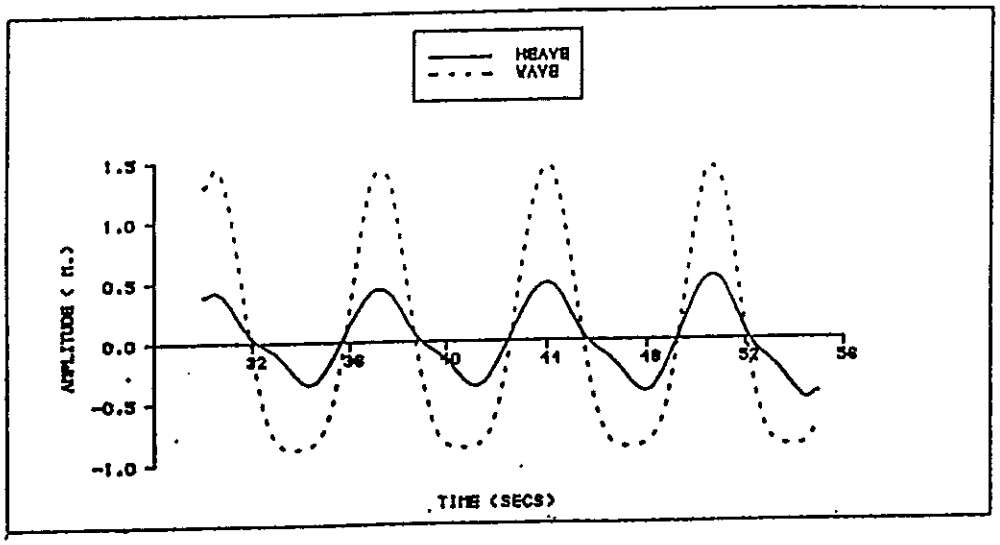

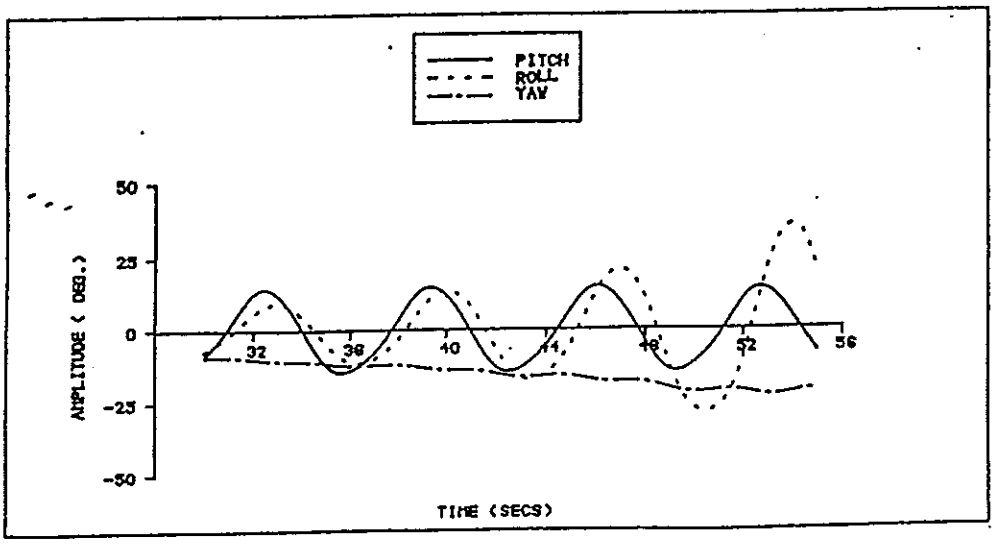

Figure 6: Coupling Between Longitudinal and Transverse Motions

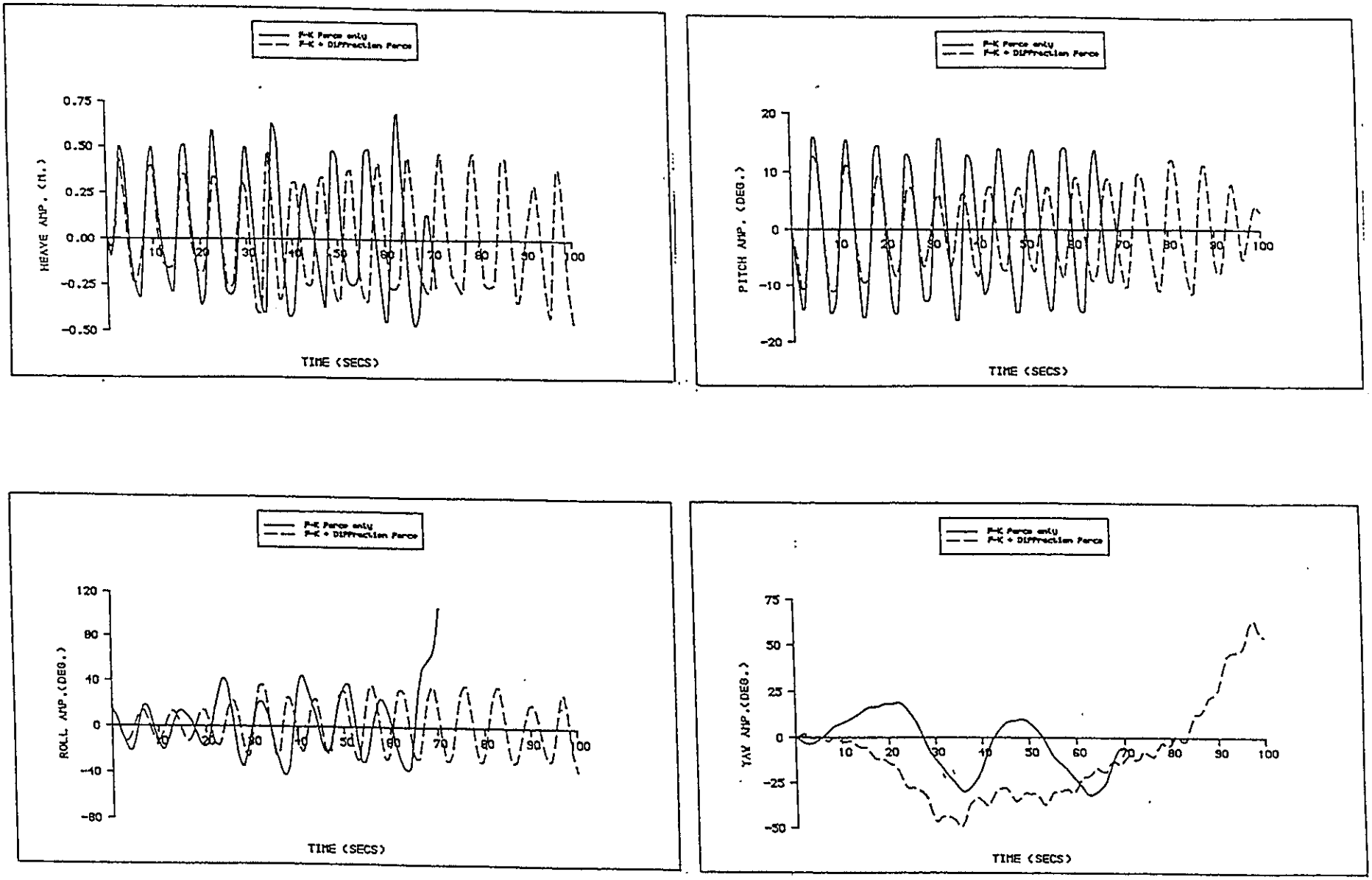

Figure 7: Influence of Wave Diffraction (V_S/V_W=0.5; L_S/L_W=1.0)

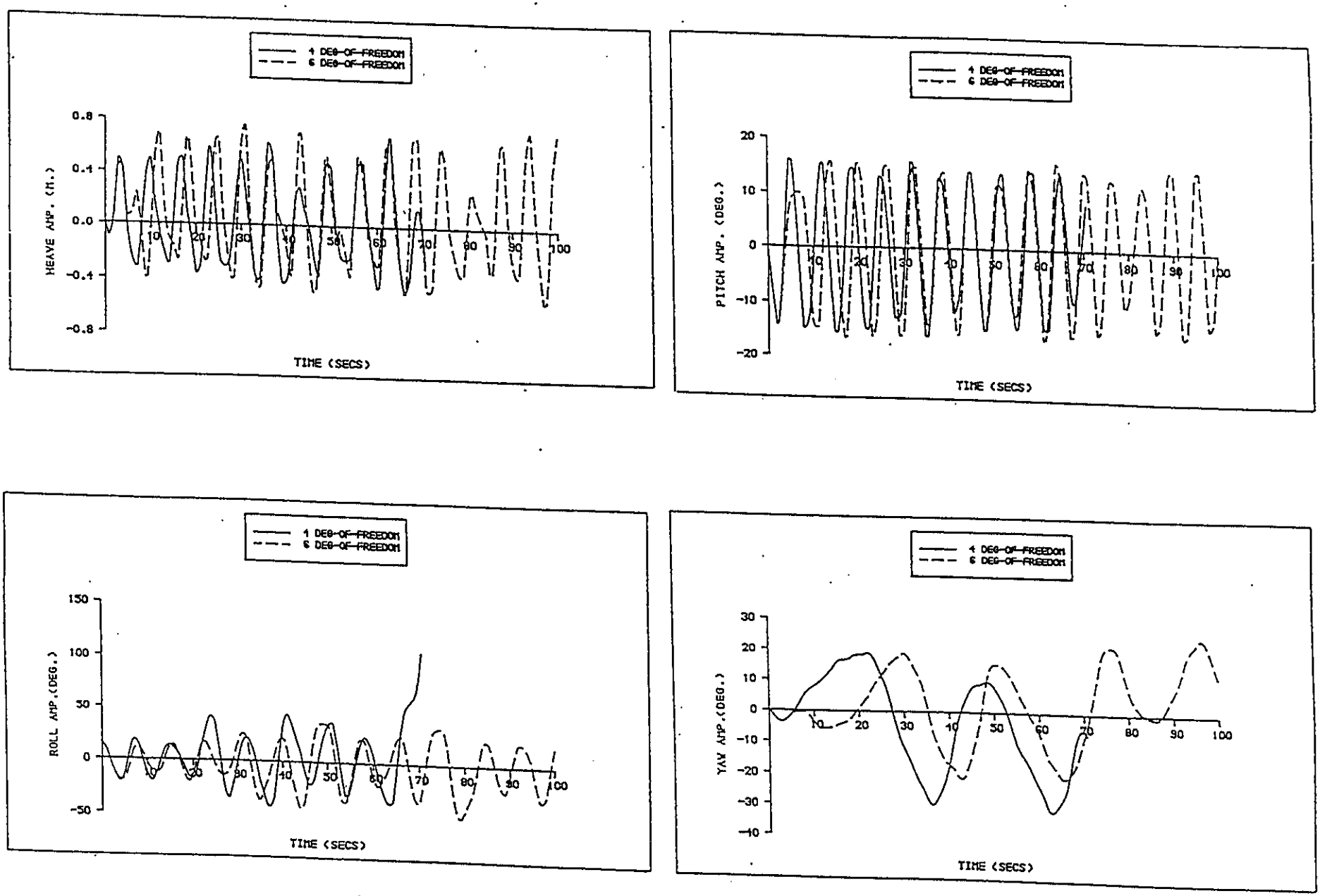

Figure 8: Influence of Surge and Sway Motions (V_S/V_W=0.5; L_S/L_W=1.0)

MECHANISM OF BROACHING-TO OF SHIPS FROM THE PERSPECTIVE OF NONLINEAR DYNAMICS

B. Bandyopadhyay C. C. Hsiung
Technical University of Nova Scotia, Halifax, Nova Scotia, Canada

ABSTRACT

This paper presents the results of an attempt to unveil the mechanism of broaching-to of ships, by a numerical and phenomenological approach with reference to qualitative prediction techniques of nonlinear dynamics. The ship and the ambient water are considered to form a *time-invariant* dynamic system. Nonlinear effects are simulated in their true forms or by their linear approximations. Four degrees of freedom in surge, sway, roll and yaw have been considered to describe the ship-dynamics. The ship manoeuvre through environmental (external) excitations is described by a semi-empirical mathematical model in the form of ordinary differential equations. This model is developed by combining theoretical and experimental modelling techniques. The equations of motion describing the total system dynamics is recasted in the compact *state space* representation, $\dot{\mathbf{x}} = \mathbf{A}\mathbf{x}$. Time-domain simulations are performed by numerically integrating these canonised ordinary differential equations.

Parametric analyses of the time domain simulation results, carried out by judiciously varying the ship's steady forward speed, relative wave heading, length and amplitude of waves, speed and direction of wind, and substantiated by graphical depictions, reveal a new mechanism for the inception and occurrence of broaching-to.

INTRODUCTION

Difficulty in steering a ship/boat in following and quartering seas, leading to the total loss of directional control despite any rudder action, under some critical parametric combinations, is termed as 'broaching-to'. Theoretical and experimental analyses of this complicated phenomenon have been carried out by several investigators [4], [6], [10], [11], [12], [13], [18], [19], [20].

Applications of qualitative prediction techniques of nonlinear dynamics through topological approach have led to new understandings of the complex ship motions in roll [7], [15], [21], the responses of moored tanker [3], [14], [16], and broaching of ships [18], under deterministic excitations. The result of a preliminary investigation into the broaching-to phenomenon by the above mentioned approach, has been introduced by the authors [2]. In this paper, unfolding of the mechanism for the occurrence of broaching-to has been exemplified by case studies. For brevity, only an outline of the simulation model, which is elaborated to some extent in [2], has been presented. For further details of the model or any other part of the paper, readers are referred to the doctoral thesis of the first author [1].

SIMULATION MODEL

The principal constituents of the model are :

I. the kinematic relations
II. equations of motion describing the ship dynamics
III. expressions for external excitations which is considered by a linear superposition of the following effects :
   (a) Quasi-steady hydrodynamic response force-couple;
   (b) Propeller and rudder force-couple;
   (c) Linear hydrodynamic memory effects;
   (d) Steady wind force-couple; and
   (e) First-order regular wave exciting force-couple.

The hydrostatic force-couple is neglected, except in roll, since effects of 'heave' and 'pitch' have been dispensed with in the present investigation.

Coordinate Systems

In developing the equations of motions, the following *right-handed*, orthogonal coordinate systems, as shown if Fig. 1, are adopted :

Inertial (x_o, y_o, z_o) : the origin is at an arbitrary point fixed in the space, with the z_o-axis directed vertically downwards.

Body (x_b, y_b, z_b) : fixed on the body (moving ship), the origin being on the centre plane at the intersection of the midship section and the designed water plane with the x_b axis directed towards the forward of the ship and the z_b axis, vertically downwards.

Positive translatory as well as rotational displacements are depicted in Fig. 1 by *arrow-heads.*

Dynamics

The equations of motion describing the dynamics of the ship motion in surge, sway, roll and yaw are :

$$\begin{aligned} m[\dot{u} - rv - x_G r^2 + z_G pr] &= X \\ m[\dot{v} + r(u+U) - z_G \dot{p} + x_G \dot{r}] &= Y \\ I_x \dot{p} - mz_G[\dot{v} + r(u+U)] - mx_G z_G \dot{r} &= K \\ (I_z + mx_G^2)\dot{r} + mx_G[\dot{v} + r(u+U)] - mx_G z_G \dot{p} &= N \end{aligned} \tag{1}$$

Kinematics

The kinematic equations, relating the velocity components in the inertial and the body coordinate systems in surge, sway, roll and yaw, are as follows :

$$\begin{aligned} \dot{x}_o &= (u+U)\cos\psi - v\cos\phi\sin\psi \\ \dot{y}_o &= (u+U)\sin\psi + v\cos\phi\cos\psi \\ \dot{\phi} &= p \\ \dot{\psi} &= r\cos\phi \end{aligned} \tag{2}$$

The kinematic effects of an incoming regular wave are considered by (u_{rel}, v_{rel}), as :

$$\begin{aligned} u_{rel} &= u + U - \sqrt{\tfrac{g\lambda}{2\pi}}\cos(\mu - \psi) \\ v_{rel} &= v - \sqrt{\tfrac{g\lambda}{2\pi}}\sin(\mu - \psi) \end{aligned} \tag{3}$$

where μ, λ and the quantity $\sqrt{g\lambda/2\pi}$ are the heading, the length and the phase-velocity of the incident wave, respectively.

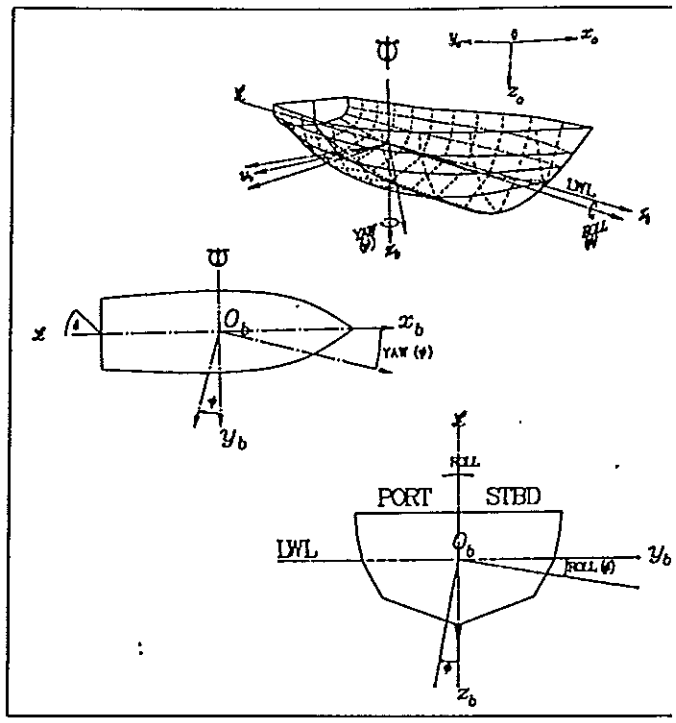

Figure 1: *Coordinate systems and sign conventions.*

The Memory Effect

The *vectorial recursive state space representation* [3] of the memory effect is :

$$\begin{aligned} \dot{\mathbf{s}}_{n-k}(t) &= \mathbf{s}_{n+1-k}(t) - \mathbf{A}_k \mathbf{s}_0(t) - \mathbf{B}_k \mathbf{v}(t) \\ &\text{with } k = 0, 1, \ldots, n; \\ &\mathbf{s}_0(t) = \mathbf{F}^*(t) \text{ and } \mathbf{s}_{n+1}(t) = 0 \end{aligned} \tag{4}$$

In equation (4), $\mathbf{s}_k$ for $k = 0, 1, \ldots, n$, are state vectors that effectively store the input history during time domain simulations (starting from suitable initial conditions) and thus contain

memory effect. The state parameter matrices $\mathbf{A}_k$ and $\mathbf{B}_k$ are optimally estimated as outlined in [3] and described in details in [1]. The final expression for memory effect is obtained as [14] :

$$\begin{aligned} \mathbf{F}_M &= [X_M, Y_M, K_M, N_M]^T \\ &= [\mathrm{a}(0) - \mathrm{a}(\infty)]\dot{\mathrm{v}}(t) \\ &+[\mathrm{b}(0) - \mathrm{b}(\infty)]\mathrm{v}(t) + \mathrm{s}_0(t) \end{aligned} \tag{5}$$

STATE SPACE REPRESENTATION

New dynamic equations are obtained by explicitly solving (1) for $\dot{u}, \dot{v}, \dot{p}, \dot{r}$ that otherwise occur linearly on both sides, in the following matrix form* :

$$\underbrace{\begin{bmatrix} \mathcal{C}_{11} & 0 & 0 & 0 \\ 0 & \mathcal{C}_{22} & \mathcal{C}_{23} & \mathcal{C}_{24} \\ 0 & \mathcal{C}_{32} & \mathcal{C}_{33} & \mathcal{C}_{34} \\ 0 & \mathcal{C}_{42} & \mathcal{C}_{43} & \mathcal{C}_{44} \end{bmatrix}}_{\boxed{\equiv \mathcal{C}}} \underbrace{\begin{bmatrix} \dot{u} \\ \dot{v} \\ \dot{p} \\ \dot{r} \end{bmatrix}}_{\boxed{\equiv \dot{\mathcal{V}}}} = \underbrace{\begin{bmatrix} rhs_1 \\ rhs_2 \\ rhs_3 \\ rhs_4 \end{bmatrix}}_{\boxed{\equiv rhs}} \tag{6}$$

The matrix $\mathcal{C}$ is a *known* quantity and the vector rhs can be evaluated for some suitable values (initial conditions) of unknown variables. Thus (6) can be solved for $\dot{\mathcal{V}}$ by the following matrix equation :

$$\dot{\mathcal{V}} = [\mathcal{C}]^{-1}\,[rhs] \tag{7}$$

Equations (2), (4) and (7) constitute the intended state-space representation $\dot{\mathbf{x}} = \mathbf{A}\mathbf{x}$ which is numerically integrated with suitable initial conditions, using the IMSL (International Mathematical and Statistical Library) routine 'DIVPAG' which employs the *Adams-Moulton* method for solving the initial value problem described by a set of ordinary differential equations and is recommended for the so-called *stiff* problems. The results of these simulations are analysed to identify the nature and the causes of the broaching-to phenomenon of ship motion.

*for details, see [1] or [2]

SIMULATION PREDICTIONS

Scope Of Calculations

The ship chosen for the investigation is a wide hull fishing boat [8], engaged along the coast of Newfoundland. The main particulars of the fishing boat are :

$L_{WL}(L) = 18.36m$, Breadth (mld) $(B) = 7.43$ m, Depth (mld) $(D) = 5.3$ m, Draft (mld) $(h) = 2.76$ m, Displacement $(\nabla) = 187.4$ m^3, Number of Propeller $(n_P) = 1$; Number of Rudder $= 1$.

The parameters representing the external excitations by wind are (i) speed and (ii) direction; and those by the waves are (i) length, (ii) heading and (iii) height. The system parameters, influencing ship manoeuvring are (i) speed of advance of the boat, (ii) rudder deflection and (iii) propeller r.p.m.

Simulation Preliminaries

It is pertinent at this point to clarify a few important concepts about the simulation algorithm. The mathematical model, as mentioned before, consists of equations (2), (4) and (7). The following items should be noted with regard to the application of the model :

Wind Effect : The wind effect is neglected in this investigation on the consideration that it can only aggravate the situation favourable to broaching, but can not initiate the same. Neglecting the wind effect in the simulation does not imply that wind forces and moments are non-existent. The boat forward speed will result in non-zero values of this effect.

Memory Effect : The parameter matrices $\mathbf{A}_k$ and $\mathbf{B}_k$ in equation (4) have been obtained by least square fits with $n = 4$ [1].

Propeller Revolution (r.p.m.) : The propeller is considered, primarily, to produce the axial thrust in the forward (surge) direction. However, the parasitic sway force and yaw moment due to the inherent hydrodynamic asymmetry in screw propellers, are also considered. The propeller revolution, r.p.m., is considered to proportionally change the propeller thrust and thereby is linked

with the ship speed.

Rudder Deflection (δ) : The rudder solely contributes to the directional control of the boat. It is deflected to restore the deviation of the course of the boat, as close as possible, to a zero mean value. The rudder deflection represents the human navigator and no rudder-autopilot is attempted in the present investigation.

Initial Conditions : The initial conditions of the dynamic system under consideration refer to the initial values of the position and orientation of the moving boat with respect to the inertial coordinate system. These variables have been designated by (x_o, y_o, ϕ, ψ) in the left hand side of equation (2). The conditions also include initial values of the perturbation velocities (u, v, p, r), which appear in the left hand side of equation (1). These initial values are essentially unknown and in the present investigation these have been set to zero under the consideration that broaching-to is a *transient* failure of ship/boat manoeuvrability through waves. This consideration stems from the systematic experimental observations [11], that the boat, while steadily moving on a straight course through calm water with *negligible* translatory as well as rotational displacements and velocities, broached when it was subjected to a *sudden* and *short* pulse of regular wave excitation.

PHENOMENOLOGICAL ANALYSIS

Conceptual understanding, often based on strong intuitions, precedes rigorous analytical or experimental exercises in the engineering analysis of a physical phenomenon. Based on this argument, an intuitive analysis of the observations on the broaching-to of ships in systematic experimental studies, has been done first in order to formulate a rational analytical method of investigation into this complicated phenomenon.

It is pertinent to recall that the mathematical model, which describes the ship/boat dynamics, has been formulated on the consideration that the ship/boat and the environment, together, form a dynamic system. Therefore, intuitive identification of the similarities between the salient features of broaching-to and the behavioural characteristics of nonlinear dynamic systems, forms the basis for the analytical investigation.

SALIENT FEATURES OF BROACHING-TO

Broaching-to, in reality as well as in the systematic experimental studies, has been identified by a large heading deviation of the ship/boat, with or without an associated large heel, despite any action from the helm, while traveling through following or quartering seas. Experimental observations on a radio-controlled free-running ship model in wind generated waves on an open water [11], revealed that broaching occurred when the model encountered, *successively*, a train of following or quartering waves. As each wave passed, the model was forced to yaw off the original heading to such an extent that the steering system was *unable to correct the heading in the time interval between the action of successive waves.* Thus it may be inferred that broaching-to takes place in a rather *short* span of time.

The phenomenological approach is based principally on the following three salient features of the broaching-to of ships, as revealed by the above mentioned experimental observations :

I. *Sudden* loss of ship manoeuvrability in waves;
II. *Large* heading deviation as a result of broaching-to; and
III. Occurrence of broaching-to in a *short* span of time.

INTUITIVE IDENTIFICATION

A phenomenological analysis of the *salient features* of broaching-to has resulted in intuitive identifications of these features with two most important behavioural characteristics of nonlinear systems as described below :

Bifurcation

The above mentioned salient features I and II implies that broaching-to may or may not lead to capsize but certainly results in a *noticeable* and *sudden* change of its state. The change of states referred to, are the changes in the orientations and motions of the ship/boat, in response

to some variations in environmental parameters, such as 'wave height' and 'relative wave heading'. This qualitative change of the state or the resulting motion of the ship/boat resembles the *bifurcation* phenomenon of nonlinear system. The bifurcation takes place at a threshold parametric value, when one or more of the system parameters is/are varied gradually [9], [16]. This similarity between 'broaching-to' and 'bifurcation' leads to the *intuitive* identification of broaching-to as a bifurcation phenomenon.

Transient failure/capsize

This mode of failure/capsize is typified by failure or collapse or capsize of a dynamic system during its *transient* motion which do not decay but grow without limit, as the system evolves. As a result, the steady state motion has not had a chance to develop. The above mentioned salient features II and III lead to the consideration that a ship/boat broaches and may also capsize subsequently, as a result of the development of a *large transient* motion. Therefore, in terms of *ultimate* safety, the emphasis of the analysis shifts to the study of the 'transient' behaviour of the nonlinear system under consideration, rather than analysing its steady states.

NONLINEAR DYNAMICS IN BROACHING

The intuitive identifications of broaching-to with *bifurcation* and *transient failure/capsize*, prompt the adoption of nonlinear system theory in *analytically validating* these identifications and subsequently in unveiling the underlying dynamics of the broaching-to phenomenon. Again, the intricacy of the mathematical model, which describes the ship motion, and the *embedded nonlinearities* in equations (7), (2) and (4), which are the principal constituents of the mathematical model, advocate against adoption of linearisation.

The Topological Concepts

Consider a moving ship/boat which is undergoing steady oscillatory motion around the prescribed course under the continuous and time variant excitation from waves and wind. From the topological perspective, this situation signifies that the boat's 'states', namely the translatory as well as the angular displacements and velocities, belong to a stable attractor, typically a 'chaotic' attractor [16], in the phase space. A *sudden* change of the ship/boat direction and/or course merely implies a *jump* of its motions from the original attractor, which represents the bounds of its current states (motions), to another stable attractor in the neighbourhood, corresponding to its new states. This jump indicates 'bifurcation' which may be *safe* or *dangerous*, depending on the severity of the jump. A bifurcation which results in a *recoverable* loss of the ship/boat directional stability is referred to as a 'safe' bifurcation. But a sudden and complete turn-around of the ship/boat heading, which is a characteristic feature of broaching, suggests a *dangerous* or *catastrophic* bifurcation from the primary stable attractor to another one, referred to in technical literature as *attractor at infinity* which is located far away from the original attractor.

THE MECHANISMS

The primary goal of this paper is to reveal the underlying dynamics of broaching-to. The following two sections discuss the revelation of the two principal constituents of this dynamics, namely the mechanism for the *inception* and the *occurrence* of broaching-to.

§1. The Inception

The concept

The intuitive identification of broaching-to as a bifurcation phenomenon suggests that a parametric analysis of the simulated motions should be done to validate the identification.

In real seas, a moving ship, acted upon by waves of frequently changing height, length and direction, will continuously change its course due to the variations in wave exciting force-couple. Analysis of such a problem by *simultaneously* considering the effect of variations of all of these parameters on motion responses, is perhaps an impossible task. A meaningful investigation can only be carried out by varying a chosen number (usually one or two) of parameters while keeping the rest fixed at some predetermined values.

The principal considerations are :

- Analysis in REGULAR waves
- TRANSIENT analysis
- PARAMETRIC analysis

Analysis in REGULAR waves : The occurrence of broaching-to in a relatively *short* span of time suggests that investigations into this phenomenon can be carried out effectively by scrutinising the 'yaw displacement', which quantifies the directional control of the boat, for a brief time period, during which it is unlikely that the wave characteristics will change noticeably. Thus the consideration of the excitations by a series of *regular* waves during the short duration of investigation is plausible. Again, systematic experimental investigations into the mechanism of broaching-to have been carried out mostly in *regular* waves in a manoeuvring tank [6], [10]. These are the possible justifications for the present investigation in regular waves.

TRANSIENT analysis : The salient features of broaching-to suggest that the boat is unlikely to lose its directional control and to subsequently broach once it has been stabilised, by the action of the rudder, in an oscillatory yaw motion with an almost *zero mean* heading deviation, if the amplitude or the frequency of the external excitations is not varied. This implies that attention should be focussed on the transient motion (response) which the boat has to overcome to arrive at a stable motion, if exists at all. In other words, broaching-to should be identified and analysed as a *transient* phenomenon.

PARAMETRIC Analysis : As indicated before, for systematic studies of this complicated phenomenon, the effects of each of the parameters on the motion responses are examined while the rest are kept to the prescribed values, e.g. only the wave amplitude, ζ_a , is varied while U, λ/L and μ are kept unchanged. Of these the ship speed, U, and the wave length ratio, λ/L , are easily perceived to have kept constant, as long as the helmsman does not change the ship speed voluntarily by varying the propeller r.p.m. and the wave length does not change appreciably within the relatively short duration of the investigation, respectively. However, the relative wave heading, μ, will vary continuously, even if the direction of wave propagation with respect to the earth-fixed (inertial) coordinate system is considered to be unchanged during the time span of the investigation, due to the deviation in boat's heading resulting from the wave action. This simplification has been adopted in the present analysis to segregate the parametric effects.

The methodology

Explanation of terms

ζ_a : the PRIMARY parameter – Nonlinear systems exhibit complicated dynamics when either the *amplitude* of the forcing function or the frequency of excitation is, or both are, varied [9], [16]. Amongst the parameters, U, μ, λ/L and ζ_a , it is ζ_a which has been considered to be directly proportional to the amplitude of the forcing function, while it does not alter the frequency of encounter, *i.e.* $|\mathbf{F}_S| = f(\zeta_a)$, but $\omega_e \neq f(\zeta_a)$. Thus the investigation begins with the wave amplitude, ζ_a , as the parameter.

ζ_a^{crit} : the CRITICAL wave amplitude – The parametric analysis calls for critical value(s) of the parameter(s) at which the qualitative change in the behaviour of the dynamic system takes place. In the present context, the critical value is the critical wave amplitude, ζ_a^{crit} .

δ_{ideal}: the STEADY rudder deflection – A new concept of an equivalent *steady* rudder deflection is introduced. A time-varying rudder deflection is usually necessary in practice to keep the boat within acceptable deviation of the heading, during its manoeuvre through waves. It is observed from trial runs of the simulation algorithm that the rudder deflection stabilises at some nearly steady value after the decay of the transients. Consequently, in the following analysis, the unsteady rudder deflection is replaced by a constant deflection from the beginning of the investigation under the presumption that the deviation in the boat's heading can be corrected, where possible, by some *time-invariant* rudder deflection during the evolution, to a steady oscillatory yaw motion

around a zero mean heading deviation, or *not at all.*

The *steady* rudder deflection has been obtained by several trials with the prediction algorithm and is termed as 'δ_{ideal}' for future references. Admittedly, this is possible only during numerical exercises. 'δ_{ideal}' has been obtained to stabilise the boat as close as possible to a zero mean heading error, in the shortest possible duration.

ψ_{broach} : the BROACHING angle – The limit of the heading error, defined as 'ψ_{broach}', beyond which the boat is considered to have broached, is a subjective decision and depends on the judgement of the investigator. In the present analysis, this limit has been chosen as 45° towards either port or starboard, *i.e.* $|\psi_{broach}| = 45°$ (Renilson [12] took this limit as 40°). However the simulation has been performed for the time span which corresponds to 35–40 forcing cycles, irrespective of whether the resulting yaw angle, ψ, at any instant of time, exceeds 45° towards port or starboard, *i.e.* $|\psi| > |\psi_{broach}|$, or not.

ψ^{peak}_{trans} : the PEAK TRANSIENT yaw angle – This concept has been introduced in order to identify the occurrence of broaching-to. Fig. 2 shows the time domain simulation of the yaw response, for $U = 7$ knots, $\lambda/L = 3.0$, $\mu = 60°$ and $\zeta_a = 0.7$ metre. The transient negative yaw displacement, ψ, indicates a heading deviation towards the port-side for quartering waves approaching from the port-side. The 'peak' value of this transient heading deviation is defined as 'ψ^{peak}_{trans}' for the future reference.

Time domain simulations: Time domain simulation results are presented in the following forms:

- Time series results – This form gives the instantaneous roll and yaw displacements of the boat in the evolution process. *Occurrence* of broaching-to is identified from the result of the yaw displacement, when $|\psi^{peak}_{trans}|$ exceeds $|\psi_{broach}|(\equiv 45°)$.
- State plane diagrams – This form summarises the boat motions in the state plane by presenting the time series result of yaw-roll displacements, as *motion trajectories.*

Fig. 2 exemplifies the above mentioned forms.

Procedure

i. Simulation is first carried out with a slower ship speed of $U = 7$ knots, corresponding to a low Froude number, F_n, of 0.268, a longer ($\lambda/L = 3.0$) and smaller ($\zeta_a = 0.5$ metre) wave, resulting in a ratio of wave height to wave length, $2\zeta_a/\lambda$, of 0.018, a larger relative wave heading ($\mu = 60°$) as compared to the experiments performed by Motora et al. [10] with a similar hull form in the range of $0.4 \leq F_n \leq 0.7$, $0° \leq \mu \leq 45°$, $1.25 \leq \lambda/L \leq 3.0$ and $0.02 \leq (2\zeta_a/\lambda) \leq 0.067$, to ensure that the boat's directional stability can be restored, after the decay of the initial transient, by a suitable time-invariant rudder deflection, δ_{ideal}.

ii. The wave amplitude, ζ_a, which has been chosen as the primary parameter, is increased slowly, while keeping other parameters, namely U, λ/L, and μ unchanged.

iii. Observe the occurrence of broaching-to from the time series results of yaw displacements, *i.e.* if $|\psi^{peak}_{trans}|$ exceeds $|\psi_{broach}|$ during its transient motion, as ζ_a is increased.

iv. Observe the change in the size of the chaotic attractor in the state plane diagram, as ζ_a is increased.

The mechanism

The evolution of a new mechanism for the inception of broaching-to has been typified in a step-by-step manner by 'case studies'. Each case-study has been illustrated by displaying the time domain simulation result and by categorically listing the pertinent *observations* and their *implications.* Finally, a summary of the observations and the inferences are given.

The Case Studies

Various case studies have been performed following the procedure described above. Repeated time domain simulations of the boat responses are performed for various combinations of the

parametric values, $U = 7.0$ knots , $\lambda/L = 3.0$, $0.5\ \text{m} \leq \zeta_a \leq 1.4$ m, and $60° \geq \mu \geq 10°$. Only the cases, pertinent to the understanding of the mechanism, are presented.

CASE I : $\mu = 60°$

Figures 2–4 exemplifies the time domain simulation results of roll and yaw displacements for the case study with $\zeta_a = 0.7$m, 1.1m and 1.4m, respectively. Examinations of these figures reveal the following observations on each simulation result.

Case I-1 : Fig. 2, for $\zeta_a = 0.7$ m

The observations

i. The yaw displacement of the boat settles to a steady oscillation after a transient motion.

ii. The absolute value of the 'peak transient yaw displacement' $|\psi^{peak}_{trans}|$ has not exceeded the 'broaching angle', ψ_{broach} ($\equiv$ 45°), and therefore, the boat is considered to have recovered its direction. The transient motions eventually decay to a steady oscillation around the zero mean value.

iii. The yaw-roll state plane diagram depicts that the trajectory has no apparent repeatability, or in other words, 'chaotic'. The space enclosed by this trajectory is the *chaotic attractor* for the transient motion.

Case I-2 : Fig. 3, for $\zeta_a = 1.1$ m

The observations

i. The observations (i) – (iii) of Case I-1 also apply to this case.

ii. $|\psi^{peak}_{trans}|$ has a value greater than that in Case I-1.

iii. The chaotic attractor in yaw-roll state plane increased in size or *expanded* as ζ_a is increased from Case I-1.

iv. δ_{ideal} has increased from that in Case I-1.

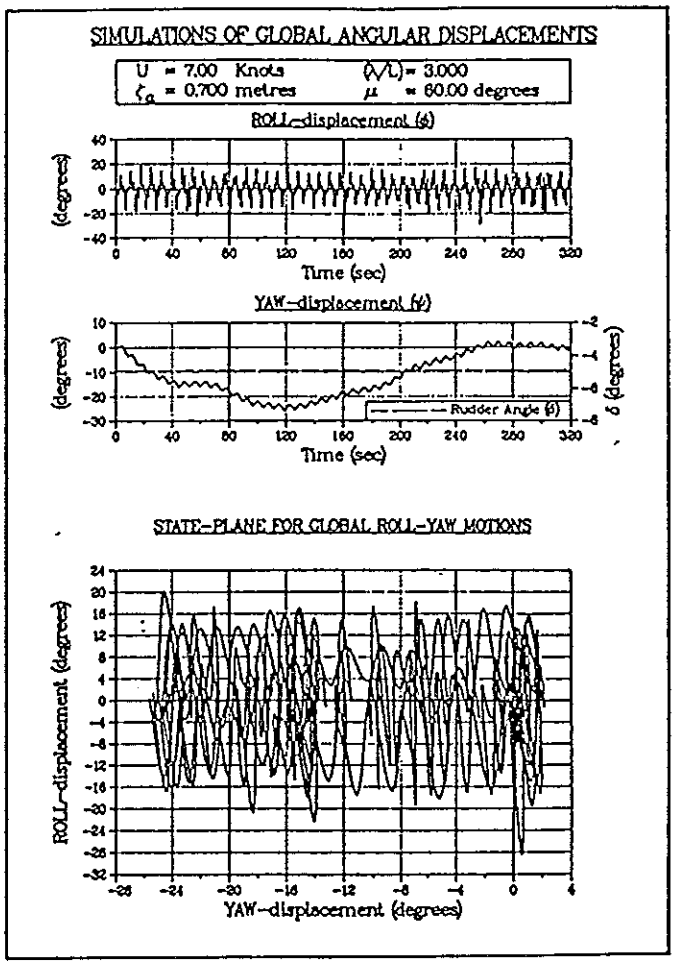

Figure 2: *Yaw and Roll displacements for U=7 knots, λ/L =3.0, ζ_a =0.7 m, $\mu = 60°$.*

Case I-3 : Fig. 4, for $\zeta_a = 1.4$ m

The observations

i. The time series result of yaw displacement shows that after the transient yaw motion, the boat's heading has been recovered by a suitable rudder deflection ($\delta_{ideal} \approx 14°$), in the same manner as shown in Cases I-1 and I-2. But in this case, the boat has been *considered to have broached* since $|\psi^{peak}_{trans}|$ has exceeded $|\psi_{broach}|$ during its transient motion.

ii. The size of the attractor has increased further from that in Case I-2.

iii. δ_{ideal} has further increased from that in Case I-2.

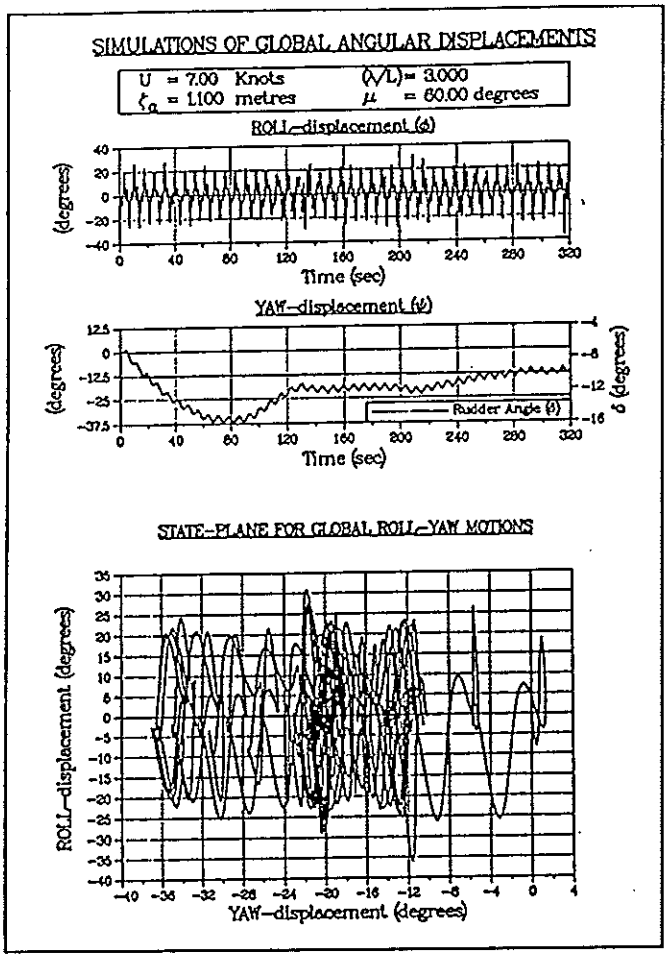

Figure 3: *Yaw and Roll displacements for U=7 knots, λ/L =3.0, ζ_a =1.1 m, $\mu = 60°$.*

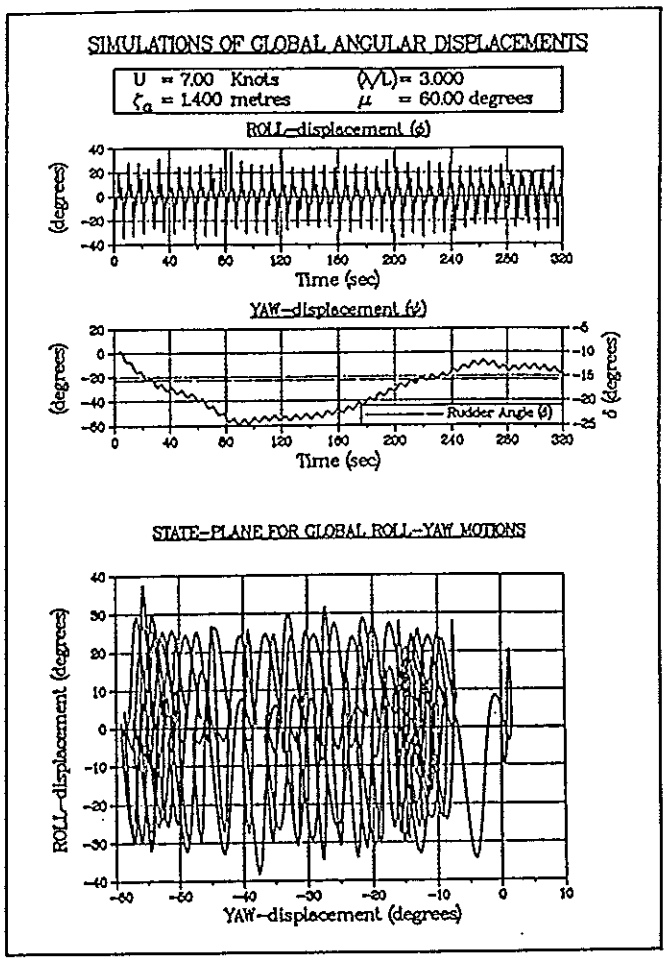

Figure 4: *Yaw and Roll displacements for U=7 knots, λ/L =3.0, ζ_a =1.4 m, $\mu = 60°$.*

Case I : the implications

i. Broaching-to occurred during the transient motion of the boat, *i.e.* it is a *transient loss* of boat manoeuvrability in waves.
ii. From topological perspective, broaching-to is related to the *expansion* of the chaotic attractor observed in the yaw-roll state plane.
iii. The expansion of the attractor is *gradual* with respect to the increase in ζ_a .
iv. The implication (iii) above signifies that the ζ_a^{crit} appears *gradually.*

CASE II : $\mu = 40°$

Figures 5–8 display the time domain simulation results for ζ_a = 0.5, 0.7, 0.9 and 1.0 metre.

Case II-1 : Fig. 5 for ζ_a = 0.5 m

The observations

i. The general characteristics of the observations for Case I-1 apply qualitatively.

Case II-2 : Fig. 6 for ζ_a = 0.7 m

The observations

i. The general characteristics of the observations for Case I-2 apply qualitatively, when compared with Case II-1.

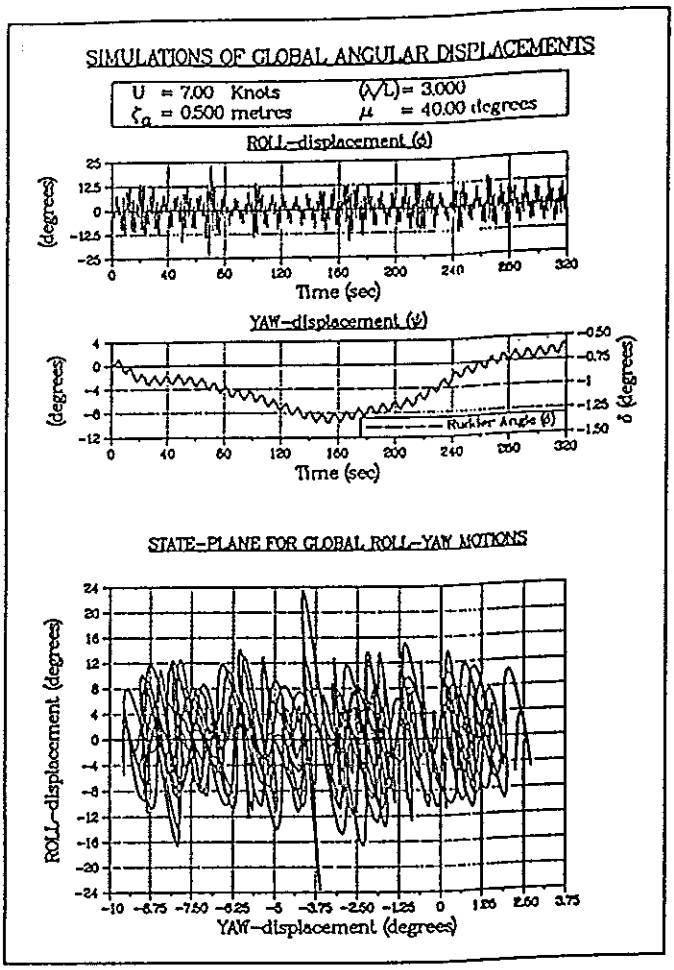

Figure 5: *Yaw and Roll displacements for U=7 knots, λ/L =3.0, ζ_a =0.5 m, $\mu = 40°$.*

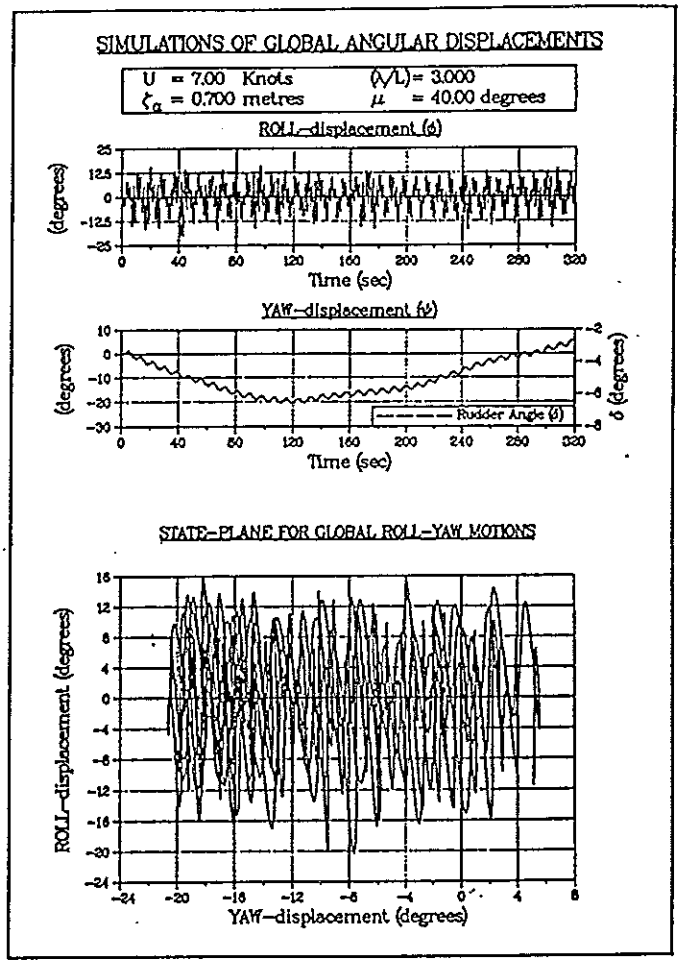

Figure 6: *Yaw and Roll displacements for U=7 knots, λ/L =3.0, ζ_a =0.7 m, $\mu = 40°$.*

Case II-3 : Fig. 7 for $\zeta_a = 0.9$ m

The observations

i. Observations (i) and (ii) of Case I-1 are valid.

ii. The size of the chaotic attractor, when compared to that of Case II-2, has *reduced* even though the wave amplitude, ζ_a , is increased from 0.7 metre to 0.9 metre, *i.e.* despite increase in ζ_a , the attractor has *shrunk*.

Case II-4 : Fig. 8 for $\zeta_a = 1.0$ m

The observations

i. The boat has *broached* during its transient motion as explained in observation (i) of Case I-3.

ii. The attractor, after shrinking in Case II-3, has again *expanded* due to the increase in ζ_a from 0.9 metre to 1.0 metre.

iii. Due to the *shrinking* of the attractor in Case II-3, the 'expansion' in this case takes the form of a *jump* in size, unlike the *continuous* and *gradual* increase as in Case I, for broaching to occur. This is apparent when the state plane diagrams in Figures 7 and 8 are compared.

iv. Due to (iii) above, ζ_a^{crit} appears more *rapidly* than in Case I (implication (iv)).

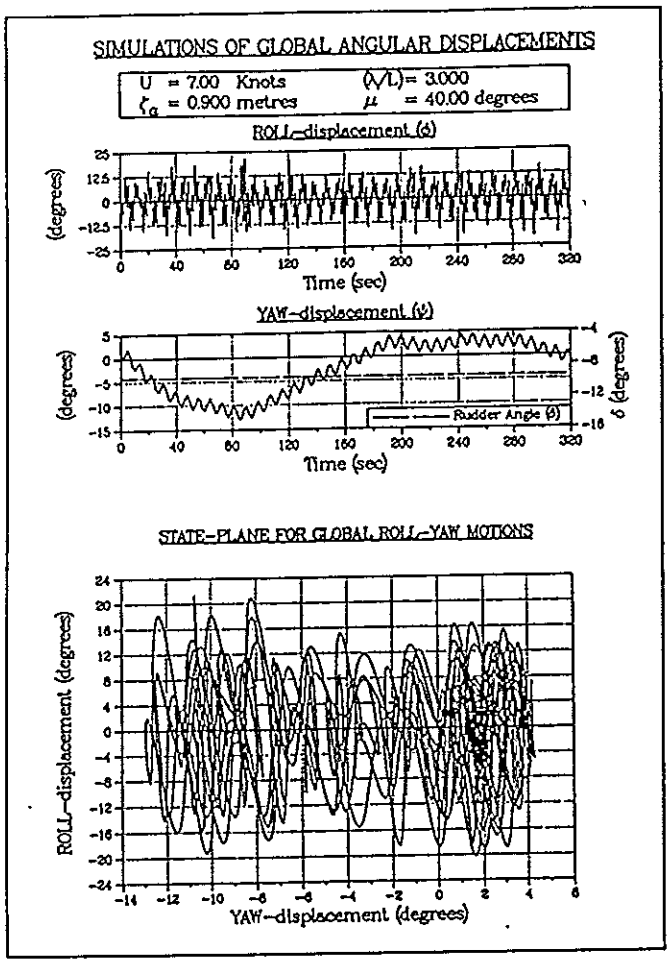

Figure 7: *Yaw and Roll displacements for U=7 knots, λ/L =3.0, ζ_a =0.9 m, $\mu = 40°$.*

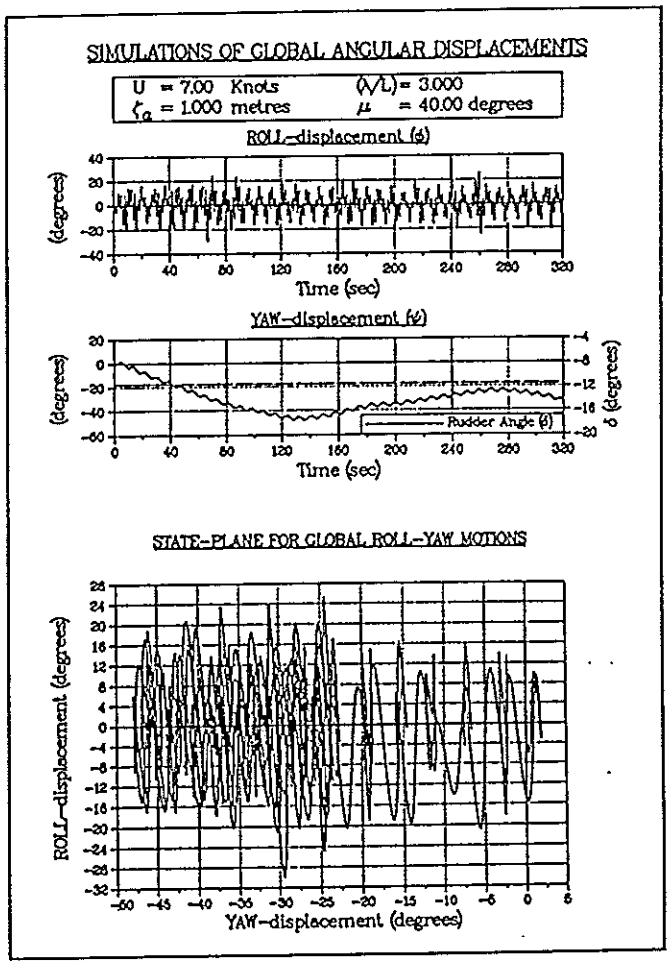

Figure 8: *Yaw and Roll displacements for U=7 knots, λ/L =3.0, ζ_a =1.0 m, $\mu = 40°$.*

Case II : the implications

i. The implications (i) and (ii) of Case I are also valid in Case II.

ii. The *rapid* appearance of ζ_a^{crit} in observation (iv) of Case II-4 results in a *sensitivity* of boat's yaw response to the change in ζ_a for values near ζ_a^{crit} .

iii. The 'jump' in size of the attractor with the increase of the parameter ζ_a , as revealed in observation (iii) of Case II-4, signifies a *bifurcation* of chaotic attractor in the topological concept [17]. This 'jump' or 'bifurcation' has been observed to have linkage with the inception of broaching-to in Case II-4.

iv. The 'bifurcation' phenomenon and the 'linkage', stated in (iii) above, *identifies the inception of broaching-to as a bifurcation phenomenon.*

CASE III : $\mu = 20°$

Figures 9–13 display the time domain simulation results for this case for ζ_a = 0.5, 0.7, 0.8, 0.84 and 0.85 metre.

Case III-1 : Fig. 9 for ζ_a = 0.5 m,
Case III-2 : Fig. 10 for ζ_a = 0.7 m,
Case III-3 : Fig. 11 for ζ_a = 0.8 m,
Case III-4 : Fig. 12 for ζ_a = 0.84 m

The observations

i. The general characteristics of the observa-

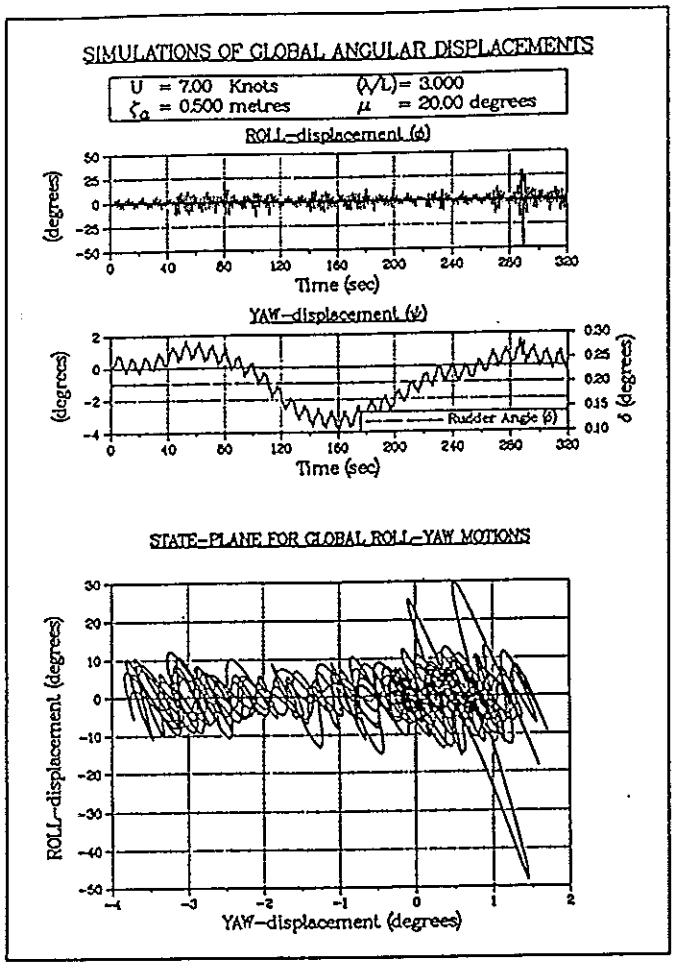

Figure 9: *Yaw and Roll displacements for U=7 knots, λ/L =3.0, ζ_a =0.5 m, $\mu = 20°$.*

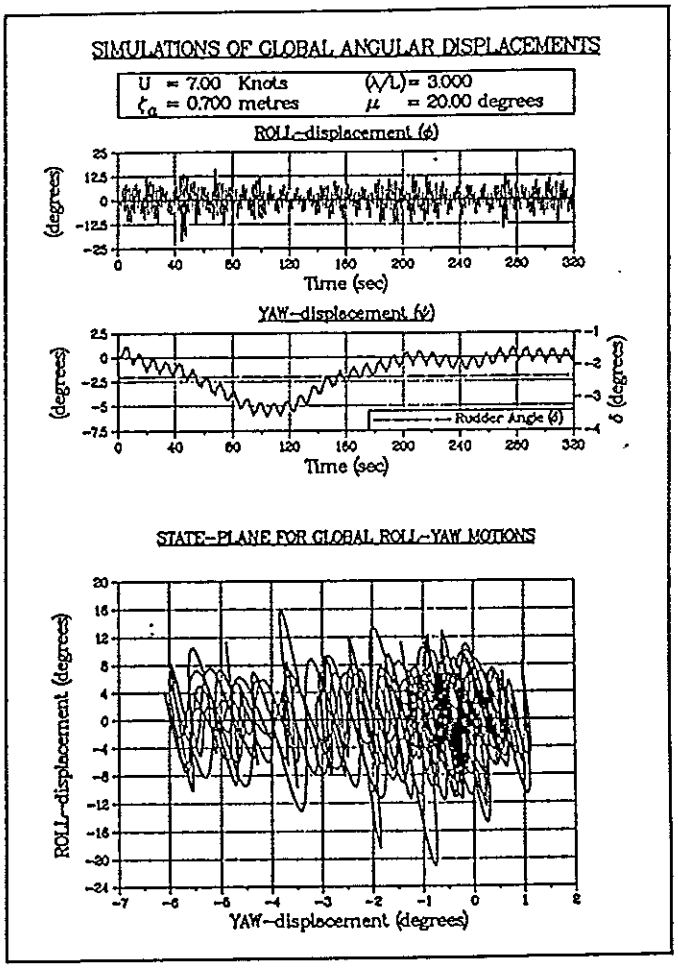

Figure 10: *Yaw and Roll displacements for U=7 knots, λ/L =3.0, ζ_a =0.7 m, $\mu = 20°$.*

tions for Case II apply qualitatively.

ii. The 'contraction' of the attractor, similar to observation (iii) in Case II-3, can be seen by comparing Fig. 12 for Case III-4 with Fig. 11 for Case III-3.

Case III-5 : Fig. 13 for ζ_a = 0.85 m

The observations

i. The general characteristics of the observations for Case II-4 apply.

ii. The 'jump' in size mentioned in observation (iii) of Case II-4 takes the form of an *explosion* in the present case, when the wave amplitude ζ_a is increased from 0.84 metre in Case III-4 to 0.85 metre. This observation is evident when Figures 12 and 13 are compared.

iii. Because of the 'explosion' in (ii) above, broaching-to occurs at almost a *threshold* value of ζ_a , *i.e.* the appearance of ζ_a^{crit} is *instantaneous.*

Case III : the implications

i. The implications of Case II are valid in this case.

ii. The 'sensitivity' mentioned in implication (ii) of Case II *intensifies* as a result of the 'explosion' referred to in observation (ii) of Case III-5.

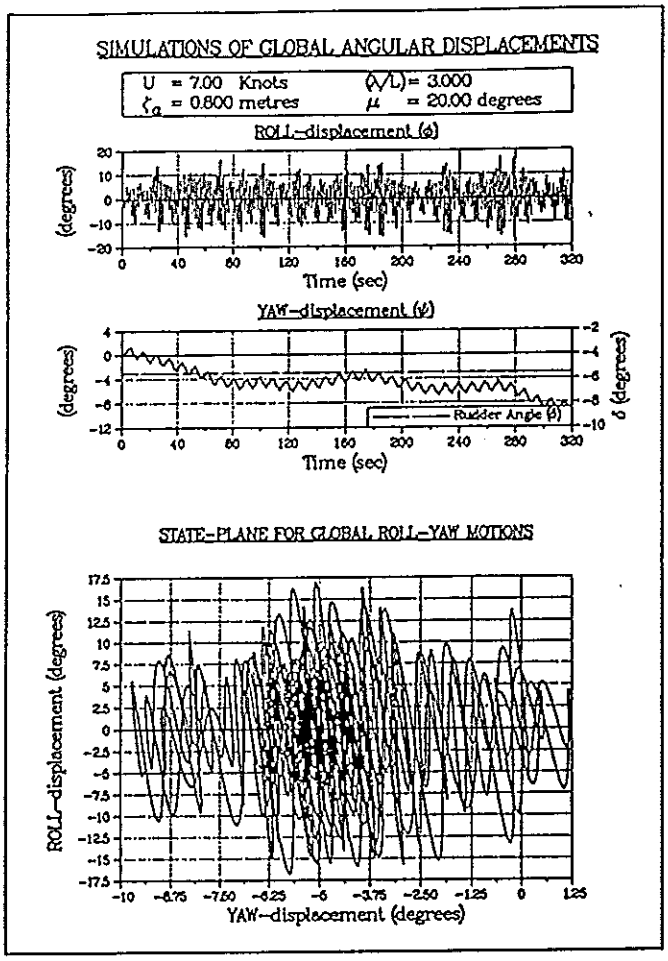

Figure 11: *Yaw and Roll displacements for U=7 knots, λ/L =3.0, ζ_a =0.8 m, $\mu = 20°$.*

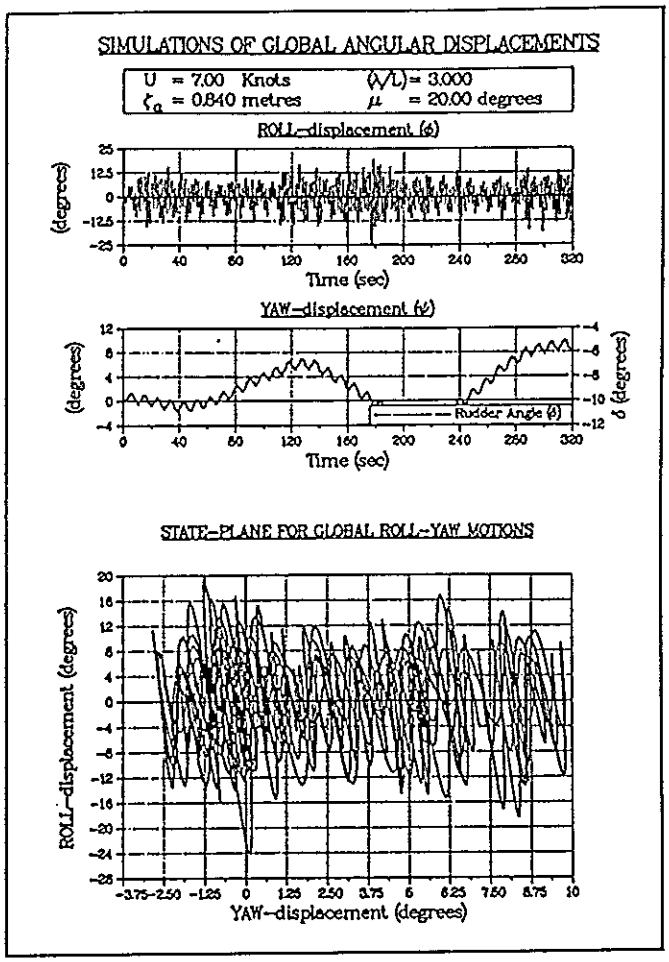

Figure 12: *Yaw and Roll displacements for U=7 knots, λ/L =3.0, ζ_a =0.84 m, $\mu = 20°$.*

THE SUMMARY

The observations

i. Broaching of the boat occurred during the transient motion in all cases.

ii. The *gradual* expansion of the chaotic attractor in the state plane, for a *larger* relative wave heading, *i.e.* $\mu = 60°$ and $50°$, as ζ_a is slowly increased.

iii. For $\mu \leq 40°$, the attractor expands, then *shrinks*, followed by a *rapid* expansion prior to broaching, as ζ_a is slowly increased.

iv. The above mentioned rapid expansion takes the form of a *jump* in size or *explosion* for smaller relative wave headings, $\mu \leq 20°$.

The inferences

i. The change in the states of the boat is reflected topologically by the variations in the size of the attractor as stated in the observations. This variation is identified as a 'bifurcation' phenomenon of a nonlinear dynamic system [16].

ii. As a natural consequence of the identification in (i) above, the inception of broaching-to has been attributed to the bifurcation of chaotic attractor, observed in the yaw-roll state plane in the form of a gradual or a rapid expansions, or an explosion of the attractor.

iii. The intuitive identification is validated in

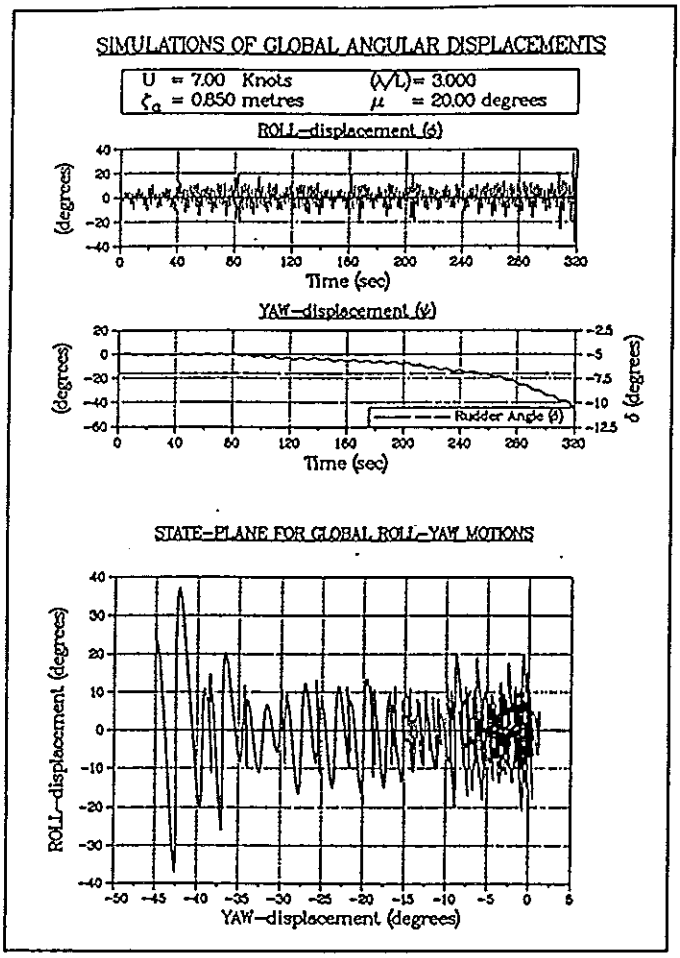

Figure 13: *Yaw and Roll displacements for U=7 knots, λ/L =3.0, ζ_a =0.85 m, $\mu = 20°$.*

(ii) above.

iv. The *gradual* expansion for $\mu = 60°$ in observation (ii) refers to the 'safe' bifurcation.

v. The 'explosion' in observation (iv) for $\mu \leq 20°$ indicates a 'dangerous' or 'catastrophic' bifurcation. The explosion was first identified by Ueda [17] and has been categorised as *interior catastrophe* by Thompson and Stewart [16].

vi. The appearance of ζ_a^{crit} for $\mu > 40°$ is gradual, but the explosion for $\mu \leq 20°$ causes ζ_a^{crit} to appear very suddenly. This results in an acute sensitivity of boat's response to parametric changes.

§2. THE OCCURANCE

The mechanism for the inception of broaching-to has been revealed by specific case studies as exemplified in §1. The case studies consist of analyses of the time domain simulation results for fixed values of ship speed, $U = 7$ knots, and wave length, $\lambda/L = 3.0$. In other words, a local analyses in the parameter space of U, λ, μ, ζ_a and δ, have been performed. To obtain a global understanding of the underlying dynamics of broaching-to, such local analyses have to be repeated for the entire parameter range. In the present context, this implies that the investigation into broaching-to, through *repeated* time domain simulation, need to be performed for different values of U and λ/L .

The concept

Principal considerations

- BROACHING ZONE diagrams
- ANALYSIS of the broaching zone diagrams

Broaching zone diagrams :

The need : It is apparent from the statements given above, that :

i. Numerous tedious trial runs of the simulation algorithm have to be carried out with various choices of the rudder deflection 'δ', in order to determine δ_{ideal}. Each of these runs has to be performed with a set of U, λ/L , μ, and ζ_a , as evident from above.

ii. The repeated time domain simulation results should be summarised in a form amicable to the intended global analysis in the total parameter space.

Elimination of the trial runs in (i) above, and the summary, mentioned in (ii), have been achieved by a unique presentation of the time domain simulation results in the form of *safe and unsafe* broaching zones in the system parameter space. The said presentation has been typified in Fig. 14.

The formation : The development of 'broaching zone diagrams' pivots around the concept that the boat would broach within the action of a certain number of forcing cycles, hereinafter termed as 'n_f ', or would not broach at all. This presumption thrives on the viewpoint that broaching-to is a 'transient' phenomenon. The consideration is that once the boat attains a *steady oscillation*, it would *not broach thereafter* under the action of the *same* external excitation. The number of forcing cycle, n_f , has been optimally chosen as 20, as some trial calculations with $n_f > 20$ have not indicated appreciable differences in the results. The time period ($\equiv T_f$) of the forcing cycle is calculated as $T_f = 2\pi/\omega_e$, where ω_e is the frequency of encounter. Thus the maximum time span, for which the boat's responses are simulated, equals to ($n_f \times T_f$).

Analysis of the diagrams

The procedure followed to unveil the mechanism of broaching-to consists of :

i. Examination of the *characteristic features* of the safe zone; and

ii. Parametric analysis of the *behavioural pattern* of the safe zone.

As a result of this analysis, a global understanding of the effects of various parametric combinations on the occurrence of broaching-to, has been obtained. This understanding leads to the conceptualisation of a new mechanism of broaching-to. Similar method of analysis has been successfully adopted in the field of nonlinear dynamics, and recently in the transient analysis of ship capsize in roll motion [4], [7], [15].

The methodology

A topological approach has been adopted to unravel the mechanism of broaching-to.

Safe and unsafe broaching zone diagrams

The broaching zone diagrams uniquely summarise the *fate*† of the boat during the transient motion under investigation, from the perspective of broaching-to. These diagrams, as displayed in Fig. 14, are the principal tool for the present investigation. Therefore, a brief discussion on their formation follows.

Formation of each figure

Individual plot : Although n_f has been chosen as 20, for the sake of clarity, the fate of the boat is noted and indicated in each plot for the lower values of n_f = 16, 12 and 8. The symbols '•', '+', '×', 'o' and '△' refer to the combinations of ζ_a and μ for which the simulation algorithm has predicted $|\psi^{peak}_{trans}| < |\psi_{broach}|$, with the *arbitrarily chosen* steady rudder deflection. In other words, each of these symbols, where exists, indicates that the chosen helm would directionally stabilise the boat in regular waves, which is described by the corresponding values of ζ_a and μ, for $n_f > 20$, $16 \leq n_f \leq 20$, $12 \leq n_f \leq 16$, $8 \leq n_f \leq 12$ and $n_f < 8$, respectively. Therefore, in the present study, *cluster* of '•' symbols, corresponding to $n_f = 20$, is considered to represent the *safe* zone in the μ - ζ_a plane, as far as the loss of ship manoeuvring through wave is concerned.

Each figure : Each figure is composed of several plots, described above, for a wide range of rudder deflections, e.g. $-20° \leq \delta \leq 10°$ in Fig. 14. The range of the rudder angle has been chosen on the basis of some trial calculations which showed that a helm in this range could directionally stabilise the boat under the wave action, if possible.

Formation of broaching zone diagrams

The broaching zone diagrams are prepared by a collection of figures, described above. The diagrams cover a range of ship speed, 8 knots $\leq U \leq$ 12 knots, and a range of wave lengths, $1.5 \leq \lambda/L \leq 3.0$. The selections of these ranges are based, respectively, on the designated service speed of the boat and on the fact that broaching-to has been observed to occur when a ship/boat encounters quartering or following waves of length in this range. The maximum value of U = 12 knots has been limited by the

†In the present context, the word 'fate' is used to indicate whether the boat maintained or lost its directional control during the period of simulation.

availability of tank test results for the total hull resistance [8].

The Mechanism

A new understanding of the occurrence of broaching-to is presented by case studies, as before.

The Case Studies

The ranges of the parameter values considered are, 8 knots$\leq U \leq$ 12 knots, $3.0 \geq \lambda/L \geq 1.5$, 0.4 m$\leq \zeta_a \leq$ 1.2 m, and $0° \leq \mu \leq 60°$.

Only the cases, pertinent to the revelation of the mechanism, are displayed in Figures 14–18.

Case I : U=8 knots, λ/L =3.0, Fig. 14

This case study forms the basis of the present investigation. It furnishes the basic features of the safe zone for the parametric combinations which give rise to the *least* likelihood of broaching-to. The subsequent case studies will be examined in comparison with this study.

The observations[‡] :

a. The safe zone does not exist for all values of the rudder deflection, $-20° \leq \delta \leq 10°$.

b. The existence of the safe zone spans *more* over *starboard* rudder than *port* rudder.

c. The boundary of the safe zone, where exists, is non-smooth or *fractal.*

d. As the rudder deflection is varied from starboard ($\delta = -20°$) to port ($\delta = 10°$), the safe zone emerges from the higher ζ_a side, moves towards the lower ζ_a side, and finally vanishes from the μ - ζ_a window, leaving a few *sparsely* located safe points for $\delta \geq 10°$. The terminology 'V_{safe} ' is used to quantify this movement for future comparisons.

e. The 'sparse' points in (d) above remain *stationary* with respect to the change in helm, $\delta \geq 10°$.

The implications*

A. The Obs(I-a) is easily comprehensible from the fact that larger rudder deflections to port ($\delta \geq 10°$) or starboard ($\delta = -20°$) will result in a ψ_{trans}^{peak} which exceeds ψ_{broach} within the stipulated time span and the boat loses its directional control. This loss is interpreted as a *voluntary* action by the helmsman.

B. Obs(I-b) implies that a starboard rudder is necessary to counteract the excitations from an incoming wave from port side ($0° \leq \mu \leq 60°$).

C. The *fractal* boundary in Obs(I-c) signifies uncertainties in the boat's response to the change in ζ_a or μ in the vicinity of the boundary. This uncertainty is conceived from the obvious *risk* that a small departure in μ or ζ_a would put the boat in the unsafe zone.

D. The implication of Obs(I-c) will be dealt with later.

Case II : U=9 knots, λ/L =3.0, Fig. 15

This case study reveals the effect of the *increase* in forward speed U when compared with Case I.

The observations

a. The Obs(I-a)–Obs(I-c) are valid equally well in this case.

b. In comparison with Case I, the safe zones exist over a *lesser* range of rudder deflection. In Case I, the safe zone *prominently* exists for $-15° \leq \delta \leq 5°$, but in this case, the range of the rudder angle reduces to $-10° \leq \delta \leq 5°$.

[‡]The observation (a) below will be referred to in the text as "Obs(I-a)". Similar referrals will be made for the observations in other cases.

*The implication (A) below will be referred to in the text as "Imp(I-A)". Similar referrals will be made for the implications in other cases.

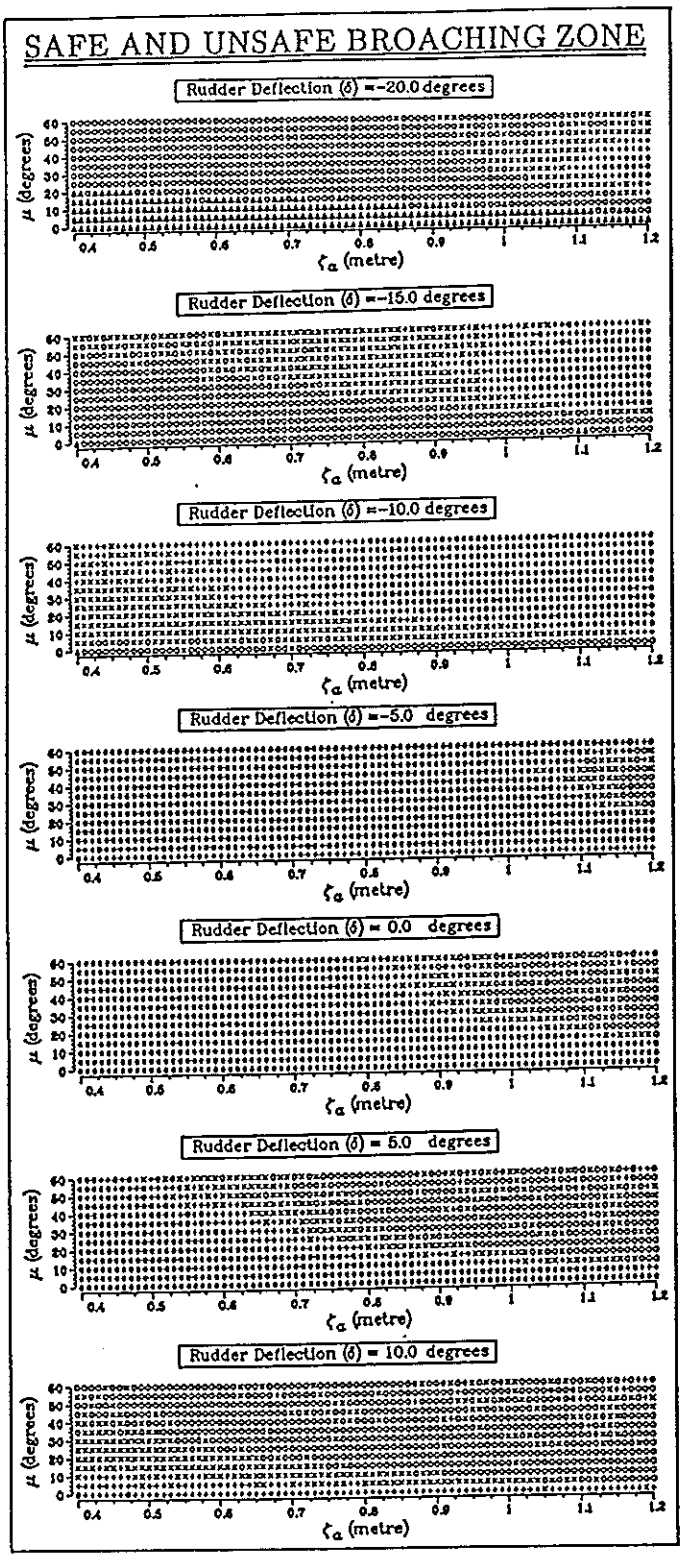

Figure 14: *Safe('•') and unsafe broaching-zones in control space without wind effect for $U = 8$ kn., $\lambda/L = 3.00$ and $\delta = -20°$ to $10°$*

c. The number of the scattered safe points, mentioned in Obs(I-d), has increased in this case, as a result of the increase in the boat speed.

d. The 'stationary' characteristics of the sparse points, as in Obs(I-e) is also observed in this case.

The implications

A. Obs(II-a) suggests that Imp(I-A)–Imp(I-D) apply equally well in this case.

B. Obs(II-b) indicates that the rudder deflection, which can avoid the loss of directional stability in this case, spans over a *narrower* range due to the increase in the boat speed. Alternatively stated, V_{safe} of Obs(I-d) *increases* for higher boat speed. From the point of view of the helmsman, this signifies that a unit (1° in the case study) rudder deflection will result *more* change in heading deviation in this case of higher boat speed. In other words, the boat's yaw response has become *sensitive* to the rudder deflection at this higher speed.

C. Obs(II-c) implies that the 'uncertainties', mentioned in Imp(I-D), increases when the boat travels faster.

CASE III : U=10 knots, λ/L =3.0, Fig. 16

This case study confirms the effect of increasing the boat speed onto the yaw response of the boat, as detailed in Imp(II-B) and Imp(II-C). It also introduces a new phenomenon of *rudder ineffectiveness.*

The observations

a. Obs(II-a) is also valid in this case.

b. The 'span' of the rudder angle, discussed in Obs(II-b), is reduced *further* in this case to $-5° \leq \delta \leq 5°$.

c. The 'sparse' safe points have increased in number and are tending to *cluster* together for $5° \leq \delta \leq 10°$.

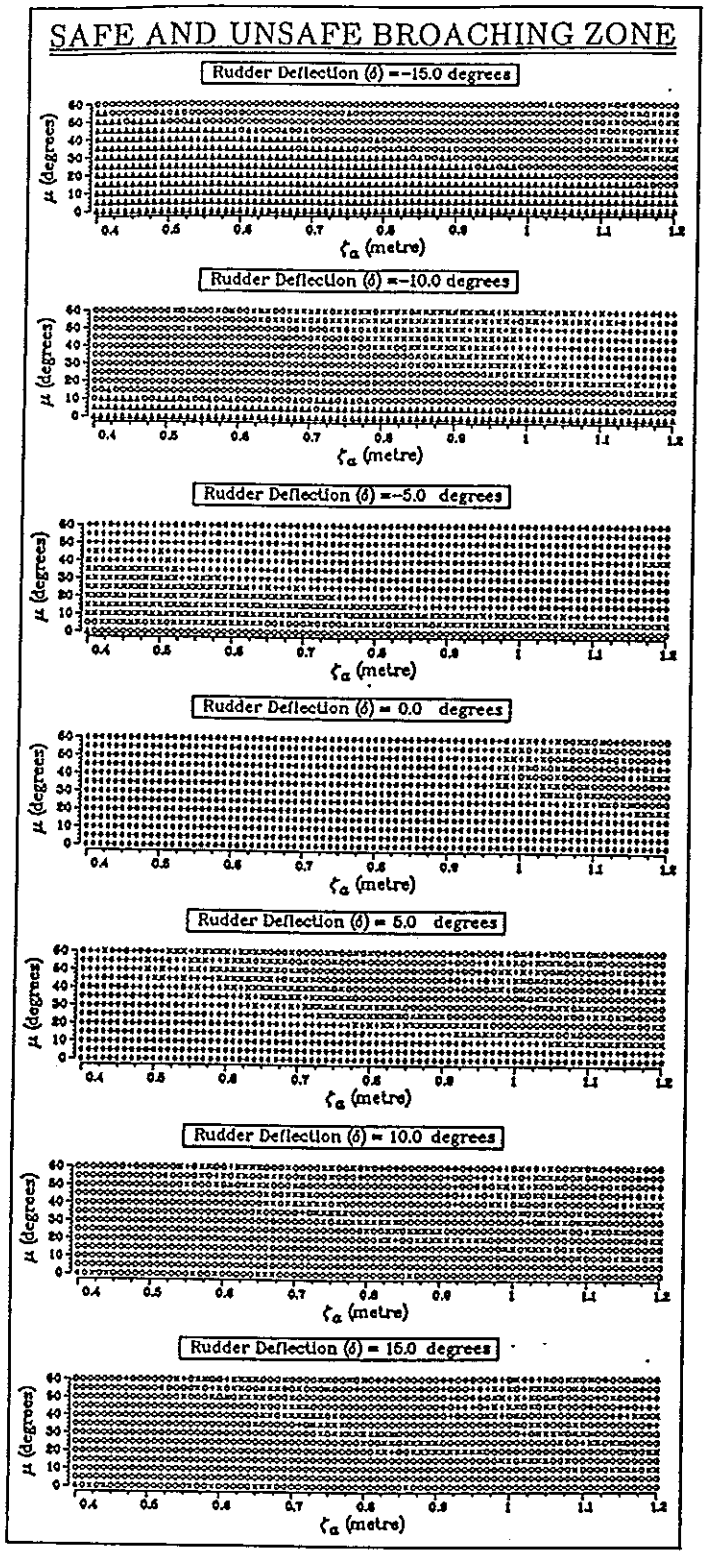

Figure 15: *Safe('•') and unsafe broaching-zones in control space without wind effect for $U = 9$ kn., $\lambda/L = 3.00$ and $\delta = -15°$ to $15°$*

d. The distribution of the *nearly clustered* safe points remain unchanged and stationary in the μ - ζ_a plane, with respect to the variation of rudder angle, in the range $5° \leq \delta \leq 10°$.

The implications

A. Obs(III-a) establishes that Imp(I-A) – Imp(I-D) are also valid in this case.

B. Obs(III-b) indicates that V_{safe} has increased and correspondingly the sensitivity, as explained in Imp(II-B), has intensified due to further increase of boat speed from 9 knots to 10 knots.

C. Obs(III-c) indicates crystallisation of the sparse points to form a *secondary* safe zone. The safe zone, which has been discussed so far, will be referred to as *primary* zone to distinguish it from the secondary zone.

D. Obs(III-d) suggests an *insensitivity* of the secondary zone to the rudder deflection. This implication signals an inception of a *rudder ineffectiveness* on the heading correction of the boat.

CASE IV : U=11 knots, λ/L =3.0, Fig. 17 & 18

This case study primarily corroborates the formation of the 'secondary zone' and the 'rudder ineffectiveness' mentioned in Imp(III-C) and Imp(III-D), respectively.

The observations

a. Obs(II-a) holds equally well in this case.

b. The secondary zone, as introduced in Imp(III-C), prominently exists for $\delta \geq 5°$ in Fig. 17 which may falsely suggest that the secondary zones, as appears in the plots for $\delta \geq 5°$, have been *annexed* to the primary safe zone of the plot for $\delta = 0°$. Fig. 18, which enlarges Fig. 17 for $0° \leq \delta \leq 5°$ with $\Delta\ \delta = 1°$, clarifies the following characteristics in this case :

(i) Both the primary and the secondary zones exist.

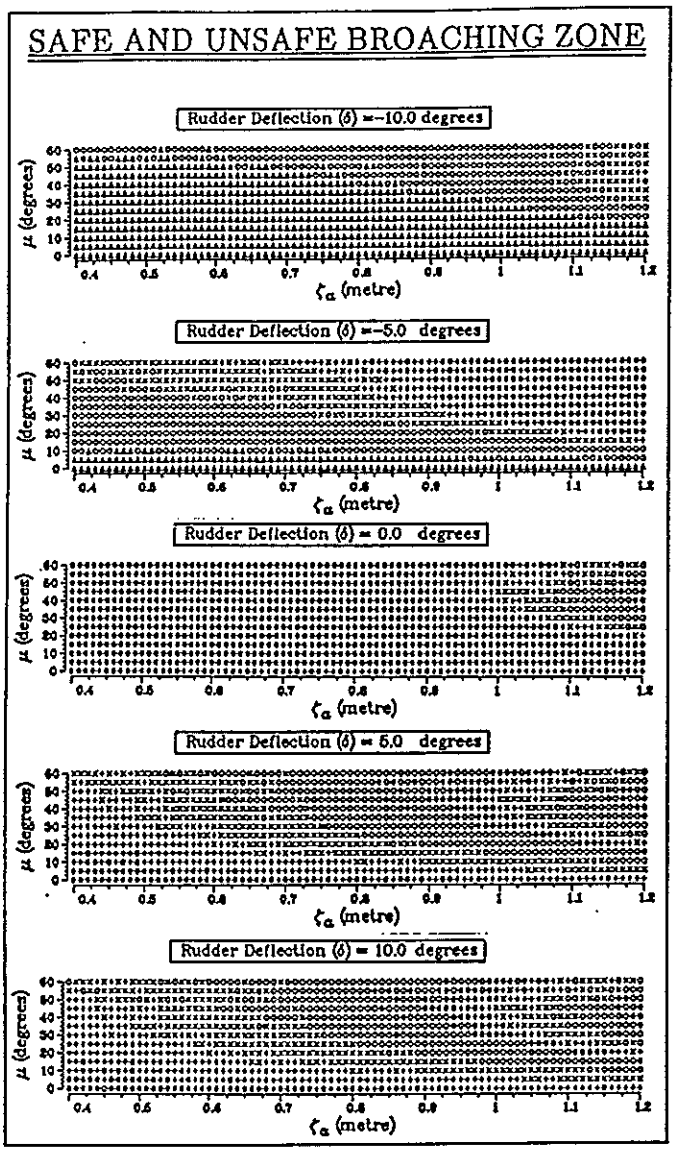

Figure 16: *Safe('•') and unsafe broaching-zones in control space without wind effect for $U = 10$ kn., $\lambda/L = 3.00$ and $\delta = -10°$ to $10°$*

(ii) The *movement* of the 'primary' zone, as noted in Obs(I-d), exists.

(iii) The *gradual emergence* of the 'secondary' zone in the μ - ζ_a window, as the rudder deflection is varied.

(iv) The secondary zone is not *annexed* to the primary zone. It is a *separate* entity.

(v) The span of the rudder angle, first mentioned in Obs(II-b), is reduced further form Case III, to $-5° \leq \delta \leq 3°$, indicating *increased* V_{safe} .

c. The secondary zone prominently exists for $\delta > 5°$ and remains stationary in the μ - ζ_a plane with respect to the variation of the rudder angle.

The implications

A. Obs(IV-b(v)) corroborates Imp(III-B) for a further increase of the boat speed and reveals *more* sensitivity of the yaw response to rudder deflection and *increased* V_{safe} .

B. Obs(IV-b(iv)) suggests that the existence of the primary and the secondary zones explains two different mechanisms of broaching-to, as detailed in (C) and (D) below.

C. The development of an increased sensitivity in (A) above, due to the movement of the primary zone with increased V_{safe} , relates the primary zone with the inception of broaching-to. It is pertinent at this point to refer to Imp(III-ii) of §1, which revealed that the sensitivity, described in (A) above, is a prime factor for the inception of broaching-to.

D. Obs(IV-c) signifies an increased 'rudder ineffectiveness' which has been first introduced in Imp(III-D). The *surf-riding* phenomenon of ship/boat also demonstrates the rudder ineffectiveness. Therefore, the prominence of the stationary secondary zone is related to the likelihood of surf-riding which has been considered to be a precursor to broaching [5], [6], [20].

E. The increase in V_{safe} in Imp(IV-A) and the prominence of the stationary secondary zone in Obs(IV-c) appears to be related. The secondary zone becomes more prominent as V_{safe} increases.

F. The implications stated in (C) and (D) above are related through the implication (E). The *stronger* inception results in a *more probable* surf-riding.

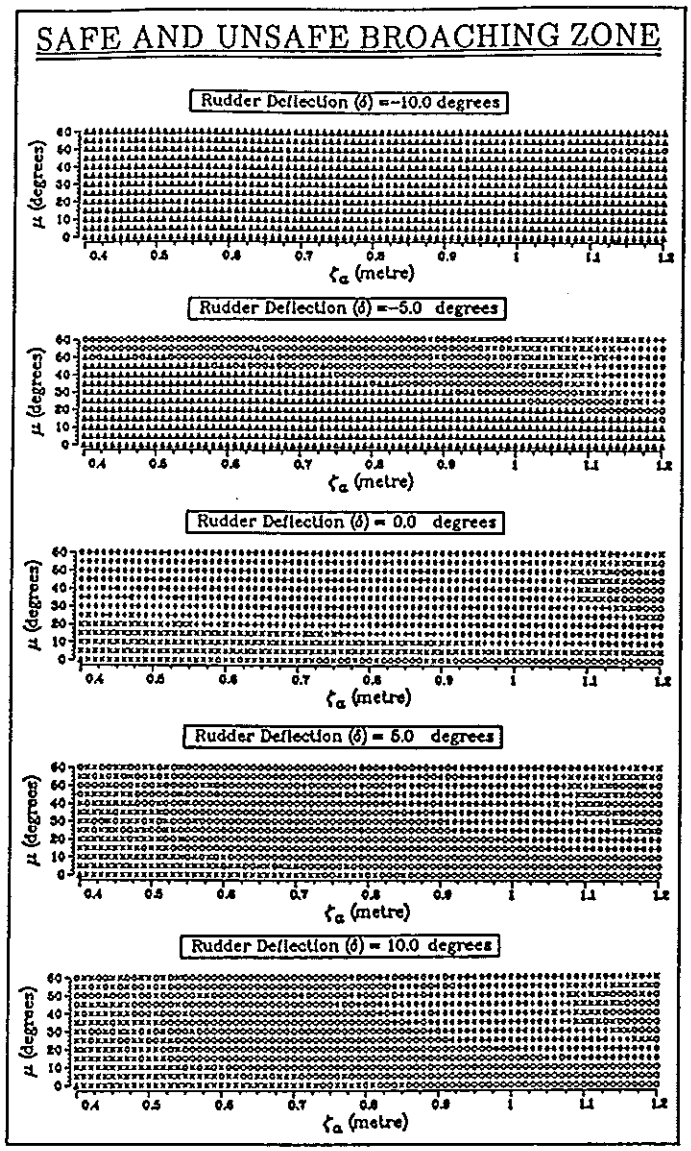

Figure 17: *Safe('•') and unsafe broaching-zones in control space without wind effect for $U = 11$ kn., $\lambda/L = 3.00$ and $\delta = -10^o$ to 10^o*

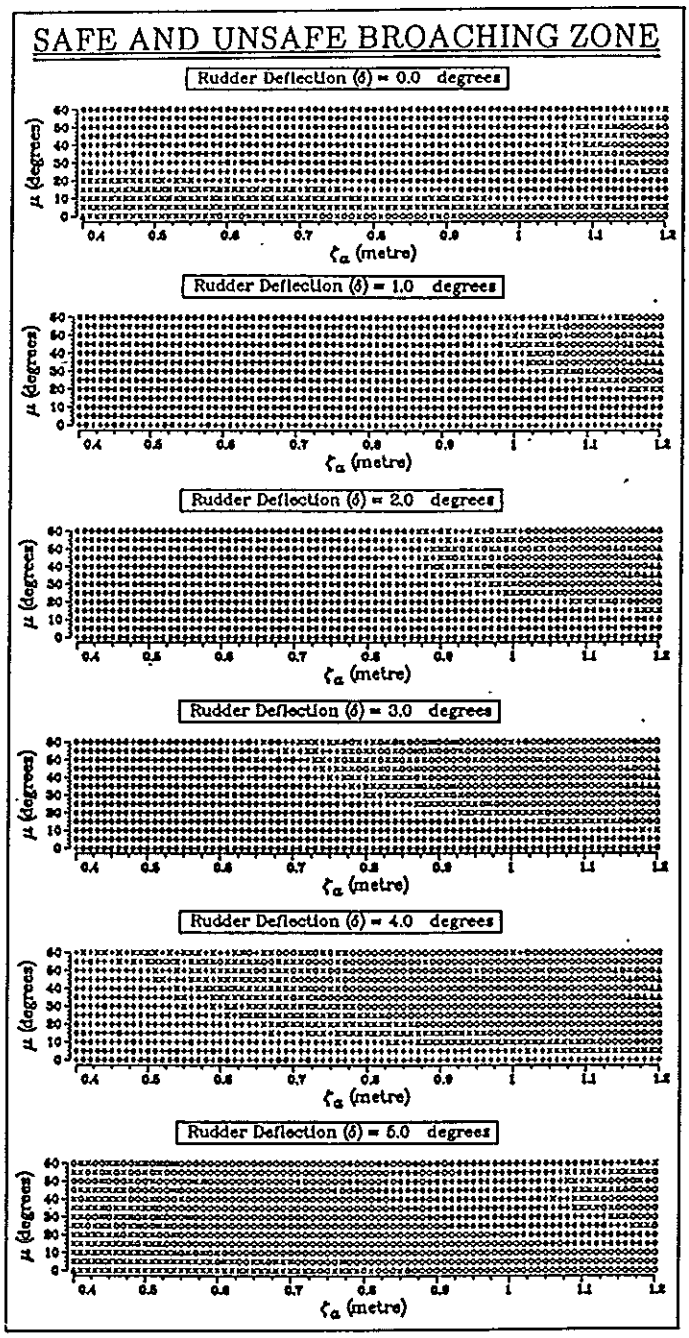

Figure 18: *Safe('•') and unsafe broaching-zones in control space without wind effect for $U = 11$ kn., $\lambda/L = 3.00$ and $\delta = 0^o$ to 5^o*

CONCLUSIONS

- The inception of broaching-to is attributed to the *bifurcation of the chaotic attractor*, observed in the yaw-roll state plane as *expansion* or increase in size of the attractor. This expansion takes the form of sudden jump in size or *explosion* in the case of *lower* wave headings.

- Due to the *explosion* of the chaotic attractor, the sensitivity *intensifies* in the cases of the *lower* wave headings, resulting in an *acute unpredictability* of the ship's heading correction by rudder deflection.

- The characteristic features of the *safe* (non-broaching) zone in the parameter space indicate *sensitivity* of the ship's yaw response to the rudder deflection under specific combinations of the parametric values.
- Finally, the occurrence of the broaching-to phenomenon is attributed to the inability (or perhaps the impossibility, depending on the severity of the situation) of the helmsman to negotiate the *unpredictability*, by applying appropriate rudder deflection at the right time.

References

[1] Bandyopadhyay, B. (1994) : 'A Nonlinear Dynamical Investigation into the Broaching-to Phenomenon of Ships'. Ph.D. Dissertation, Department of Mechanical Engineering, Technical University of Nova Scotia, Halifax, Canada.

[2] Bandyopadhyay, B. and Hsiung, C.C. (1993) : 'Identification of Ship's Broaching-to As Bifurcation Phenomenon'. *Proceedings of the International Conference On Marine Simulation And Ship Manoeuvrability*, St. John's, Newfoundland, Canada, vol.1, pp. 11–21.

[3] Jiang, T., Schellin, T.E. and Sharma, S.D. (1987) : 'Maneuvering Simulation of a Tanker Moored in a Steady Current Including Hydrodynamic Memory Effects and Stability Analysis'. *Proceedings of International Conference on Ship Manoeuvrability, London, England*, v. 1, n. 23, pp. 1–12.

[4] Kan, M. (1992) : 'Chaotic Capsizing'. *Proceedings of 20th ITTC Meeting on Seakeeping Performance*, ITTC.SKC-KFR, Osaka, Japan, pp. 155–180.

[5] Kan, M. (1990) : 'Surging of Large Amplitude and Surf-riding of Ships in Following Seas'. *Naval Architecture and Ocean Engineering*, edited by Society of Naval Architects of Japan, vol. 28, pp. 49–62.

[6] Kan, M., Saruta, T., Taguchi, H., Yasuno, M. and Takaishi, Y. (1990) : 'Model Tests on Capsizing of a Ship in Quartering Waves'. *Proceedings of Fourth Conference On Stability of Ships and Ocean Vehicles*, Naples, Italy, pp. 109–116.

[7] Kan, M., Saruta, T., Taguchi, H. and Yasuno, M. (1990) : 'Capsizing of a Ship in Quartering Seas (Part 2 : Chaos and Fractal in Capsizing Phenomenon).' *Journal of the Society of Naval Architects of Japan* vol. 168, pp. 211–220. (in Japanese); *Naval Architecture and Ocean Engineering*, edited by Society of Naval Architects of Japan, vol. 29 (1991), pp. 49–60 (in English).

[8] Karppinen, T.O. and Molyneux, W.D. (1984) : 'Wide Beam Fishing Vessels : Results of Resistance and Wake Survey Experiments With Model Hulls 350 and 352.' *Report no. LTR-SH-363*, Institute for Marine Dynamics, St. John's, Newfoundland, Canada.

[9] Moon, F.C. (1987) : 'Chaotic Vibrations'. John Wiley and Sons, New York, U.S.A.

[10] Motora, S., Fujino, M., Fuwa, T. (1982) : 'On the Mechanism of Broaching-to Phenomenon'. *Proceedings of Second Conference On Stability of Ships and Ocean Vehicles*, Tokyo, Japan, pp. 535–550.

[11] Oakley, O.H. Jr, Paulling, J.R. and Wood, P.D. (1974) : 'Ship Motions and Capsizing in Astern Seas'. *Proceedings of 10th Symposium on Naval Hydrodynamics*, pp.1–51.

[12] Renilson, M.R. (1982) : 'An Investigation into the Factors Affecting the Likelihood of Broaching-to In Following Seas'. *Proceedings of Second Conference On Stability of Ships and Ocean Vehicles*, Tokyo, pp. 551–564.

[13] Rutgersson, O. and Ottosson, P. (1987) : 'Model Tests and Computer Simulations – An Effective Combination for Investigation of Broaching Phenomena'. *Transactions of SNAME* , vol. 95, pp. 263–281.

[14] Sharma, S.D., Jiang, T., Schllin, T.E. (1988) : 'Dynamic Stability and Chaotic Motions of a Single Point moored Tanker'. *Proceedings of the 17th Symposium on Naval Hydrodynamics*, The Hague, pp. 543–563.

[15] Thompson, J.M.T. and Soliman, M.S. (1990) : 'Fractal Control Boundaries of Driven Oscillators and Their Relevance to Safe Enginnering Design'. *Proceedings of Royal Society, London, England*, vol. A, no. 428, pp. 1–13.

[16] Thompson, J.M.T. and Stewart, H.B. (1986) : 'Nonlinear Dynamics and Chaos'. John Wiley and Sons, New York, U.S.A.

[17] Ueda, Y. and Akamatsu, N. (1980) : 'Chaotically Transitional Phenomena in the Forced Negative-Resistance Oscillator'. *IEEE Transaction Circuit System*, vol. CAS-28, pp. 217–224.

[18] Umeda, N. (1994) : 'Broaching of a Fishing Vessel in Following Seas' *Fishing Boat World*, January, pp. 26–30.

[19] Umeda, N. and Renilson, M.R. (1993) : 'Broaching in Following Seas – A Comparison of Australian and Japanese Trawlers'. *Bulletin of National Research Institute of Fisheries Engineering of Japan*, no. 14, March issue, pp. 175–187.

[20] Umeda, N. (1990) : 'Probabilistic Study on Surf-Riding of a Ship in Irregular Following Seas'. *Proceedings of Fourth Conference On Stability of Ships and Ocean Vehicles*, Naples, Italy, pp. 336–343.

[21] Virgin, L.N. (1987) : 'The nonlinear rolling response of a vessel including chaotic motions leading to capsize in regular seas'. *Applied Ocean Research*, v. 9, n.2, pp. 89–95.

Capsize Criteria for Nonlinear Coupled Heave and Roll Oscillations in Beam Seas

Pompiliu Donescu and Lawrence N. Virgin,
School of Engineering, Duke University, Durham, NC 27708

Abstract

The coupled (heave and roll) oscillations of a ship in transverse sinusoidal waves are considered. In contrast to much of the recent research in this area nonlinear effects, fluid--structure interaction and geometry of a realistic vessel are included in the analysis. The ship hull is described by a set of realistic transverse sections and fluid influence coefficients are computed using three-dimensional linear interpolation from tables taking into account the instantaneous waterplane and the frequency of the waves.

Because of the highly nonlinear and complex nature of the governing equations of motion the main thrust of this paper is based on numerical simulation.

The fundamental forcing parameters of this problem are the wave height and wave frequency. As expected, large response amplitudes occur for large wave height and proximity of the fundamental frequency of the waves to a natural frequency of the vessel. However, nonlinear effects have a strong influence on these results. Several initial conditions of the system were chosen and therefore transient effects are an integral part of this study. Combinations of wave parameters leading to either steady-state motion or capsize are mapped out as `safe' and `unsafe' conditions respectively.

Suggestions are made concerning how this information could be incorporated into a relatively simple criterion.

Introduction and main assumptions

Traditionally, the study of ship dynamics and capsize has evolved from rather simplistic concepts based on the essentially static consideration of restoring moments and the GZ curve. Incorporation of dynamic effects has progressed along two lines. First, fully coupled but linear equations of motion have been developed including probabilistic wave action (Price and Bishop, 1974; Rawson and Tupper, 1983). Second, uncoupled roll motion in its fully nonlinear context has also received recent attention (Virgin, 1987). This latter approach has been stimulated by rapid progress in the theoretical understanding of nonlinear dynamics and chaos, and is the basis of the current paper. Recent contributions to nonlinear ship dynamics include the work of Falzarano et al. (1992) and Thompson et al. (1992).

The aim of this paper is to study coupled heave and rolling motions in regular transverse seas. The restoring moment is not considered from the stability arm diagram. An enhanced analysis is dedicated to Froude-Krylov forces as, usually, these forces are "dominant for all waves conditions" (de Kat and Paulling, 1989). Also the fluid influence coefficients are computed using a simplified model but they are not constant and depend on the position of the ship and on wave frequency because the motion is dominated by the forcing frequency.

Once the equations of motion have been established they can be solved numerically starting from a given set of initial conditions. A multitude of data can be generated in this way and some typical responses and their dependence on certain excitation parameters are delineated. It is important to try to establish some simple rules based on this complicated nonlinear behavior.

Recently, Thompson et al. (1991, 1992) have developed a safety criterion based on the fractal erosion of the stable basin of attraction. Paulling and de Kat (1989) have studied multiple degree of freedom motion in severe seas in the time domain. Falzarano (1992) has also concentrated on nonlinear dynamics of vessels in severe seas. Most of the older and some of the more recent work has used the vanishing stability angle as the capsize condition although a few other alternatives have been considered. Virgin (1988) has established an approximate capsize criterion based on the total energy of a single degree of freedom oscillation. Also Liapunov functions have been used by a few researchers to establish the

boundedness of the motion (Caldeira-Saraiva, 1990 and Ozkan, 1985).

The computed capsize boundaries are compared with a condition based on the underlying potential energy of the system. Suggestions for future work are developed.

Equations of motion

In deriving the equations of motion two systems of coordinates are considered: a fixed system $Ox_1y_1z_1$ and a frame of reference attached to the ship Oxyz. Fluid forces have been computed by considering the fluid incompressible and inviscid, and its motion irrotational. Assuming the motion is described by Laplace's equation for the velocity potential and linearized boundary conditions at the mean wave elevation, superposition of incoming wave potential, radiation potential and diffraction potential is used. Froude-Krylov forces and fluid influence coefficients are more accurately computed and diffraction potential is neglected (Rawson and Tupper, 1983; Thompson et al., 1992). The equations of motion are derived from momentum balance:

$$(\Delta + M_{33})\,\ddot{z}_{1G} + L_{33}\dot{z}_{1G} + (\Delta - \rho V \cos\alpha)\,g = M_{33}\ddot{z}_{1V} + L_{33}\dot{z}$$

$$(J_{xx} + M_{44})\,\ddot{\varphi} + L_{44}\dot{\varphi} + \rho g V\left((z - z_G)\sin(\varphi - \alpha) - (y - y_G)\cos(\varphi - \alpha)\right) = M_{44}\ddot{\alpha} + L_{44}\dot{\alpha}$$

where:

- z_{1G} - heave displacement in the fixed frame of reference (Fig. 1.);
- φ - roll angle;
- α - wave angle at the ship middle plane;
- Δ - ship displacement;
- J_{xx} - moment of inertia of the ship mass (only);
- M_{33}, L_{33}, M_{44}, L_{44} - fluid influence coefficients;
- V - displaced volume;
- g - gravitational constant;
- y, z - center of volume V in the frame of reference attached to the ship;
- y_G, z_G - mass center of the ship;

- z_{1v} - wave height at the ship middle plane;
- ρ - water density.

The displaced volume, its center and the fluid influence coefficients are computed using strip theory:

$$M_{ii} = \int_L m_{ii}\, dL$$

$$L_{ii} = \int_L l_{ii}\, dL$$

$$m_{33} = \rho \frac{\pi}{8} b^2 \mu_{33}$$

$$l_{33} = \rho \omega \left(\frac{b}{2}\right)^2 \nu_{33}$$

$$m_{44} = \rho \pi d^4 \mu_{44}$$

$$l_{44} = \rho \omega d^4 \nu_{44}$$

where

- $b = b(x)$, $d = d(x)$ - ship breadth and draught at the section x for the current waterplane;
- m_{ii}, l_{ii} - coefficients per unit length;
- μ_{ii}, ν_{ii} - nondimensional coefficients.

The nondimensional coefficients are based on Lewis forms or the transverse sections in order to solve the 2D potential flow around each section. Further details of this derivation can be found in Donescu and Virgin (1993).

In the above equations several terms are nonlinear (Jordan and Smith, 1987). The restoring force and moment depend nonlinearly on the heave displacement and roll angle because of the ship shape and of the large amplitude motion. The fluid influence coefficients (added masses and damping coefficients) are computed for each position of the ship and thus are nonlinear functions of ship position. They also vary with the wave frequency. The forcing terms are also nonlinear because of added masses and damping coefficients although the wave is assumed sinusoidal. The restoring moment is not determined from the static stability diagram, but the ship volume was computed for each instantaneous heave and roll displacement and wave position. This is an important extension since the submerged volume

of the ship is no longer assumed constant.

Numerical simulation

Because of the complexity of the problem and the aim of considering a real ship shape numerical simulations form the basis of the current study. Numerical methods are becoming increasingly widespread and sophisticated (Parker and Chua, 1989, and de Kat and Paulling, 1990). The results of the simulations are summarized as diagrams of wave length-wave height showing the capsize-no capsize domains. The ship is assumed to capsize when the roll angle is greater than the angle of vanishing stability for its volume in still water. Also zones determined by the number of transient cycles until ship capsize are emphasized. For refinement purposes each such domain is attached a shade. The huge number of necessary simulations to emphasize the boundary between the domains imposed a heuristic procedure of refining the initial mesh. This procedure is based on the fact that a coarse cell is refined only if its corners have different shades. Several levels of refining are considered.

Simulations were conducted on a 15000 tdw ship based on a specific Romanian cargo vessel (Fig. 2) with the following characteristics:

- length between perps L_{pp} = 147.00 m;
- breadth B = 22.80 m;
- depth of the ship D = 13.20 m;
- draught T = 9.6 m;
- block coefficient C_B = 0.65.

The results of a typical simulation are shown as time series in figure 3. Figure 3(a) shows a typical wave profile corresponding to a wave height of 30 m and wave length of 330 m. The ship under consideration is then subject to this wave with initial conditions (heave and roll displacements and velocities) (-0.7, 0.0, 0.0, -0.1). Figure 3(b) shows the resulting relative roll angle as the continuous line. The absolute roll angle is shown in figure 3(c). Also shown in figures 3(b) and 3(c) are the results of simulations based on slightly different wave conditions. In these cases the ship capsizes after a few transient oscillations, i.e. 3.59 and 7.44 wave periods prior to capsize.

Contour plots were obtained showing the safe domain and the unsafe ones for a fine grid of wave parameters. The unsafe regions are also divided according to the number of wave periods in which capsize occurs. Inspection of the diagrams shows the capsize (unsafe) domain appears for waves with maximum angles larger than a specific value depending on the ship and on initial conditions. However, the boundary between capsize and no capsize can be very complicated. In fact, an interesting feature of this plot is observed when one considers a specific wave length of 300 m. For wave height of less than 20 m the motion is stable but for wave heights above 20 m and up to approximately 25 m capsize occurs within the first two transient cycles. However, for wave heights between 25 and 28 m capsize does not occur. Although this is somewhat counter-intuitive it is a feature not uncommon in nonlinear dynamical systems.

Although they are not presented here, simulations for different initial conditions have been performed and they show that if the initial conditions are in the sense of the excitation the ship is less likely to capsize or capsizes after a longer period (Fig 4). By contrast, initial conditions contrary to the forcing decrease the safe areas in the parameter space and also capsize occurs more suddenly.

The shaded figures can be used for sea-keeping purposes. They represent important information in terms of whether the actual direction of the ship is safe for a given sea. The domains manifest a fractal nature, i.e. showing geometric self similarity at any scale, which may show that chaos is present in the system dynamics (Virgin, 1987-1989).

Figure 5 shows a 3-D plot of the maximum roll angle as a function of the wave parameters. It is apparent that the maximum roll angle grows rapidly as the capsize boundary is approached, hence the build up of roll angle may occur quite suddenly as the wave conditions change. Clearly, this figure augments figure 4 in the sense that the capsize regions in figure 4 relate to the regions which are included in the plateau of figure 5.

Towards a capsize criterion

Clearly the mechanism of capsize is a very complicated process even when the mathematical model is based on various simplifications. Sensitivity to initial conditions and

wave parameters means that isolated simulations are of little value and therefore a relatively simple criterion is sought which provides some kind of lower bound to the onset of large amplitude motion leading to capsize.

Here, we attempt to show how capsize corresponds to escape from the local potential energy well, the shape of which is determined primarily from the geometry of the vessel. Figure 6 shows 3-D and contour plots of the potential energy as a function of heave and roll displacements. The symmetric saddle points are associated with the angle of vanishing stability. It is also apparent that the energy surface is not at all symmetric with respect to the heave displacement.

The proposed criterion is based on limiting transients to remain within an energy 'watershed'. This watershed is defined by the locus of points with a minimum gradient length which contains the saddles and the maximums of the potential energy surface shown in figure 6. A useful analogy is to consider a ball rolling on this energy surface. Escape corresponds to capsize. Wave forcing is in some sense analogous to shaking this surface. If the excitation is strong it is clear that the ball is more likely to escape over the saddle points.

It is desired to restrict the motion to be contained within a subset of this surface. A safety factor can be incorporated by restricting the allowed region even further. Figure 7 illustrates this approach as a phase projection in the heave-roll plane relative to the wave. In figure 7(a) the motion is initiated and it can be seen that despite relatively large amplitude transient behavior the ship does not capsize, and the condition is not violated. In figure 7(b) the wave height is increased slightly, the capsize condition is violated and capsize occurs (i.e. the relative roll angle exceeds the angle of vanishing stability) very soon after. To illustrate the conservative nature of this approach consider figure 7(c) where motion that does not ultimately result in capsize but does violate the stability criterion. Hence, this combination of wave height and frequency is considered an unsafe wave action.

A summary of the proposed criterion is then shown as a function of wave parameters in figure 8. It can be seen that the criterion acts as a lower bound for stable rolling motion, i.e. no capsize when compared with figure 4. Although this criterion is ad hoc in nature it is based on the underlying (nonlinear) characteristics of the vessel albeit with damping and forcing neglected. It should be pointed out that these curves correspond to a single set of initial conditions, but since the set chosen are associated with a near rest state they may be

viewed as close to a worst case since significant transients are caused.

Conclusions

The coupled heave-roll motion of a ship in beam seas has been studied. The restoring forces and the fluid influence coefficients are computed as nonlinear functions of ship position and wave frequency.

The governing equations of motion are solved numerically for a variety of wave conditions. It is shown that the resulting behavior is very complicated, including possibility of counter-intuitive behavior. Due to sensitivity of the system an approximate criterion is suggested such that a lower boundary is developed for the stable (i.e. non-capsizing) motion.

This work represents the early stages in an on-going program of research to investigate realistic ship dynamic behavior and ways of developing useful tools based on the underlying (nonlinear) physics of the problem.

Acknowledgment

The authors gratefully acknowledge the support of the Army Research Office.

References

Donescu, P., Virgin, L.N. - "Nonlinear coupled heave and roll oscillations of a ship in beam seas", ASME Winter Meeting, New Orleans, 1993.

Falzarano, J., Shaw, S., Troesch, A. - "Application of Global Methods for Analyzing Dynamical Systems to Ship Rolling Motion and Capsizing", *International Journal of Bifurcation and Chaos*, Vol. 2, pp. 101-115, 1992.

Jordan, D. W., Smith, P. - *Nonlinear Ordinary Differential Equations*, Oxford University Press, Oxford, 1987.

Thompson, J.M.T., Rainey, R.C.T., Soliman, M.S. - "Mechanics of ship capsize under direct and parametric wave excitation", *Phil. Trans. R. Soc. Lond.* A (1992) 338, pp. 471-490.

de Kat, J. O., Paulling, J.R. - "The Simulation of Ship Motions and Capsizing in Severe Seas", *SNAME Transactions*, vol. 97, pp. 139-168, 1989.

Parker, T. S., Chua, L. O. - *Practical Numerical Algorithms for Chaotic Systems*, Springler-Verlag, 1989.

Rainey, R. C. T., Thompson, J. M. T. - "The Transient Capsize Diagram - A New Method of Quantifying Stability in Waves", *Journal of Ship Research*, 35, pp. 58-62, 1991.

Rawson, K. J., Tupper, E. C. - *Basic Ship Theory*, Vol. 2, Longman Group, Ltd., London, 1983.

Thompson, J.M.T., Stewart, H. B. - *Nonlinear Dynamics and Chaos*, Wiley, 1986, London.

Virgin, L. N. - "The Nonlinear Rolling Response of a Vessel Including Chaotic Motions Leading to Capsize in Regular Seas", *Applied Ocean Research*, Vol. 9, pp.89-95, 1987.

Virgin, L. N. - "Approximate Criterion for Capsize Based on Deterministic Dynamics", *Dynamics and Stability Systems*, 4, pp. 55-70, 1989.

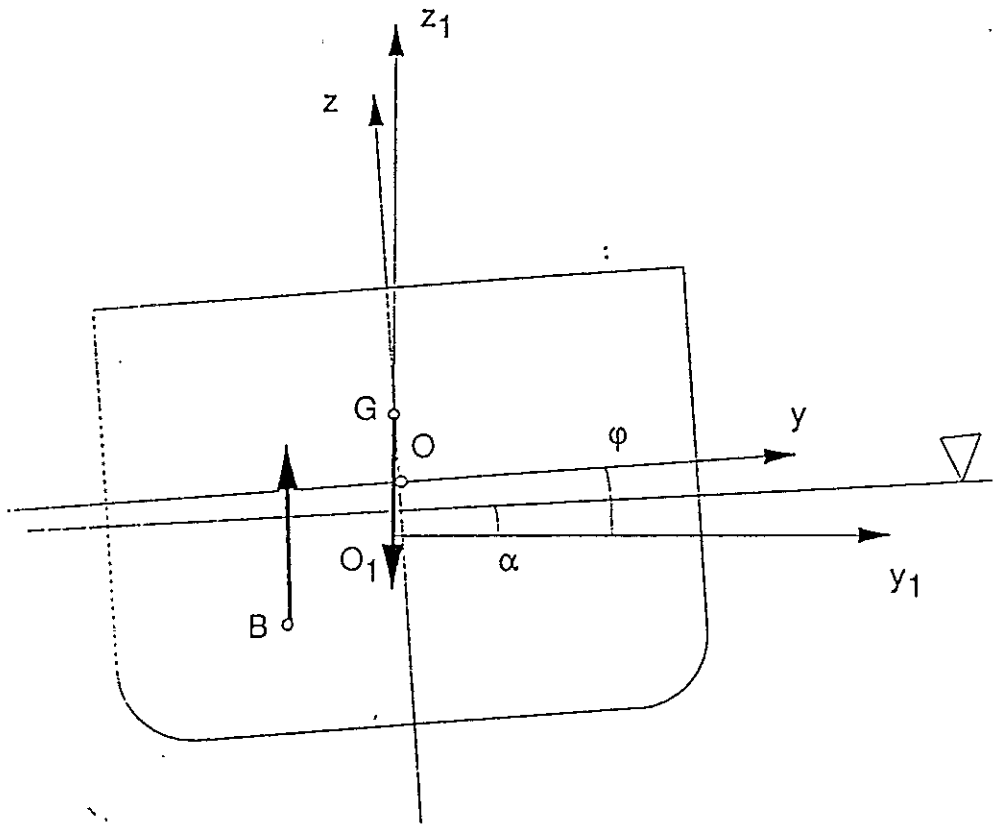

Fig 1. Heave and roll oscillations: frame of reference, displacements and forces acting on the ship

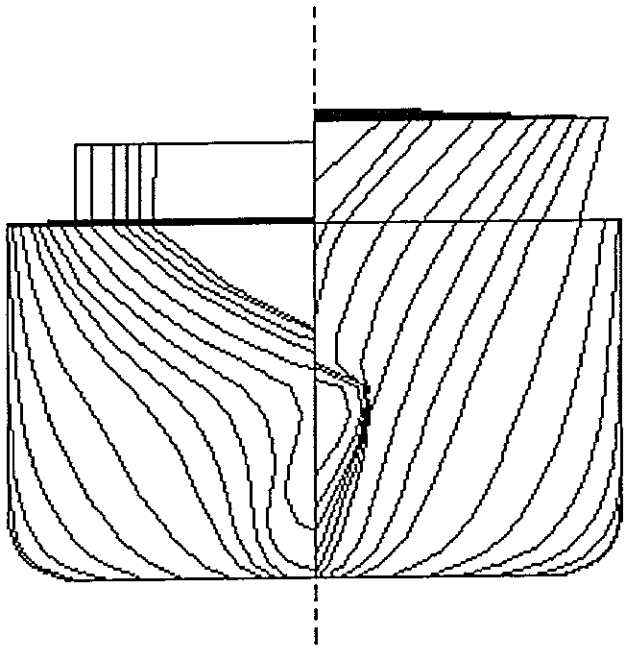

Fig 2. Cross-sectional geometry of the vessel
(33 sections)

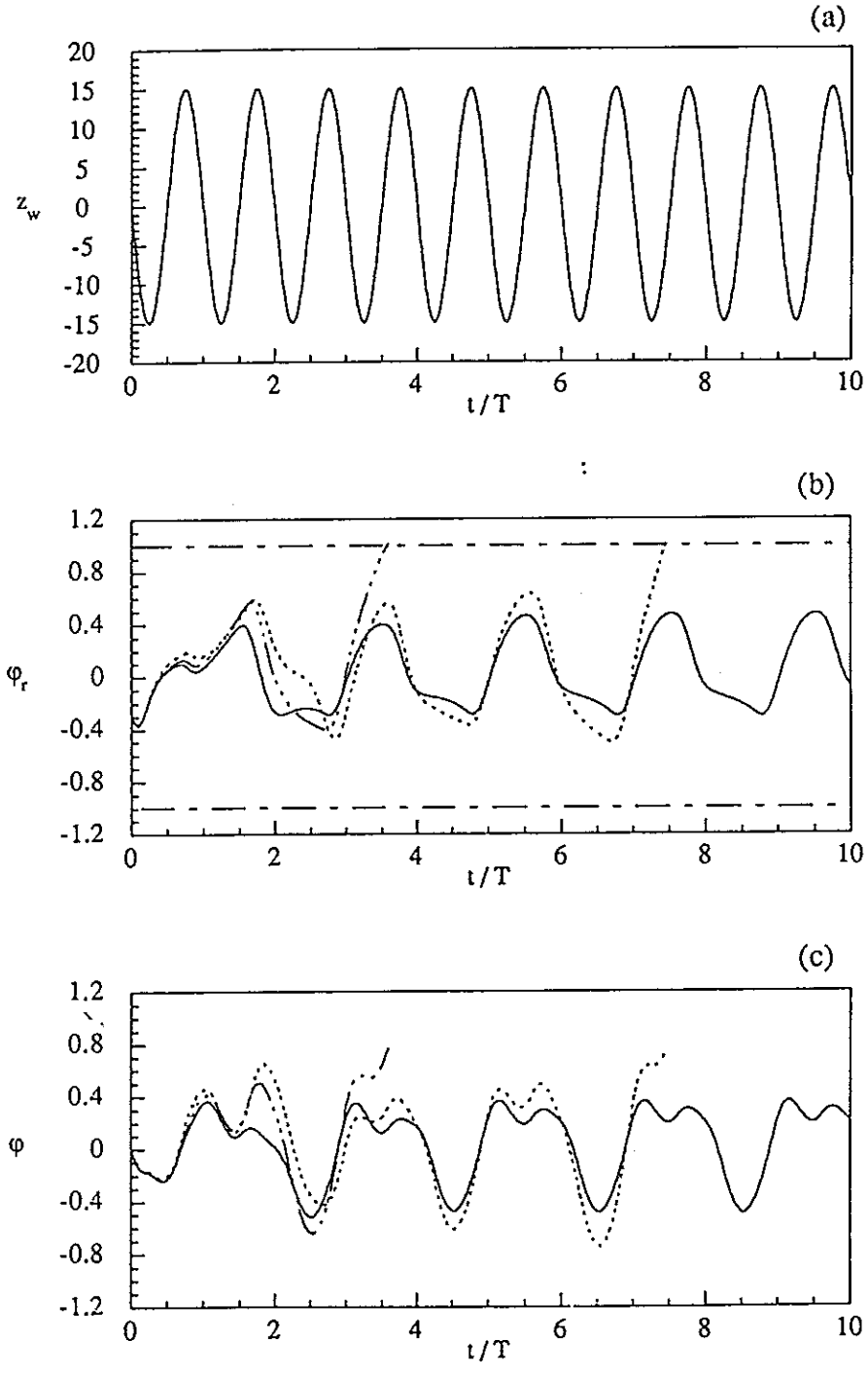

Fig 3. Times series; (a) typical wave(h_w=30m, l_w=330m);
(b) relative roll angle; (c) absolute roll angle;
(___ h_w=30m, l_w=330m; _ ... _ h_w=30m, l_w=320m; . . . h_w=31m, l_w=320m)

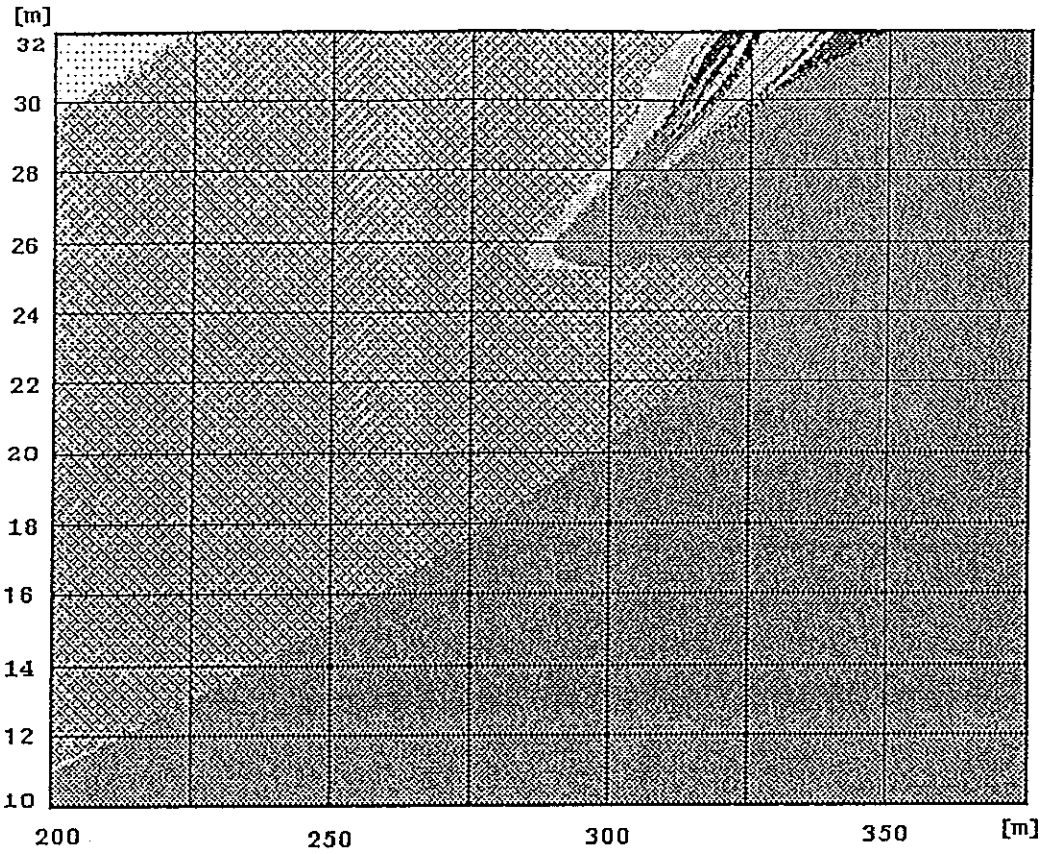

Fig 4. Capsize diagram; the shades are codded according to the number of transient oscillations prior to capsize.

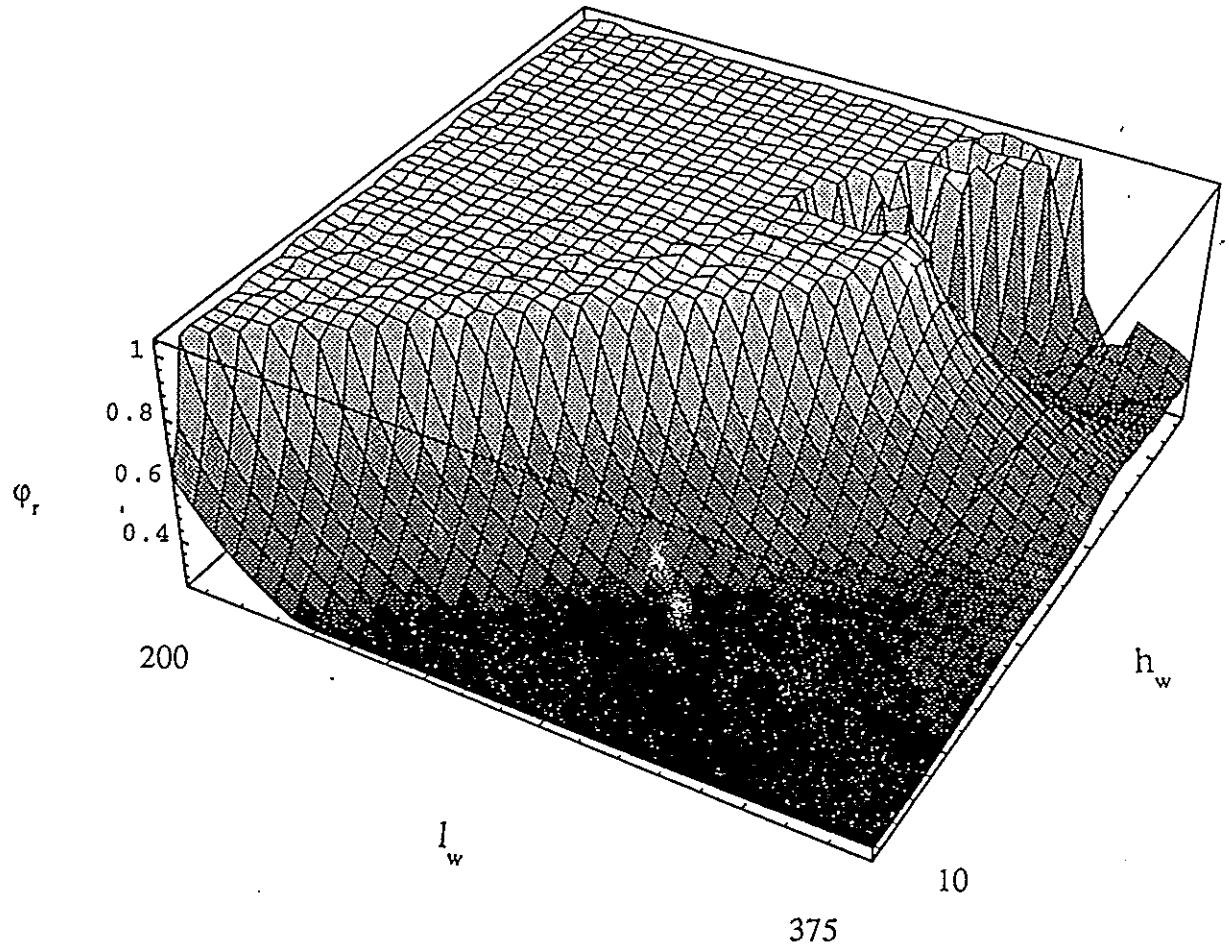

Fig 5. Maximum φ_r (relative roll angle) excursion

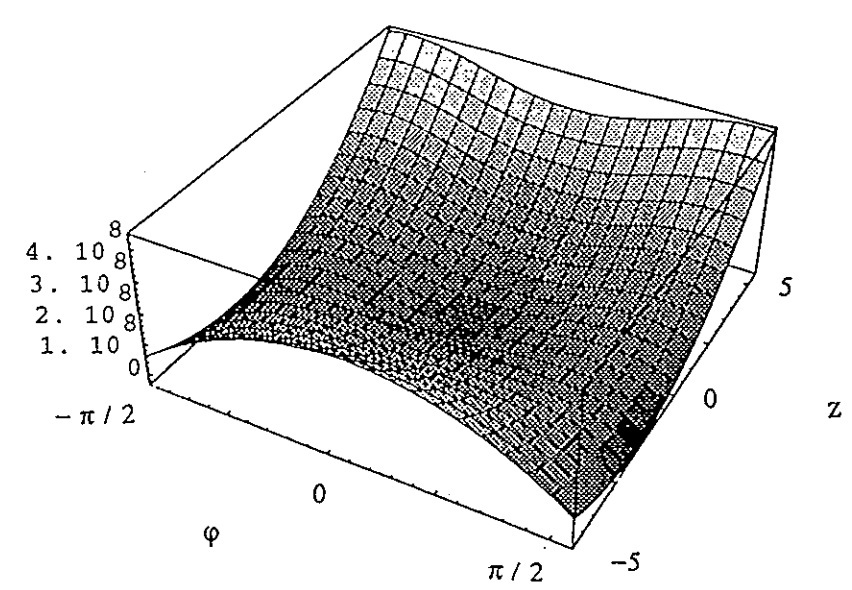

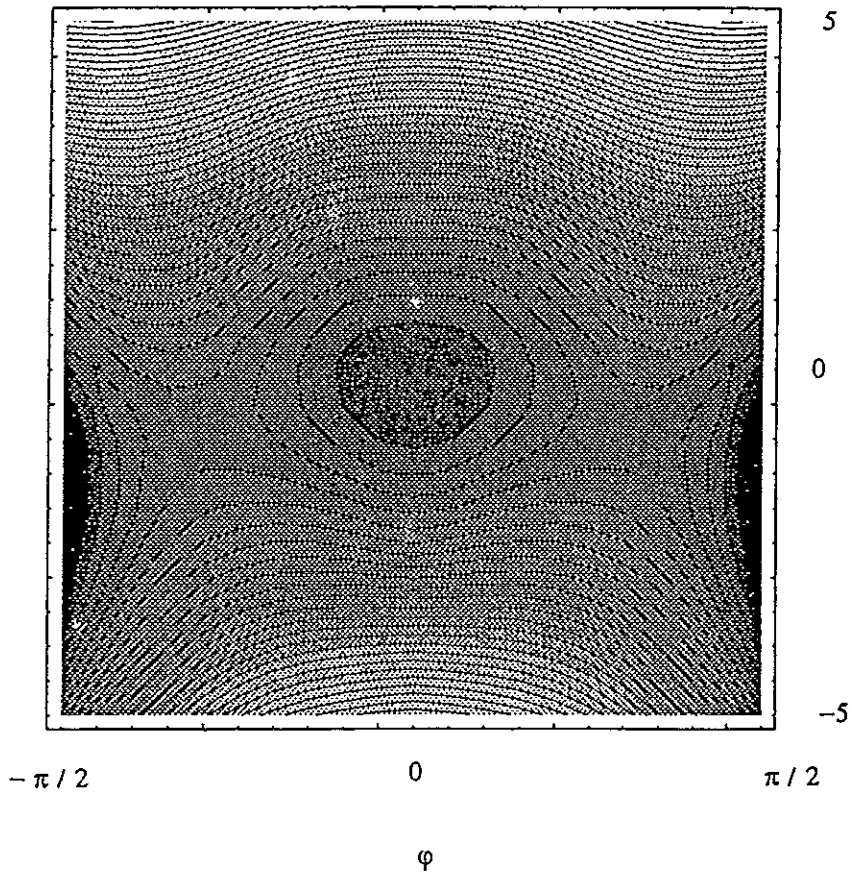

Fig 6. Potetial energy surface;
(a) 3-D plot; (b) contour plot

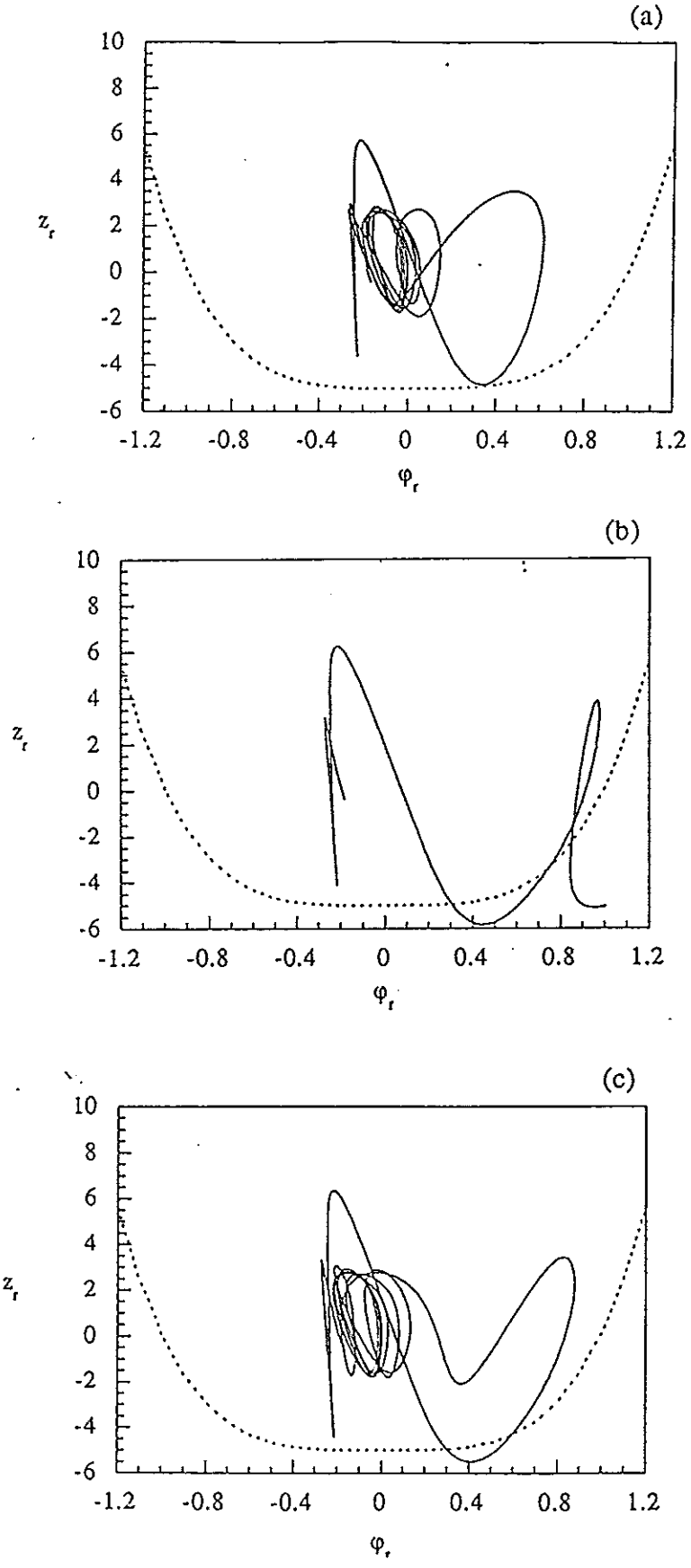

Fig 7. Phase projection (___) and capsize criterion (...);
(a) h_w=10m, l_w=200m; (b)h_w=11m, l_w=200m;(c)h_w=12m, l_w=215m

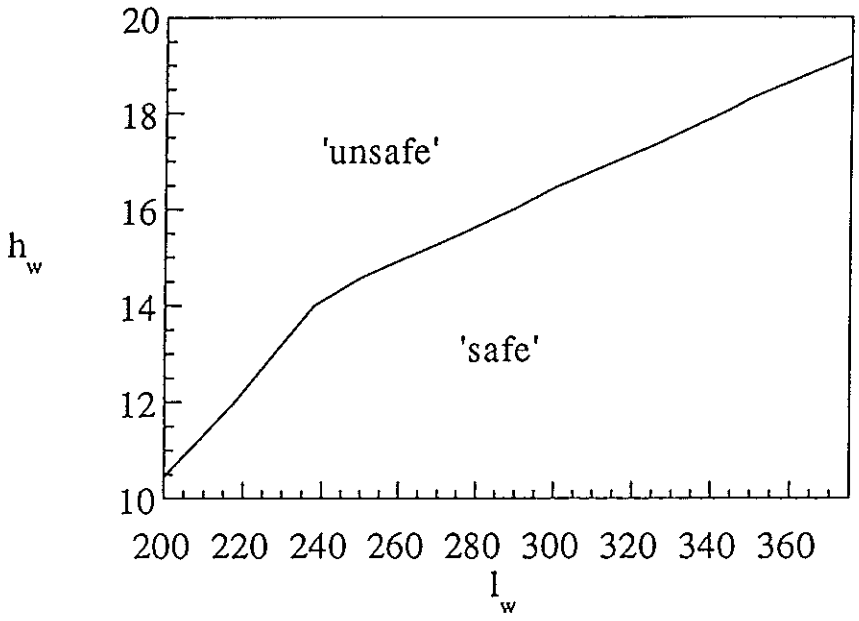

Fig 8. Capsize criterion based on the 'watershed'.

The probability distribution of rolling amplitude of a ship in high waves

Huang Xianglu Gu Xiechong Bao Weiguang
Shanghai Jiao Tong University
PRC

Abstract

The probability distribution function of the rolling amplitude of a ship with S-type stability curve in high waves was derived by using the stochastic averaging method. Some results of different S type stability curves and damping were presented and discussed. Also in the paper the influence of shipping water on the probability distribution was demonstrated by a time domain numerical simulation.

1.Introduction: The rolling of a ship in high waves is an important factor in the determination of ship stability especially from the dynamic point of view. As early as 60 decade,Rahola has stressed the dynamic effect of ship rolling in the determination of ship stability. After that,several regulations have been established for governing the ship stability which take this point into consideration. No matter what the importance of the role of the rolling amplitude, the determination of the magnitude of the rolling amplitude in those regulations remain harsh. Almost all of the regulations use average rolling amplitude by some empirical formula in which only a few of the parameters have been involved. The reason of such situation is the lack of the knowledge of ship rolling in high sea especially in random waves. The nonlinear ship oscillation in random waves is a difficult task in ship motion theory,since the nonlinear character of the motion equation leads to the invalidation of the assumption of the normal distribution of the solution which is the base of the derivation of probability distribution in linear cases. In nonlinear cases,the form of distribution has to be determined according to the specified motion response system.

In 60 decade,Caughey[1] proposed a method in which the Markov process theory was used to derive the probability function of the output of a nonlinear discrete system. The idea of such derivation is that the output of a nonlinear first order system may be Markovian provided the input signal is a white noise. Using the Markov process theory,we can determine the probability function of the process by solving the corresponding Fokker-Planck equations.The shortcome of the method is that it is unreasonable for us to assume that the wave be substituted by a white noise. But the basic idea of substitute the original process by a Markov process is very important,it may give a way to break through the barrier of finding the probability distribution function for several nonlinear systems. Two Russian scientists Stratonovich[2] and Khasminskii[3] have found the criteria of replacing the output of a nonlinear system by a dispersion process and establish the relation between the equation of the system and the process parameters. Roberts[4][5] first applied such method to a nonlinear large amplitude rolling equation in which both the restoring and damping function are represented by a polynomial up to third order. In order to fulfill the requirement of KS limit theorem,Roberts transformed the original nonlinear rolling equation into a first order equation system with a pair of new variable energy level and phase angle. Under some conditions

which is imposed on the equation he succeeded in finding the probability function of rolling amplitude for both the nonlinear restoring and damping. Comparison between the theoretical results and its correspond experimental result show satisfactory conformation.

In the derivation of Roberts,as for nonlinear restoring functions he only considered the stability curves which can be represented by a third order polynomial. This means only ships with so-called soft restoring character are considered. But as we know a large number of ships especially for ships require better seakeeping quality such as the container ship always have a hard or S-type stability curves. The rolling amplitude for such kind of ships will have much more importance. In this paper we extent Roberts work to such ships by fitting the restoring curve with a fifth order polynomial. Since the solution of roll motion depends on the form of the restoring function we should at first find out the solution of the free rolling . We will explain the process of derivation in next sections.

Another interesting problem related to the rolling amplitude is the influence of shipping water. Due to the complexity of the problem,both theoretical and experimental researches are scarce. In this paper,an attempt was made to simulate numerically the rolling of a ship in a beam sea with water shipping to the deck. The calculation proceeded in time domain in which a scheme proposed by Dillingham[6] was used to treat the deck water. Some of the results obtained are presented and discussed.

2.Theory: There are two kinds of calculations involved in this paper. One is the determination of large amplitude rolling probability distribution function,which related to the application of KS limit theorem. The other is the calculation to investigate the influence of shipping water on the rolling of a ship in random beam sea,which is a time domain integration of a nonlinear complicated motion equations. The aim of our work is not to develop or modify the theory,only use such method as a tool to solve our problem,so we will not describe these theory in detail,only introduce them briefly to make the statement more clear. Reader who interest in the theory can refer to [1]-[6].

For the large rolling amplitude problem,we use the same method as Roberts,the only difference between our work and Roberts is the type of stability curves. In the following we explain some points which related to the change of the stability function in the procedure of the derivation of the distribution function.

According to Roberts,the rolling amplitude was replaced by the energy level V and phase angle θ,the motion equation was transformed into a first order equation system of V and θ. Assuming that the damping of roll motion is small compared with the wave excitation the equation will have the form which fulfill the requirement of KS limit theorem:

$$\dot{V}=-\epsilon^2 A_1(V)+\epsilon b_1(V,\theta,Y)$$

$$\dot{\lambda}=-\epsilon^2 A_2(V)+\epsilon b_2(V,\theta,Y)$$

in which:

V——————————— energy level

θ——————————— angle of roll motion

λ——————————— the phase angle which is induced by higher order nonlinearity

Y(t)——————————— excitation moment

ϵ——————————— smallness parameter,which corresponds to the damping magnitude

$$A_1(V)=\frac{1}{T(V)}\int_0^{T(V)} f(V,\theta)\sin\theta d\theta$$

$$A_2(V)=\frac{1}{T(V)}\int_0^{T(V)} f(V,\theta)\cos\theta d\theta$$

$$b_1(V,\theta,Y)=\sin\theta(2V)^{\frac{1}{2}}Y(t)$$

$$b_2(V,\theta,Y)=\frac{\cos\theta}{(2V)^{\frac{1}{2}}}Y(t)$$

According to KS limit theorem the response process V weakly convergent to a dispersion process provided ϵ approaches to zero,the dispersion and drift coefficients of the process are related with the term of A and b in the transformed motion equation as follows:

$$m=A+\int_{-\infty}^{0}<E(\frac{\partial b}{\partial Z})(b')_{t+\tau}>d\tau$$

$$DD'=\int_{-\infty}^{\infty}<E(b)_t(b')_{t+\tau}>d\tau$$

in which the subscript ' denote the transpose.

After we got the coefficients of the process it is straight forward to derive the probability function from the corresponding Fokker-Planck equations. So,the main problem for us is to find out the expression of the terms A and b.

It is understood that the phase angle θ of roll appeared in the term b is the rolling motion characteristic,which is represented by the undamped free rolling of the ship. In other words,it is the solution of the following equations:

$$\ddot{\psi}+F(\psi)=0$$

Roberts has found the solution of the equation of the third order restoring function. In our case,the solution of the equation with fifth order restoring functions are needed. We will illustrated the procedure of solving such equation in following paragraph.

The calculation of the rolling of a ship in waves with shipping water on deck are proceeded in time domain. The motion equation of the ship rolling which is to be integrated as an initial problem are expressed as follows:

$$A\ddot{\theta}+\int_{-\infty}^{t}K(t-\tau)\dot{\theta}(t)d\tau+F(\theta)=M_W(t)+M_D(t)$$

in which:

A——————————the moment of inertia of ship
$F(\theta)$—————————— restoring function of ship rolling motion
$M_W(t)$—————————— wave exciting moment
$M_D(t)$—————————— moment induced by the shipping water

The term of convolution integral represents the hydrodynamic forces induced by the ship motion,while the function K(t) involved in this integration is the so-called retardation function. In this paper,a time domain Green's function method were used to generate such retardation function. The quantity and motion of the shipping water are calculated by a scheme proposed by Dillingham in which the shallow water theory was used to modeling the motion of the deck water,and to solve the deck water motion equations the random choice method are utilized. The wave as a input of the calculation were generated by using the Longuet-Higgins model,the spectrum used in the random wave trace generation are ITTC spectrum. The resulted rolling motion trace were treated statistically which gives the correspond histogram,from which by comparing the results between those considering shipping water or without shipping water,some conclusions may be drawn.

3.The solution of the undamped free rolling equation with fifth order restoring function:

Before solving the equation,we should determine the coefficients of the fifth order polynomial to be fitted with a given S-type restoring curve. It will be more convenient if we normalize the restoring curve by the angle at which the stability moment become zero(not zero point). It is shown in Appendix that the normalized fifth order restoring function has the form of:

$$F(\psi)=\psi+(C-1)\psi^3-C\psi^5$$

Then the undamped normalized free rolling equation should be:

$$\ddot{\psi}+\psi+(C-1)\psi^3-C\psi^5=0$$

After integration this equation will have the form:

$$\frac{1}{2}\dot{\psi}^2=V-[\frac{1}{2}\psi^2+\frac{1}{4}(C-1)\psi^4-\frac{1}{6}C\psi^6]$$

This equation also can be expressed in following form:

$$\dot{\psi}^2=\frac{1}{3}C(a^2-\psi^2)(b^2-\psi^2)(c^2+\psi^2)$$

$$a^2<b^2$$

let

$$u=\frac{1}{\psi^2}$$

$$\dot{u}^2=\frac{4}{3}C(a^2u-1)(b^2u-1)(c^2u-1)=8V(u-\alpha)(u-\beta)(u-\gamma)$$

in which:

$$V=\frac{1}{6}Ca^2b^2c^2$$

$$\alpha=\frac{1}{a^2};\beta=\frac{1}{b^2};\gamma=\frac{1}{c^2}$$

$$\alpha>\beta>0$$

$$u=\alpha+(\alpha-\beta)\tan^2\theta$$

$$\dot{\theta}^2=2V(\alpha+\gamma)[1-\frac{\beta+\gamma}{\alpha+\gamma}\sin^2\theta]$$

its solution will be:

$$\omega_1 \tau = \int_0^{\varphi} \frac{d\theta}{[1-k^2\sin^2\theta]^{\frac{1}{2}}}$$

Here:

$$\omega_1 = \sqrt{2V(\alpha+\gamma)}$$

$$k^2 = \frac{\beta+\gamma}{\alpha+\gamma} < 1$$

So:

$$u = \alpha + (\alpha-\beta)\frac{sn^2(\omega_1\tau,k)}{cn^2(\omega_1\tau,k)}$$

$$\psi = \frac{acn(\omega_1,k)}{\sqrt{1-\frac{a^2}{b^2}sn^2(\omega_1,k)}}$$

This is the solution of the free undamped rolling of a ship has fifth order restoring function.By using such solution in the calculation of the terms b we can solve the S-type stability problem.

4.Calculation of the stationary rolling amplitude probability: The calculation of the probability distribution function is the same as Roberts. By considering the case of stationary roll,which means no capsize happen the left hand side of the Fokker-Planck equation become zero. Then the solution of equation can be expressed in the form:

$$P_s = \frac{K}{V\mu(V)}\exp[-\int_0^V \frac{\beta A_1(\zeta)-\pi\alpha(\zeta)}{\pi\zeta\mu(\zeta)}d\zeta]$$

in which: K is a parameter which guarantee the integral of the distribution over its entire range be unity.

$$\mu(V) = \sum_{n=1}^{\infty} S_n^2 S_\chi[n\omega(V)]$$

$$\alpha(V) = \frac{1}{2}[\mu(V)+\nu(V)]$$

$$v(V)=\sum_{n=1}^{\infty} C_n^2 S_X[n\omega(V)]$$

S_n, C_n are the Fourier coefficients of the sine and cosine part of the undamped free oscillation of rolling motion $\theta_0(t)$.

$$\sin\theta_0(t)=\sum_{n=1}^{\infty} S_n \sin\frac{2\pi nt}{T}$$

$$\cos\theta_0(t)=\sum_{n=1}^{\infty} C_n \cos\frac{2\pi nt}{T}$$

$$S_X(\omega)=\int_{-\infty}^{\infty} W_X(\tau)\cos\omega\tau d\tau$$

$$W_X(\tau)=E[x(t)x(t+\tau)]$$

in this paper the spectrum of Dalzell which is the spectra of wave slope were used. the form of such spectrum is:

$$S_X(\omega)=S(\omega_p)H_s(\omega^*)$$

$$H_s(\omega^*)=\frac{1}{\omega^*}\exp-[\frac{1+\frac{\pi}{8}}{4\omega^{*4}}+\frac{\pi}{16}\omega^{*2}-\frac{1}{4}-\frac{3\pi}{32}]$$

$$\omega^*=\frac{\omega}{\omega_p}$$

According to this theory,a program of calculate the probability distribution of the rolling amplitude both for ships with fifth or third order stability curve was developed,which was running on a personal computer of 486.

5.The effect of the nonlinearity of the stability curves on the statistical distribution of the rolling amplitude

By using the above mentioned method,a series of ships with different kinds of stability curve were calculated. In order to clarify the influence of the nonlinearities of the terms in the equation,both fifth and third order restoring function and linear ,quadrature damping are included. The parameters and its ranges used in the calculation are listed in table 1. The results of the probability distribution are shown in fig2-5,while the amplitude corresponds to the cumulate probability of 0.99 for every situation are listed in table 1. The form of the

restoring curves of S-type used in the calculation are also shown in fig 1. The parameters of the restoring function attribute to the cases denoted in the figs are: Case 1 : third order polynomial. case 2: fifth order with C=1.2. case 3: fifth order with C=2.0. case 4:fifth order with C=5.0.

It is clear from the calculated results,that the effect of the nonlinearity of the restoring curve is significant. The resulting amplitude of the ship with fifth order curve is small compared with third order curve. The more the intensity of fifth order term the smaller the resulting amplitude. The significance of the influence of nonlinear term is increasing with the magnitude of the rolling amplitude. It is seen from the last column of table 1,the amplitude of 99 percent probability of the ship with fifth order curve,which has the coefficient C as 5 is 0.4595 rad,while the correspond value of the ship with third order restoring curve will be 0.6474, about 29 percent greater than the S-type condition. Considering that the value correspond to the linear restoring function are even large than third order case,it is worth to take this factor into consideration if the safety problem are dealing with.

Table 1 : The amplitude with cumulative probability 0.99

	a=0.3 b=0.0	a=0.0 b=1.0	a=0.1 b=1.0	a=0.01 b=0.1
Third order	0.2203	0.2849	0.2388	0.6474
C=1.2	0.2218	0.2810	0.2382	0.5728
C=2.0	0.2176	0.2753	0.2342	0.5368
C=5.0	0.2047	0.2577	0.2211	0.4595

6.Comparison between the time domain simulation and theoretical prediction:

As Roberts has done in his work,we proceeded the time simulation of the motion of a equation with fifth order restoring function. In the calculation,Dalzell spectrum were used to generate the wave slope time series. The length of the time trace is 409.6sec,while the spectrum resolution of 0.02 was used.The histogram of the rolling amplitude was calculated from the simulated time series. Fig 6-7 show that the conformation between the theoretical predicted distribution curve and the simulated histogram is good.

7.The time domain simulation of a ship rolling in beam waves with shipping water on deck:

In order to investigate the influence of shipping water on the probability distribution of the rolling amplitude in random beam waves,a numerical calculation program has been developed in Ship Hydrodynamic Laboratory of Shanghai Jiao Tong University according to the method as we mentioned in section two. The wave series or time series of wave height and slope was generated numerically by using Longuet-Higgins model. The length of the time trace used in the calculation is about fifteen minutes. The ship used in the calculation is a ship with moderate size. The particulars are as follows:

Length over all: 61.5 M
Beam : 8.26 M
Draught: 3.8 M
Displacement: 1024 Ton
The metacentric height of ship were varied in the calculation to investigate the influence of shipping water. The stability curve of the ship were assumed to be of third order.

The time trace of rolling angle were calculated for following ship conditions:
Metacentric height: 0.5 M 0.25 M
Freeboard height : 0.4 M

The wave height and period is 3 meter and 8 sec.

The time trace of ship rolling angle were analyzed statistically,and the resulted histogram of rolling amplitude(Maximum) are shown in Fig 8-9.the theoretical distribution of maximum value,the Longuet-Higgins distribution also included in the graphs. Some of the time traces of the rolling angle and deck water quantity obtained in the calculation were also shown in fig 10-11.

It can be seen from the histograms obtained in these calculation,the effect of shipping water always increase the rolling amplitude. Comparison between the histogram with the Longuet-Higgins theoretical distribution which corresponds to the linear case,show that they conform well when the shipping water effect were ignored,but will have significant discrepancy when the shipping water effect were account for. The shipping water resulted in a significant skewness in the rolling amplitude distribution with a trend of increasing the tail of the distribution curve.

Acknowledgement:
This work was supported by the science foundation of CSSC. The support from the state key laboratory of ocean engineering is grateful acknowledged.

Reference:
1.Caughey T.K. 1963 Derivation and application of the Fokker-Planck equation to discrete nonlinear dynamic systems subjected to white random excitation. Journal of the acoustical society of America 35 (11)

2.Stratonovich R.L. 1964 Topics in the theory of random noise. Gordon and Breach New York

3.Khasminskii R.Z. 1966 A limit theorem for the solution of differential equations with random right hand sides. Theory of probability and its applications vol.11(in russia)

4.Roberts J.B. 1982 A stochastic theory for nonlinear ship rolling in irregular sea. Journal of ship research vol.26 No.4

5.Roberts J.B. 1982 Effect of parametric excitation on ship rolling motion in random waves. Journal of ship research vol.26 no.4

6.Dillingham J.T. 1981 Motion of a vessel with water on deck. Marine Technology 18(1)

APPENDIX:

The fitting of the S-type restoring curves:

In order to express the restoring curves with S-type character,a polynomial at least up to fifth order should be explored. This is due to the requirements of the restoring curve should be asymmetric,has two zero points and at least one point of inflexon. We assume that the restoring curve has following form:

$$G(\varphi)=C_1\varphi+C_3\varphi^3+C_5\varphi^5$$

it is clear this curve will have at least two zero points $\varphi = 0,\varphi=\varphi^* > 0.\varphi^*$is the angle at which the restoring moment diminish. $C_1>0$. When φ is small,the restoring curve should be upper to the tangent line through the original point,that is:

$$G(\varphi)>C_1\varphi$$

or

$$C_3\varphi^3+C_5\varphi^5>0$$

or

$$C_3+C_5\varphi^2>0$$

so,$C_3 > 0$. In order to guarantee the zero point φ^*exist,C_5 should be less than zero.

It is convenient to normalize the restoring curve by the angle at which restoring moment diminishes. For this reason we at first calculate the angle of stability diminish by solving the following equation:

$$C_1+C_3\varphi^2+C_5\varphi^4=0$$

The roots of this equation are:

$$\varphi^2=\frac{C_3\pm\sqrt{C_3^2+4C_1(-C_5)}}{2(-C_5)}$$

in which the positive root:

$$\varphi^{*2}=\frac{C_3+\sqrt{C_3^2+4C_1(-C_5)}}{2(-C_5)}$$

Then we obtain the diminish angle of stability $\varphi^* > 0$. Another root of the equation is negative:

$$\varphi_1^2=\frac{C_3-\sqrt{C_3^2+4C_1(-C_5)}}{2(-C_5)}$$

and:

$$|\varphi^{*2}|>|\varphi_1^2|$$

Introduce a parameter C

$$C=-\frac{\varphi^{*2}}{\varphi_1^2}>1$$

then

$$\frac{C_5}{C_1}=\frac{1}{\varphi^{*2}\varphi_1^2}=-\frac{C}{\varphi^{*2}}$$

$$\frac{C_3}{C_1}=-\frac{(\varphi^{*2}+\varphi_1^2)}{\varphi^{*2}\varphi_1^2}=\frac{1}{\varphi^{*2}}(C-1)$$

Introduce a new normalized variable of rolling angle and time:

$$\psi=\frac{\varphi}{\varphi^*}$$

$$\tau=\omega_0 t$$

in which:

$$\omega_0=\sqrt{C_1}$$

By dividing the original motion equation with $\omega_0\,\varphi^*$,we will obtain following normalized equation:

$$\ddot{\psi}+\psi+(C-1)\psi^3-C\psi^5=0$$

as we have used in section 3.

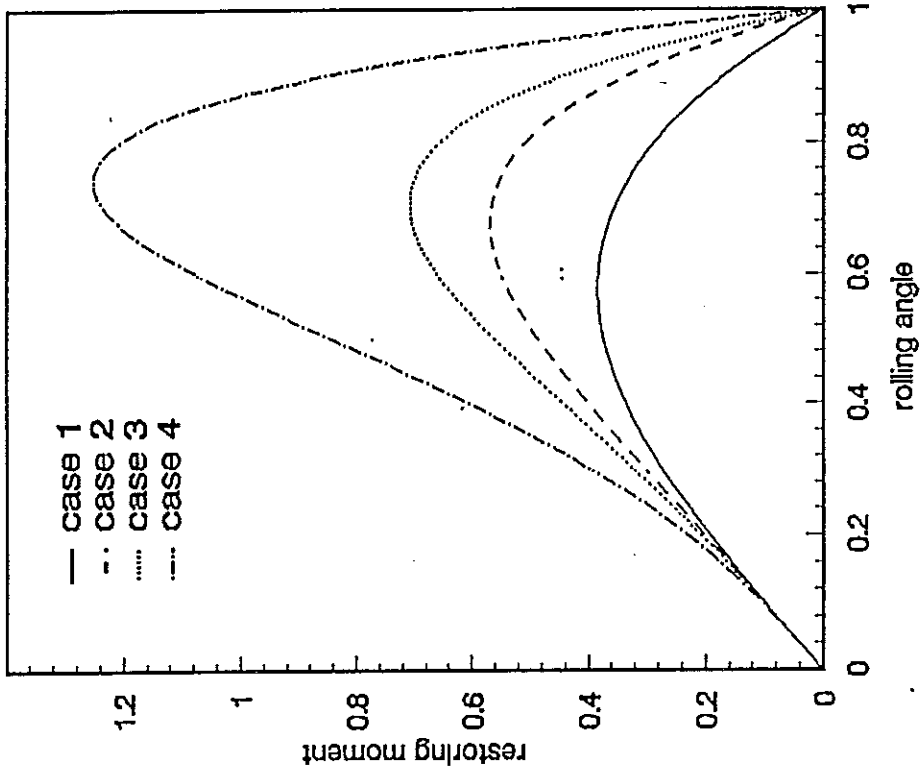
case 1
case 2
case 3
case 4
restoring moment
rolling angle
0
0.2
0.4
0.6
0.8
1
1.2
0
0.2
0.4
0.6
0.8
1

Fig. 1

Fig: 2

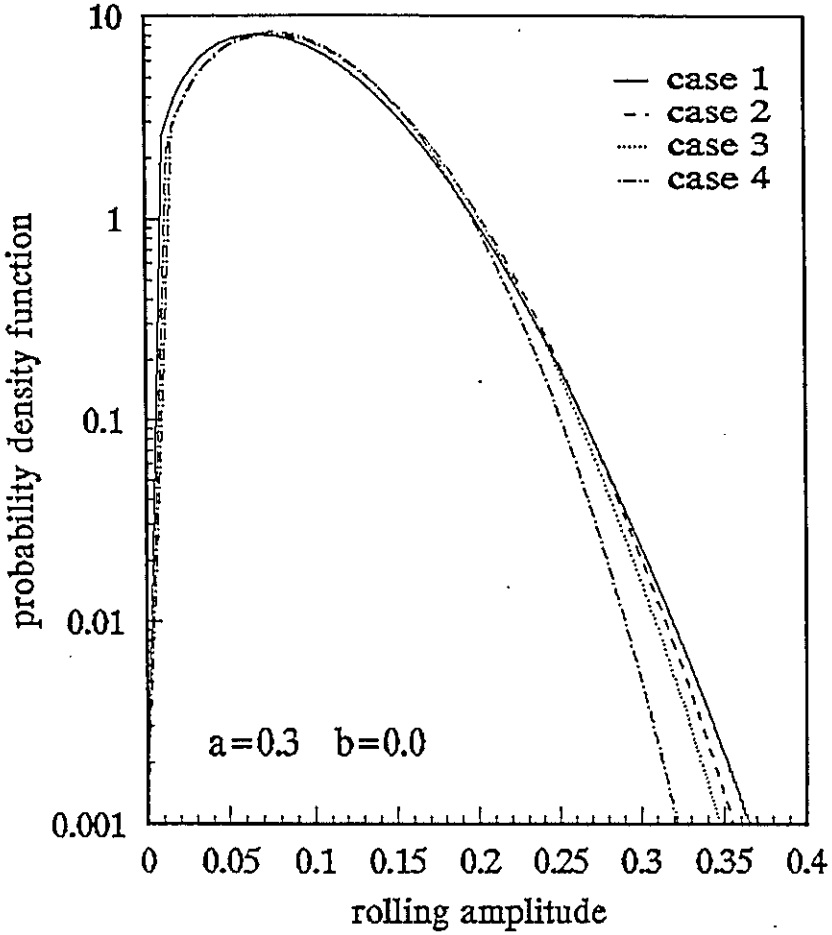
10
1
0.1
0.01
0.001
probability density function
case 1
case 2
case 3
case 4
a=0.3 b=0.0
0
0.05
0.1
0.15
0.2
0.25
0.3
0.35
0.4
rolling amplitude

Fig. 3

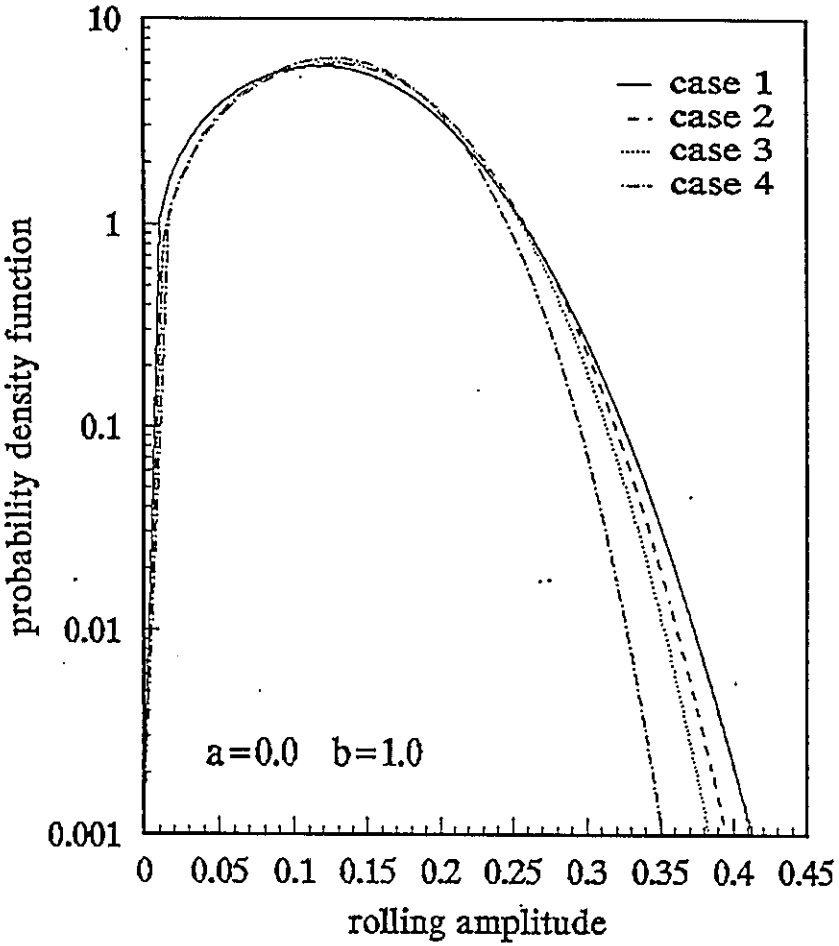
10
1
0.1
0.01
0.001
probability density function
case 1
case 2
case 3
case 4
a=0.0 b=1.0
0 0.05 0.1 0.15 0.2 0.25 0.3 0.35 0.4 0.45
rolling amplitude

Fig. 4

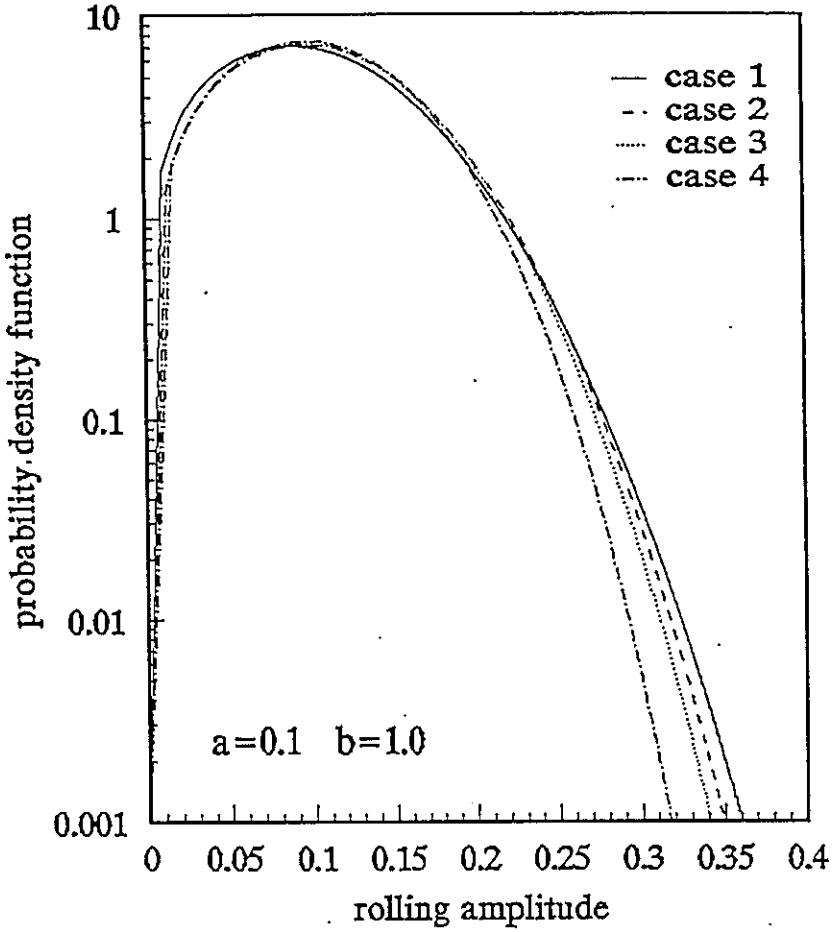
10
1
0.1
0.01
0.001
probability density function
case 1
case 2
case 3
case 4
a=0.1 b=1.0
0
0.05
0.1
0.15
0.2
0.25
0.3
0.35
0.4
rolling amplitude

Fig. 5

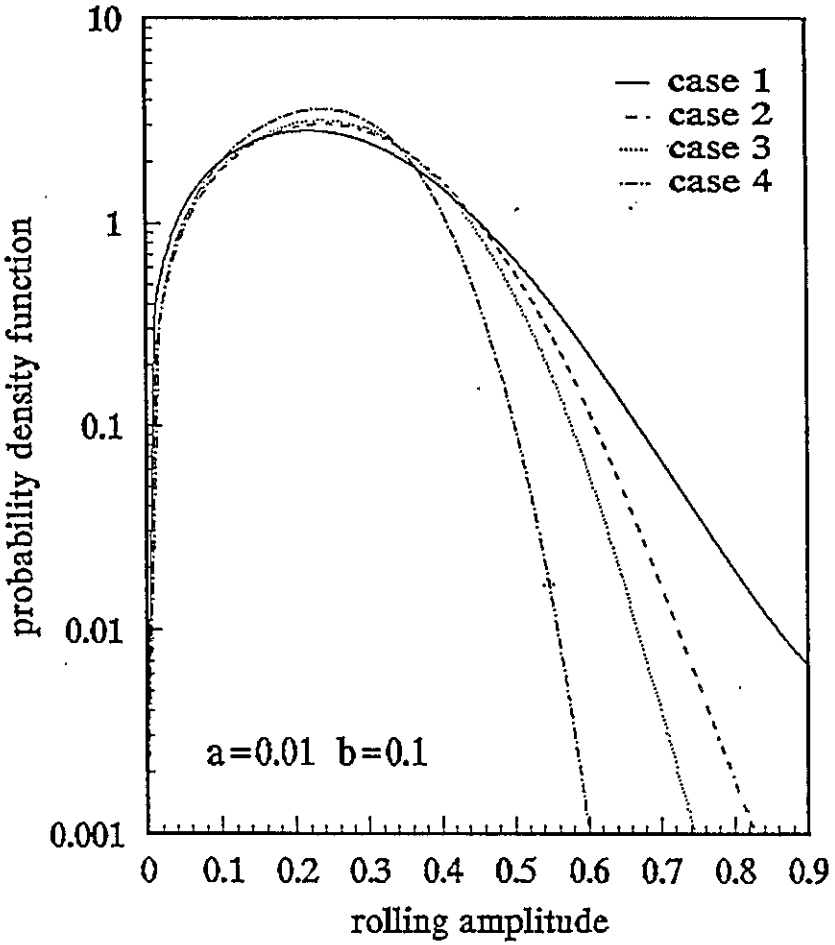
10
1
0.1
0.01
0.001
probability density function
case 1
case 2
case 3
case 4
a=0.01 b=0.1
0 0.1 0.2 0.3 0.4 0.5 0.6 0.7 0.8 0.9
rolling amplitude

FIG. 6 ROLL. a=0.3 C=1 C3=.2 C5=-1.2

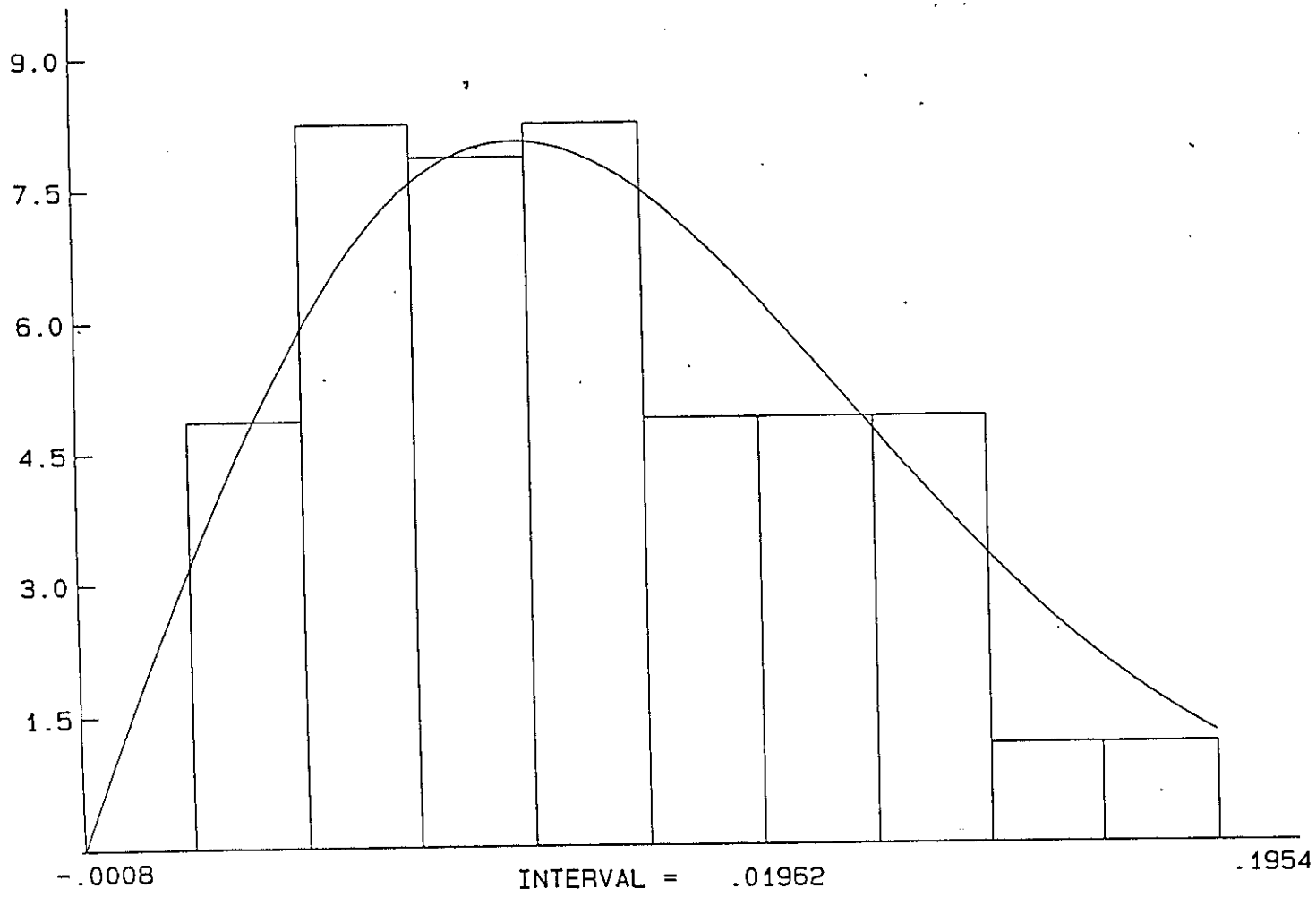

FIG. 7 ROLL a=.3 b=0 C=1 C3=4 C5=-5

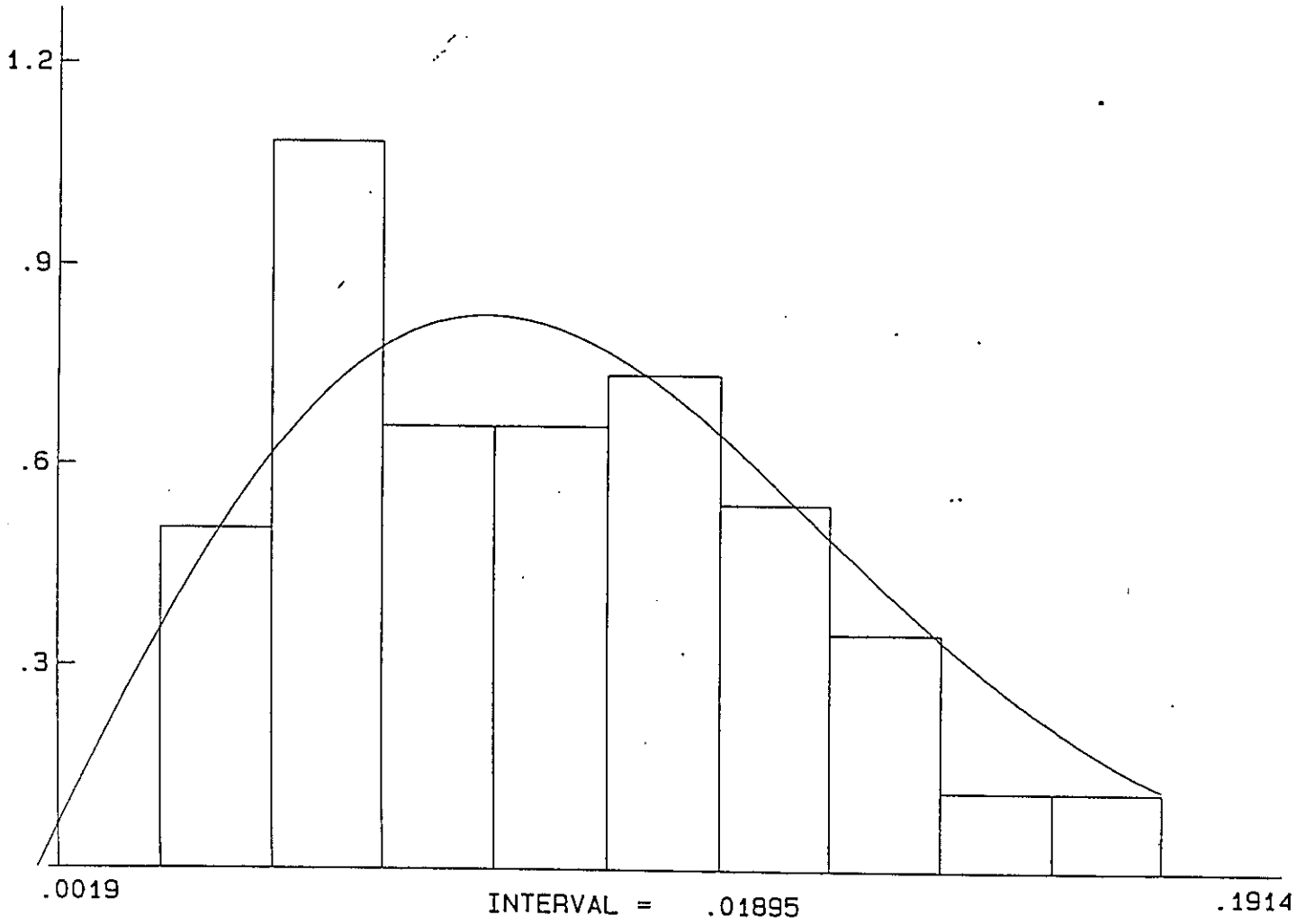

Fig 8a : ROLL H=3 T=8 GM=.25 NO DECKWATER

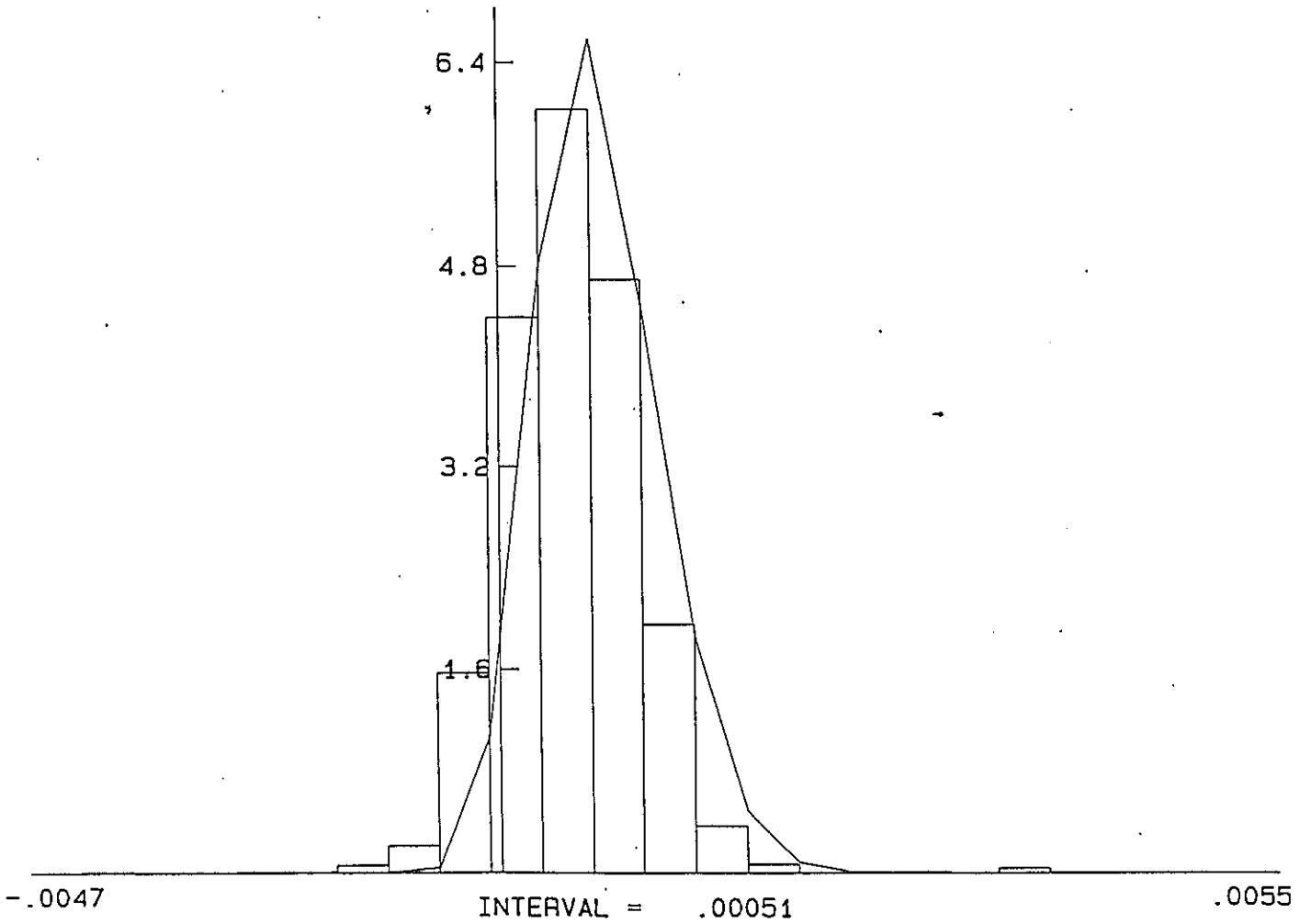

Fig 8b : ROLL H=3 T=8 GM=.25 HD=.4

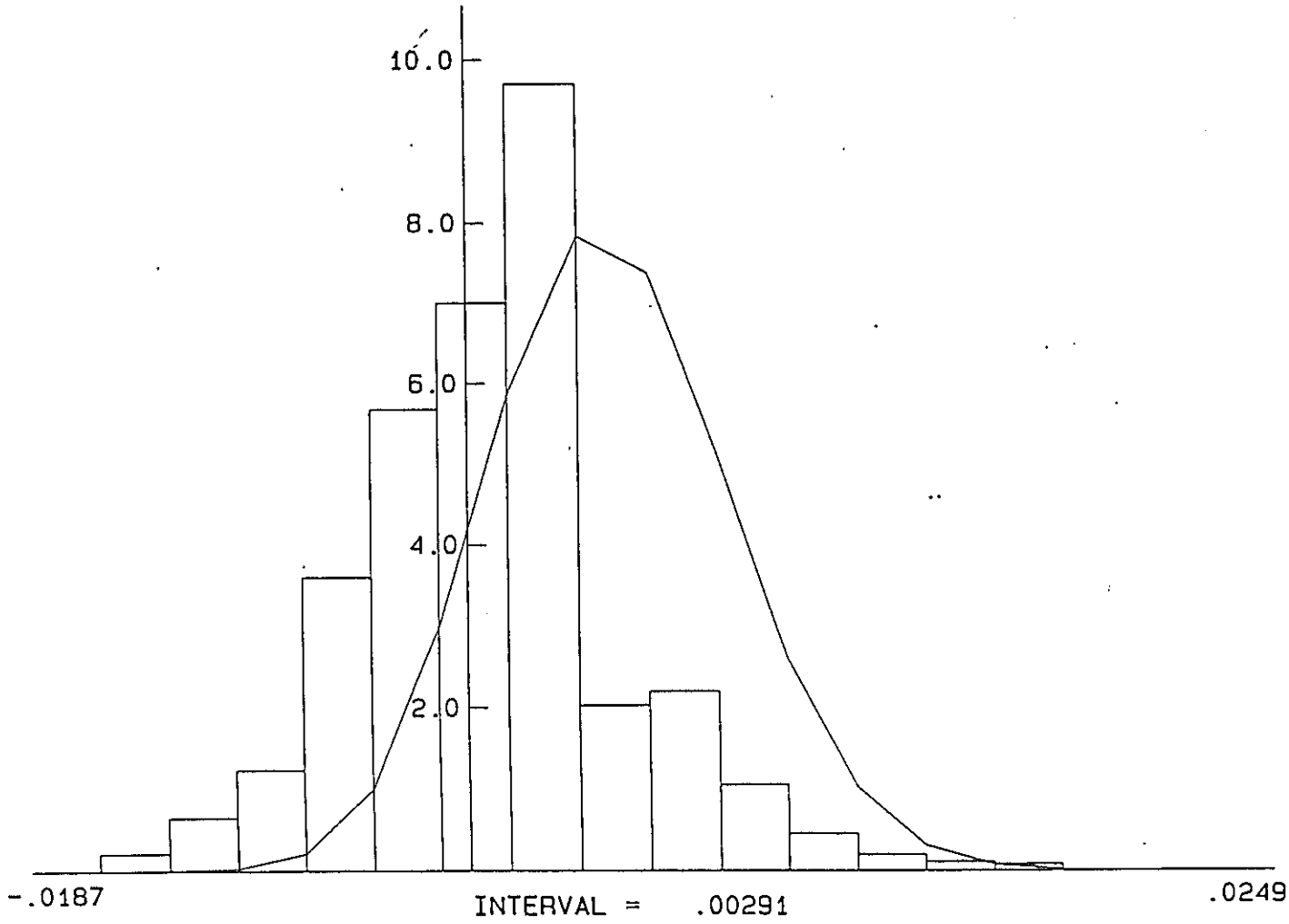

Fig 9a : ROLL H=3 T=8 GM=.5 NO DECKWATER

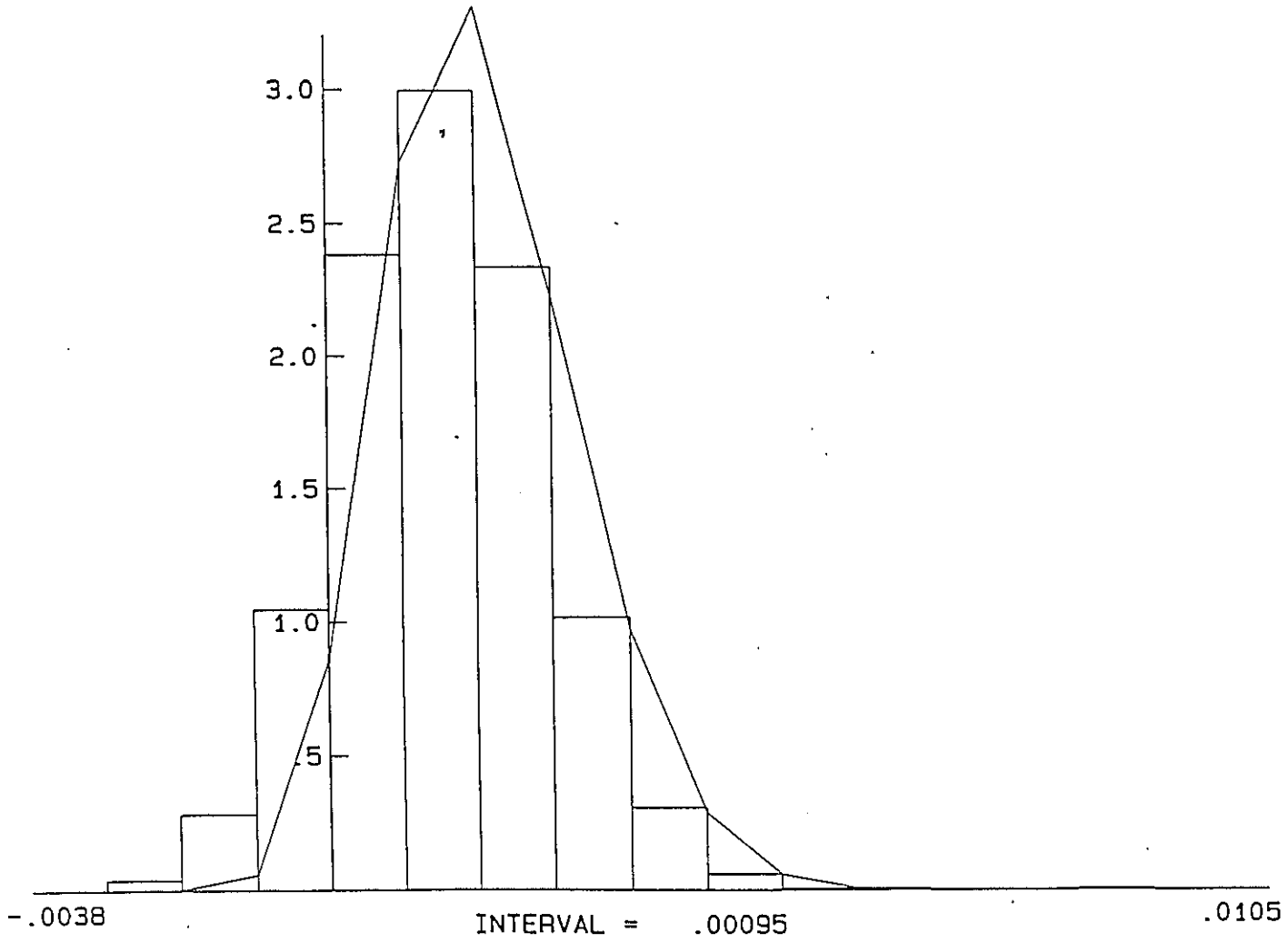

Fig96 : ROLL H=3 T=8 GM=.5 HD=.4

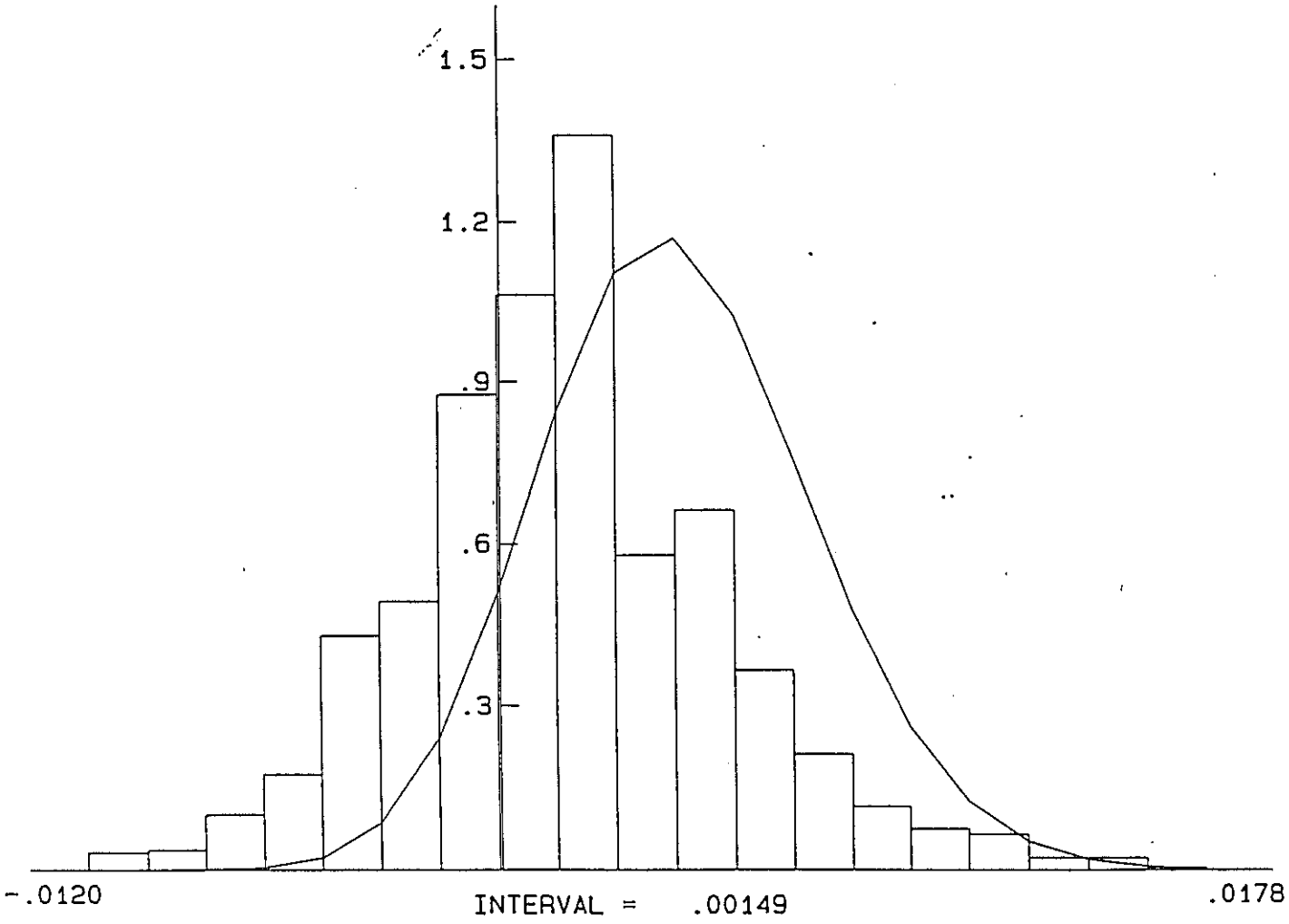

H=3 T=8 GM=0.5

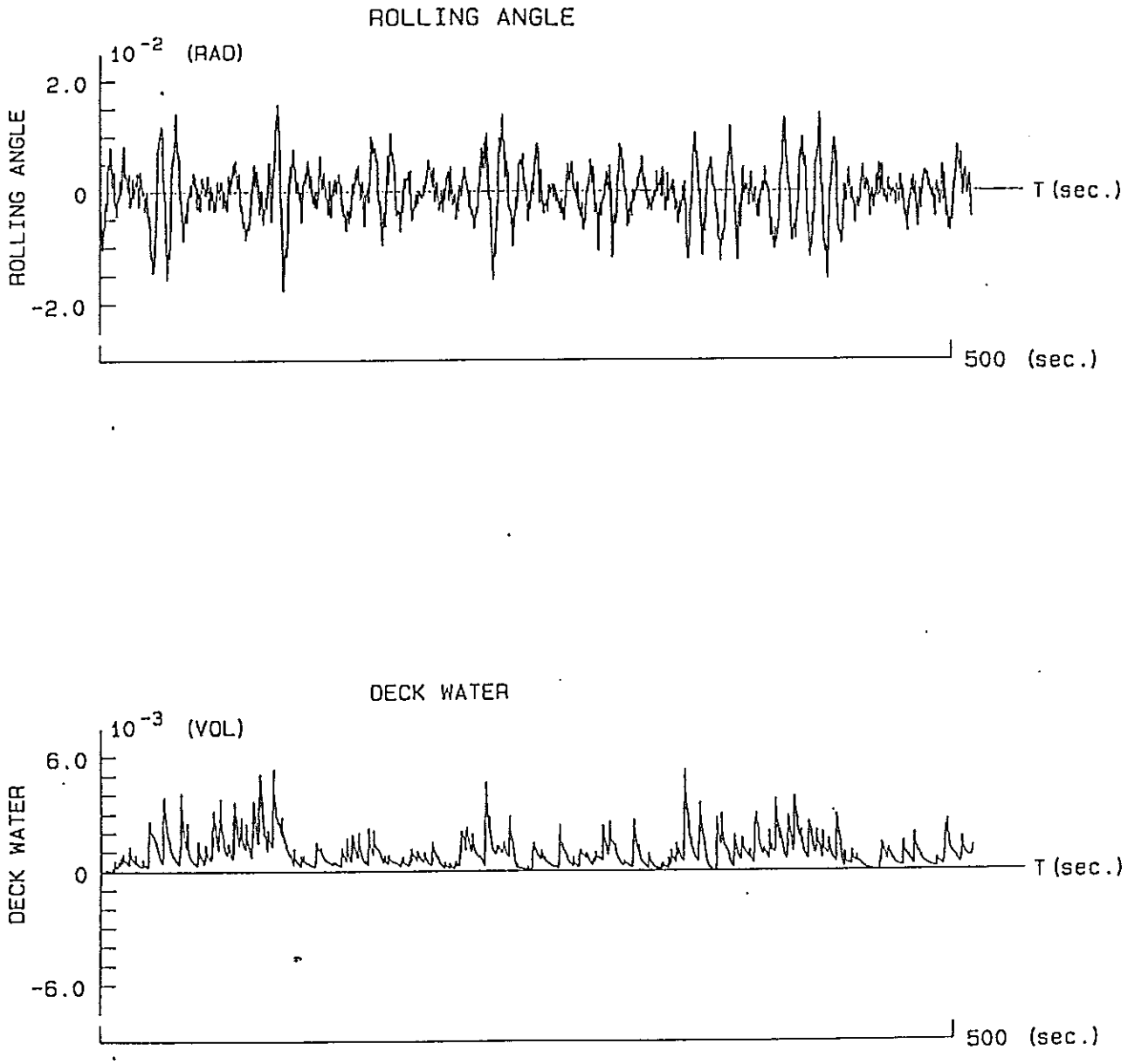

FIG10.

H=3 T=8 GM=0.25

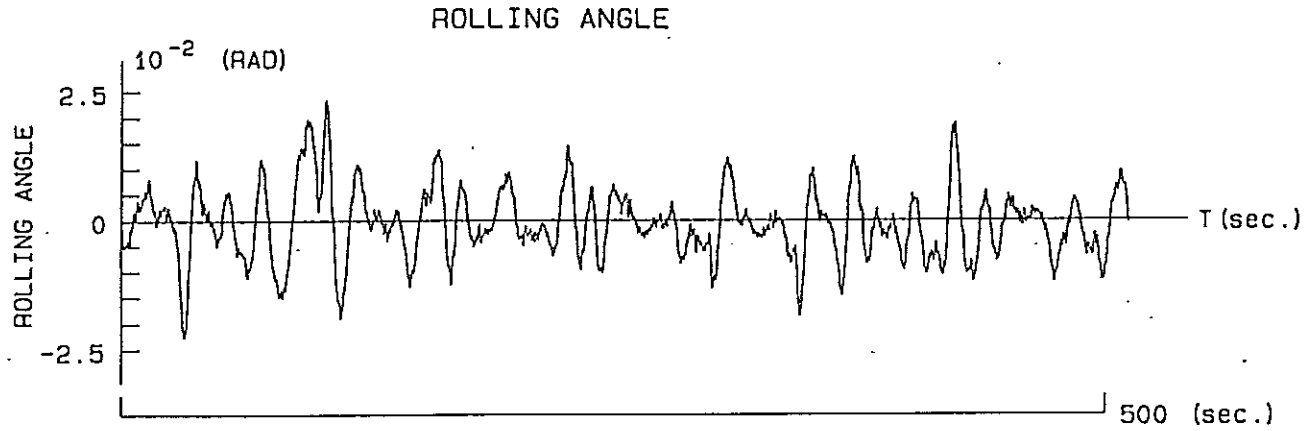

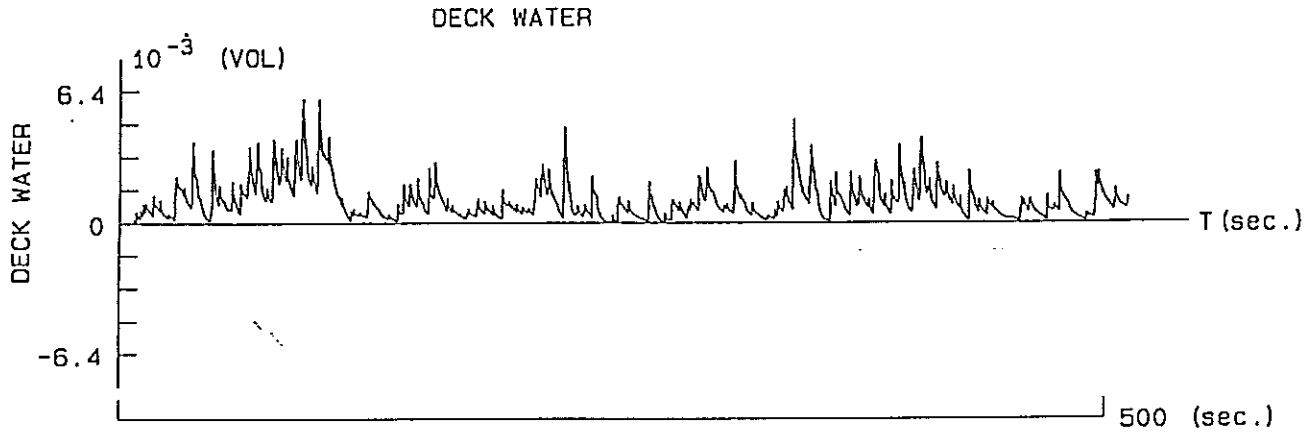

Fig 11

Transverse Stability of Ships in Waves in Consideration of Ship Generated Waves

Z. J. Huang C. C. Hsiung
Centre for Marine Vessel Design and Research
Technical University of Nova Scotia
Halifax, Nova Scotia, Canada B3J 2X4
Tel:(902)420-7954; Fax:(902)423-6711

Abstract

The righting moment of a ship in waves is computed with the consideration of the incident and diffracted waves around the ship, and the steady wave due to the ship advancing at a constant speed. The three-dimensional panel method is employed for the wave field and the righting moment computation. The influence of wave length, heading, frequency and amplitude of the incident wave as well as the effects of the ship's forward speed and the ship motion are studied. It has been found that the righting moment of a ship in waves is related to all these factors. It can not be adequate if the righting moment is only computed in calm water or with the consideration of the incident waves. Results for various conditions are presented and discussed.

Introduction

For the large amplitude ship motion in waves, including ship capsizing in severe seas, the righting moment should be determined by the instantaneous ship position and actual wave field around the ship. Two factors that resist capsizing are the viscous roll damping and the righting moment. Therefore, accurate computation of the righting moment in the actual wave field is critical to the safety analysis of ships.

The wave field around the ship consists of incident waves and ship generated waves. The ship generated waves are radiated waves caused by the ship oscillatory motion; diffracted waves due to the interference of the ship hull to incident waves; and steady waves due to the ship advancing in water with a constant speed. When only the incident wave is considered, it has been found that the transverse stability of a ship in the incident wave is quite different from that in calm water. For instance, the righting moment is dramatically reduced when a ship is positioned at the wave crest in a following sea [1] [2].

The righting moment was also computed using the instantaneous wetted surface in an undisturbed incident wave field in the simulation of ship motion and capsize [3]. However, the ship generated waves should not be ignored for the transverse stability calculation, and their contribution needs to be carefully studied. In our computation, for instance, the diffracted wave accounts for 40% of the total wave amplitude amidships at beam seas and 30% at quartering seas when the wave length equals the ship length. Also, the steady wave may increase the righting moment if its trough is amidships.

The steady waves, or the so-called Neumann-Kelvin waves, and the diffracted waves are calculated by using the three-dimensional panel method. The radiated waves are not considered at the present study. The ship hull including the deck space is approximated by discretized panels. Since the panel method is used, the ship form can be slender or full and there is no restriction on the wave direction. The righting moments are calculated by taking account of the incident

wave, steady wave, diffracted wave, sinkage and trim at different wave headings, wave lengths and forward speeds.

Since the wave field around the ship and the actual ship position in waves are varying with time, the calculation is carried out in the time domain with various relative positions of the ship to the incident wave crests. The ship's hull and deck space are discretized into panels. At each time step, the actual wetted hull surface is calculated based on the wave surface and the ship position. Then, the pressure on all the wetted panels is computed.

The deformed wave elevation is not symmetrical to the longitudinal centerplane, therefore, unlike in the calm water situation the righting moment no longer becomes an odd function about the ship's upright position. In the sense of hydrostatics, the stable equilibrium position corresponding to zero righting moment is obtained at a heel angle leaning towards the incoming wave.

The computation of the traditional righting lever in calm water is carried out with heeling angles at the static equilibrium between the ship weight and its buoyancy. However, when the ship is in waves its position is governed by the dynamic equilibrium, i.e. the equation of ship motion. Hence, the computation should be performed for an arbitrary position due to the ship motion.

In the following sections, the computational procedure is described. The computed righting moment vs. heel angle is presented with the following parameters: wave direction, wave length, and ship forward speed, as well as relative positions of the ship to the incident wave crest, the steady wave and the diffracted wave. The relationship between the righting moment and the above-mentioned parameters, and the effects of steady and diffracted waves, sinkage and trim on the transverse stability are discussed.

Methodology

Three coordinate systems are adopted in the present studies, as shown in Fig.1. Let $OXYZ$ be the space-fixed coordinate system with the OXY-plane on the calm water surface and the OZ-axis being positive upwards. The second coordinate system $oxyz$ is a moving system which moves with the same arbitary horizontal excursions as that of the center of gravity of the ship. In the present studies, we consider the ship has a constant forward speed U in the OX-direction. The oxy-plane always coincides with the OXY-plane, the ox-axis is in the same direction as the OX-axis and the oz-axis is positive upwards. The third coordinate system $o_1x_1y_1z_1$ is ship-fixed with the $o_1x_1y_1$-plane coincides with the OXY-plane when the ship is in its static equilibrium position, and the o_1z_1-axis is positive upwards.

It is convenient to describe the steady wave, incident wave and diffracted wave, and the oscillatory ship motion in the $oxyz$-system. The ship geometry and the righting moment will be expressed in the $o_1x_1y_1z_1$-coordinate system. To take account of the effect of large amplitude ship motion on the restoring moment, it is required to determine the new position of the ship at each time instant. The ship motions are represented by $(\xi_1,\xi_2,\xi_3,e_1,e_2,e_3)$, in which, (ξ_1,ξ_2,ξ_3) are the displacements off the origin o_1, and (e_1,e_2,e_3) are the Euler angles of the ship in space.

Making use of the Euler angles (e_1, e_2, e_3), the ship-fixed coordinate system and the steady moving coordinate system can be related as:

$$\begin{pmatrix} x \\ y \\ z \end{pmatrix} = \begin{pmatrix} \xi_1 \\ \xi_2 \\ \xi_3 \end{pmatrix} + [R] \begin{pmatrix} x_1 \\ y_1 \\ z_1 \end{pmatrix} \qquad (1)$$

where the transform matrix $[R_m]$ has been derived as follows:

$$[R] = \begin{pmatrix} c_2c_3 & s_1s_2c_3 - c_1s_3 & c_1s_2c_3 + s_1s_2 \\ c_2s_3 & s_1s_2s_3 + c_1c_3 & s_1s_2s_3 - s_1c_3 \\ -s_2 & s_1c_2 & c_1c_2 \end{pmatrix} \qquad (2)$$

and $c_i = cos(e_i)$, $s_i = sin(e_i)$; for $i = 1, 2, 3$. Also we have:

$$X = Ut + x; \quad Y = y; \quad \text{and} \quad Z = z \qquad (3)$$

where U is the ship's forward speed.

In this work, we assume that

a. the wave field can be represented by potential flow;

b. the wave field around the ship hull is the superposition of the incident wave, steady wave and diffracted wave;

c. in computing the righting moment, the ship is heeled to different angles, the wave field is not affected by the change of the heel angle; and

d. the ship's forward speed and heading are constant.

The incident wave elevation is given in the following form :

$$\begin{aligned}\zeta_i(x,y,t) &= a_i cos[k(X cos\beta + Y sin\beta) - \omega t + \epsilon_i] \\ &= a_i cos[k(x cos\beta + y sin\beta) - \omega_e t + \epsilon_i] \quad (4)\end{aligned}$$

where a_i is amplitude of the incident wave, ω is the incident wave frequency in $OXYZ$ system, ϵ_i is the phase lag, β is direction of the incident wave propagation with $\beta = 180^\circ$ as head seas, and $k = \frac{\omega^2}{g}$.

The canonical potential function of incident wave is given as:

$$\phi_i(x,y,z) = \frac{ig}{\omega} exp\{ik(x cos\beta + y sin\beta) + kz\} \quad (5)$$

By using the superposition principle, the velocity potential of the deformed wave field can be given as follows:

$$\begin{aligned}\Phi(x,y,z,t) &= \phi_s(x,y,z) \\ &+ a_i(\phi_i(x,y,z) + \phi_d(x,y,z))e^{-i\omega_e t} \quad (6)\end{aligned}$$

where ϕ_s is the steady wave potential and ϕ_d is the diffracted wave potential.

The steady wave

A steady wave system around the ship is generated as the ship is advancing in calm water at a steady forward speed. The velocity potential of the steady wave can be expressed as:

$$\phi_s(x,y,z) = -Ux + \bar{\phi}(x,y,z) \quad (7)$$

where $\bar{\phi}$ can be determined by solving the Neumann-Kelvin problem:

$$\nabla^2\bar{\phi}(x,y,z) = 0, \quad \text{in the fluid domain} \quad (8)$$

$$(\frac{\partial^2}{\partial x^2} + \frac{g}{U}\frac{\partial}{\partial z})\bar{\phi}(x,y,z) = 0, \text{on } z = 0 \quad (9)$$

$$\frac{\partial\bar{\phi}(x,y,z)}{\partial n} = Un_1 \quad \text{for } (x,y,z) \text{ on } \bar{S} \quad (10)$$

and the radiation condition

$$\bar{\phi}(x,y,z) = \begin{cases} o(1/R) & \text{for } x > 0 \text{ and } R \to \infty \\ O(1/R) & \text{for } x < 0 \text{ and } R \to \infty \end{cases} \quad (11)$$

where $R = \sqrt{x^2 + y^2}$.

By applying the second Green identity, the solution of the above problem can be found in the form:

$$\begin{aligned}\bar{\phi}(x,y,z) &= \frac{1}{4\pi}\int\int_{\bar{s}} \sigma_s(Q)G_s(P,Q)ds \\ &- \frac{U}{4\pi g}\oint_c \sigma_s(Q)G_s(P,Q)dl \quad (12)\end{aligned}$$

where σ_s is the source strength distributed on the hull surface, G_s is the three-dimensional Green function of the Neumann-Kelvin problem, $\bar{s}$ is the mean wetted hull surface below the waterline and c is the waterline contour, $P(x,y,z)$ is the field point, and $Q(x,y,z)$ is the source point. Furthermore, if the ship has a transom, vortex analysis is also carried out for the steady wave system [4].

Once the potential function has been solved, the steady wave elevation can be calculated from:

$$\zeta_s(x,y) = -\frac{U}{g}\frac{\partial\bar{\phi}(x,y,z)}{\partial x} \quad (13)$$

The computer program developed in [4] has been employed to compute the steady wave surface in this work.

The diffraction wave

As a ship encounters with the incident wave, the wave will be diffracted by the ship hull. In this paper, the work in [5] is further extended to compute the diffracted wave elevation. The three-dimensional panel method is employed in the computation.

The diffracted wave potential is solved from the following boundary value problem.

$$\nabla^2\phi_d(x,y,z) = 0 \quad \text{in the fluid domain} \tag{14}$$

$$\left[(i\omega_e - U\frac{\partial}{\partial x})^2 + g\frac{\partial}{\partial z}\right]\phi_d(x,y,z) = 0 \quad \text{on } z=0 \tag{15}$$

$$\frac{\partial\phi_{kj}}{\partial n} = -\frac{\partial\phi_d(x,y,z)}{\partial n} \text{ on } \bar{s} \tag{16}$$

and the radiation condition at far field.

The solution of diffracted wave potential is expressed in terms of the three-dimensional Green function:

$$\phi_d(x,y,z) = \frac{1}{4\pi}\int\int_{\bar{s}}\sigma_d(Q)G_d(P,Q)ds \tag{17}$$

where σ_d is the source strength distributed on $\bar{s}$, and G_d is the Green function in the unsteady diffraction problem. $P(x,y,z)$ is the field point, and $Q(x,y,z)$ is the source point.

After solving ϕ_d, the wave elevation around the ship hull at time t will be calculated from:

$$\zeta_d(x,y,t) = -\frac{1}{g}\frac{\partial\phi_d(x,y,0,t)}{\partial t} + \frac{U}{g}\frac{\partial\phi_d(x,y,0,t)}{\partial x} \tag{18}$$

The restoring moment

Once the steady and diffracted waves are computed, the wave elevation around the ship hull is constructed as follows:

$$\zeta(x,y,t) = \zeta_s(x,y) + \zeta_i(x,y,t) + \zeta_d(x,y,t) \tag{19}$$

The total pressure including the static and dynamic componemts is:

$$p(x,y,z,t) = -\rho g(z-\zeta) - \rho\frac{\partial\Phi}{\partial t} - \frac{1}{2}|\nabla\Phi|^2 \tag{20}$$

In the ship motion analysis, the righting moment is the roll restoring moment which is caused by the hydrostatic pressure related to the ship motion displacement and the water surface elevation. The dynamic pressure of the incident wave field gives contribution to the Froude-Krylov force, the dynamic pressure of the diffracted wave produces the diffraction force, and the dynamic pressure of the steady wave yields the steady force. The isobaric surface can not be given explicitly in the deformed waves.

For an arbitrary ship motion, the hydrostatic pressure at point (x_1, y_1, z_1) is:

$$\begin{aligned} p_s(x_1,y_1,z_1,t) = -\rho g[&\xi_3 - x_1 sin(e_2) \\ &+y_1 sin(e_1)cos(e_2) \\ &+z_1 cos(e_1)cos(e_2) - \zeta(x,y,t)] \end{aligned} \tag{21}$$

where

$$\begin{aligned} x = \; &\xi_1 + x_1(cos(e_2)cos(e_3) \\ &+y_1(sin(e_1)sin(e_2)cos(e_3) \\ &-cos(e_1)sin(e_3)) \\ &+z_1(cos(e_1)sin(e_2)cos(e_3) \\ &+sin(e_1)sin(e_2)) \end{aligned} \tag{22}$$

$$\begin{aligned} y = \; &\xi_2 + x_1 cos(e_2)sin(e_3) \\ &+y_1(sin(e_1)sin(e_2)sin(e_3) \\ &+cos(e_1)cos(e_3)) \\ &+z_1(sin(e_1)sin(e_2)sin(e_3) \\ &-sin(e_1)cos(e_3)) \end{aligned} \tag{23}$$

With the above transformation, the wave elevation corresponding to point (x_1, y_1, z_1) can be calculated in the $oxyz$-system.

The nonlinear restoring moment about the centre of gravity of the ship is calculated by integrating the pressure distribution over the instantaneous wetted ship hull beneath the wave surface:

$$\begin{aligned} M_r(t) = -\int\int_{s(t)} &p_s(x_1,y_1,z_1,t) \\ &((y_1-y_{1g})n_3 - (z_1-z_{1g})n_2)ds \end{aligned} \tag{24}$$

where $s(t)$ is the instantaneous wetted surface, (x_{1g}, y_{1g}, z_{1g}) is the center of gravity of the ship in

the ship-fixed coordinate system, and (n_1, n_2, n_3) is the unit outward normal of the ship hull in the ship-fixed coordinate system. Both the ship motion displacements and wave elevation are involved in computing the righting moment.

Results and Discussion

The body plan of a ship hull, taken from Ref. [6], is shown in Fig. 2, and is used as the computational example for illustration. We did not include its bulwark in computation. The ship length is $L = 15^m$, beam $B = 3^m$, draft $T = 1.2^m$ and displacement $\Delta = 37.8^{tons}$, respectively.

The deformed wave amplitudes amidships are calculated for different wave frequencies. The computed results are compared with the experimental data given in Ref.[6]. The deformed wave amplitude amidships in beam seas is shown in Fig. 3, where the amplitude is expressed in the dimensionless form, which is defined as:

$$\bar{\eta} = \frac{\text{amplitude of deformed wave}}{\text{amplitude of incident wave}} \qquad (25)$$

The value of $\bar{\eta}$ being greater than one means that the incident wave is augmented. It can be seen that the wave elevation at the weather side (W.S.)is higher than that at the lee side (L.S.). The ship hull is like a breakwater and provides a relative calm water area at the lee side. Since the wave length decreases as the frequency increases, the wave motion is limited to a thin layer of water close to the free surface in short waves. Incident waves will be almost completely reflected at the weather side at high frequency. Hence, at the lee side, smaller wave motion amplitudes are obtained at higher wave frequencies. These phenomena can be observed in experimental measurements as well as in numerical computation. The computed deformed wave amplitudes in oblique sea with $\beta = 120^o$ are also shown in Fig.4. The comparison between the computed results and experimental data shows satisfactory agreement.

Computations have been carried out for $\lambda/L = 1.0$, $a_i/\lambda = 0.02$, $\beta = 15$ degrees and $F_n = 0.0$, to investigate the effects of incident and diffracted waves on the righting moment. Note that the incident wave amplitude is taken as $a_i = 0.3^m$ in all the computations in this paper.

The nondimensional x-coodinate of the incident wave crest is defined as:

$$\xi = \frac{x_{crest}}{L} \qquad (26)$$

where x_{crest} is the x-coordinate of the incident wave crest in the $oxyz$-system; θ is the heeling angle of the ship in degrees; and the nondimensional righting moment is defined as:

$$\bar{M} = \frac{M_r}{\Delta B} \qquad (27)$$

where B is the beam of the ship and Δ is the weight of the ship.

In the following figures, negtive righting moment at a positive heel angle (the ship heels to the starboard side) indicates that the righting moment will pull the ship back to its stable equilibrium position. This definition is the same as in the ship motion analysis.

Fig. 5 shows the righting moment in the incident waves (i.w.). The righting moment reaches a maximum value when the wave trough is amidships, and reaches the minimum value when the wave crest is amidships. This indicates that the wave location relative to the ship has a significant effect on the righting moment. The righting moment in calm water is also presented for comparison.

The three-dimensional plot for the righting moment in incident waves is shown in Fig. 6. The righting moment at various wave crest locations can be found in this figure. The variation of the righting moment as the wave crest travels from stern to stem can be clearly observed. With the energy balance analysis [7], this plot can provide a deeper insight into the ship's capability to avoid capsizing in waves.

Fig. 7 shows the righting moment with both the incident and diffracted waves (d.w.). At the wave crest location $\xi = 0.4$, the maximum righting moment is about 15 % greater than that in the

incident wave. The righting moment is no longer an odd function of the heel angle.

The three-dimensional plot of righting moment with incident and diffracted waves is given in Fig. 8. It can be seen that, unlike in Fig. 5 where only the incident wave is considered, the righting moments for the wave crest at stern and stem are different. When the wave crest is at $\xi = 0.4$ the righting moment is greater than that for the wave crest at the stem.

The effect of the wave heading on the righting moment is given in Fig. 9. All the wave conditions, except the wave heading, are the same as above and both the incident and diffracted waves are considered. The ship hull used in the computation is longitudinally symmetrical about the midship, so that, in the incident wave, the righting moment is an odd function of heel angle and the stable equilibrium is at $\theta = 0^0$ if $\beta \neq 90°$. However, when the diffracted wave is considered, the righting moment curve shifts and the stable equilibrium position is at a heel angle towards the incoming wave instead of leaning away from the incoming wave. This is different from the righting moment in calm water and in incident waves.

The effect of wave length is shown in Fig.10, where two wave lengths $\lambda/L = 0.5$ and $\lambda/L = 1.0$ are chosen. At $\lambda/L = 0.5$, when the ship heels to the port-side, the righting moment is greater than that as the ship heels to the starboard side. The righting moments in these two waves are quite different.

In order to investigate the steady wave (s.w.) effect, the steady wave field is computed at Froude number $F_n = 0.2$. In Figs. 11 to 15, $a_i/L = 0.02$, $\lambda/L = 1.0$, and $\beta = 15°$. The righting moments in calm water and in a steady waves are compared and shown in Fig. 11. For this particular ship at $F_n = 0.2$, the steady wave causes 8 % increase in the righting moment. This effect depends on the steady wave elevation and its crest location, and therefore ship speed. Since the steady wave is transversely symmetrical about the ship's longitudinal centre plane, the righting moment in steady wave is an odd function of the heel angle.

Fig. 12 shows the three-dimensional plot of the righting moment with all three waves considered. The results with all three waves at $\xi = 0.4$ and with only the steady waves are shown in Fig. 13 for comparison. When the ship is advancing with a constant speed, the maximum righting moment in waves increases about 10 %.

In consideration of these three waves, the righting moment is computed for the ship with and without sinkage and trim (s.+t.). The sinkage and trim used in the computation are -0.05 *m* and -2.0 *degrees*, respectively. The ship's volume displacement increases for the given sinkage and trim. Since the righting moment directly depends on the displacements of ship motions (or the ship position in space), the effects of sinkage and trim will also indicate the effects of the ship motions in waves. Therefore, the precedure for righting moment computation can be directly applied to the ship motion analysis and the dynamic stability studies. The three-dimensional plot is given in Fig. 14 and comparison of results with and without sinkage and trim is shown in Fig. 15. It can be seen that in the case of sinkage= -0.05^m and trim= -2.0^{deg}, the righting moment is increased.

From the above computational examples, we find that the righting moment in waves is related to many factors, such as the wave field, loading conditions and ship motions. It is different from the righting moment in calm water, where one righting lever curve is used to represent the ship's capability to avoid capsizing. In this paper, we only present the computed righting moment for one ship for two wave lengths and two wave headings to illustrate the effects of diffracted wave, steady wave and the sinkage and trim. However, more computations and analyses are required in order to evaluate the transverse stability of a ship with the computational procedure given in this paper.

Conclusions

A procedure for computing the righting moment of a ship in waves is illustrated in this paper. The computation takes into account of the incident

wave amplitude, wave length, wave direction, ship's forward speed, ship motion displacements in six-degrees-of-freedom. The effects of steady and diffracted waves are also studied. Computed results for a given ship are presented. However, these effects can be different from one ship to another. Therefore, in studying dynamic stability and ship safety in waves, all effects should be considered and carefully evaluated.

Some interesting phenomena have been revealed. For instance, if the diffracted wave is considered, the stable equilibrium position heels towards the incoming waves. The steady wave changes the maximum righting moment depending on where the steady wave crest located. From the computational example, it can be seen that the diffracted wave has a stronger influence on the righting moment than the steady wave, and makes the righting moment quite different from that in calm water or in incident waves.

The computational procedure can be directly applied to nonlinear ship motion analysis and dynamic stability studies. Further work is required to evaluate the ship's capability to avoid capsizing based on the time-varying righting moment as computed in this paper.

Acknowledgement

This work was supported by the Natural Sciences and Engineering Research Council of Canada. The authors are grateful to Dr. L. Cong for his help in computing the steady wave field.

References

[1] J. R. Paulling. The transverse stability of a ship in a longitudinal seaway. *Journal of Ship Research*, Vol. 4, No. 1, March 1961.

[2] M. Hamamoto and K. Nomoto. Transverse stability of ships in a following sea. In *The 2nd International Conference on Stability of Ships and Ocean Vehicles*, Tokyo, Japan, 1982.

[3] Jan O. de Kat. The numerical modeling of ship motions and capsizing in severe seas. *Journal of Ship Research*, Vol.34, No. 4, December 1990.

[4] L. Cong. *Application of Source Analysis to the Wave-Making Problem for Ships with or without a Transom Stern.* PhD thesis, Technical University of Nova Scotia, Halifax, Nova Scotia, Canada, 1992.

[5] C.C. Hsiung and Z.J. Huang. Comparision of the strip theory and the panel method in computing ship motion with forward speed. In *Symposium on Selected Topics of Marine Hydrodynamics*, St. John's, Nfld, August 1991.

[6] Shin Chanik. The prediction of the deck wetness in oblique waves and effect of shipping water on stability of ships. In *The 4th International Conference on Stability of Ships and Ocean Vehicles*, Naples, Italy, 1990.

[7] C. Kuo, et al. Ship stability criteria based on time-varying restoring moment. In *Safeship Seminar*, London, March 1982.

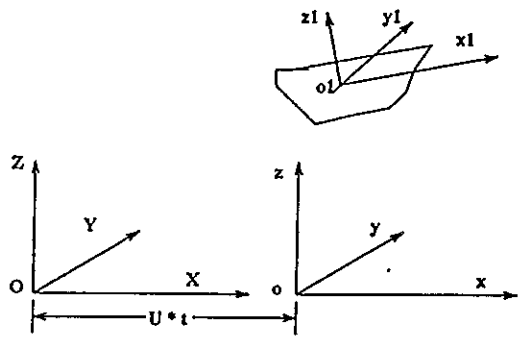

Figure 1: The Coordinate Systems

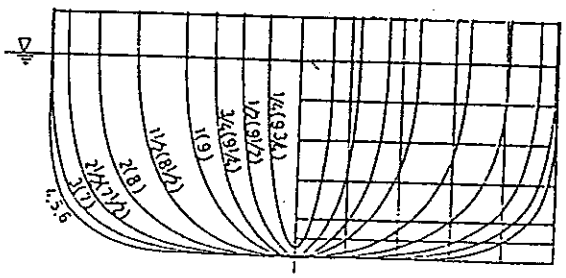

Figure 2: Body Plan of the Ship Hull

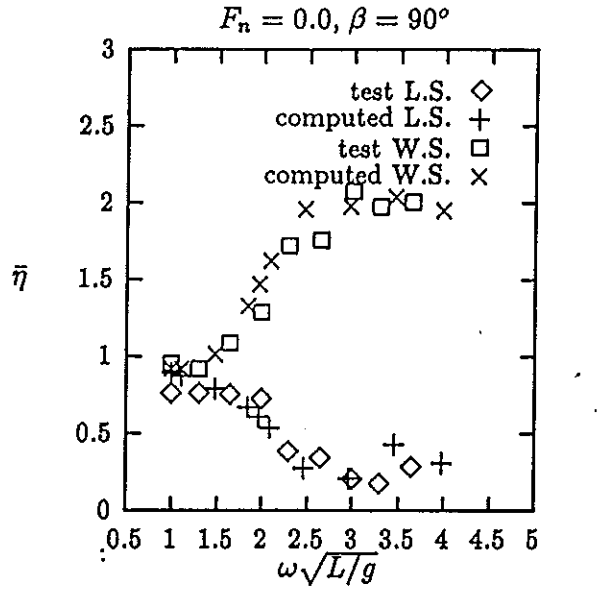

Figure 3: Deformed Wave Amplitude, $\beta = 90°$

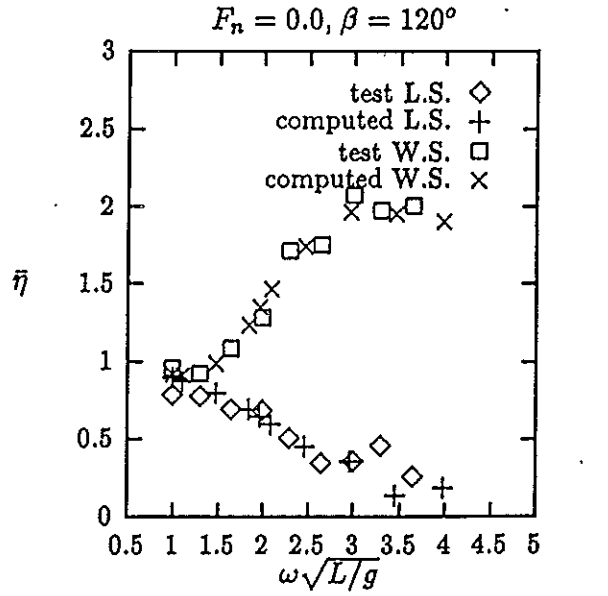

Figure 4: Deformed Wave Amplitude, $\beta = 120°$

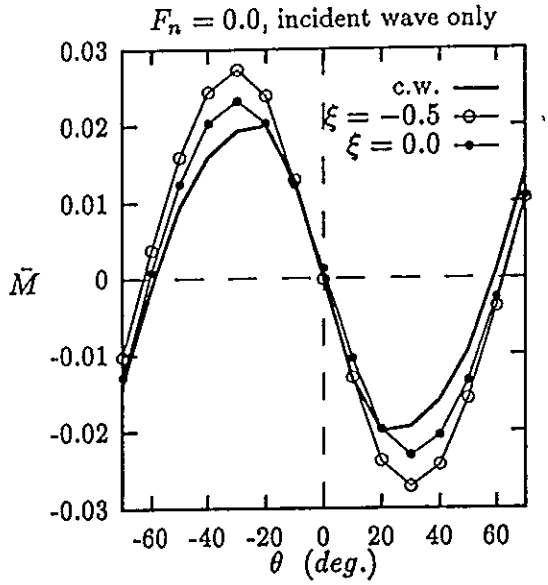

Figure 5: Effect of Incident Wave Location

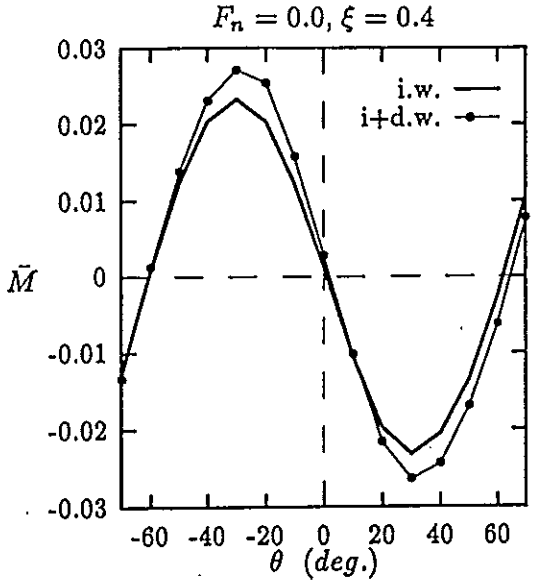

Figure 7: Effect of Diffracted Wave

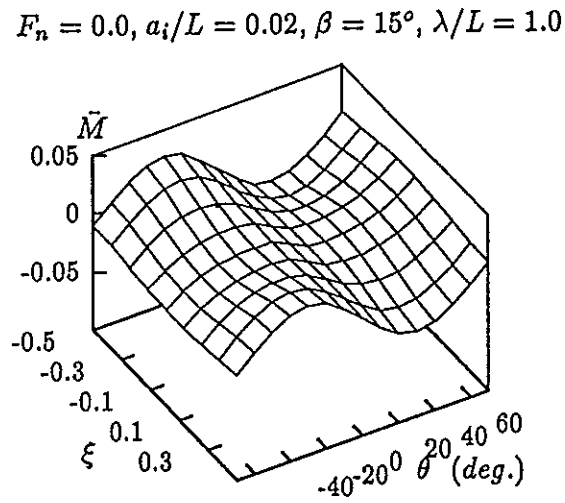

Figure 6: Rghting Moment in Incident Wave

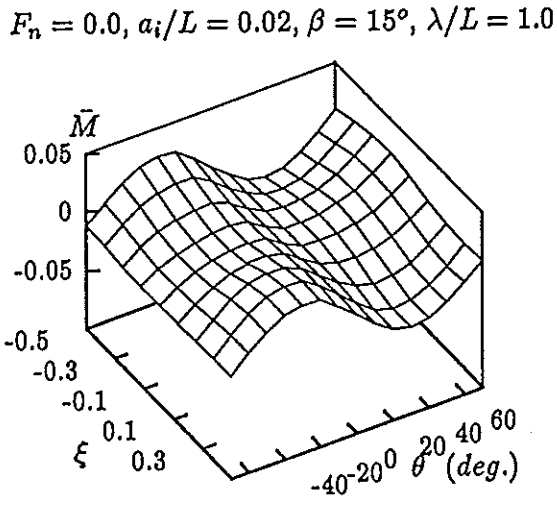

Figure 8: Righting Moment in I. and D. Waves

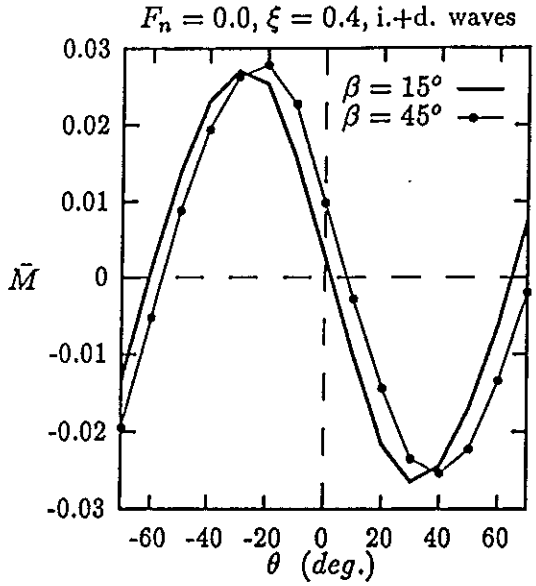

Figure 9: Effect of Wave Direction

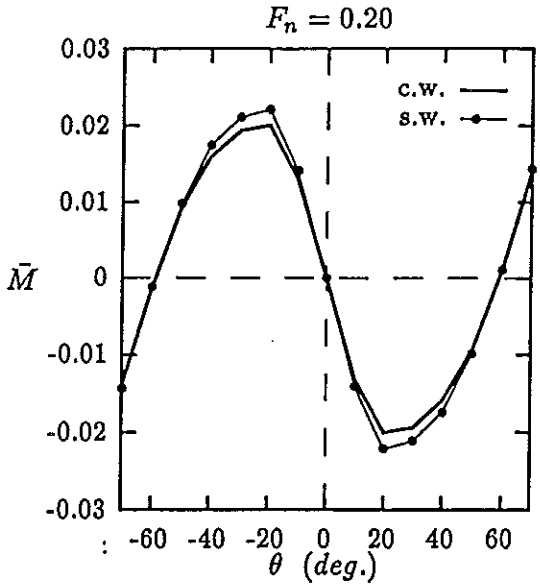

Figure 11: Effect of The Steady Wave

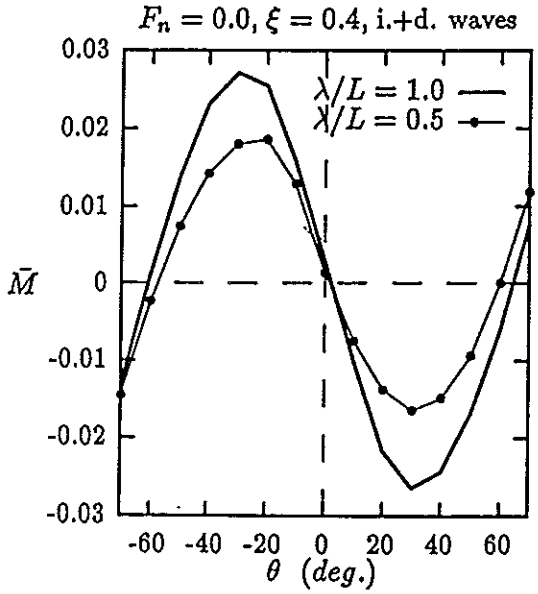

Figure 10: Effect of Wave Length

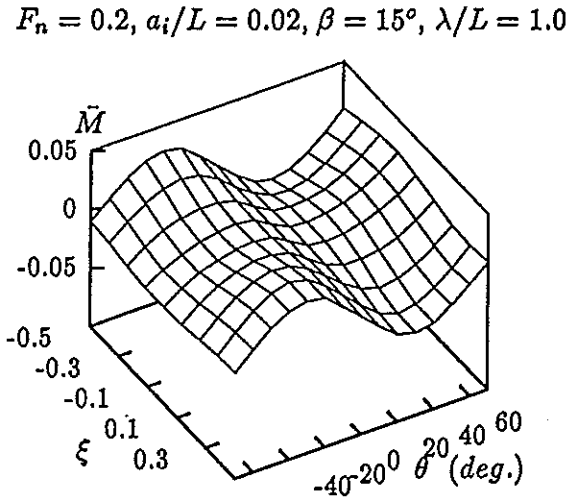

Figure 12: Righting Moment in S.+I.+D. Waves

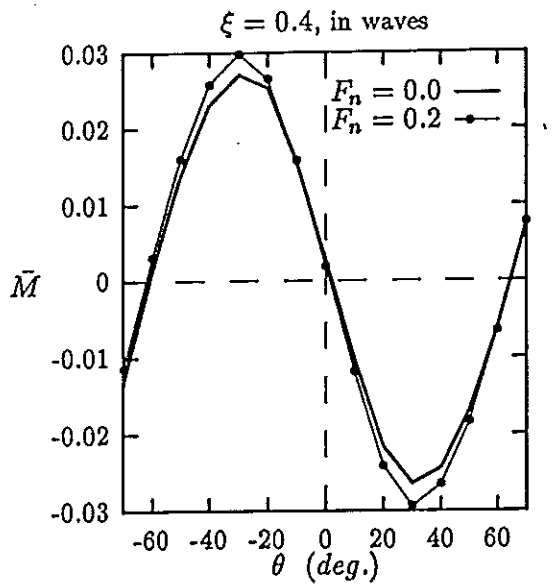

Figure 13: Effect of of the Forward Speed

$F_n = 0.2, a_i/L = 0.02, \beta = 15^o, \lambda/L = 1.0$

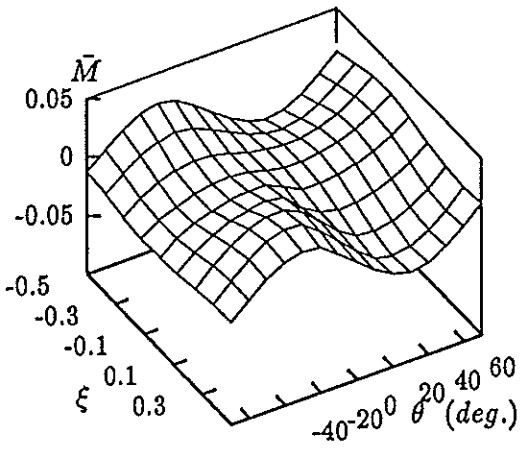

Figure 14: Righting Moment with Sinkage and Trim

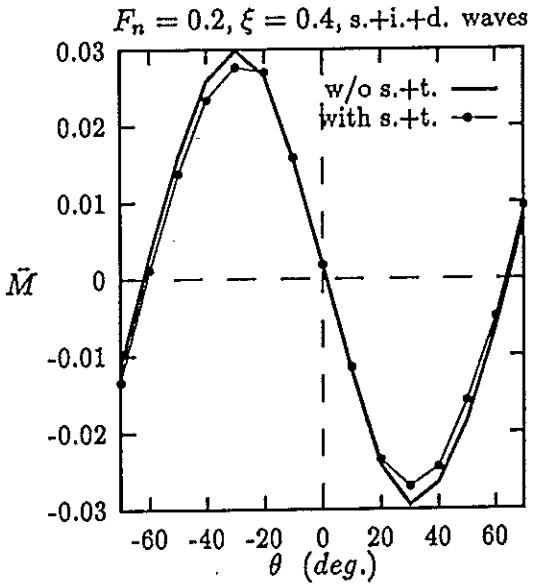

Figure 15: Effect of Singkage and Trim

Victor G. Sizov
Yuri L. Vorobyov

THE CORRELATION OF SHIP HULL FORM AND HER STATIC STABILITY DIAGRAM.

The correlation between the ship hull form and her static stability diagram (SD) is theoretically investigated. The value of metacentric height (MH), named "critical", at which SD changes from "hard" to "soft" type, is obtained. Three special ship hull forms are investigated (body of revolution, body whith vertical side walls and parallelepiped-form body), and exact formulae are gained. The approximate formulae to calculate "critical" MH for real hull forms are given. The inverse problem is investigated:. how to determine appropriate hull form for a given SD. Two special hull forms, that provide exact solutions, are studied, and the solution for bi-similar ship hull form is discussed in details.

Nomenclature.

B - beam of a vessel;
d - dynamic stability arm;
h_g - generalised metacentric height (MH);
h_1 - limiting value of MH;
h_o - initial MH;
I_x - waterline central moment of inertia for equivolumed inclinations;
$l = \frac{M_r}{\gamma\Delta}$ - static stability arm (restoring moment arm);
M_r - restoring moment;
r - metacentric radius;
r_1 - metacentric radius in the limiting case;
r_o - initial metacentric radius;
S - area of waterline;
T - draft of a vessel;
Z_g - elevation of the center of gravity over the moulded base;
γ - sea water specific weight;
Δ - displacement of a ship;
$\rho=\rho(\theta)$ - equation of horizontal cylinder hull form in polar co-ordinates;
θ - angle of inclination;
θ_s - angle, which corresponds to zero restoring arm $l(\theta_s)=0$.

1. INTRODUCTION.

The thorough study of the vessel's seaworthiness in connection with the navigational safety demonstrates deep correlation of her SD type and the behaviour of the vessel in confused seas. There are "soft" and "hard" types of SD. SD is of a "soft" type when the restoring moment increases with the angle of inclination slower, than it comes from the metacentric formula. In this case the curve $M_r(\theta)$ runs below

the tangent to this curve in the origin. If the curve $M_r(\theta)$ near the origin is arranged above the tangent mentioned, and the restoring moment increases with the angle of inclination quicker than linearly, in that case SD is of a "hard" type (Fig.1). The type of SD coincides with the characteristic properties of the behaviour of ships in waves. The amplitude-frequency curve (AF curve) has one frequency interval of unstable roll mode if SD is of a "soft" type. When SD is of a "hard" type, two such intervals may exist. Both ship hull form and MH value determine SD type. There are hull forms with the "soft" type of SD under all possible values of MH. One of such forms is the body of revolution. But for typical vessels the type of SD may be changed with variation of h_0 value. The value of h_0 corresponding to the change in SD type is called the limiting value h_1. The evaluation of h_1 for different hull forms is described in the following paragraph.

2. THE EVALUATION OF h_1.

Let us expanse $l(\theta)$ as an odd function in terms of θ:

$$l(\theta)=l'(\theta)+l'''(\theta)\frac{\theta^3}{3!}+l^{v}(\theta)\frac{\theta^5}{5!}+.. \tag{1}$$

From fig.2 it comes, that for any value of θ:

$$r(\theta)=h_g(\theta)+a+d(\theta), \qquad a=r_o-h_o \tag{2}$$

On differentiating of (2) twice with respect to θ and taking into consideration, that

$$d''(\theta)=l'(\theta)=h_g(\theta) \tag{3}$$

it comes:

$$l'(\theta)=r''(\theta)-h_g''(\theta)=h_g(\theta) \tag{4}$$

Repeating the differentiation two times, one gets

$$l''(\theta)=r''(\theta)-h_g(\theta) \tag{5}$$

$$l^{v}(\theta)=r^{iv}(\theta)+h_g(\theta). \tag{6}$$

From (1),(4),(5),(6) the series for $l(\theta)$ comes in a form

$$l(\theta) = h_o\theta + (r'' + -h_o)\frac{\theta^3}{3!} + (r^{IV} - r'' + h_o)\frac{\theta^5}{5!} +.. \tag{7}$$

According to (7), the type of SD depends on the sign of the difference $(r_o''-h_o)$:

if $r_o'' > h_o$, SD is of a "hard" type, and if $r_o'' < h_o$, SD is of a "soft" type. So for the limiting value of MH such an equality follows:

$$h_1 = r_o'' \tag{8}$$

From the hull symmetry one gets $r_o' = 0$, and for the metacentric radius, which corresponds to the limiting situation in accordance to (8), the approximate formula may be taken in a form:

$$r_1(\theta) = r_o + \frac{1}{2} h_1 \theta^2. \tag{9}$$

This is the equation of the limiting parabola for the function $r(\theta)$. So if the initial part of the curve $r(\theta)$, calculated using the theoretical hull lines, is above the parabola (9), real SD is of a "hard" type; in the opposite situation it is of a "soft" type (fig.3).

An approximate formula for h_1 comes from (9) in the case the initial part of the curve $r(\theta)(\theta \le 15^0)$ is known

$$h_1 = \frac{2}{\theta^2}[r(\theta) - r_o]. \tag{10}$$

3. CALCULATIONS FOR THREE SPECIAL HULL FORMS.

Let us investigate special hull forms, first being the hull with circular frames (body of revolution). In this case $r(\theta) \equiv r_o$ $r''(\theta) = 0$ and for any $h_o > 0$ $r'' - h_o < 0$ and SD is of a "soft" type. It is obvious, as soon as for a body of revolution SD is a sine function.

For a ship hull with vertical side walls

$$r(\theta) = \frac{r_0}{\cos^3\theta}, \quad r''(\theta) = 3r_0 \frac{1 + 3\sin^2\theta}{\cos^5\theta}, \quad r_0'' = 3r_0. \tag{11}$$

From (8) and (11) one has

$$h_1 = 3r_0. \tag{12}$$

So, SD is of a "soft" type, if $h_0 > 3r_0$, that practically cannot be realized for ordinary vessels. That is why for all vessels with vertical side walls SD is of a "hard" type. For the rectangular pontoon (parallelepiped) SD type depends on the value of Z_g. As soon as in this case

$$r_0 = \frac{B^2}{12T}, \quad h_1 = 3r_0 = \frac{B^2}{4T} \quad \text{and} \quad h_0 = \frac{1}{2}T + \frac{B^2}{12T} - Z_g,$$

SD will be of a "soft" type, if

$$\frac{Z_g}{T} < \frac{1}{2} - \frac{1}{6} \cdot \frac{B^2}{T^2}. \tag{13}$$

The boundary curve, dividing the zones of different SD types, is given on fig 4.

4. THE POSITION OF SIGNIFICANT SD POINTS.

The formula (2) for r(q) is useful for control of SD drawing and its significant points position. The curve $h(\theta)=r(\theta)-a-d(\theta)$ has to be drawn together with SD using the same coordinate system. The extrema and zeros of $h(\theta)$ curve locate the points of inflection and extrema of $l(\theta)$ curve. Both $l(\theta)$ and $h(\theta)$ curves are given on fig.5 for an ordinary bulk carrier.

The control mentioned is specifically desirable for SD with unusual form. Such an example is given on fig.6.

The trawler "Narfi" [1] from Iceland with the forecastle and the poop (Δ = 1440t, h_o = 0,69m) has SD with two maxima and one minimum. Evidently that $h(\theta)$ - curve helps to check the location of extrema and points of inflection in between.

5. THE INVERSE PROBLEM. SAMPLES.

Before formulating the inverse problem, it is essential to mention, that for the given value of a (2) two functions: $r(\theta)$ and $l(\theta)$ are synonymous and determined either by (2), or by Volterra type convolution integral equation:

$$\int_0^{\theta} r(\varphi)\cos(\theta-\varphi)d\varphi = l(\theta)+a\cdot\sin\theta \qquad (14)$$

In particular, if $r(\theta)$ is taken in a form: $r(\theta)=r_0+\frac{1}{2}h_0\theta^2$, for some range of the static stability arm $l(\theta)$ in this range is expressed by linear function $l(\theta)=h_0\theta$, and SD is a straight line. If SD is taken in a form of quadratic parabola:

$$l(\theta)=h_0(\theta-\frac{\theta^2}{\theta_s}), \qquad (15)$$

the function $r(\theta)$r(q) is the cubic parabola

It is obvious, that the function $r(\theta)$ can be realized by innumerable set of hull forms. So, the additional conditions are to be formulated to determine the unique hull form, which corresponds to a given function $r(\theta)$.

In the case the horizontal cylinder is floating with his axe of symmetry in still water plane, the equivolumed waterlines are running along the mentioned axe being the axe of inclination simultaneously. The cross-section equation in polar coordinates is $\rho=\rho(\theta)$, the waterline width is $2\rho_0$.

For the case of unit hull length

$$I(\theta)=\frac{2}{3}\rho^3(\theta) \qquad \Delta=\int_0^{\pi/2}\rho^2(\theta)d\theta, \qquad r(\theta)=\frac{1}{\Delta}I(\theta). \tag{17}$$

Let us for example find the cylinder hull form with linear SD (fig.7), which corresponds to the function $r(\theta)$, given by formula (9).

For $I(\theta)$ it comes:

$$I=I_0(1+k\theta^2), \qquad I_0=\frac{2}{3}\rho_0^3 \qquad k=\frac{\Delta\cdot h_0}{2I_0}, \tag{18}$$

$2\rho_0$ being the initial waterline width.

The hull form is described by the following equation:

$$\rho(\theta)=\rho_0\sqrt[3]{1+k\theta^2}. \tag{19}$$

The value of k depends on relative metacentric height $\frac{h_0}{B}$, and for its evalution such an equation comes:

$$\Delta=\rho_0^2\int_0^{\pi/2}(1+k\theta^2)^{2/3}d\theta=\rho_0^2 I(k) \tag{20}$$

The binominal integral $I(k)$ cannot be expressed using elementary functions. For metacentric height it is easy fo find

$$\frac{h_0}{B}=\frac{2}{3}\cdot\frac{k}{I(k)}=\varphi(k) \tag{21}$$

The graph of $\varphi(k)$ is given on fig.8, and the cylindrical hull forms with linear SD are given on fig.9 for different values of $\frac{h_0}{B}$

6. THE INVERSE PROBLEM FOR BISIMILAR HULL FORMS.

Let us consider the problem of the determination of three-dimensional hull form for a given SD.

To simplify the problem, we take a ship hull of bisimilar form (according to classification of prof.Mark G. Krein [2]):

$$y=\pm f(x)\cdot\psi(z). \tag{22}$$

In this case all frames are similar, as well as waterlines. Moreover, the waterlines are taken symmetrical, i.e. f(x) is an even function of x. The over-surface part of the middle frame is given, while its under-water part must be determined. If SD is given, $I_x(\theta)$ becomes a known function. This function

cannot be taken as desired, as soon as it is related with displacement and freeboard of a vessel. Moreover, the limiting angle of inclination, to which the function $I_x(\theta)$ may be specified, cannot be taken arbitrarily. This angle is equal to the angle of inclination of the equivolumed waterline, that passes the keel line, otherwise the problem is either indefinite, or inconsistent. If $_f$ is the volume of the over-surface part of the hull (reserve of buoyancy), the limiting angle is equal to 90º. If $_f \gtrless \Delta$, the angle mentioned is $\frac{more}{less}$ than 90º.

Let us take the Cartesian coordinate system *Oxyz* with its origin *O* on the free surface, waterline axis *Ox* pointed fore, axis *Oy* - to the starboard, and axis *Oz* - vertically upward. The positive heel angle corresponds to the inclination to the starboard. The over-surface part of the middle hull section (MHS) is decribed by the given equation: $y_1 = \varphi_1(z_1)$. If the unknown equation of the under-water part of MHS is taken in the form: $y_2 = \varphi_2(z_2)$, the problem of evaluating of the hull form, that corresponds to the given SD, may be formulated in the following way. It is necessary to find the function φ_2, related by the equalities:

$$y_2 = f(x) \cdot \varphi_2(z_2), \tag{23}$$

$$z_2 = z_f - (y_2 + y_f)tg\theta \tag{24}$$

This function has to satisfy the following equation:

$$\frac{2}{3}\int_0^{L/2}(y_1^3 + y_2^3)dx - y_f^2\int_0^{L/2}(y_1 + y_2)dx = I_x(\theta)\cos^3\theta. \tag{25}$$

The coordinates (y_f, z_f) of the axis of inclination may be found from the formulae

$$y_f = \int_0^{\alpha}\rho(\theta)\cos\theta d\theta \quad z_f = \int_0^{\alpha}\rho(\theta)\sin\theta d\theta. \tag{26}$$

The differential metacentric radius $\rho(\theta)$ and the area of waterline *S* are given by the equalities:

$$\begin{aligned}\rho(\theta) = \frac{4}{S\cdot\cos\theta}\{&\int_0^{L/2}[y_1^2 tg(\nu+\theta) + y_2^2 tg(\mu-\theta)]dx - \\ &-y_f\int_0^{L/2}[y_1 tg(\nu+\theta) - y_2 tg(\mu-\theta)]dx - \\ &-\frac{1}{2}y_f^2\int_0^{L/2}[tg(\nu+\theta) + tg(\mu-\theta)]dx\},\end{aligned} \tag{27}$$

$$S = \frac{2}{\cos\theta} \int_0^{L/2} (y_1 + y_2) dx, \tag{28}$$

$$tg\nu = \frac{d\varphi_1(z_1)}{dz_1}; \qquad tg\mu = \frac{d\varphi_2(z_2)}{dz_2} \tag{29}$$

The iterative method of the approximatee determination of the under-water part of MHS form was worked out for a simplified hull with $f(x)=(1-x^2)$. The calculations are conducted step-wise for fixed values of heel angle (for example, within 10°). The frames inside the interval of the heel angle changes are approximated by straight-line segments. The angles of inclination to the horizontal plane of the segments mentioned are changed to satisfy all identities and conditions of the problem. It is an external cycle of iteration. Inside every iteration the step-by-step approach method is used for evaluating the equivolumed waterline position for the fixed angle of inclination. The program is worked out, based on the given formulae to realize the computations in accordance with the procedure mentioned. Special calculations, performed to run a check on the solution, showed good correlation between the given hull form and the calculated hull form, which is approximated by straight-line segments.

CONCLUSION

The theoretical statements, discussed in the paper, give the possibility to go deeper into understanding of the communication between the hull form and the ship stability characteristics. These statements may be used both in studying the ship dynamics theory and for the practical estimating of the stability characteristics of the ships, especially those of the non-standard forms.

REFERENCES

1.Sevastyanov N.B. Stability of the fishing vessels (In Russian).- Leningrad, "Sudostroyeniye" Publishers, 1970.
2.Kostyukov A.A. The theory of ship waves and ship resistance (In Russian). - Moscow, "Sudpromgiz" Publishers, 1959.

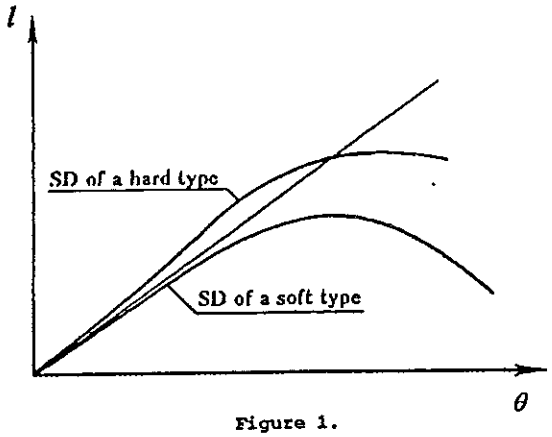

Figure 1.

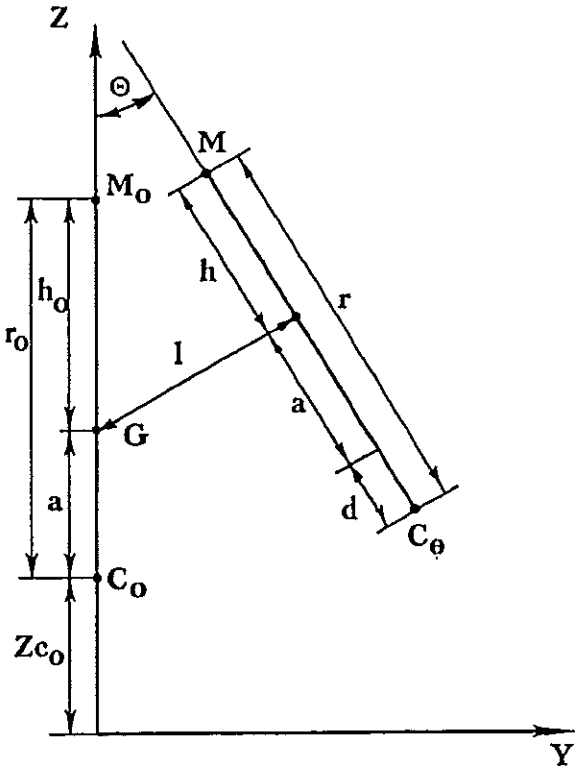

Figure 2.

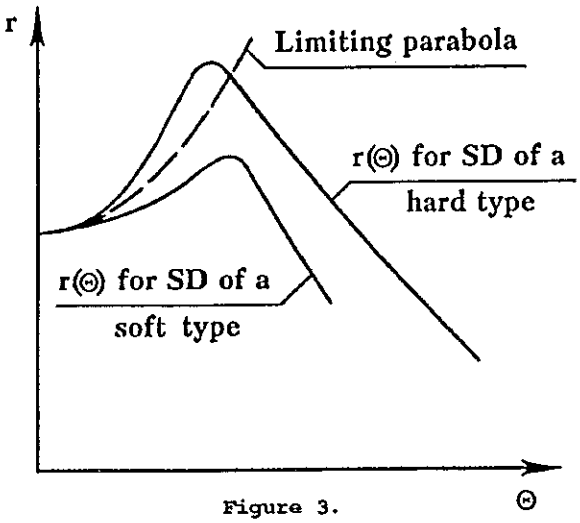

Figure 3.

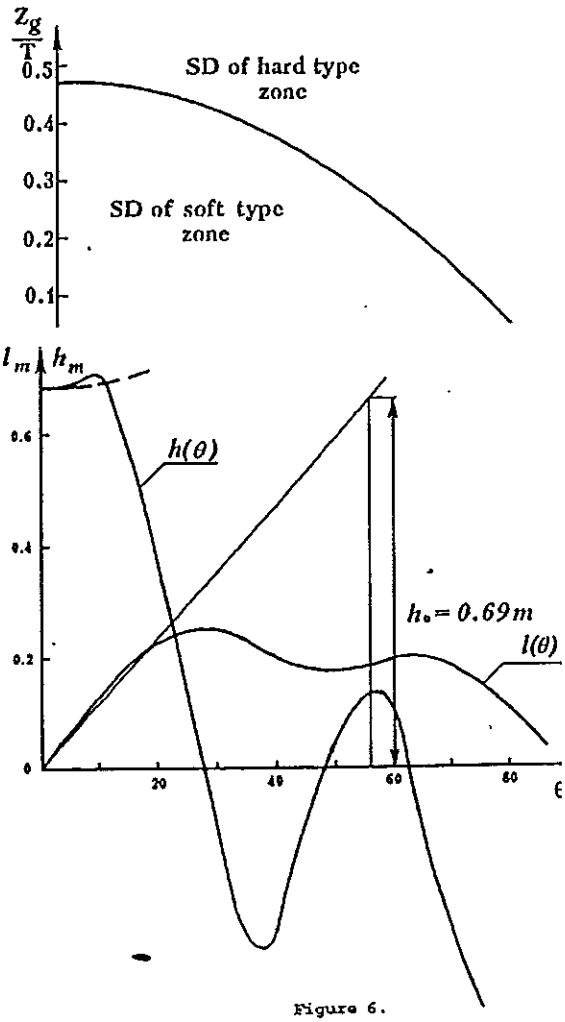

Figure 6.

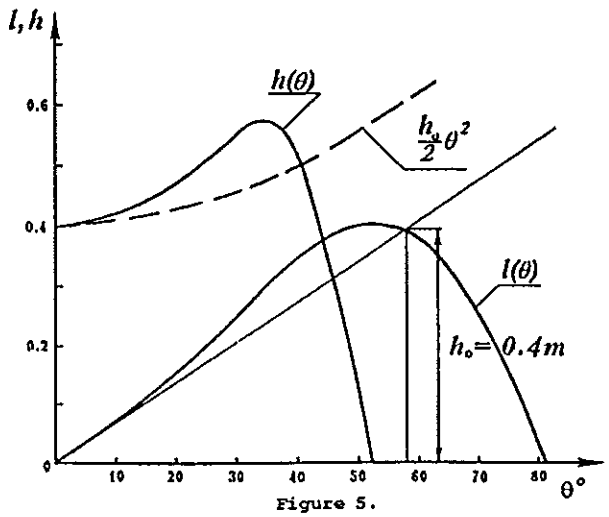

Figure 5.

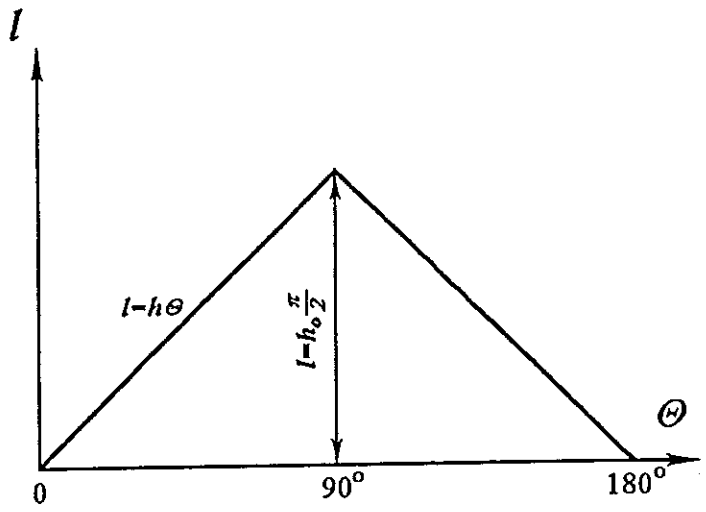

Figure 7.

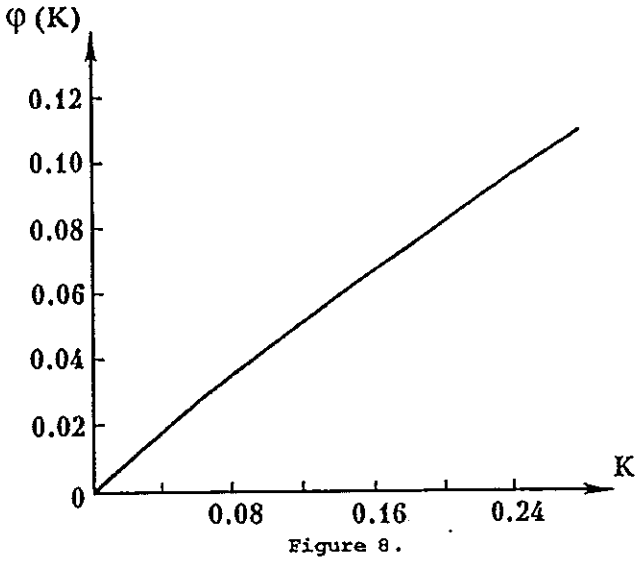

Figure 8.

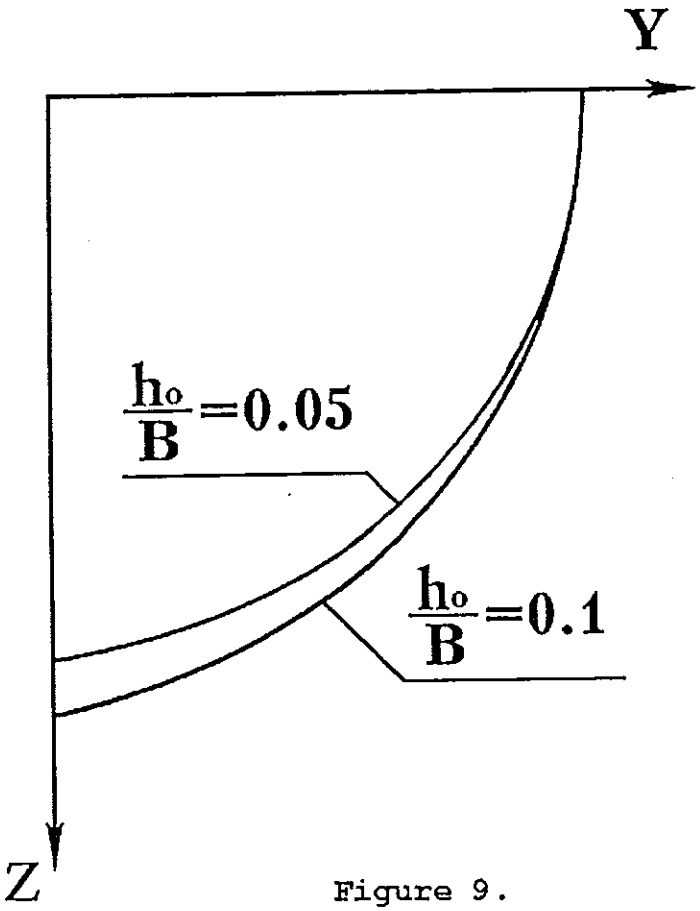

Figure 9.

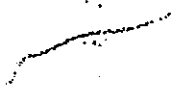

On the Statistical Properties of the Metacentric Height of Ships in Following Seas

Mikael Palmquist
Div. of Naval Architecture
KTH, Royal Institute of Technology
S-100 44 Stockholm, Sweden

Abstract

Systematic numerical computations of the metacentric height GM in regular waves are presented in terms of mean values and amplitudes of the first harmonic variation. Significantly larger variations are found for two hull forms of RoRo-type than for a more traditional hull form. Timedomain simulations are then used to compute GM-spectra's and statistics in irregular seas. These simulations show that the random process of GM is non-linear, exhibiting a low frequency process. This slowly varying part of GM reduces the absolute values of large minimum peak values, producing skewed distributions.

Application of linear response theory for prediction of the process at wave encounter frequencies shows good agreement with simulations. Further, an approximate non-linear method, in which the slowly varying process is considered a function of the envelope of the linear variation, is evaluated. Statistical distributions obtained by the proposed method shows qualitatively fair agreement with distributions obtained from simulations.

INTRODUCTION

Because of the random nature of the sea, the behaviour of ships at sea is also essentially random. Concerning linear wave induced motions and loads, probabilistic methods are well established and in practical use. However, when dealing with non-linear mechanisms, the probabilistic approach is not as straightforward as in the linear case, although still attractive. The dynamic stability of ships in waves is generally such a non-linear problem.

In the research field of ships dynamic stability, quite some efforts has been devoted to the development of improved intact stability criteria's, many of those from a probabilistic point of view. This research avenue has in recent years been strengthened by the progress of probabilistic methods concerning safety in many other areas, for instance reliability based structural design and risk analysis in offshore technology.

With the possibility of probabilistic stability criteria's in mind, this paper deals with the metacentric height GM of ships in irregular seas as a random process in time. This is motivated since GM fluctuations in waves is considered to be important for the onset of pure loss of stability and parametrically excited roll in following waves. It is strongly acknowledged that the metacentric height can not alone be used to describe large rolling amplitudes leading to damages or capsize, because of the non-linear nature of the restoring moment at large angles. However, it is believed that it can be used as a ground for describing the

occurrence of possible dangerous situations, or in the probabilistic sense, the probability of encountering potentially dangerous situations. The basic idea of identifying dangerous conditions without concern to the actual non-linear motions has for instance been discussed by Bishop et. al. /1/.

GM fluctuations in regular following waves, and means of predicting these fluctuations, has for a long time been subject to much interest, /2, 3/ amongst many others. However, there seems to be a lack of a solid foundation for determining the practical implications of these fluctuations, since their importance are highly dependant on the combination of ship size, speed range and operating areas etc. Therefore it seems appropriate to investigate the possibilities of establishing a probabilistic approach to GM(t) in random seas, which could provide a reference frame for at least qualitative, but hopefully also quantitative, risk assessment.

In /4/, Dunwoody presented a linear derivation relating the energy spectrum of GM(t) to the wave energy spectrum. This technique was then used by the same author in /5/, in which an idealised model was used to study the parametrically excited roll response to such GM fluctuations in terms of GM spectra's. GM(t) was assumed to be a stationary, ergodic, Gaussian process.

Another approach to GM fluctuations in irregular seas is the "effective wave" concept, introduced by Grim /6/ in the early 1960s. This approach has then been applied and further developed by others, for instance by Helas /7/ and Umeda et. al. /11/. Its basic concept is that the instantaneous wave profile along a ship travelling in following waves may be replaced by a regular wave with wave length equal to the ship length. The amplitude of the effective wave is determined in a least square sense, which is assumed to minimise the righting arms fluctuations between the irregular wave and the regular one. This concept may to some extent be regarded as probabilistic since the effective wave heights becomes Rayleigh distributed, hence effective wave heights may easily be determined for certain probabilities of excess. Because of the nature of this approach, it has been applied to the pure loss of stability problem. However, this approach does not deal with the random process of righting arms in itself.

Since complete time-domain simulations, for making statistical evaluations of the GM process, is costly in computer time, it is today not a practical tool for these purposes. It therefore seems appropriate to develop simplified methods in this respect, which constitutes a part of this study.

In the light of investigating GM(t) as a random process, the main objectives of this paper are:

- To show that GM(t) is a non-linear, and therefore, nonGaussian process, which may be idealised as the sum of a linear Gaussian process and a slowly varying non-linear process.

- To investigate the influence of non-linearities on the statistical properties of GM.

- To show that the linear part of GM(t), expressed in terms of spectral density, may be determined by the linear response theory.

The modern hull forms A and C are, with their large B/T ratio and flare, representative for the hull forms of RoRo ships. The conventional hull form D should not be regarded as a ship found in practice, because of the large B/T ratio in relation to it's hull form. Still, it is interesting in comparing the importance of actual hull shapes at constant main dimensions.

GM FLUCTUATIONS IN REGULAR WAVES

For the three different hull forms, GM fluctuations has been computed in regular waves with amplitudes ranging from 0.3 m to 6.0 m, and for wave frequencies from 0.1 rad/s and 1.15 rad/s. In each regular wave, GM was computed in 19 equally spaced phase steps over a wave passage. Assuming that the GM fluctuation as function of the wave phase a in a regular wave may be expressed as a Fourier series:

$$GM(\alpha) = GM_{SW} + \Delta\overline{GM_m} + \sum_{n=1}^{\infty}\{A_n \cos(n\alpha) + B_n \sin(n\alpha)\} \quad (3)$$

and that it is a fair approximation to neglect orders of $n \geq 2$. Then we can write:

$$GM(\alpha) = GM_{SW} + \Delta\overline{GM_m} + GM_1 \cos(\alpha - \mu)$$

$$\text{where} \quad GM_1 = \sqrt{A_1^2 + B_1^2}\ , \quad (4)$$

$$\mu = \arctan\left(\frac{B_1}{A_1}\right)$$

In figure 2, the change in mean GM, $\Delta\overline{GM_m}$ and the amplitude of the first harmonic GM variation, GM1, are shown as functions of wave amplitude and dimensionless wave length λ/L_{PP}, for the three hull forms investigated.

As expected, the modern hull forms A and C shows significantly larger GM variations than the conventional hull form D. This agrees with the general opinion that modern hull forms, like A and C, are more sensitive to the influence of wave profile on righting levers, and that maximum fluctuations occurs in wave lengths close to the ship length. Concerning the changes in mean GM, relatively small differences are found between the three hull forms. The magnitude of these changes compared to GM1 are not generally negligible at wave lengths of interest.

The GM_1 obtained by Fourier analysis will include contributions from higher odd orders of the non-linear system. This is shown by the deviations from linearity for GM_1 as a function of wave amplitude. Nevertheless, the GM_1 variation of 1st order in wave amplitude is predominate.

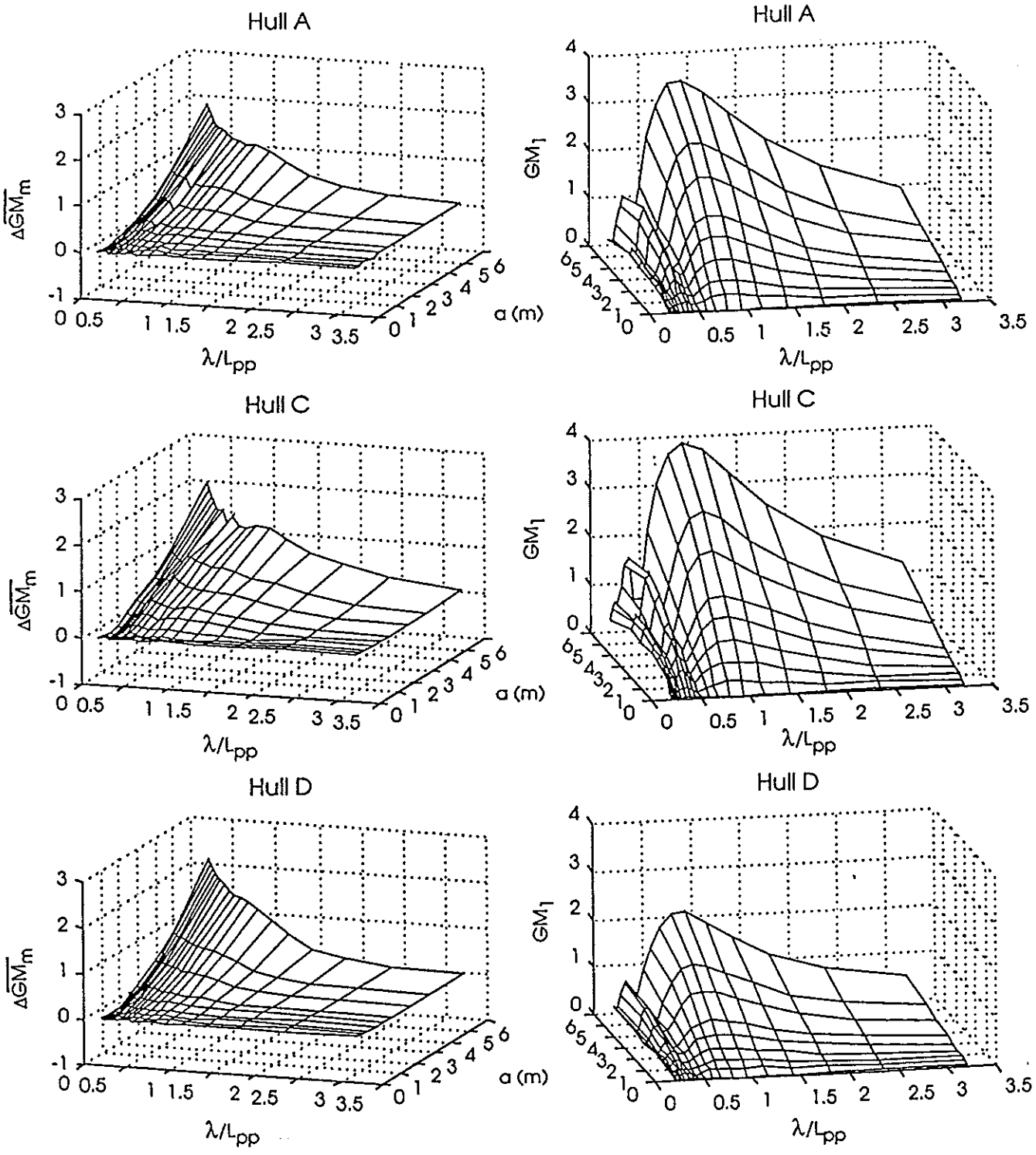

Figure 2. Difference in mean GM (diagrams to the left) and amplitude of 1st order GM variation (to the right) in regular waves, as functions of wave amplitude and dimensionless wave length.

• To investigate whether the slowly varying GM process, and hence the entire non-linear process, may be approximately estimated from the GM response in regular waves using a narrow band approach.

MAJOR ASSUMPTIONS OF GM CALCULATIONS

The computations of GM fluctuations in this paper are based on the widely used quasi-static approach where the only external forces on the hull are the Froude-Krylov forces. The implication of the quasi static approach, i.e. neglecting vertical radiation and diffraction forces, is in practice an assumption of low frequencies of encounter. This applies to encounter frequencies reasonably far below the natural frequencies of heave and pitch. The quasi-static assumption does not necessarily mean a pure Froude-Krylov assumption. It is known that forward speed radiation has some influence on the righting arms variations, /8, 9/, which may to some extent be taken into account in quasistatic calculations if the ship's own wave system is known. This effect has been reported to influence the results both as an increase or decrease of stability depending on the speed. However, the magnitude of this change is not generally large, so that it seems reasonable to neglect this effect with respect to the considerable complexities this would introduce.

The calculations of GM in waves in this work are performed by integrating the undisturbed incident wave pressure field over the momentarily submerged hull surface S. The Froude-Krylov forces and moments are obtained from the pressure integrations:

$$\vec{F} = \iint_S p\vec{n}\,dS \qquad (1)$$

$$\vec{M} = \iint_S p(\vec{r} \times \vec{n})\,dS$$

where p is the undisturbed wave pressure field including Smith's effect

$\vec{n}$ is the unit vector normal to the surface element dS

$\vec{r}$ is the vector from the center of gravity to dS

Computer code for this purpose has been developed and is also part of a more general time-domain simulation program for ship motions and manoeuvring, described in /13/. At each time step the pressure integration is repeated to find the quasi-static equilibrium. In this paper, GM is computed as:

$$GM(t) = \frac{1}{\nabla \rho g}\left(\frac{dM_{Roll}(\phi, t)}{d\phi}\right)_{\phi=0} \qquad (2)$$

In the present study, only the case of longitudinal waves has been considered, which is motivated by the conceptual nature of this work. It is, however, recognised that quartering seas, where roll exciting wave forces are present, has shown to be more dangerous in many cases. Therefore, one should point out that the approach of this paper is not limited to longitudinal seas. For relative wave directions less than some 20 degrees, the GM fluctuations in regular waves can be obtained from those in longitudinal waves by using the projected wave length, see Hua and Rutgersson /14/.

An advantage of the quasi-static, Froude-Krylov assumption is that the statistical properties of GM becomes timeinvariant, which follows from considering wave elevation as a stationary and homogeneous process. Hence the statistical properties of GM are the same if it is based on GM-samples at randomly selected locations or at a fixed location, asymptotically with the number of samples of course. This justifies computing GM(t) in irregular waves at zero speed, the statistical properties remain the same at any speed, although the accuracy of GM(t) may decrease as the encounter frequency increases.

As a summary, this work makes the following basic assumptions:

- For ships travelling in following waves, continuous quasistatic equilibrium is assumed.
- The pressure distribution in the incident waves is not disturbed by the presence of the ship. The pressure due to water particle orbital motion (Smith's effect) is included in the pressure field.

INVESTIGATED HULL FORMS

Three different hull forms with large B/T-ratio are investigated in this study, figure 1. These hull forms has earlier been subject to stability investigations by Huss /10/ (in which a hull form B was also used, explaining the alphabetic inconsistency). Hull A and C represents modern hull forms with pronounced flare. A has a conventional after body, while C has a wide transom stern. D is a traditional hull form with very little flare, and has been obtained by stretching and scaling a Series 60 model.

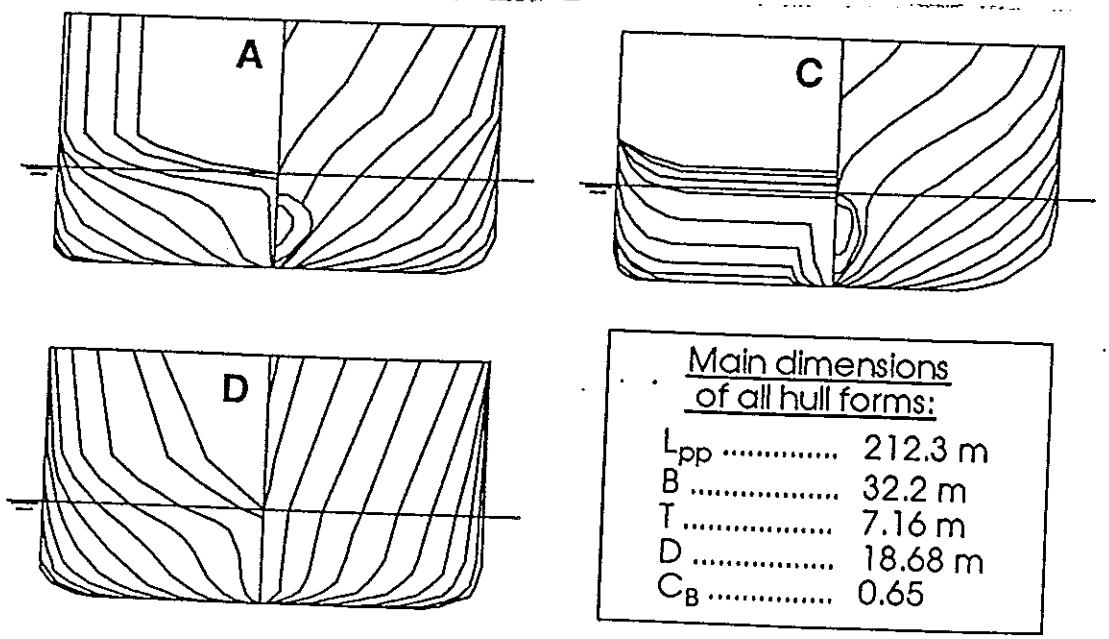

Figure 1. Investigated hull forms and main dimensions.

GM AS A RANDOM PROCESS IN IRREGULAR SEAS

For a ship at sea, the metacentric height will constitute a random process in time. Since GM(t) is considered an important factor for the onset of pure loss of stability and parametrically excited roll in following waves, one would wish to be able to describe this process in statistical terms.

Considering the results of GM fluctuations in regular waves, with significant changes in mean GM, one basically expect GM(t) in irregular seas to be a non-linear process and hence have a non-Gaussian nature. This is confirmed by time-domain simulations based on the quasi-static approach earlier mentioned. In figure 3, histograms of ΔGM(t) for the three hull forms clearly shows how the distributions are skewed. These histograms are based on simulations of approximately 2 hours in real time, divided into shorter sequences (126 s), each with new random wave component phases, to avoid repetition of the wave form. The higher sensitivity of modern hull forms to the wave profile with respect to GM fluctuations is also apparent in the histograms of figure 3.

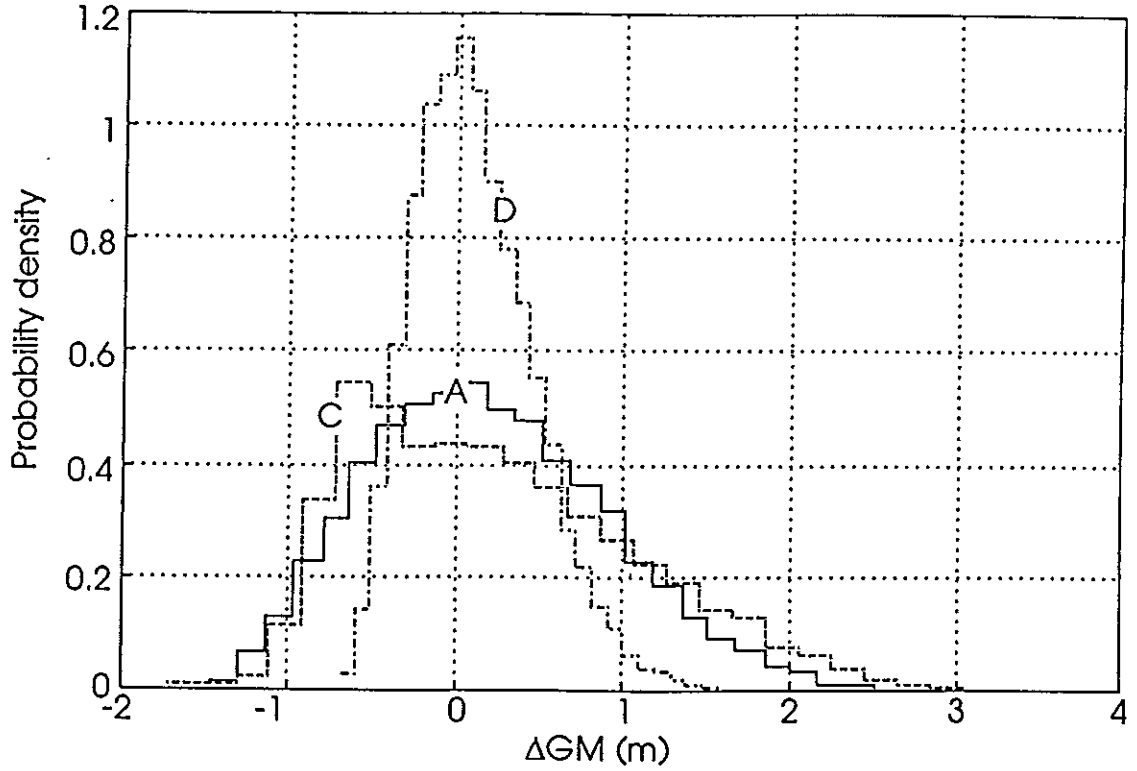

Figure 3. Histograms of $\Delta GM(t)$ in irregular waves for the three hull forms (ISSC wave spectra with H_s=6 m and T_m=12 s).

The characteristics of the random process ΔGM(t) for hull C in terms of it's moments of distributions is shown in table 1. While the mean and variance are dimensional quantities, the 3rd and 4th moments, that is the skewness and kurtosis, are defined in such a way as to make them non-dimensional. The skewness and kurtosis are pure numbers which characterises only the shapes of the distributions in relation to the gaussian distribution (skewness and kurtosis equal to 0). Positive skewness means a tail extending out towards more positive x-values, and positive kurtosis means a more peaked distribution. The results of table 1 are, due to computer time, based on shorter simulations than those of figure 3, approximately 40 minutes in real time.

The difference in mean GM follows in general the characteristics from regular waves, that is an increase with wave height and decrease with wave period, for small wave heights the difference in mean may be slightly negative. The skewness of the distributions is, with the exception of the case Hs=2 m and Tm=16 s, positive, while the kurtosis, with the same exception, is negative.

		Mean		
		Hs		
		2	*6*	*10*
Tm	*8*	-0.0136	0.2525	0.5526
	12	-0.0276	0.1366	0.3294
	16	-0.0245	0.0328	0.1537

		Variance		
		Hs		
		2	*6*	*10*
Tm	*8*	0.1210	0.7914	1.7664
	12	0.0868	0.6632	1.5894
	16	0.0370	0.3534	0.8801

		Skewness		
		Hs		
		2	*6*	*10*
Tm	*8*	0.1204	0.3032	0.2378
	12	0.1831	0.5345	0.4763
	16	-0.3333	0.4960	0.5519

		Kurtosis		
		Hs		
		2	*6*	*10*
Tm	*8*	-0.4115	-0.6122	-0.6567
	12	-0.2522	-0.4378	-0.5248
	16	0.7890	-0.2919	-0.5105

Table 1. Moments of ΔGM(t) distributions for hull form C from simulations at different Hs and Tm of the ISSC wave spectra.

The deviations of the simulated ΔGM distributions from Gaussian distributions are mainly due to the presence of a low frequency component, which, in a quasi-harmonic sense, can be regarded as a slowly varying average related to the change in mean GM in regular waves. In the power spectra's of GM(t) the slowly varying component is represented by isolated energy at frequencies below wave frequencies, although the power spectrum can not convey the non-Gaussian properties of the signal. Figure 4 shows an example of a GM time series, and it's decomposition into two separate signals. The decomposition has been performed by filtering GM(t) in the frequency domain, with a cut-off frequency corresponding to the frequency dividing the low frequency energy from the encounter frequency energy (approx. 0.25 rad/s in fig. 4).

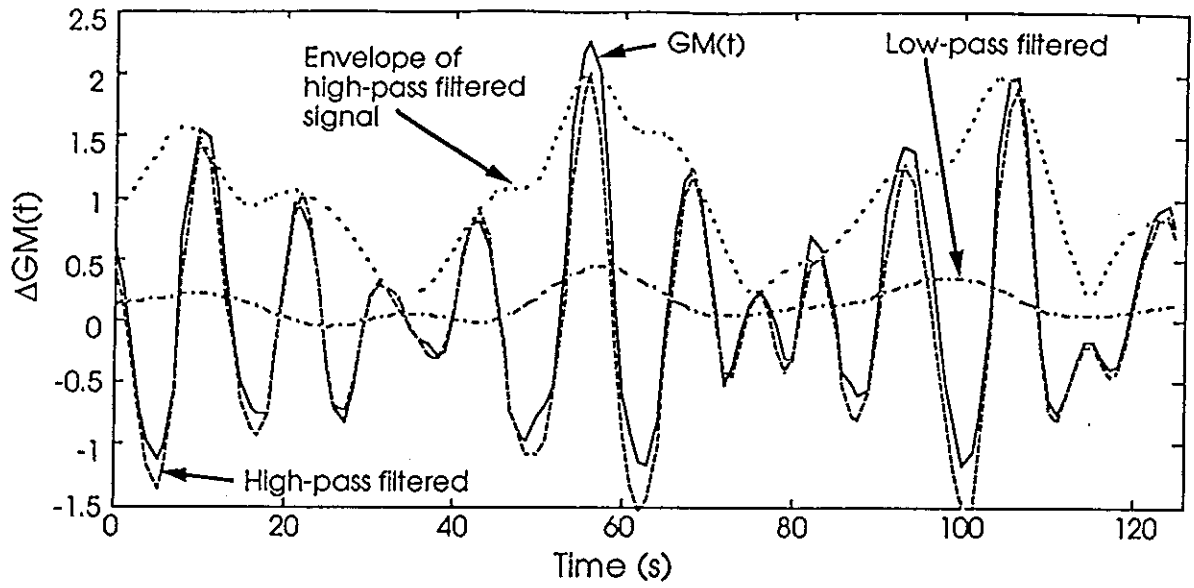

Figure 4. Example of a time series of GM(t) and it's filtered components (hull C, Hs=6 m, Tm=12 s).

In the following, it will be assumed that the GM(t) process can be regarded as a sum of a linear encounter frequency process and a slowly varying process, the high-pass and lowpass filtered signals in figure 4 respectively.

ESTIMATION OF THE ENCOUNTER FREQUENCY PART OF GM(t)

Although the energy of GM(t) at encounter frequencies includes contributions from higher orders, this process will here be regarded as a linear, zero mean, Gaussian process GMlin(t). For a linear system with Gaussian input in spectral representation, the output spectrum is directly related to the input by a transfer function describing the linear input/output relation as function of frequency. Considering GMlin(t) to be the output from a linear system, it's spectral density is determined by:

$$S_{GM}(\omega) = \left| f_{GM}(\omega) \right|^2 S_w(\omega) \tag{5}$$

where $f_{GM}(\omega)$ is the transfer function of $GM_{lin}(t)$

$S_w(\omega)$ is the wave energy spectrum

The "exactly" linear transfer function fGM can easily be determined from the results in regular waves, from the GM variation at small wave amplitudes:

$$f_{GM}(\omega) = \left(\frac{dGM_1(\omega, a)}{da} \right)_{a=0} \tag{6}$$

From the results in regular waves it is observed that the 1st harmonic variation GM1 is weakly non-linear with respect to wave amplitude. In order to account for the non-linear effects, an ad. hoc. approach has also been applied for the calculations of f_{GM} in which f_{GM} has been obtained by a "linearization" of GM1(w,a). In this approach the Rayleigh p.d.f. of wave amplitudes of the actual sea state has been used as a weighting function, giving:

(7)

$$f_{GM}(\omega) = \int_a GM_1(\omega, a) \frac{2}{R_a} e^{\left(-a^2/R_a\right)} da$$

where R_a is the Rayleigh parameter of the wave amplitude distribution.

In figure 5, GM spectra's obtained by transfer functions calculated from equation (6) and (7) are compared to the corresponding spectra's obtained by fourier transforms of time-domain simulation results.

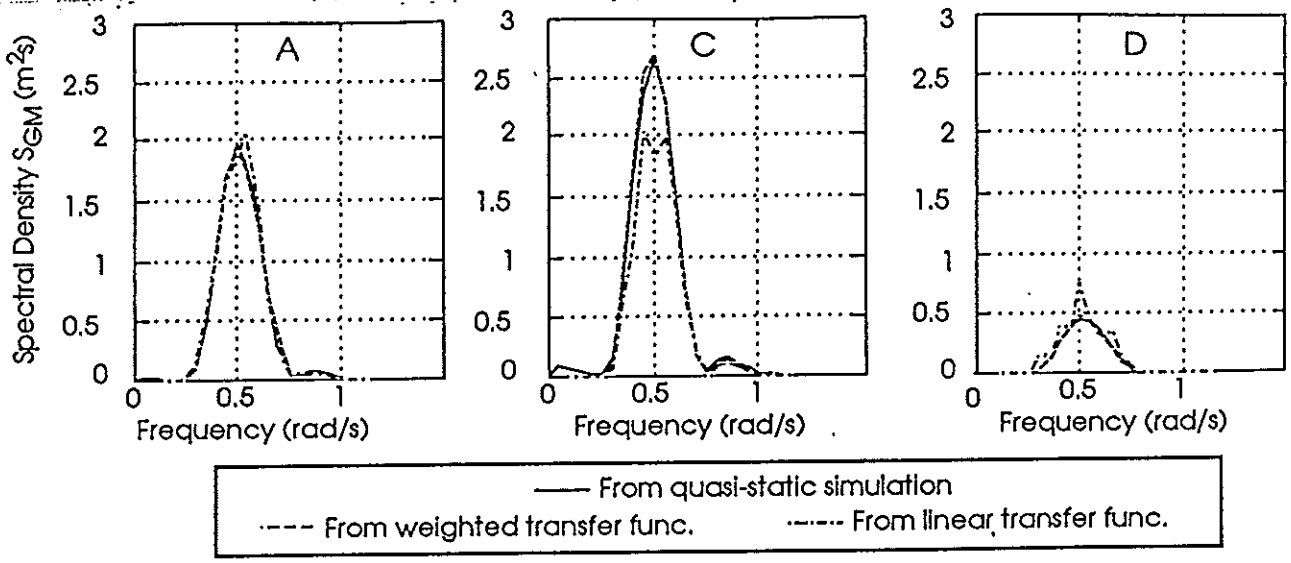

Figure 5. GM spectra's for the three hull forms. Comparison of spectra's from simulation and spectra's obtained by linear response theory (ISSC wave spectra, H_s=6 m, T_m=12 s).

For hull C, comparisons of the 0th spectral moment;

$$m_0 = \int_{\omega} S_{GM}(\omega)\, d\omega \qquad (8)$$

for different significant wave heights and mean periods are made in table 2. The low frequency "bulge" was excluded in the m_0 evaluations for the simulation spectra's. Good agreement is found, especially bearing in mind that the square root of m_0 equals the standard deviation of $GM_{lin}(t)$. Higher spectral moments has also been found in good agreement between simulations and predictions. As seen in table 2, predicted spectra's based on weighted transfer functions are in all the cases closer to the simulated spectra's than the "exactly" linear ones. However, since this weighting technique has a rather weak theoretical foundation, it has not been pursued in the following investigations of this paper.

Hull C		Spectral area m_0 of $GM_{lin}(t)$ (simulated / predicted with weighted trf / predicted with linear trf)		
		Hs		
		2	6	10
T_m	8	0.120 / 0.102 / 0.078	0.773 / 0.830 / 0.706	1.696 / 1.770 / 1.962
	12	0.087 / 0.072 / 0.057	0.651 / 0.652 / 0.513	1.556 / 1.469 / 1.425
	16	0.037 / 0.034 / 0.027	0.349 / 0.315 / 0.247	0.866 / 0.734 / 0.686

Table 2. Comparison of m_0, simulation versus predictions for different sea states (ISSC wave spectra).

THE SLOWLY VARYING PART OF GM(t)

The slowly varying part of GM(t) is an effect due to even orders of the system in which the wave elevation $\eta(t)$ is the input and GM(t) the output. Under multi-tone input as in irregular waves, this is further complicated by the introduction of sum frequency terms. Low frequency energy is a general feature of non-linear systems, and analogies can be made between this problem and ,for example, drift forces and added resistance. However, the reasons for studying these low frequency processes may differ. Concerning drift forces on a offshore platform for instance, the reason may be to avoid or predict resonant conditions at low frequencies, when the natural frequency can coincide with frequencies of such slowly varying forces. But, in the present case, we have no detailed interest in the slow process in itself. What is wanted is a way to describe it's influence on the entire process GM(t). Therefore, an approximate approach is motivated.

In regular, harmonic waves, both the change in mean GM and the amplitude of the 1st harmonic variation are functions of wave amplitude and frequency. By combining those functions one can establish relationships between $\Delta \overline{GM}_m$ and GM1 which are frequency dependant. By fitting a polynomial to the numerical relationship, $\Delta \overline{GM}_m$ can be expressed as: (9)

$$\Delta \overline{GM}_m(\omega, GM_1(\omega)) = c_1(\omega) GM_1(\omega) + c_2(\omega) GM_1(\omega)^2 + \ldots + c_n(\omega) GM_1(\omega)^n$$

where $c_1, c_2, .., c_n$ are frequency dependant polynomial coefficients.

Provided that $\eta(t)$ is sufficiently narrow banded in character, so that all the wave energy is concentrated close to the peak frequency ω_p, the linear GM variation GMlin(t) will also be narrow banded. The 1st harmonic GM variation GM1 in regular waves will then, in narrow banded irregular waves, be slowly varying with time, described by the envelope function of GMlin(t). The envelope function of GMlin(t) is defined as:

$$\rho_{GM}(t) = \sqrt{GM_{lin}(t)^2 + \hat{GM}_{lin}(t)^2} \qquad (10)$$

where $\hat{GM}_{lin}(t)$ is the Hilbert transform, see for instance /15/, of $GM_{lin}(t)$.

So, for sufficiently narrow banded seas, the slowly varying GM process is obtained by combining equation (9) and (10):

$$\Delta GM_s(t) = c_1(\omega_p)\rho_{GM}(t) + c_2(\omega_p)\rho_{GM}(t)^2 + \ldots + c_n(\omega_p)\rho_{GM}(t)^n \qquad (11)$$

This expression can in fact be regarded as an asymptotic relation as the bandwidth of the wave elevation process approaches zero.

Narrow band assumptions are widely used in many areas, often leading to reasonable results. In practice, the meaning of "sufficiently narrow banded" is of course not a strict statement. Usually the bandwidth of a process is discussed in the time scale, that is in frequency or period. But, for the present case, the physical problem is mainly a geometrical one, and should therefore be related to space (wave length) rather than time. Unfortunately, because of the quadratic relationship between wave frequency and wave length, the bandwidth with respect to wave length is larger than with respect to frequency. In defending narrow band assumptions, one may for practical reasons argue that severe seas have been observed to have considerable smaller bandwidth than standard two-parameter wave spectra's.

The validity of the present approach to estimate the slowly varying process can be qualitatively indicated by comparing $\Delta GMs(t)$ against $\rho_{GM}(t)$ from simulations to the polynomial function of equation (11). Figure 6 shows two such plots for an ISSC wave spectra with Hs=6 m and Tm=12 s (left plot) and a narrow banded (right plot), 3 wave components, wave spectra with Hs=6 m and the same modal frequency as the used ISSC spectra ($\approx$0.37 rad/s). The plots consists of 2520 samples. As expected, the correlation is more clear in the extremely narrow banded case. Here, the polynomial agrees quite well with the sampled points, which are more concentrated although some outlier points are present. The reason for those outlier points is not clear. For the ISSC wave spectra case, the higher order polynomial correlation does not seem motivated. However, linear fits fails to predict the correlation at small significant wave heights, where $\Delta GMs(t)$ is concentrated in the slightly negative region. A solution could be to use linear fits weighted by a suitable function with respect to wave heights.

For real wave spectra's it is not obvious which frequency to choose for computing the polynomial coefficients of equation (11). The first reason for this is the asymmetry of real wave spectra's, and secondly that those spectra's are wide enough for admitting changes of the characteristic frequencies between the waves and the response. For instance, depending on the transfer function the response may be located at frequencies corresponding to the tail of the wave spectra. This complicates the practical applications of a narrow band approach. In this study the
modal frequency of $S_{\zeta_{GM}}$ has been chosen for estimations of the polynomial correlation between ΔGMs(t) and $\rho_{GM}(t)$.

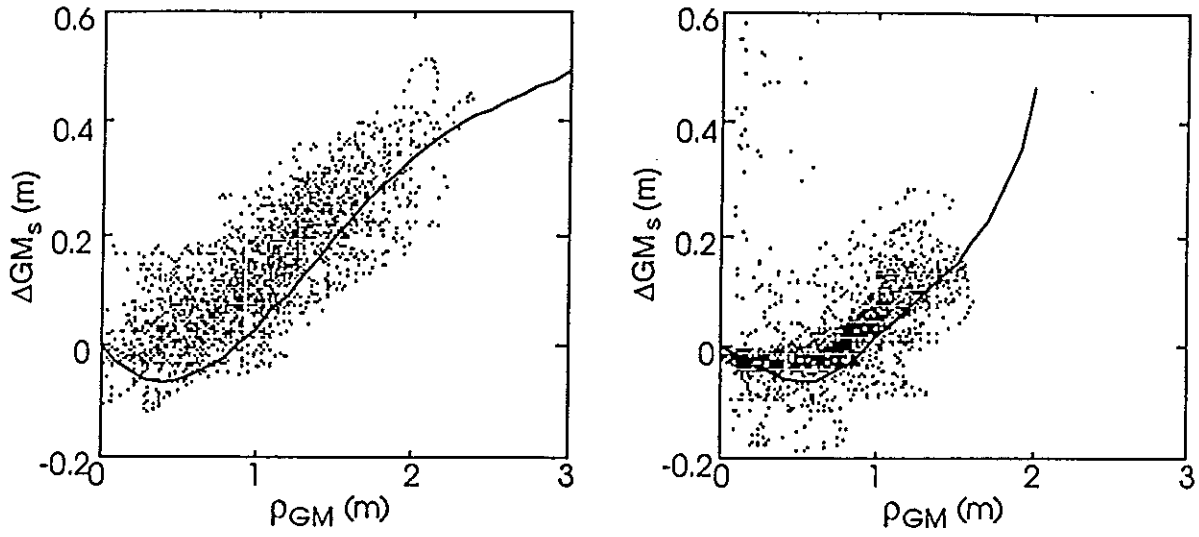

Figure 6. Plots of $\Delta GM_s(t)$ versus $\rho_{GM}(t)$ from simulations. The solid line is the polynomial function (5th degree), see equation (6), estimated from the results in regular waves.

PREDICTION OF GM(t) AND IT'S STATISTICAL PROPERTIES

If the linear GM variation GMlin in spectral representation, $S_{\zeta_{GM}}(w)$, can be estimated by the use of linear response theory, and if the slowly varying process ΔGMs(t) can be approximated as a function of the envelope of GMlin , then the entire non-linear process ΔGM(t) can be approximately expressed as:

(12)

$$\Delta GM(t) = GM_{lin}(t) + \Delta GM_s(t) =$$
$$= \sum_i \sqrt{2 \cdot S_{GM_i} \cdot \Delta\omega} \cdot \cos\left(-\omega_i t + k_i x(t) + \varepsilon_i\right) + f\left(\rho_{GM}(t)\right)$$

where ε_i are uniformly distributed random phases in the interval $\{0, \ 2\pi\}$.

Hence, any statistical properties of ΔGM(t) can be numerically estimated by means of direct simulation of equation (12). The computer time for this analysis, compared to that of complete simulations involving iterative pressure integrations over the submerged hull at each time step, is small.

For the estimation of the probability density function of minimum GM in relation to GM in still water, ΔGMmin, an even more effective Monte-Carlo simulation procedure can be used. Since the envelope function of a process coincides with peak values of that process, an estimate for the p.d.f. of ΔGMmin can be computed through randomly generated peak values following the peak value distribution. For a peak value $\breve{GM}_{LIN_j}$ of the linear GM process, the minimum, non-linear, GM becomes:

$$\Delta GM_{min_j} = -\breve{GM}_{lin_j} + f\left(\breve{GM}_{lin_j}\right) \tag{13}$$

where f is the function of equation (11).

The linear GM process is assumed to be a Gaussian, narrow banded, process, from which it follows that it's peak values can be considered Rayleigh distributed. By rewriting the Rayleigh cumulative probability function in closed form, a large number of Rayleigh distributed samples $\breve{GM}_{LIN_j}$ can easily be generated from uniformly random probabilities.

Monte-Carlo simulations according to equation (12) and (13) has been made for comparison with results from complete time-domain simulations at Hs=6 m and Tm=12 s. Figure 7 shows histograms of ΔGM and ΔGMmin for the three hull forms. For the ΔGMmin histograms, the Rayleigh p.d.f. of the linear variation has been added to show the influence of the slowly varying process. The predicted statistics of ΔGM is generally in good agreement while the minimum peak distributions are not very well predicted, although the tail behaviour of the predicted ΔGMmin distributions is between those from the simulation and Rayleigh distributions. This means that the predictions are conservative. In figure 7, the same kind of comparisons are made for hull C at two different sea states. Here, the predictions are in better agreement and it is seen that the prediction method is able to account for the non-conservatism in neglecting the slow variation at small wave heights. Generally speaking, the present approach to account for the influence of the slow variation in the statistical properties are qualitatively satisfactory.

Some problems of applying narrow band assumptions in practice has earlier been discussed in this paper. As then mentioned, the modal frequency of the GM response has been used for estimating the slowly varying process. Computations has shown that better agreement for the predicted distributions, especially in the tail of the ΔGMmin p.d.f., are obtained by choosing a somewhat higher frequency for this polynomial correlation. It seems however difficult to motivate this on a theoretical basis, but the author believes that the accuracy of the proposed approach can be improved in this way. This must of course be verified by systematic numerical calculations or, if possible, analytically.

A technique for estimation of the correlation of the slowly varying part, which has not been applied at this stage, is to use weighted linear correlation instead of higher order polynomials. For linear correlation, equation (13) becomes:

$$\Delta GM_{min_j} = \breve{G}M_{lin_j}(k - 1) \tag{14}$$

where k is a linear coefficient.

Since $\breve{G}M_{lin}$ are considered Rayleigh distributed with a Rayleigh parameter R, one can easily show that ΔGM_{min} is also Rayleigh distributed, and with a Rayleigh parameter:

$$R' = (k - 1)^2 R \ , \quad k \neq 0$$

Hence, this would provide a simple way of predicting the minimum GM p.d.f. with consideration to the slowly varying process, eliminating the need for Monte-Carlo simulations.

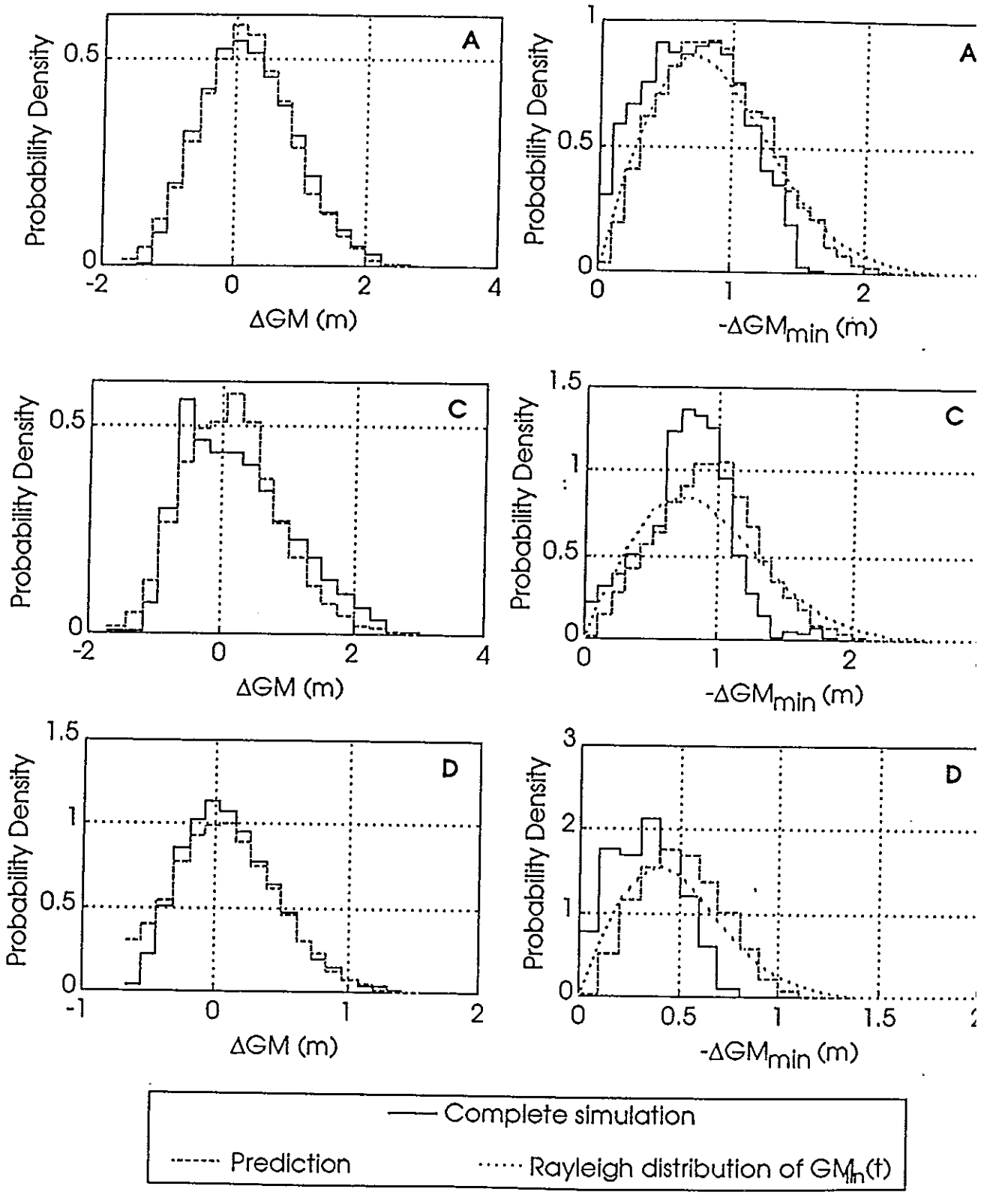

Figure 7. Histograms of $\Delta GM(t)$ (left side) and ΔGM_{min} (right side) for the three hull forms, simulation versus prediction (ISSC wave spectra, H_s=6 m, T_m=12 s).

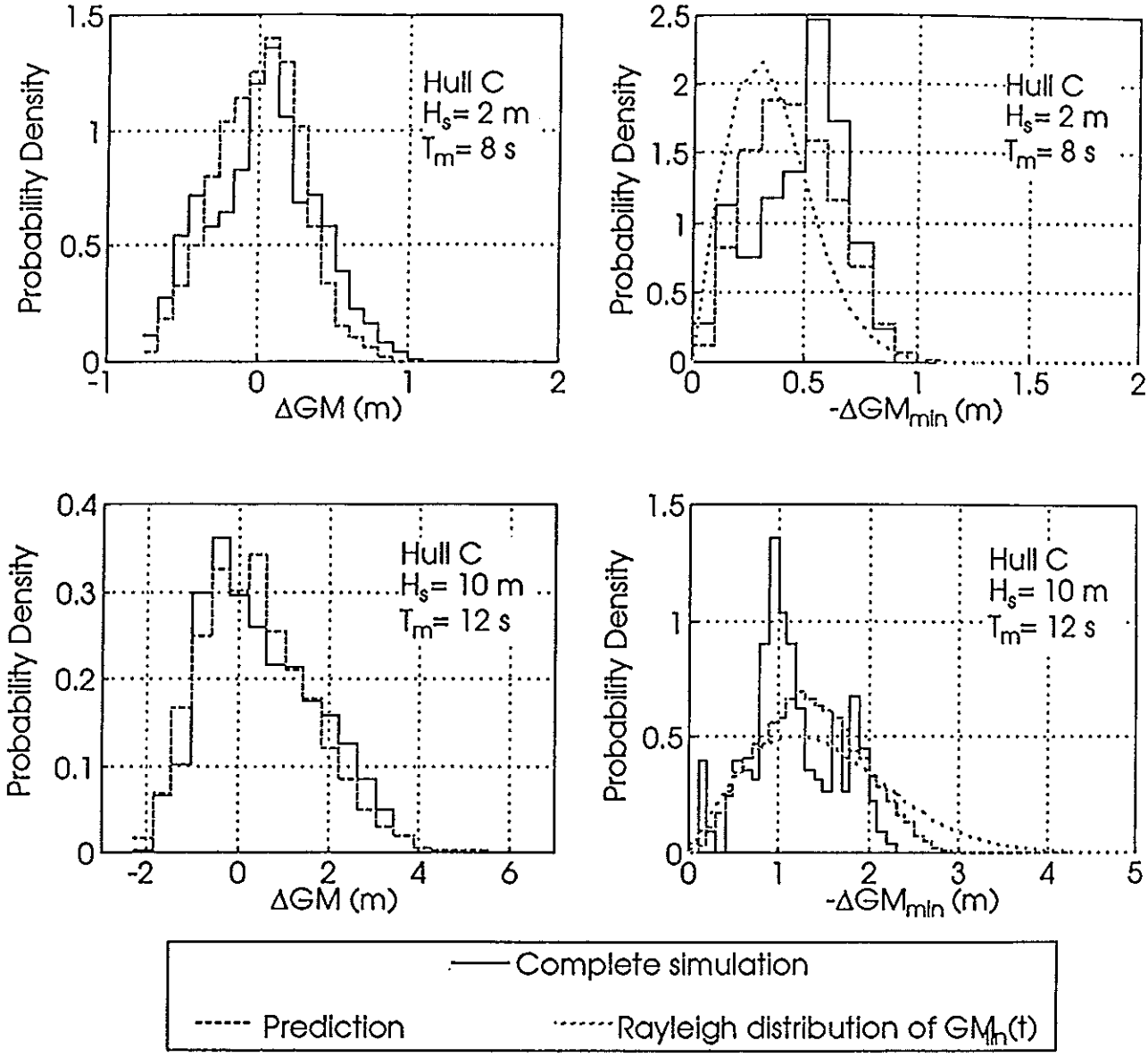

Figure 8. Histograms of $\Delta GM(t)$ (left side) and ΔGM_{min} (right side) for hull C in two different sea states, simulation versus prediction.

DISCUSSION ON PRACTICAL APPLICATIONS

For practical applications of a probabilistic approach to
ships dynamic stability in following waves, the frequency of encounter is of vital importance. The statistical properties investigated in this paper, that is the distributions of momentary GM and minimum peak values, are time-invariant and does not deal with this part of the problem. They do, however, constitute a foundation for a developed approach taking speed, relative wave direction, natural frequencies of roll etc. into account. For example, it is known that the pure loss of stability only occurs at low frequencies of encounter when small righting moments are maintained for a sufficiently long period of time. Therefore, the method for estimating the distributions of Δ GM(t) and Δ GMmin of this paper could be used to estimate probabilities of duration of excursion. In the authors opinion, such a joint probability distribution could be archived either by simulation of equation (12) or by assuming GM(t) to be narrow banded and quasi-harmonic, directly putting GM(t) into a time scale. For at least smaller ships, the surge motion can influence the time periods of low stability /11/, which in that case should be taken into account.

Considering parametrically excited roll motion, it is
reasonable to believe that the slowly varying process is of very little importance, and that the linear variation alone governs the problem as assumed in /5/. However, there is a possibility that the slowly varying part may have the effect of modulating the natural frequency of roll, since the mean GM will momentarily increase in a group of large GM variations. Another approach to the parametrically excited roll could be the concept of wave groups, see Blocki /12/ amongst others, applied to the GM process instead of the wave elevation, in which the probability of a critical run of large GM amplitudes becomes part of a risk assessment formulation.

Finally, some general remarks on stability criteria development. A very important question is what the actual aim of new criteria should be. What kind of events do we wish to avoid, or at least decrease the probability of, by using these new criteria? Looking at casualty statistics and accident investigations, one may draw the conclusion that ship casualties are very complicated sequences of events, interacting and triggering others. The "theoretical" pure capsize is an event rarely found in real life, except possible for small vessels such as pleasure and fishing vessels, for which the problem is even more complicated due their greater sensitivity to single energetic events such as breaking waves. For example, shift of cargo is almost always present to some extent, and often the triggering factor, in the accident chain of ship capsizes. One may therefore argue that shifting of cargo would constitute a kind of limiting event which criteria should focus on. This kind of approach could be combined with demands on redundancy in the system, e.g. survivability of a ship after shifting of cargo.

Another interesting question is how to incorporate the operation of ships in the work of criteria development. Clearly, many casualties could have been avoided by operational decisions if only the danger in the situations had been apprehended. So, in the authors opinion, much would be gained by finding appropriate ways of transferring the present knowledge on the dynamic stability of ships into the operation, i.e. to shippers, masters etc. General new criteria for the dynamic stability, based on the present knowledge, could have a significant negative effect on efficiency, simply because this is very complicated problems. This is a reason for

working with probabilistic approaches for short term statistics, since this yields a connection to operational conditions.

CONCLUSIONS

The metacentric height GM of ships in following irregular waves has been investigated as a random process by means of numerical computations. The work has been based on assuming quasi-static equilibrium and that the only external forces are the Froude-Krylov forces.

The conclusions of this work may be summarised as:

• By comparisons of the GM response in regular and irregular waves for three different hull forms, it is clearly shown that the characteristics of modern hull forms significantly increases the GM variations.

• GM of the investigated ships in following random seas is a non-linear, and therefore non-Gaussian, process. The most important non-linear feature is the existence of a slowly varying process, having the general effect of reducing the absolute values of minimum GM. Hence, neglecting this effect can be highly conservative, except for very moderate sea states.

• The GM fluctuations at encounter frequencies, that is with the slowly varying part filtered out, can be accurately estimated through linear response theory.

• A simple method has been developed for prediction of the non-linear GM fluctuation in random seas. In this method, the slowly varying component is expressed as a function of the envelope of the linear variation. Comparisons of statistical distributions using the developed method and time-domain simulation results shows that the method is capable of predicting the statistical characteristics caused by non-linearity. The quantitative accuracy could however be improved.

REFERENCES:

1. Bishop, R.E.D, Price, W.G. and Temarel, P.: "On the Role of Encounter Frequency in the Capsizing of Ships", STAB 82, Tokyo, oct, 1982

2. Paulling ,J.R.: " The Transverse Stability of a Ship in a Longitudinal Seaway", J.S.R., vol. 4, March, 1961

3. Hamamoto, M. and Nomoto, K.: "Transverse Stability of Ships in a Following Sea", STAB 82, Tokyo, Oct, 1982

4. Dunwoody, A.B.: "Roll of a Ship in Astern Seas - Metacentric Height Spectra", J.S.R., vol. 33, no. 3, Sep 1989

5. Dunwoody, A.B.: "Roll of a Ship in Astern Seas - Response to GM Fluctuations", J.S.R., vol. 33, no. 4, Dec 1989

6. Grim, O.: "Beitrag zu dem Problem der Sicherheit des Schiffes im Seegang", Schiff und Hafen, Heft

6, 1961

7. Helas, G.: "Intact Stability of Ships in Following Waves", STAB 82, Tokyo, Oct, 1982

8. Lipis, A.V. and Voitkounski Y.I.: "Consideration of the Influence of a Ship's Own Wave System on Ship Stability When Moving in Following Waves", STAB 90, Naples, sep, 1990

9. Blume, P. and Hattendorff, H-G.: "An Investigation on Intact Stability of Fast Cargo Liners", STAB 82, Tokyo, oct, 1982

10. Huss, M.: "The Stability of Ships in Waves; A Comparative Study of Modern Hull Forms with Large B/T Ratio", Report TRITA-SKP 1060, The Royal Institute of Technology, Stockholm, 1988

11. Umeda, N. et. al.: "Probabilistic Study on Ship Capsizing due to Pure Loss of Stability in Irregular Quartering Waves", STAB 90, Naples, sep, 1990

12. Blocki, W.: "Ship Safety in Connection with Parametric Resonance of the Roll", ISP, feb, no 306, 1980

13. Hua, J. and Palmquist, M.: "A Description of SMS", The Royal Institute of Technology, Div. of Naval Architecture, (Report to be printed 1994)

14. Hua, J. and Rutgersson, O.: "A Study of the Dynamic Stability of a RoRo-Ship in Waves", to be presented at STAB 94, Florida, 1994

15. Longuet-Higgins, M.S.: "Statistical Properties of Wave Groups in a Random Sea State", Phil. Trans. R. Soc. London, A 312, 1984

NOMENCLATURE

a	Wave amplitude
A_n, B_n	Fourier coefficients
c_i	Polynomial coefficient
C_B	Block coefficient
GM_{SW}	GM in still water
$\Delta \overline{GM_m}$	Change of mean GM in regular waves
GM_1	Amplitude of 1st harmonic GM variation in regular waves
$\Delta GM(t)$	Difference between momentary GM(t) and GM_{SW}
ΔGM_{min}	Difference between minimum peak values of GM(t) and GM_{SW}
$GM_{lin}(t)$	Linear GM process in irregular waves
$\hat{GM}_{lin}(t)$	Hilbert transform of $GM_{lin}(t)$
$\Delta GM_s(t)$	Difference between slowly varying GM process and GM_{SW}
$\breve{GM}_{lin}$	Peak value of $GM_{lin}(t)$
$f_{GM}(\omega)$	Transfer function of $GM_{lin}(t)$
$\rho_{GM}(t)$	Envelope function of $GM_{lin}(t)$
H_s	Significant wave height
T_m	Zero-crossing wave period
L_{pp}	Ship length between perpendiculars
M_{Roll}	Froude-Krylov roll moment
R, R', R_a	Rayleigh parameters
S_{GM}	Spectral density of $GM_{lin}(t)$
S_W	Spectral density of $\eta(t)$
t	Time
ω	Frequency
$\Delta\omega$	Frequency increment
ω_p	Modal frequency
$\eta(t)$	Wave elevation
k_i	Wave number of spectral component
ϕ	Roll angle
∇	Volume displacement
ρ	Density of salt water
λ	Wave length

ON THE ROLLING MOTION INSTABILITY INDUCED BY SAIL ACTION

Boccadamo G.,Tortora E.
UNIVERSITY OF NAPLES 'FEDERICO II'
Naval Architecture and Marine Engineering Dept.

De Rosa S.,Lecce L.
UNIVERSITY OF NAPLES 'FEDERICO II'
Department of Aeronautical Engineering

Abstract

Generally the sail is considered a stabilizing device able to damp rolling motion. However, with some combination of course sailed, wind speed, sail trim, sail and hull-keel characteristics, the sail can actually transfer energy from the wind to the vessel rolling motion, which becomes unstable and therefore tends to grow with time.

In a previous work/7/the main factors governing this phenomenon have been individuated by means of both a theoretical approach and of a set of dynamic tests on a sail model in the wind tunnel.

In the present paper results of a more complete set of wind tunnel experiments, carried out in order to investigate the effect of the sail shape and aspect ratio and of the reduced frequency have been reported.An analytical expression of the unsteady aerodynamic rolling moment acting on a sail has also been derived and numerical results have been compared to the experimental ones. A worked example highlights the applications of the above results.

NOMENCLATURE

a = added mass
b = damping coefficient
b' = sectional damping coefficient
c_H = restoring coefficient
c = chord lenght
c_s = spring constant
C_L = lift coefficient
C_D = drag coefficient
I_{xx} = mass moment of inertia of the boat about x-axis
k = $\omega c/V_A$; reduced frequency
k_{xx} = geometrical radius of gyration
M =aerodynamic moment
S = area
V_A = wind speed
V = boat speed
α = angle of attack
β = angle of course sailed
δ = logarithmic decrement

δ_m = sail trim angle
η = heel angle
ρ = mass density
ω = circular frequency

Subscripts

A = sail
K = keel
H = hull

INTRODUCTION

In the last years during ocean racings many boats have experienced knocked down.

It is opinion of many researchers that this behaviour of the sailing boats is due to the recent trends in design, whose only purpose has been to achieve improvements in speed despite of seaworthiness.

Statical stability calculations don't allow to estimate the actual behaviour of the sailing boat, which depends on many factors such as displacement, mass of inertia, damping, restoring and aerodynamic moment acting on the sails, which are the factors governing the seakeeping characteristics of the boat.

Probably every sailorman has experienced heavy rolling motion. This phenomenon can be observed on boats of every size and even in flat sea so that it is natural to look for the causes in aerodynamic reasons. (Marchaj/2/)

Generally the sail is considered a stabilizing device able to damp the rolling motion. However, with some combination of course sailed, wind speed, sail trim, sail and hull-keel characteristics, the sail can actually transfer energy from the wind to the vessel rolling motion, which becomes unstable and therefore tends to grow with time.

The aim of this study is to analise the rolling motion of the boat in still water and under the action of the aerodynamic moment, assuming that the motion of the boat is reduced to one degree of freedom.

In a preceeding work the study was confined to the initial stability.

A linear mathematical model based on a quasi-stationary approach was drawn for the determination of the aerodynamic moment induced on the sail by the rolling motion.

Two series of experimental tests in the wind tunnel were carried out:
- static tests, to determine the stationary aerodynamic coefficients of the sail;
- free oscillatory dynamic tests, to assess the stability of the sail and to compare the results with those theoretically obtained.

Such comparison showed that the linear quasi stationary approach allows to individuate the main factors governing the phenomenon and predict the pattern of the experimental results, while on the other hand, the comparison evidenced that non-linear

and unsteady effects have to be taken into account to achieve a reasonable accuracy.

Therefore a non-linear mathematical model for the determination of the aerodynamic moment has been drawn and correction terms have also been built up in the expression of the aerodynamic moment to address the unsteady effects.

Static and free oscillatory dynamic tests have been again carried out, this time using two different sail models to assess the influence of sail shape too.

Theory

The assumed equation of an uncoupled rolling motion for the sailing boat in calm sea is:

$$(I + a)\ \ddot{\eta} + (b_H + b_K)\ \dot{\eta} + c_H\ \eta = M(\eta,\dot{\eta})$$

Attention is to be devoted to the damping terms and to the aerodynamic moment M.

In the above equation b_H is the linear wave damping coefficient, which can be calculated using the strip theory together with a multiparameter conformal transformation technique./3, 4/. The problem constituted by the particular shape of the sailing boat sections due to the presence of the keel can be overcome choosing enough transformation parameters; the nineteen parameter transformation reproduces the sectional shape with reasonable accuracy. However, calculations show that this damping term is far less than the others.

Particularly, the keel has the most important role in dissipating rolling energy. The keel damping is mainly caused by the variation of the lift force due to the rolling motion. The following expression for the keel damping coefficient:

$$b_K = \frac{1}{2}\rho_w k^2_{xx_K} S_K V \frac{dC_{LK}}{d\beta_K} \qquad (1)$$

derived by the authors /7/, has been adopted.

The aerodynamic moment M is the crucial term, because it can transfer energy from the wind to the rolling motion which therefore can become unstable.

As first approach, assuming that the rolling amplitude is very small and neglecting unsteady effects, a linear expression has been derived:

$$M(\eta,\dot{\eta}) = \frac{\delta M}{\delta \dot{\eta}}\dot{\eta} = -\frac{1}{2}\rho_A k^2_{xx_A} S_A V_A C_{\delta Y_A}\ \dot{\eta} \qquad (2)$$

where the coefficient C_{dY_A} under the above hypothesis does not depend on the amplitude nor on the frequency of the motion.

The validity of the above expression has been tested by means of wind tunnel experiments. The values of the theoretical coefficient C_{dY_A} were compared with the experimental ones, obtained as:

$$C_{\delta Y_A exp} = \frac{2}{\rho_A k^2_{xx_A} S_A V_A} \frac{c}{\omega} \frac{\delta_{A exp}}{\pi} \qquad (3)$$

The comparison showed that the non-linear and unsteady effects are to be taken into account.

Moreover, two important findings were highlighted by the experiments:

- the frequency of the motion under the action of the wind is in practice equal to the natural frequency of oscillation of the system (measured in absence of wind);

- the pattern of the recorded time-history resembles a sinusoid of varying amplitude.

These findings suggest that the non-linearity is weak and located in the damping of the system, which means that the moment M depends only on the roll angle and velocity.

In the appendix the following non-linear expression has been derived for the aerodynamic moment:

$$M\left(\eta,\dot{\eta}\right) = \frac{1}{2}\rho_A \int_{r_1}^{r_2} V_{1m} c(r) \left(C_L(\alpha) V_A \cos\beta_A + C_D(\alpha) V_A \sin\beta_A \cos\eta - C_D(\alpha)\dot{\eta} r \right) r \, dr \qquad (4)$$

where:

$$V_{1m} = \left[\left(V_A \cos\beta_A\right)^2 + \left(V_A \sin\beta_A \cos\eta - \dot{\eta} r \right)^2 \right]^{1/2}$$

$$\cos\alpha = \frac{V_A \cos\beta_A \cos\delta_m + \left(V_A \sin\beta_A \cos\eta - \dot{\eta} r \right) \sin\delta_m}{V_{1m}}$$

and $C_L(\alpha)$, $C_D(\alpha)$ are measured by static tests.

In deriving the above expression the quasi-stationary hypothesis has not yet been removed.

Fig. 1 shows the pattern of the function $M(\eta,\dot{\eta})$ versus $\dot{\eta}$ at $\eta = 0$ and for several values of the angle β_A, together with the straight lines corresponding to the linear expression (2); it is evident that the non linearity of eq(4) is weak, well in agreement with the experimental result.

The previous considerations suggest the opportunity of using the classic method of equating the work per cycle done by the damping terms to the variation of the kinetic energy of the motion

in order to calculate the variation per cycle of the motion amplitude.

According to this method, the work per cycle of the aerodynamic moment is:

$$W_A = \int_T M\omega \eta_A \cos\omega t dt \qquad (5)$$

where η_a is the amplitude of the cycle;
the work per cycle done by the linear damping terms is:

$$W_{H+K} = -(b_H + b_K)\ \omega\ \eta_a^2\ \pi$$

the variation of the kinetic energy is:

$$\Delta E \cong m\ \omega^2\ \eta_a\ \Delta\eta$$

so equating:

$$\Delta\eta = \frac{W_A + W_{H+K}}{m\omega^2\eta_a}$$

If the sum $W_A + W_{H+K}$ is positive the motion amplitude grows and therefore the motion becomes unstable if, as the amplitude increases, the energy dissipated W_{H+K} never becomes greater than the work W_A done by the aerodynamic moment

the eq. (5) does not take into account the unsteady effects; obviously the phenomenon is actually much more complex being the air flow non stationary. Therefore a correction is introduced in eq (5):

$$W_A = \omega\ \eta_a \int_T C_1(k) M \cos(\omega t + C_2(k)) dt \qquad (6)$$

where C_1 is a coefficient which reduces the amplitude of the aerodynamic moment and C_2 is the phase delay of the aerodynamic moment with respect to the rolling velocity.

Both these two coefficients are reasonably function of the reduced frequency k and can be calculated, in first approximation, by means of the Theodorsen function C(k), which can be applied in absence of flow separation:

$$C_1(k)\ \exp\ iC_2(k) = C(k)$$

Eq(6) has been used to predict the behaviour of the experimental system.

The equation governing such system is assumed to be:

$$I\ddot{\eta} + b\dot{\eta} + c_s\eta = M(\eta, \dot{\eta})$$

Because the frequency of the motion is equal to the natural frequency of the system, we can put

$$m\omega^2 = c_s$$

so that the variation of amplitude per cycle can be calculated as:

$$\Delta\eta = \frac{W_A - c_s \eta_A^2 \delta_0}{c_s \eta_A^2}$$

where δ_0 is the natural logarithmic decrement and c the spring constant of the system which can be easily measured.

WIND TUNNEL TESTS

Test equipment

The experimental tests were carried out in the closed circuit low-speed wind tunnel of the Institute of Aircraft Design, that have an open test chamber with ellipse jet section of 0.9x 0.6 metres.

The test models were two rigid sails R1 and R2 made of aluminium plate of 3 mm thickness and with circular arc section having the following main dimensions

	R1	R2
span	0.38 mt	0.40 mt
chord	0.26 mt	0.095 mt
chamber to chord	0.19	0.2

Such dimensions of the test model were chosen in order to reduce to a minimum the blockage effect and meantime having the maximum test Reynold number.

The model both for static and dynamic test was connected to the force and moment measuring balances by a stiff vertical tube. At the same time the balances were connected to the external wind tunnel supporting frame, that have a three axes moving capabilities, through a pivoting system that provide the angle of attack variation during the test. In both tests in order to expand the testing range of angle of attack, a two plate turntable system was interposed between the model and the balances, giving the possibilities to obtain a 120 degrees of angle of attack variation and, in the dynamic test case, the capabilities to change both the angle of attack α and the angle between the chord of the model and the model sensing direction δ_m (fig.1).

Static test

To measure the static aerodynamic forces acting on the sail model, a series of tests were carried out using a two component strain-gauged balance that permits to obtain the aerodynamic forces along two directions, fixed respect to the model chord. Simple geometrical transformation gives the conventional lift and drag aerodynamic coefficients. The results obtained are reported in fig. 2, and 3 where, for the range of the angle of attack from 0° to 90° that has been evaluated (due to the symmetry of the model), the curves $C_L = C_L(\alpha)$ and $C_D = C_D(\alpha)$ are shown for the two tested sails.

Dynamic tests

In order to evaluate the rolling stability of the sail model, dynamic tests were carried out connecting the same model used in the static tests with an elastic suspension system, previously used during the stall flatter study of a bridge section (Lecce et al. [6]), and giving to the model the possibility to freely oscillate as a one degree of freedom system.

The free oscillation method has been employed to investigate the unsteady aerodynamic rolling moment acting on the sail model. The tests were conducted both with and without wind, using always the same impulse force to start the motion. The free oscillation of the rolling motion was recorded and plotted. From these plotted data the frequency of oscillation and the free damping decay (the logarithmic decrement) were obtained for each testing condition that is defined by the two angles δ_m and β_A, the wind speed and the frequency of the oscillation without wind ω_0 (two different values obtained changing the inertia rolling moment of the sail model were investigated). The testing conditions were as follows:

TABLE 1

	Test n	β_A	δ_m	V_A	ω	K
sail R1	1-6	130°-180°	$1/2\beta_A$	17.3	19.23	0.289
"	7-12	"	"	15.25	22.93	0.391
sail R2	1-6	"	"	17.3	19.23	0.105
"	7-12	"	"	15.25	22.93	0.142

COMPARISON BETWEEN THEORY AND EXPERIMENT

Figg. 5 ÷ 11 show the experimental curves of the amplitude of the oscillating motion compared with the theoretical ones. As it can be seen, the pattern of the experimental curves is quite well predicted by the theory in many cases although in other cases the predicted decay is different from the experimental one

A more concise comparison between theory and experiment is presented in figg. 12÷15, where the coefficient $C_{\delta y A exp}$ given by eq. (3) is plotted together with the theoretical values obtained by

$$C_{\delta Y_A} = \frac{b_{Aeq}}{1/2\rho_A K_{xx}^2 S_A V_A}$$

in which the equivalent linear damping is given by

$$b_{Aeq} = -W_A/\pi\omega\eta_a^2 \qquad (7)$$

and has been evaluated at the mean value of amplitude. In the above eq. (3) δ_{Aexp} has been calculated as difference between the mean value measured during the test and the natural damping decay of the system.

The above figures show that the range of β_A angle in which the coefficient C_{dY_A} become negative, that is in which the sail transfer energy to the motion of the system, is underestimated by the theory in the case of the sail R1, while the opposite applies in the case of the sail R2.
Probably the prediction could be improved adopting a theory valid also in presence of flow separation, as for instance the Ragget theory, for the determination of the coefficients C_1 and C_2. This shall be subject of a future work.

However taking also into account the experimental accuracy, the authors feel that the proposed procedure can give an indication on the behaviour of an actual boat as highlighted in the following section.

APPLICATION TO A SAILING BOAT

As application of this study the preceeding considerations have been applied to a sailing boat, the main particulars of which were:

L_{OA} = 12.00 m T = 2.17 m
B = 3.64 m S_A = 123 m^2
Δ = 8207 Kg S_K = 2.5 m^2
ω_0 = 0.80 rad/s.

For this frequency the damping coefficient of the hull b_H is equal to 0,0688 KN·m·s.

The equivalent linear damping coefficient b_A of the sail calculated by means of eq. C are reported in the following table:

TABLE II b_A (KN m s)

		Va (Knots)				
β_A	δ_m	10	15	20	25	30
180	90	-7.16	-13.1	-19.2	-25.6	-32.3

The damping coefficients b_K of the keel, calculated by means of eq. 1 and using for $\frac{dC_L}{d\beta_H}$ the expression given in Norwood [5], are reported in table III as a function of the speed of the boat:

TABLE III b_K (KN m s)

V (Kn)	2	4	6	8	10
b_K	10.3	20.6	31.0	41.3	51.6

It should be noted that the linear wave damping is negligible.

From the values reported in the above tables it can be deduced that in a windlee course (b_A=180 deg.) the sum $b_H + b_K + b_A$ is negative, and therefore the boat is initially unstable, when the boat speed is lover then a limit value depending on the wind speed. For instance, being V_A=30 knots the limit value is about 6 knots.

The non-linear expression of the aerodynamic moment, togheter with the energetic approach, allows to determine the value of the motion amplitude at which the work done by the aerodynamic moment is balanced by the energy dissipated by the keel.

Fig. 16 shows the curves of W_A and of W_K for several boat speeds.

At v=2 Kn, the equilibrium is reached at a rolling motion amplitude of over 30 degrees; the equilibrium amplitude decrease as the boat speed inceases: at 4 Kn it is about 12 deg at boat speed greater than than 6 Kn the damping due to the keel makes the rolling motion initially stable.

The above results confirm that very dangerous situations can occourr in a windlee course, after the spi is raised and before the boat has reached her steady speed.

CONCLUSIONS

A sailing boat at windlee course can experience a very high heeling angle due to sail action.

The non linear procedure reported in the paper gives a quantitative evaluation of the heeling angle which can be reached in such conditions.

Further improvement is needed to better address the unsteady effects in presence of flow separation.

ACKNOWLEDGEMENTS

The research has been financially supported by MURST 40% and CNR funds.

REFERENCES

1) C.A. Marchaj, "Seaworthiness: the Forgotten Factor", Adlar Coles Ltd., 1986.
2) C.A. Marchaj, "Instability of Sailing Craft Rolling", The Ancient Interface Conference, California, November 1971.
3) R.E.D. Bishop, W.G. Price, P. Temarel, "Hydrodynamic Coefficient of Some Swaying and Rolling Cylinders of Arbitrary Shape", International Shipbuilding Progress, Vol. 27, March 1980.
4) R.E.D. Bishop, W.G. Price, P.K.Y. Tam, "The Representation of Hull Section and its Effect on Estimated Hydrodynamic Actions and Wave Response", Trans RINA, 1978.
5) J. Norwood, Jr., "High Speed Sailing", Adlar Coles Ltd., 1979.
6) L. Lecce, F. Marulo, M. Como, L. Pagnini. "Theoretical and Experimental Study of Torsional Flutter of Cable Stayed Long Span Bridges", AIMETA Conference, Italy, 1984.
7)-Boccadamo G., Lecce L., Tortora E.: 'On the Rolling Instability induced by Aerodynamic Forces' IMAM'93 Conference, Varna, Bulgaria, November 1993.

APPENDIX - Expression of the aerodynamic moment $M(\eta,\dot{\eta})$

With reference to fig.17, the following two sets of reference axes have been adopted:
- equilibrium reference system C XYZ, which has the indisturbed motion of the boat, where:
the longitudinal axis X is the line of intersection of the centre line plane and the design waterplane, positive towards the bow;
the vertical axis Z is perpendicular to the still water plane and positive upwards;
the Y axis is positive to starboard to have a right hand system.
e_1, e_2, e_3 are the unit vectors of the X,Y,Z axes resp.
The X axis is assumed to be the axis of rotation in an uncoupled rolling motion.

- sail axes C lmn fixed in the sail, with:
n in the direction of the mast, positive upwards;
m in the direction of the mean chord of the sail;
l to have a right hand system.
n, m, l are the unit vectors of the n, m, l axes resp.

The position of the sail system with respect to the equilibrium system XYZ is defined by:
η angle of roll measured about the longitudinal fixed axis X (or the angle between the Z and n axes)

δ_m sail trim angle, between the mean chord and the simmetry plane (XZ plane) of the boat or between the m and Y axes when the boat is in the upright position (i.e. for η =0)

Finally, the direction of the horizontal apparent wind velocity V_A is individuated by the apparent wind angle (or course sailed angle) β_A, between V_A and the X axis.

Under a linear approach, the aerodynamic moment can be expressed as:

$$M(\eta,\dot{\eta}) = \frac{\delta M}{\delta \dot{\eta}}\dot{\eta}$$

where the derivative is to be evaluated at $\eta = 0$ and $\dot{\eta} = 0$
The procedure which leads to the following expression of this derivative is reported in the previous paper.

$$\frac{\delta dM}{\delta \dot{\eta}_4} = -\rho_{xx}^2 \frac{1}{2}\rho_A dS_A V_A C_{\delta Y_A}$$

where:

$$C_{dY_A} = \cos\beta_A\left(-C_L\sin\beta_A + C_D\cos\beta_A + \frac{dC_L}{d\alpha}\cos\beta_A + \frac{dC_D}{d\alpha}\sin\beta_A\right) +$$
$$+2\sin\beta_A\left(C_L\cos\beta_A + C_D\sin\beta_A\right)$$

and ρ_{xx} is the radius of giration of the sail area about the rolling axis.

Non-linear expression of the aerodynamic moment

The relations between the unit versors of the equilibrium and of the sail reference systems are:

$$e_1 = \sin\delta_m\ l + \cos\delta_m\ m$$

$$e_2 = -\cos\dot{\eta}\cos\delta_m\ l + \cos\dot{\eta}\sin\delta_m\ m - \sin\dot{\eta}\ n$$

$$e_3 = -\sin\dot{\eta}\cos\delta_m\ l + \sin\dot{\eta}\sin\delta_m\ m + \cos\dot{\eta}\ n$$

Let us consider a strip of sail of area dS, at a distance r from the axis of roll.

The apparent wind speed can be expressed as:

$$V_A = -V_A\cos\beta_A\ e_1 - V_A\sin\beta_A\ e_2$$

and the velocity p induced on the strip by the rolling velocity as:

$$p = r\dot{\eta}\ (\cos\eta\ e_2 + \sin\eta\ e_3)$$

adding these velocities, the total speed on the strip in the sail system is:

$$v = \left(-V_A\cos\beta_A\sin\delta_m + V_A\sin\beta_A\cos\eta\cos\delta_m - r\dot{\eta}\cos\delta_m\right) l +$$
$$+\left(-V_A\cos\beta_A\cos\delta_m - V_A\sin\beta_A\cos\eta\sin\delta_m + r\dot{\eta}\sin\delta_m\right) m +$$
$$+ V_A\sin\beta_A\sin\eta\ n =$$
$$= V_l\ l + V_m\ m + V_n\ n$$

Neglecting the V_n component, in the plane of the strip acts the speed V_{lm} whose modulus is:

$$|V_{lm}| = \sqrt{V_l^2 + V_m^2}$$

while the angle of attack is given by: $\cos\alpha = -\frac{V_m}{|V_{lm}|}$

The force acting on the strip is:

$dF = (dL\cos\alpha + dD\sin\alpha)\,l + (dL\sin\alpha - dD\cos\alpha)\,m$

being dL , dD the lift and drag forces in the direction of , and normal to V_{lm}, which can be expressed as:

$$dL = \frac{1}{2}\rho_A |V_{lm}|^2 C_L\, c(r)\, dr$$

$$dD = \frac{1}{2}\rho_A |V_{lm}|^2 C_D\, c(r)\, dr$$

Assuming that the force dF is applied on the n axis and integrating the contributions of each strip we finally obtain the desired expression for the aerodynamic moment:

$$M\left(\eta,\dot{\eta}\right) = \frac{1}{2}\rho_A \int_{r_1}^{r_2} V_{lm} c(r)\left(C_L(\alpha)V_A\cos\beta_A + C_D(\alpha)V_A\sin\beta_A\cos\eta - C_D(\alpha)\dot{\eta}r\right) r\, dr$$

where:

$$V_{lm} = \left[(V_A\cos\beta_A)^2 + \left(V_A\sin\beta_A\cos\eta - \dot{\eta}r\right)^2\right]^{1/2}$$

$$\cos\alpha = \frac{V_A\cos\beta_A\cos\delta_m + \left(V_A\sin\beta_A\cos\eta - \dot{\eta}r\right)\sin\delta_m}{V_{lm}}$$

are function of r.

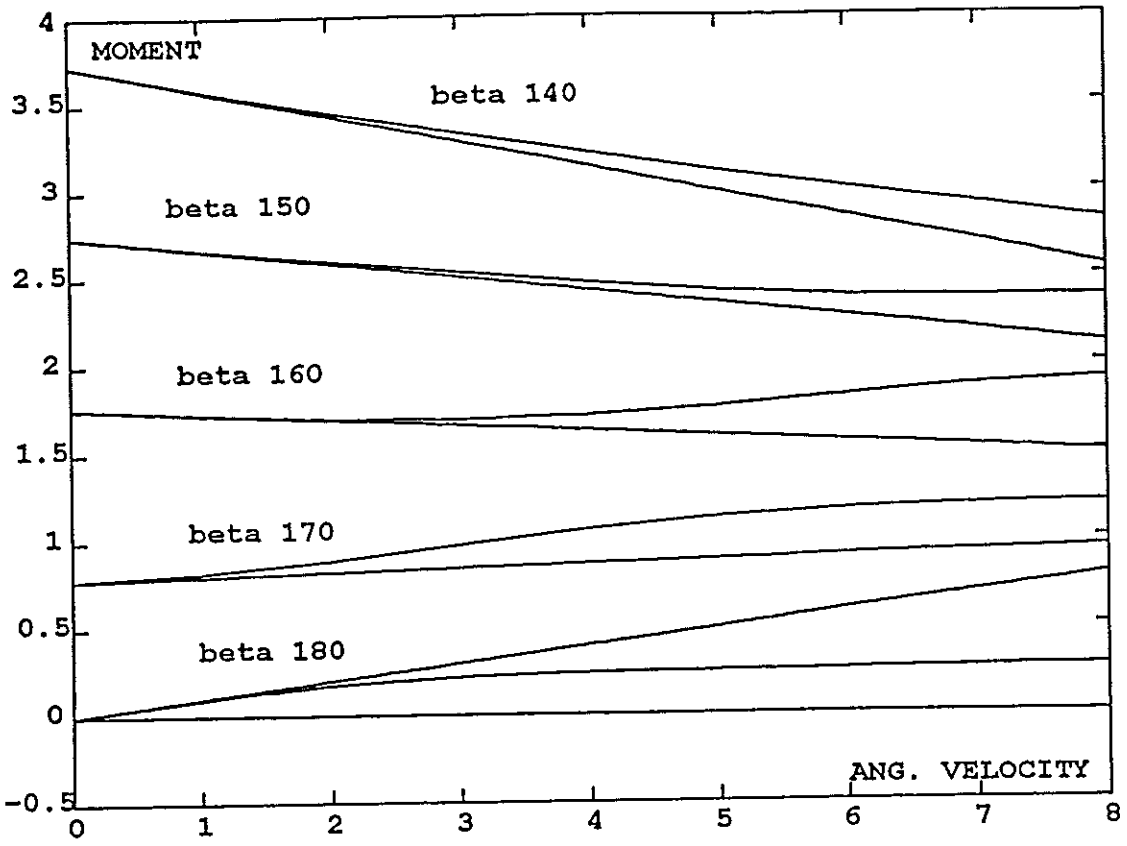
MOMENT
beta 140
beta 150
beta 160
beta 170
beta 180
ANG. VELOCITY
4
3.5
3
2.5
2
1.5
1
0.5
0
-0.5
0
1
2
3
4
5
6
7
8

Fig. 1

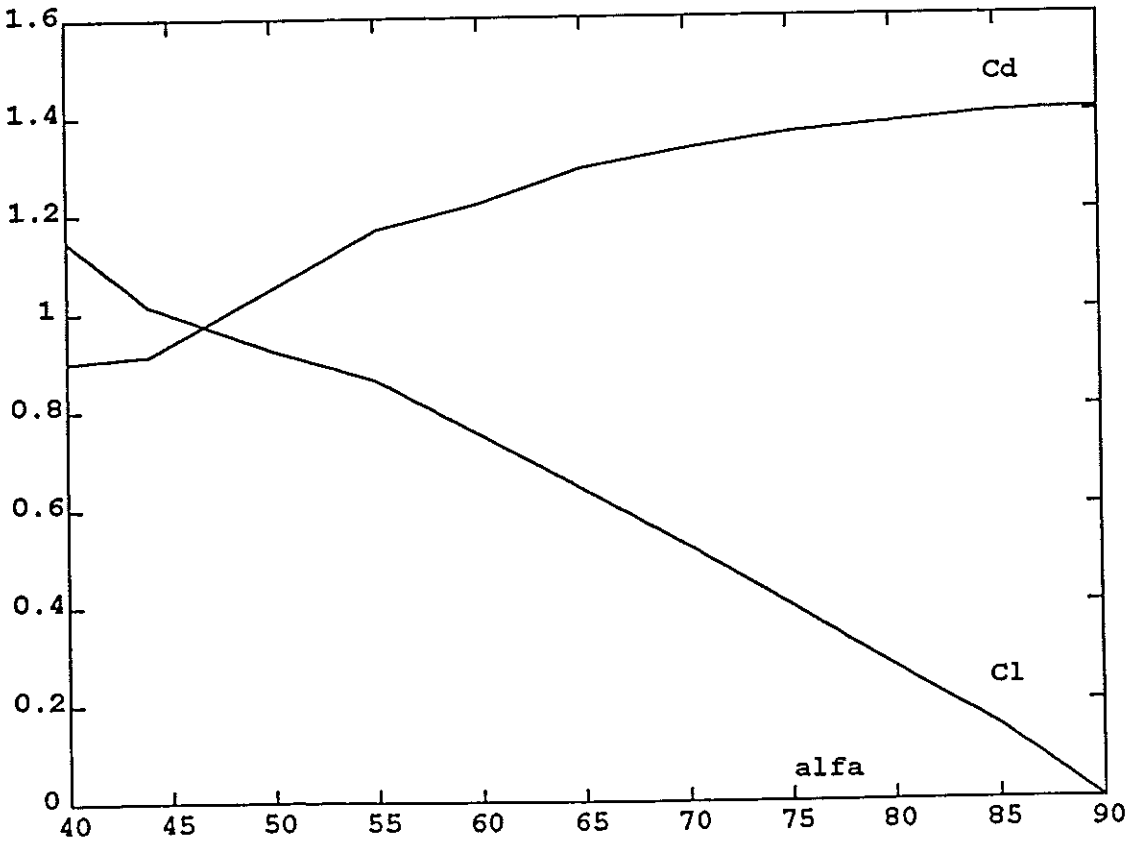
Cd
Cl
alfa
1.6
1.4
1.2
1
0.8
0.6
0.4
0.2
0
40
45
50
55
60
65
70
75
80
85
90

Fig. 2

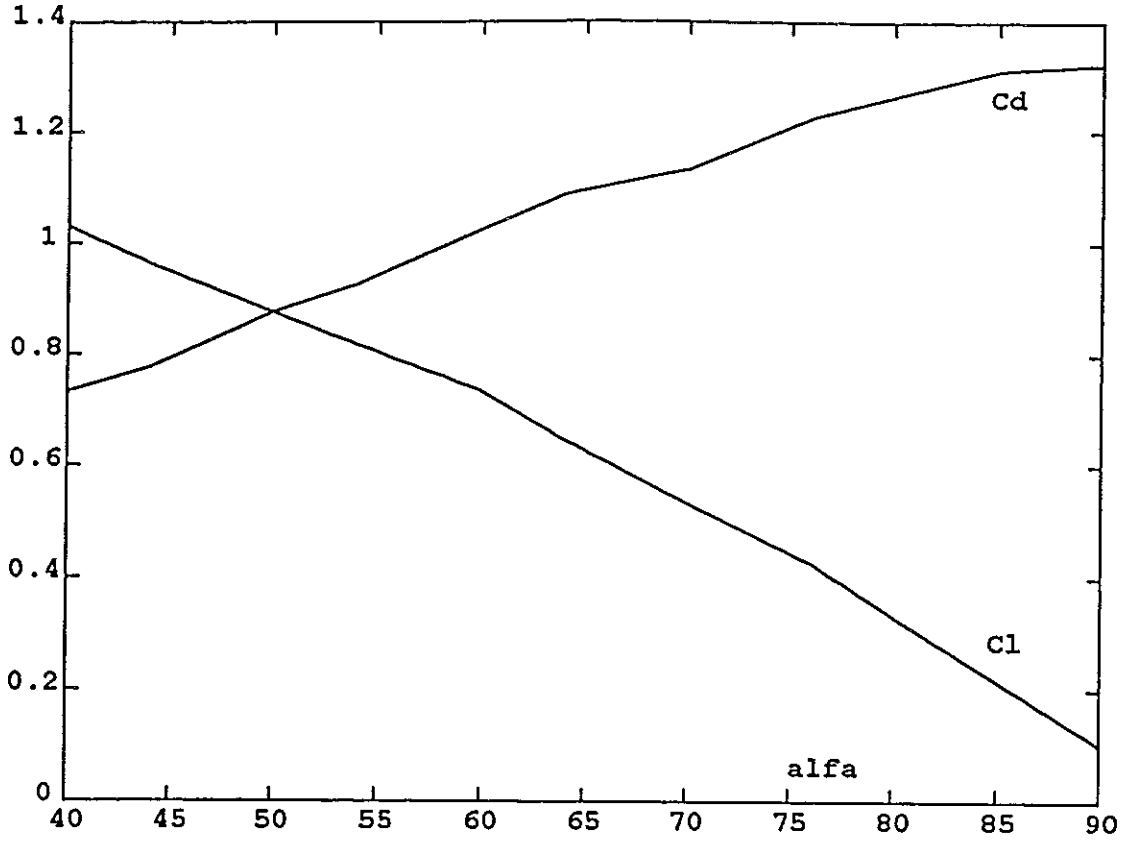
1.4
1.2
1
0.8
0.6
0.4
0.2
0
Cd
Cl
alfa
40
45
50
55
60
65
70
75
80
85
90

Fig. 3

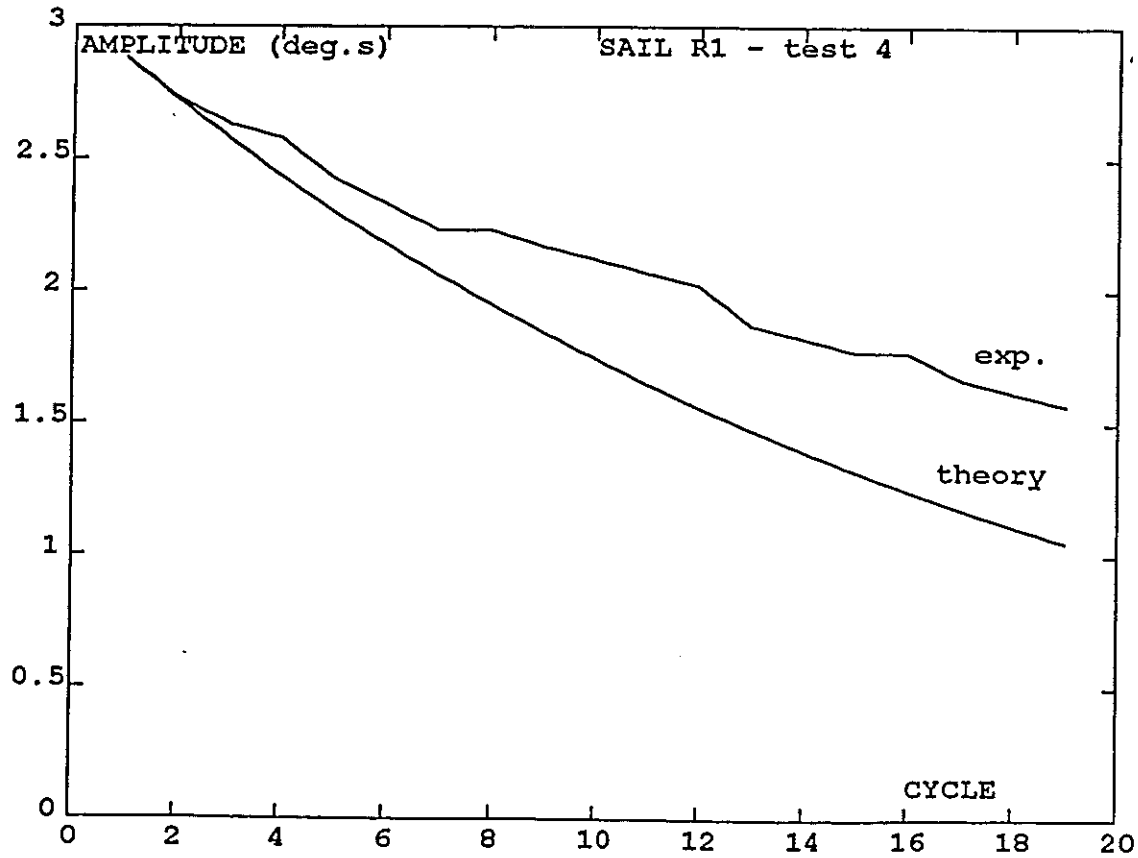
AMPLITUDE (deg.s)
SAIL R1 - test 4
3
2.5
2
1.5
1
0.5
0
exp.
theory
CYCLE
0
2
4
6
8
10
12
14
16
18
20

Fig. 4

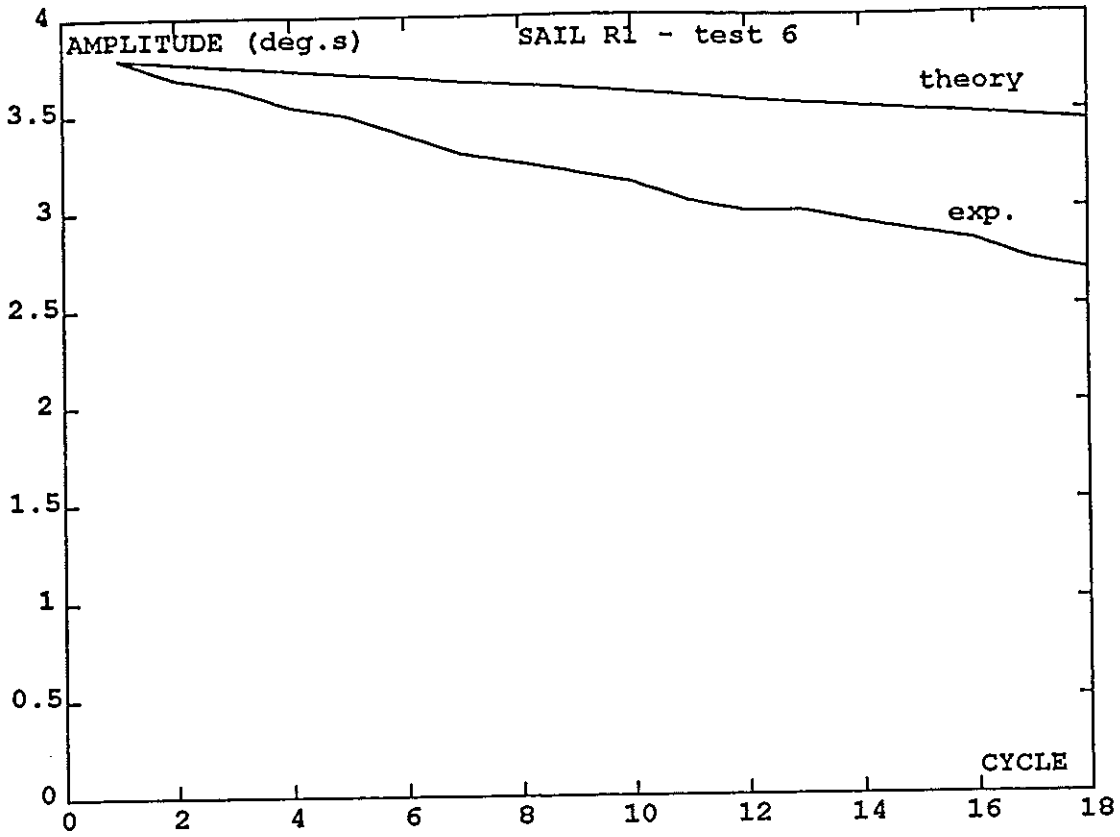
AMPLITUDE (deg.s)
SAIL R1 - test 6
theory
exp.
CYCLE
0
0.5
1
1.5
2
2.5
3
3.5
4
0
2
4
6
8
10
12
14
16
18

Fig. 5

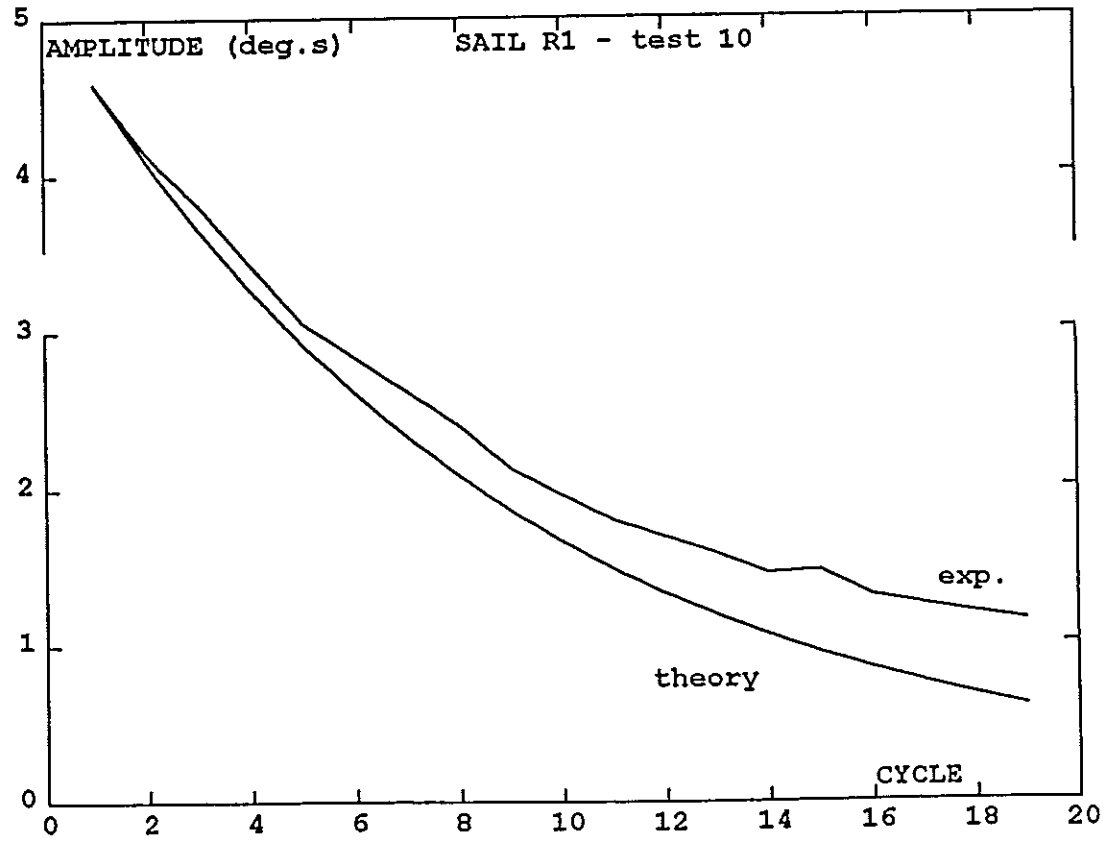
AMPLITUDE (deg.s)
SAIL R1 - test 10
exp.
theory
CYCLE
0
1
2
3
4
5
0
2
4
6
8
10
12
14
16
18
20

Fig. 6

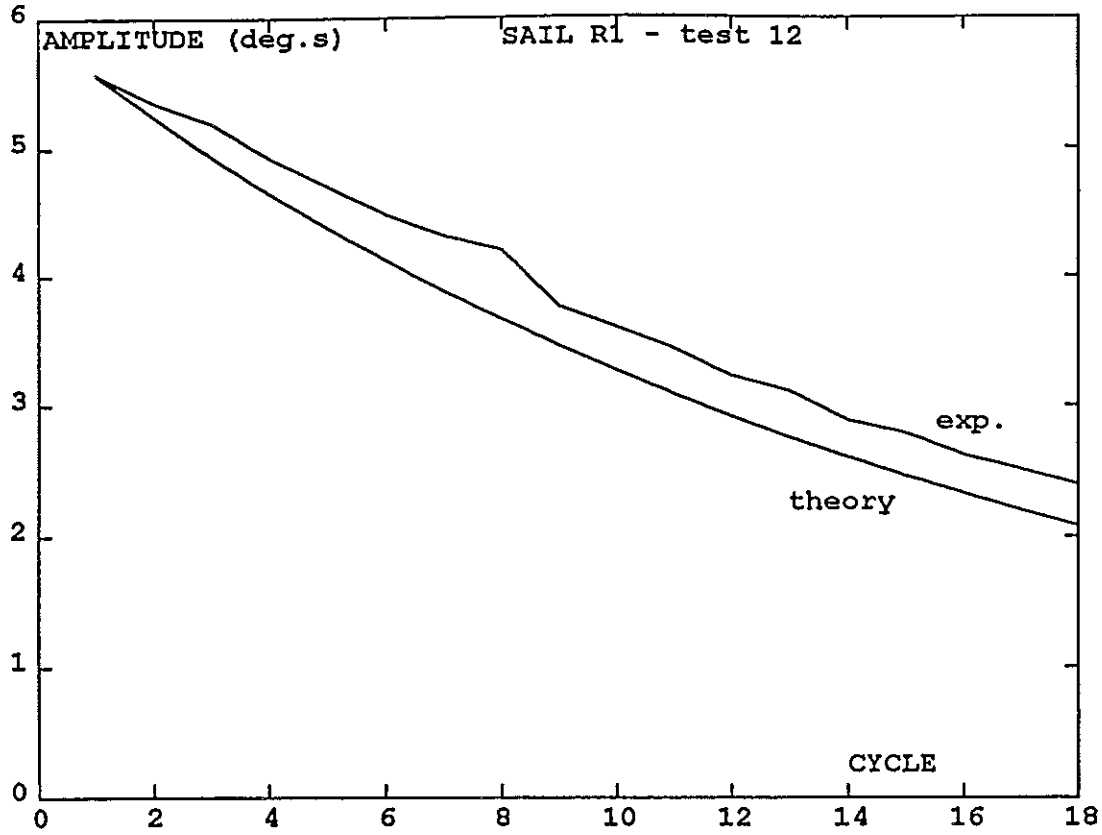
AMPLITUDE (deg.s)
SAIL R1 - test 12
exp.
theory
CYCLE
0
1
2
3
4
5
6
0
2
4
6
8
10
12
14
16
18

Fig. 7

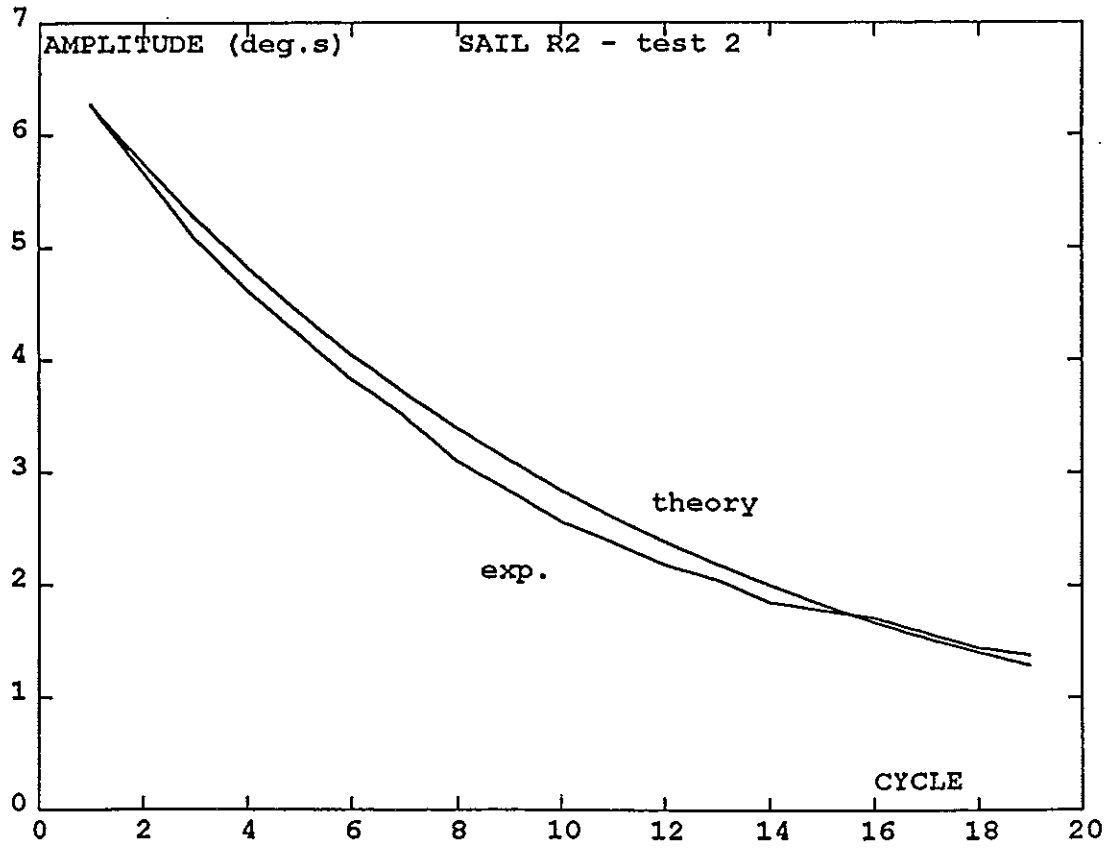
AMPLITUDE (deg.s)
SAIL R2 - test 2
theory
exp.
CYCLE
0
1
2
3
4
5
6
7
0
2
4
6
8
10
12
14
16
18
20

Fig. 8

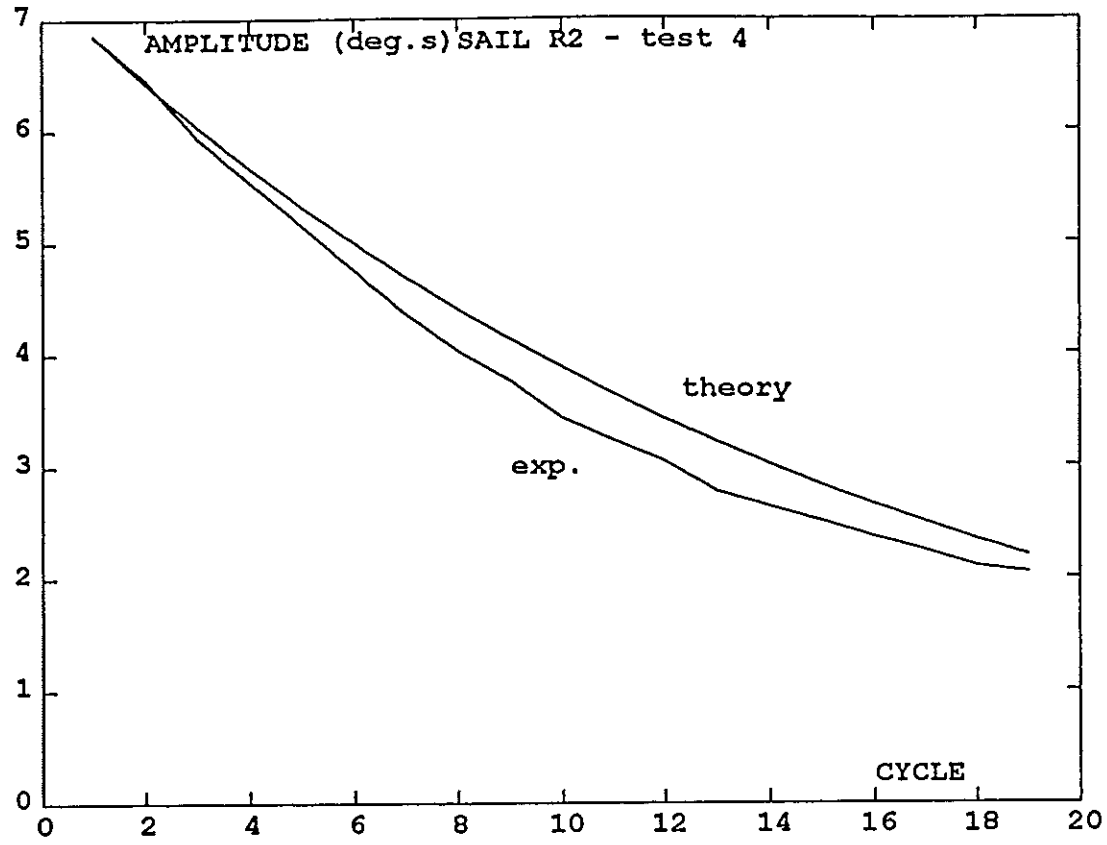
AMPLITUDE (deg.s)SAIL R2 - test 4
theory
exp.
CYCLE
0
1
2
3
4
5
6
7
0
2
4
6
8
10
12
14
16
18
20

Fig.9

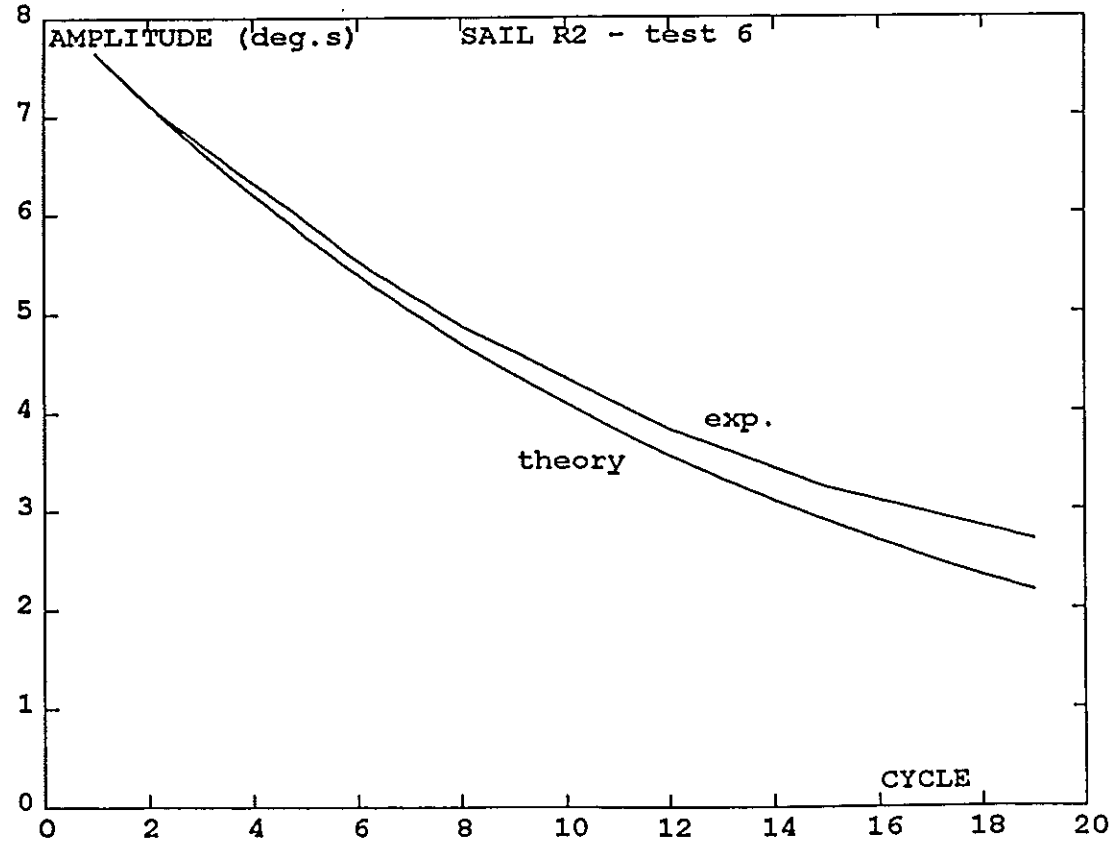
AMPLITUDE (deg.s)
SAIL R2 - test 6
exp.
theory
CYCLE
0
1
2
3
4
5
6
7
8
0
2
4
6
8
10
12
14
16
18
20

Fig.10

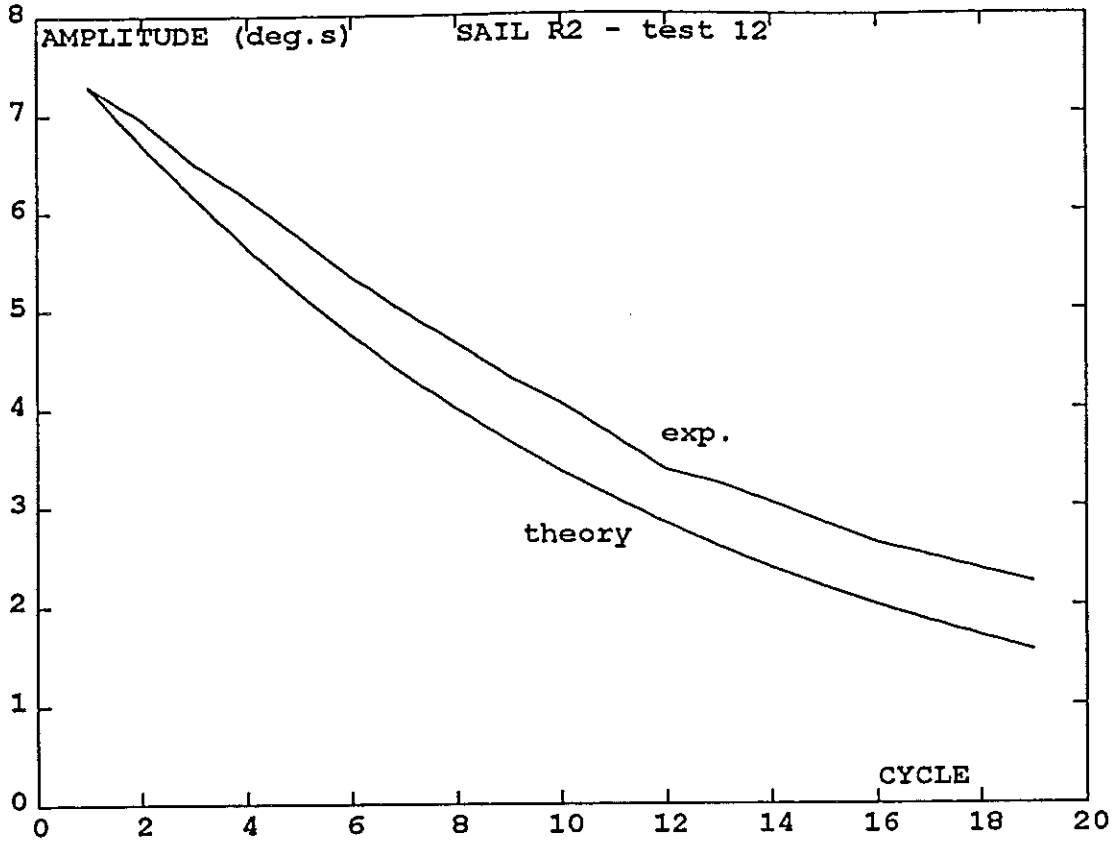
AMPLITUDE (deg.s)
SAIL R2 - test 12
exp.
theory
CYCLE
0
1
2
3
4
5
6
7
8
0
2
4
6
8
10
12
14
16
18
20

Fig11

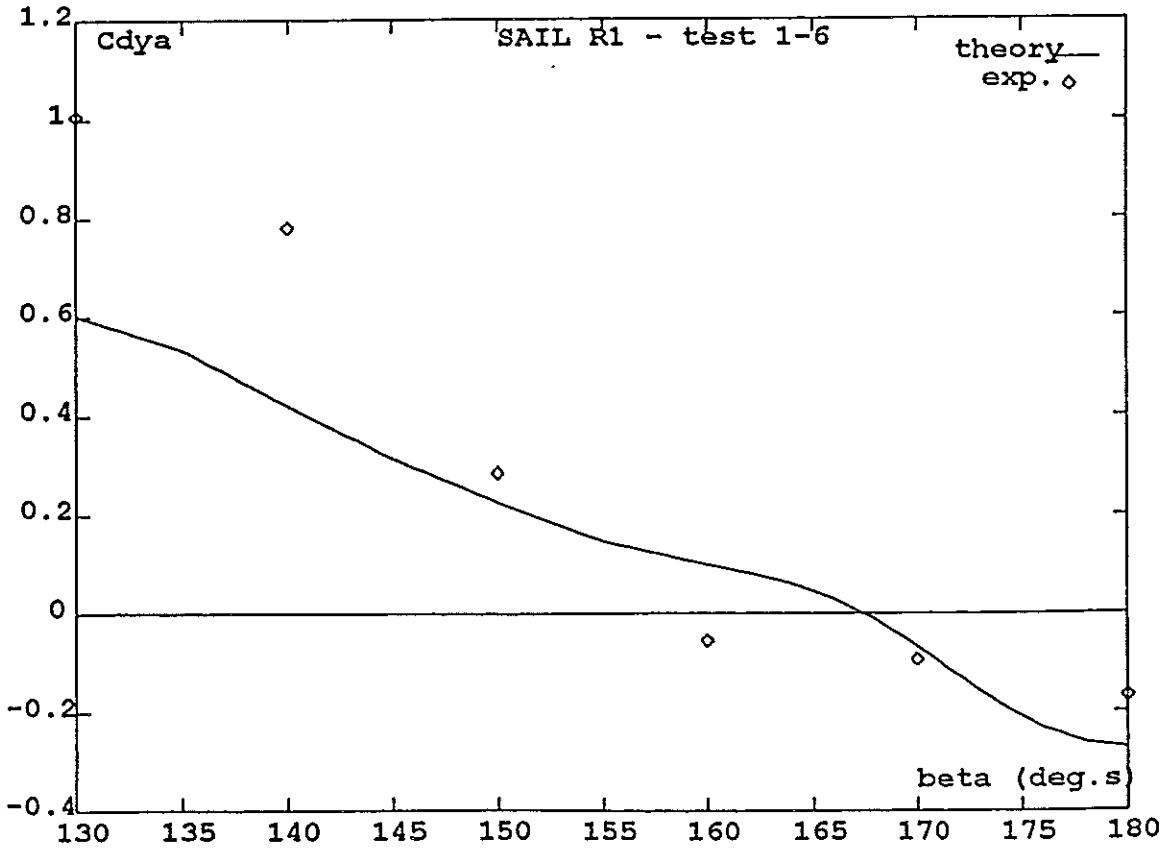
Cdya
SAIL R1 - test 1-6
theory
exp.
beta (deg.s)
1.2
1
0.8
0.6
0.4
0.2
0
-0.2
-0.4
130
135
140
145
150
155
160
165
170
175
180

Fig.12

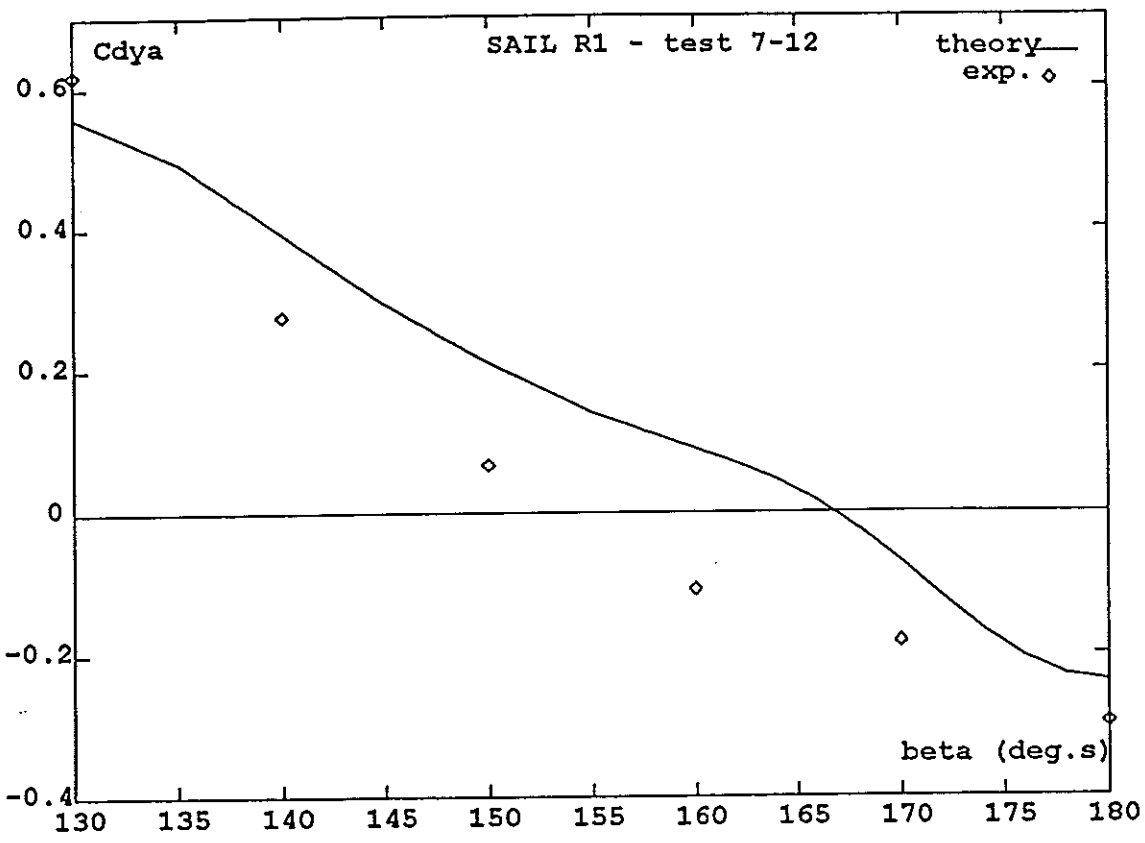
Cdya
SAIL R1 - test 7-12
theory
exp.
0.6
0.4
0.2
0
-0.2
-0.4
beta (deg.s)
130
135
140
145
150
155
160
165
170
175
180

Fig.13

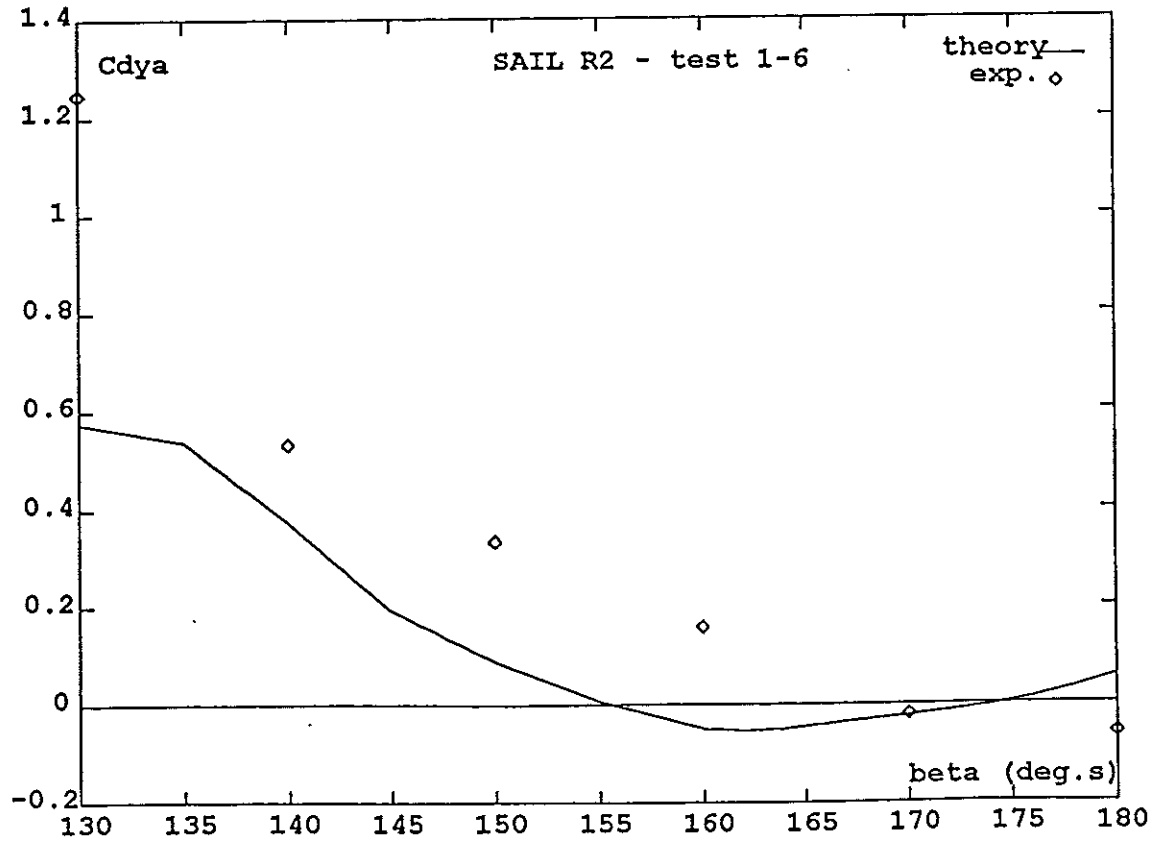
Cdya
SAIL R2 - test 1-6
theory
exp.
1.4
1.2
1
0.8
0.6
0.4
0.2
0
-0.2
beta (deg.s)
130
135
140
145
150
155
160
165
170
175
180

Fig.14

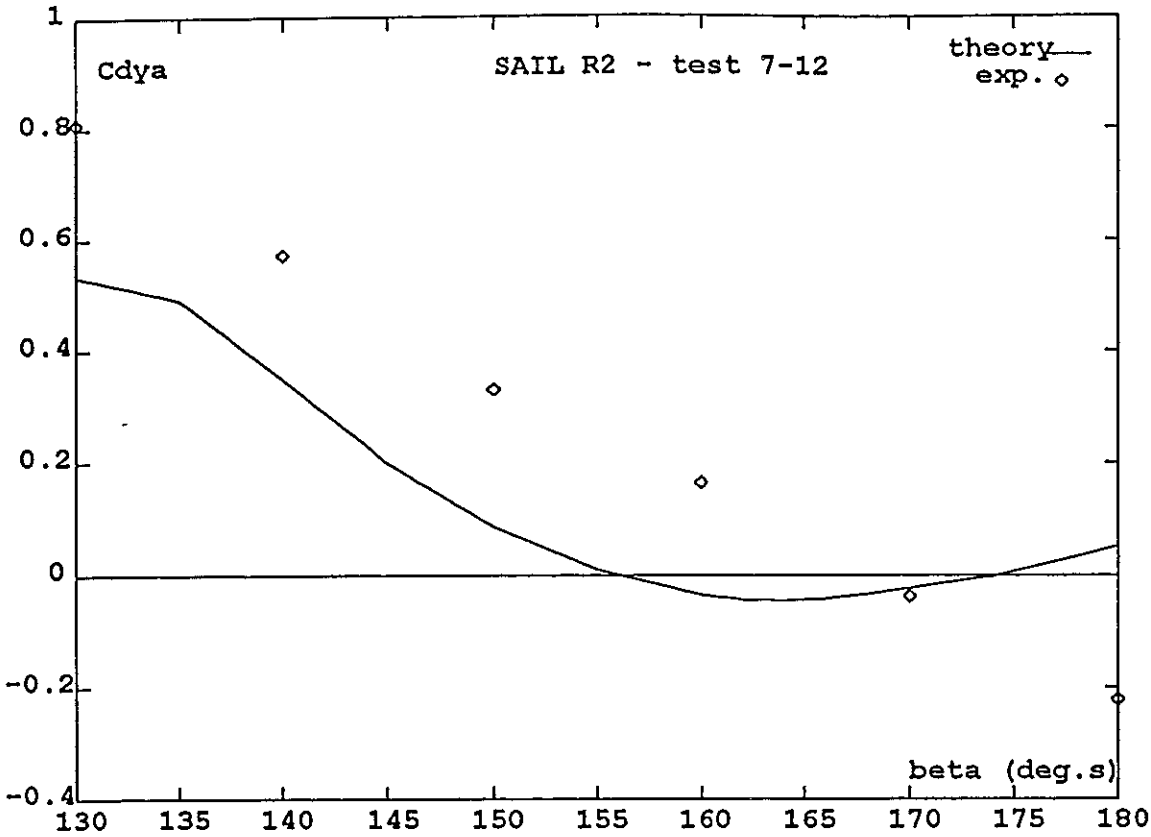
Cdya
SAIL R2 - test 7-12
theory
exp.
1
0.8
0.6
0.4
0.2
0
-0.2
-0.4
beta (deg.s)
130
135
140
145
150
155
160
165
170
175
180

Fig.15

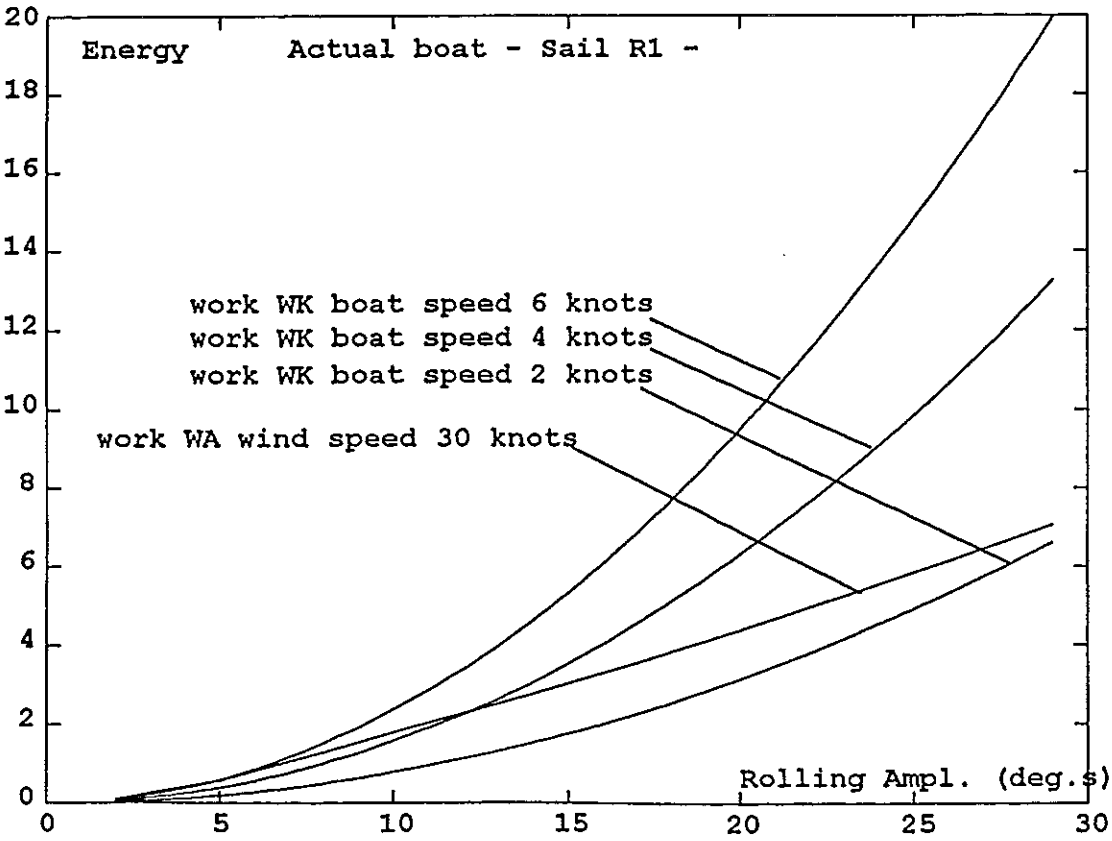
Energy
Actual boat - Sail R1 -
work WK boat speed 6 knots
work WK boat speed 4 knots
work WK boat speed 2 knots
work WA wind speed 30 knots
Rolling Ampl. (deg.s)
20
18
16
14
12
10
8
6
4
2
0
0
5
10
15
20
25
30

Fig.16

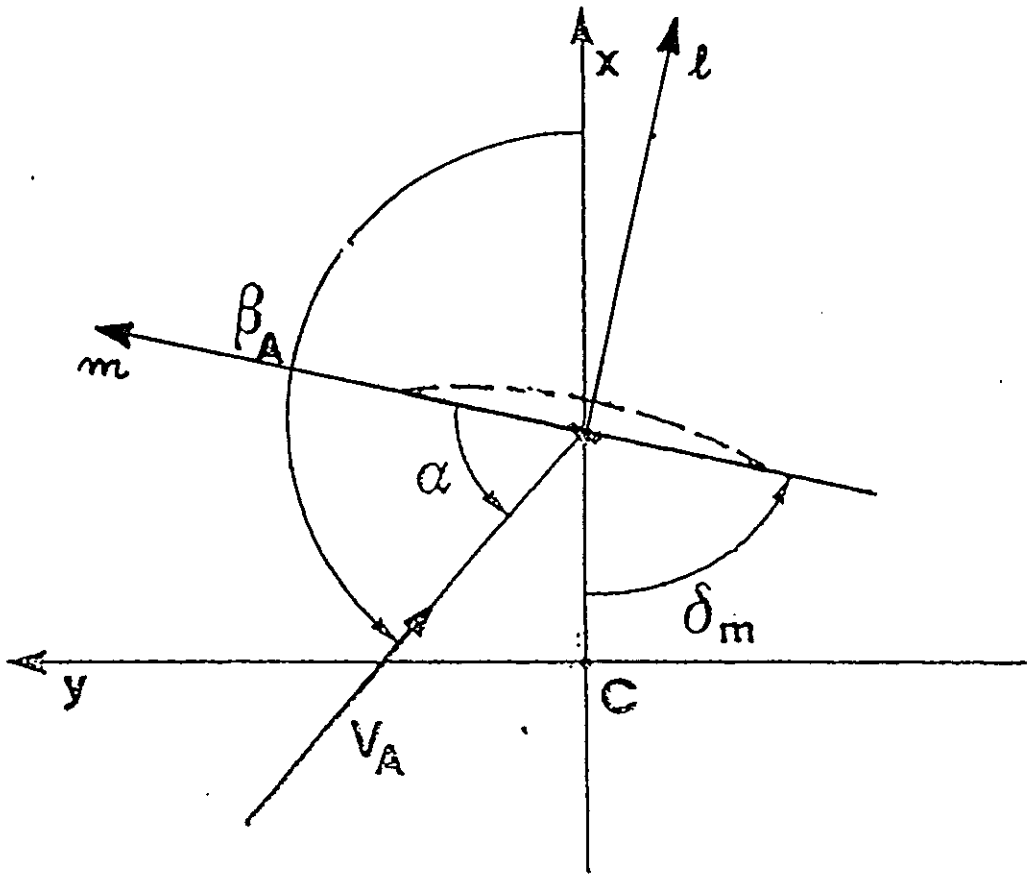

Fig. 17

5th International Conference on
Stability of Ships and Ocean Vehicles,
STAB'94, Melbourne, Fla, USA Nov. 1994

OPERATIONAL FACTORS IN STABILITY SAFETY OF SHIPS IN HEAVY SEAS

S. Grochowalski *, J.B Archibald **, F.J. Connolly **, C.K. Lee *
* National Research Council Canada,
** Canadian Coast Guard

ABSTRACT

The relationship between design stability, operational parameters, and overall stability safety is discussed. The most important operational factors which directly affect the probability of capsizing, are identified. The experimental results of the capsizing research carried out by the National Research Council and the Canadian Coast Guard are analyzed in detail in order to find a correlation between wave parameters, course angle and ship speed on the one hand and ship susceptibility to capsizing on the other . The results of the analyses are presented. The main physical phenomena involved in capsizing are identified. The influence of operating parameters on these phenomena and their contribution to capsizing is presented. The dangerous combination of operational factors is detected and a future form of practical operational criteria is discussed.

1. INTRODUCTION

In an endeavour to improve stability safety of ships, the efforts of researchers and regulatory agencies are focused on development of new, adequate theoretical models of ship capsizing in waves, and subsequently, relevant stability criteria and standards. Stability criteria regulate inherent features of a ship (design stability) to insure that the ship itself has the capability to navigate safely in heavy seas.

The efforts to develop better criteria and standards must be continued, but it becomes more and more obvious that even the best criteria will not provide absolute safety. In practical terms, it seems impossible to design a ship to be absolutely stable in all wave and loading conditions, although designers should aim for this objective.

Stability safety is a complex problem in which not only the inherent features of a ship but also the action of its crew determine whether the ship will survive in critical conditions. The skills of the crew and their correct reaction in a dangerous situation may well decide between survival and disaster. This "human factor" should be taken into consideration in the overall analysis of safety against capsizing and it has become recognized by technical experts and legislators.

The changing attitude to stability is reflected in the work of the international research community, in particular, at the International Maritime Organization (IMO). In IMO's Code of Intact Stability of Ships, the stability requirements and standards have been supplemented by some paragraphs related to operational aspects of stability safety, as for instance:

"Compliance with the stability criteria does not ensure immunity against capsizing, regardless of the circumstances, or absolve the master from his responsibilities. Masters should therefore exercise prudence and good seamanship having regard to the season of the year, weather forecasts and the navigational zone, and should take the appropriate action as to speed and course warranted by the prevailing circumstances". (Paragraph 2.3)

Present stability standards, based mainly on the GZ curve, do not provide any direct indication of how the dynamic behaviour of a ship in waves would decrease stability safety, or what combination of waves and ship operations constitutes a threat of capsize. In addition to "prudence and good seamanship", the masters need such information in order to make correct decisions. In recognition of this problem, the IMO Sub-Committee on Stability and Load Lines and on Fishing Vessel Safety (SLF) established in February 1992 an International Correspondence Group to develop a manual for safe operation in following and quartering waves.

The manual, when developed, has to link a ship's dynamic features with its inherent stability and clearly indicate which operational parameters affect stability safety, and what is their dangerous combination. Theoretical studies, together with results of model experiments, should provide a solid basis for finding these relationships.

The Institute for Marine Dynamics of the National Research Council of Canada, together with the Canadian Coast Guard, have been carrying out research in ship capsizing for a few years. Comprehensive model tests of ship dynamics in quartering and extreme waves were performed, which yielded a significant insight into the capsize mechanism of small ships. The results of the tests have been re-examined from the viewpoint of the correlation between the operational factors and a ship's susceptibility to capsizing. Some of the results of the analyses are presented in this paper.

2. STABILITY SAFETY

Every ship has its own dynamic features and its individual stability characteristics. They depend on ship geometry and the distribution of mass. These two elements define the inherent stability and the dynamic behaviour in waves and wind.

The design stability represents the inherent ability of the ship to withstand a heeling action caused by external forces, and to return to the upright position when those forces cease. This ability is evaluated by means of stability criteria, based mainly on the static restoring moment in calm water (GZ curve) and some modifications for inclusion of some wave effects and stipulated external heeling moments.

The dynamic response to the action of waves and wind depends on the ship's dynamic features, on the wave and wind characteristics, and on some operational parameters which influence the degree of interaction between the ship and the environment. These parameters are ship's speed and course angle relative to wave direction.

The magnitude and energy of a ship's response to actual environmental conditions and operational parameters, determine whether the potential energy attributed to the inherent stability can counterbalance the dynamics of the heeling action. If the dynamics of motion in waves exceed a certain level, the ship will capsize.

As the ship's speed and course angle influence strongly the magnitude of energy exerted on the ship by the environment, there is room for improvement of stability safety by appropriate selection of these two parameters. Thus, the overall stability safety is determined not only by the design stability characteristics, but also by the operation in actual environmental conditions. The logical relationship between design stability and operational safety is presented in Fig.1.

As design stability depends on the loading condition, operators can influence stability by appropriate distribution of loads when taking on cargo in a port. This aspect of safety is well known, and masters use their knowledge, the stability booklet and, more and more, computer programs to optimize the loading location, and to estimate the resultant design stability characteristics.

Once the loading is complete, and the ship leaves port, the stability characteristics are usually fixed (except for those vessels which load or unload at sea). So, the operational parameters which are within the master's discretion during the voyage are course and speed. In heavy seas, the master should select a combination of these parameters so that the dynamic behaviour of the ship will not exceed a certain safe level and the vessel will not be threatened with capsizing. However, this is not such an easy task. It is difficult to predict in heavy weather conditions, how the change of the

operational parameters will affect ship's behaviour and its survival potential, and what is the optimum combination of course and speed.

The crew's comprehension and skills need to be enhanced by a set of guidelines developed in advance and based on sound analysis of the ship's dynamics and stability in waves. The guidelines should be a part of ship stability documentation. Such guidelines are currently under development at IMO.

3. OPERATIONAL GUIDANCE TO THE MASTER

A general consensus was reached at the IMO forum that navigation in following and quartering seas constitutes the largest threat to stability safety, and requires special attention and analyses.

Two main approaches to development of stability operational guidance are under way at present.

The first consists of a set of detailed criteria for each potentially dangerous situation, developed for each individual ship and for certain selected wave parameters (as for instance the Russian proposal in IMO doc.SLF 37/3/5).

Every ship has its individual dynamic characteristics and responds to wave actions in its own way. It has its own dangerous combinations of speed, course angle, loading conditions and wave parameters. The guidance should reflect these individual characteristics in order to provide accurate and relevant advice to the master. However, the variety and number of criteria for various possible scenarios, for each set of wave parameters, and for each loading condition, make it practically impossible to use this approach effectively on board a ship in heavy seas. The method requires use of a computer on the ship, supported by a specially developed software package. The evaluation of stability safety and the recommendation on appropriate action should be available in a simplified manner and not as complicated analyses of sets of graphs.

It must be pointed out that the detailed criteria are based mainly on theoretical models. Some of them are simplified and very often do not represent adequately ship behaviour in steep waves. Some phenomena involved in extreme wave conditions still await their mathematical representation. It will be some time before the full, complex behaviour of a ship in high waves will be described mathematically, modelled by computer, and as a result, the computerized advice to the master will be available. Yet, this direction will eventually provide the solution to the problem.

The second approach does not provide specific evaluation of an individual ship. Instead, it provides general guidelines, with a diagram indicating the dangerous combinations of operational conditions for all types of ships and wave parameters. A polar diagram composed of ship's speed related to wave velocity (represented by wave period) V/T, and of heading angle α, is currently under discussion at IMO (as the Japanese proposal in IMO doc. SLF 36/3/4 and SLF 37/3/2). Since the proposed polar diagram requires estimation of three operational factors only - ship's speed, course relative to waves, and wave period - it can be easily used on board ships. It does not include any stability characteristics, but assumes that the ship satisfies appropriate stability standards. The dangerous zone on the diagram provides only an indication of the most unfavourable combinations of operational conditions, and not the criterion whether the ship will survive or capsize.

Regardless of which approach is taken, the relevance and quality of the guidance developed will depend on:

- the adequacy of the theoretical models used,
- which dangerous physical phenomena are considered and modelled,
- which scenarios are included.

Development of adequate guidelines requires careful and detailed examination of various operational situations and physical phenomena experienced by ships in heavy seas when navigating in following or quartering courses. Results of the Canadian research reported in [1] have been thoroughly examined from the viewpoint of dangerous combinations of operational factors, occurrence of dangerous phenomena and their

contribution to capsizing.

The study was performed for a small fishing trawler of 19.75m length. The model tests were carried out in quartering, extremely steep and breaking waves, both periodic and irregular. The wave length ranged from 0.95 - 3.5 of the model's length, and the model's speed covered the range of Fn = 0.12 - 0.35. Four loading conditions were tested: port departure IA and IB, and full load IIA and IIB. Conditions IA and IIB satisfied the IMO stability requirements, while IB and IIA did not.

Some results and conclusions from the analysis are presented in the following sections.

4. SURF-RIDING, RIDING ON A WAVE CREST, BROACHING

Surfing and broaching are considered as the two main dangerous phenomena specific for ship operation in following and quartering seas. If they occur, the ship is threatened by loss of control and by capsize. Elimination of the likelihood of occurrence of surfing and broaching is considered as one of the principal goals of the operational guidance. In order to achieve this goal, the criteria used in the guidance must provide true relationships between the operational conditions and the ship's dynamics leading to surf-riding.

Surf-Riding

Numerous studies were carried out in the past and various authors formulated criteria of surf-riding. It is known that, besides the ship form, the combination of speed, course angle and wave parameters determines whether the ship will surf or not.

In the theoretical studies it is usually assumed that the ship runs exactly in following sinusoidal waves. The standard surge equation is used to determine the conditions in which the periodical surge disappears and the ship starts running at the wave speed, at the same position "forever". Using this definition, some authors found that surf-riding may occur when ship's speed is larger than $1.8\sqrt{L}$ which corresponds to Fn = 0.30 (for instance [3]), while others assume $v = 1.4\sqrt{L}$ (i.e. Fn = 0.23) as the critical speed (as in [5]). Although the influence of wave steepness is sometimes indicated, the above values are considered as the minimum speed above which the phenomenon may occur, depending on wave parameters.

In the real world, a ship operating in heavy seas does not meet the ideal conditions assumed in the theoretical models, particularly when operating in quartering waves. Wave parameters change in time, the course angle changes during wave action, and surf-riding, if it occurs, never lasts "forever". It ends after some time because the hydrodynamic conditions change with time.

From the stability point of view, it is important how long surfing lasts in comparison with the roll period. If it lasts longer than 50% of the roll period, the ship will always reach its maximum heel angle while still surfing, which is extremely dangerous.

In order to find out under which conditions surf-riding occurs in extremely steep, following and quartering waves, the Canadian model tests [1] have been re-analyzed in detail. All the model runs in which clear surfing occurred with a steady position of the model in a wave over a certain significant time, were identified. The model speed, heading angle and wave parameters at which the event occurred, were determined.

The tests showed that, beyond the classic surf-riding on the front slope of a wave usually modelled theoretically, another type of surf-riding may occur. In large, extremely steep waves a ship advancing with less speed may accelerate dramatically as a results of a wave impact on the stern. The ship's speed increases and usually it matches the wave velocity when the crest is in the midships zone. The ship then moves with the wave, remaining on the wave crest for a certain time. If this riding lasts over a significant portion of the roll period, the reduction of the ship's restoring potential on the crest may coincide with a large roll angle, water on deck or any other heeling moment, and the ship may capsize. Some authors would call such an event as a "marginal surf-riding". This, however, is not precise, and because the described case has a special meaning to stability safety, it has been called here as "riding on a wave crest", in order to emphasize the steady position of the crest

at the midship over a certain significant time.

In this analysis, the surf-riding (or riding on the crest) was defined as a case in which a visible riding of the model in the same position relative to the wave, excluding transitional time, lasted more than 30% of the natural roll period. The average time of riding was over 40% of the natural roll period, ranging rom 30% to 65%. All the identified surf-riding events, including riding on the crest, are collated in the form of a polar diagram presented in Fig. 3 A,B,C.

The lengths of waves which caused the surfing are related to the model length and are distinguished by different symbols. The results of testing, both in regular and in irregular waves, are put together. There was no clear pattern to the results which would suggest that a large individual wave in a group of irregular waves causes different behaviour of the model than a corresponding one in a sequence of periodic steep (quasiregular) waves.

The dangerous zone of operation (from a capsizing point of view) in irregular seas, derived from the principle of maximum energy concentration in irregular following seas, and introduced in the first Japanese proposal [4], is marked on all the graphs as reference lines, for easy comparison of all results.

In examining the surfing criteria, a question arose as to which speed and course angle should be taken as the reference values on the graphs. In irregular waves, where a large wave may form unexpectedly after a relatively long period of small or moderate waves, and hit the ship on the stern, the speed and course angle shortly before the impact decide the subsequent behaviour of the ship. In the case of running in a group of subsequent large waves (group of large waves in irregular seas), the speed and course angle vary strongly due to large surge and yaw, and it does matter at which time point the values are taken for the validation of the criteria. The difference can be seen in Fig.3 A,B,C where the same events are presented, but the model's speed and course angle are determined at different time points: in graph A, the speed and heading angle are taken at the moment of wave impact on the stern; in B, the speed and heading are taken when the model's speed reached the maximum value (i.e. during surfing); and in C, the speed is taken as the average speed during one period before the wave impact, while the heading angle is the average angle between the position in the wave trough and the wave impact at the stern (movement of the ship in front of the coming wave). The latter combination was used in all further analyses.

Comparison of the corresponding points in Figs. 3A and 3B (the speed at the moment of impact and at surf-riding) shows how a dramatic increase of ship's speed is generated by the impact of an extremely steep wave. It can also be seen from Fig. 3C that the majority of the cases of surfing occurred at a heading angle within the range of 0° - 20°.

Furthermore, surfing on waves which are almost equal to the model's length ($\lambda/L = 0.95$) are located in the upper part of the diagram. This means that relatively high initial speed is needed in order to bring the ship to surfing. The longer wave (and thus larger wave height) results in a smaller initial speed at which the riding occurs. At the wave length $\lambda/L \geq 2.0$ many surf-riding events occurred at relatively low initial speed, below that of $1.8\sqrt{L}$. This fact was carefully examined, and a clear pattern was found which indicates the influence of wave length on the occurrence of surfing and riding on the crest. The results are shown in Fig. 4. The cases when clear riding occurred but lasted less than 30% of the roll period, are included here, and named "marginal riding".

It can be seen that, for the wave length to be equal to the ship's length, surf-riding occurs at $Fn = 0.3$, which confirms theoretical considerations. In longer waves, the riding occurs at a smaller Fn, and thus at a smaller ship's speed. In waves longer than two ship lengths, surf-riding was observed at $Fn = 0.23$, while marginal riding occurs even at a smaller speed. It seems that this value, corresponding to $V = 1.4\sqrt{L}$, could be used as a criterion for surf-riding in extreme waves.

The reason for this behaviour is that natural waves are not symmetric (Fig.2). The troughs are long, the peaks narrow, steep and high. The longer waves apply more impact energy on the ship, causing large accelerations even at small initial

speed. Furthermore, the length of the wave in comparison with the ship's length determines whether there is sufficient distance for the ship to accelerate as a result of wave impact on the stern. If the wave length is not sufficient, the bow sits in the foregoing wave crest while the stern is pushed by the next crest, and the ship will not achieve sufficient acceleration to match the wave velocity. In the tests performed, the vast majority of surfing events occurred on waves with the length λ/L = 1.5 - 3.0, with the largest concentration for λ/L = 2.0 - 2.5.

Broaching

Typical broaching-to phenomena were observed as well. The recorded events are presented in Fig. 5. It can be seen that broaching occurred in waves twice as long as the model, or longer. Furthermore, it usually happened when the course angle was about 30 deg., and generally at smaller initial speeds than those leading to surf-riding. No broaching-to was observed in waves λ/L = 0.95 - 1.42 although the waves were extremely steep.

5. ANALYSIS OF CAPSIZE EVENTS

All the capsize events have been analyzed in detail in order to detect physical phenomena which contributed to it, and to discover the main cause of capsizing. The following factors were detected:

- poor stability
- wave impacts
- influence of deck in water
- influence of water on deck
- stability reduction on a wave crest
- surf-riding or riding on a wave crest
- broaching
- dynamic rolling

In each of the analyzed cases, more than one phenomenon was identified. They occurred either simultaneously in combination, or in a certain logical sequence. The results of the analysis are presented in Table 1. The factor which was dominating or directly causing the capsize, is identified in the table by a circle, and indicated in all the graphs.

Careful review of the table does not give any clear pattern for the main causes of capsize. A large spread of the factors indicates that in steep, quartering waves various phenomena may result in capsizing, and it is hard to predict which one will dominate. Yet, in each individual case, the combination of the phenomena is logical and consistent with the overall dynamic situation.

In the light loading condition (IA and IB) the model was very responsive to wave impacts and the dominating causes of capsize were those related to large dynamics in waves, namely "deck in water" and "broaching". For full load (IIA), when the model sat deeply in the water, the most visible causes were "water on deck" and "stability reduction on a wave crest".

In an attempt to find some correlation between capsizing and operational conditions, the model's speed (Fn), heading angle (α) and wave parameters in relative form (steepness H/λ and wave length/model length ratio λ/L) are collated for all capsize events in Table 2. It can be seen that, in the light loading condition (IA, IB), all the capsize events happened as a result of action of waves twice as long as the model, or larger. At the full load condition (IIA), only three capsizes happened in waves λ/L = 1.42 caused by stability reduction on the wave crest and water on deck, while the rest of them occurred in much larger waves.

The capsize events happened in the full range of operational speed of the ship (Fn = 0.10 - 0.34). No direct indication of the influence of the speed can be found from the table, except that broaching which caused a capsize, occurred usually at high speed and in large waves.

In order to examine if there is any pattern to the operational parameters at which most of the capsizes occurred, all the runs tested were put in the polar diagram . The capsize events are distinguished from non-capsizing runs. Additionally, broaching and surf-riding events which did not cause a capsize, are distinguished.

Fig. 6 presents all the runs at light loading conditions IA and IB. At the condition IA, the design stability is satisfactory and thus only two capsizes happened in large, steep waves (Fig. 6A)

which constitutes 5% of all the runs at this condition.

For condition IB, where the design stability was not sufficient, 16 capsizes were recorded, which constitute 55% of the tests. All but two are located in the area limited by V/T = 0.9 - 1.6 and α = 20 - 35 deg. There were surf-riding and broaching events at relatively high V/T but they did not cause capsizing.

Similarly, the results for the full load conditions IIA and IIB are presented in Fig. 7. In the 30 runs in quartering waves at loading condition IIA, 14 ended with capsize (47%). No capsize happened at the IIB condition, at which the design stability was very good (range of the GZ curve was 90 deg.). Most of the capsize events (65%) lie in the same area as in the condition IB.

All the runs analyzed are collated in Fig. 8. It can be seen that most of the capsizes (75%) are concentrated in the area limited by V/T = 0.8 - 1.6 and α = 20 - 35 deg. This area is below the dangerous zone proposed originally by Japan. There were many surfing and riding events, mainly in the zone, but they did not cause capsizing. There were no capsizes in beam waves (α = 90 deg.)

Clear concentration of the capsize events in the area limited to certain V/T and α provides some ground for establishment of a "dangerous zone" of operational parameters, which should be avoided in heavy seas. Such a zone reflecting the results presented here, was proposed to IMO by Canada in the document [2] and is shown in Fig.9.

The results presented in Table 1, Table 2 and Figs. 6-9 can be summarized as follows:

1. The tests confirmed that a good design (inherent) stability is a paramount condition for stability safety. Only two capsizes occurred for good stability characteristics in the same operational conditions in which the model capsized many times when it had the GZ curve below the IMO criteria.

2. There is a clear and strong influence of the wave length to ship's length ratio (λ/L) on ship's behaviour and on the probability of capsizing in following and quartering seas. No capsize occurred in the smaller waves. Only three capsizes happened in waves of λ = 1.42L. The rest occurred in waves of λ = 2L and longer. In steep waves, the energy exerted on a ship depends on the wave height. The longer the wave, the larger the wave height, and thus the larger the energy applied to the ship. The hydrodynamic forces on a ship depend on the instantaneous shape of the immersed part of the hull in the wave. In the case of natural waves, where the troughs are long while the peaks are narrow, steep and high, the most unfavourable wave length is longer than in the case of regular, sinusoidal waves which are usually applied in theoretical considerations. In Fig. 2 , the difference in the shape of the immersed hull in natural steep waves in comparison with a sinusoidal wave is shown schematically. It can be seen that the steep wave with greater length supports approximately the same portion of the hull as the sinusoidal one with a smaller length. However, the height of the steep wave is larger while the configuration of the rest of the immersed hull causes larger reduction of the restoring capability of the ship. The experiments showed that the most unfavourable length of the natural steep waves lies in the range λ/L = 1.5 - 3.0.

3. It is hard to find any explicit form of dependence of the occurrence of capsizing on the operational factors. The operational parameters affect or generate various physical phenomena which are involved in capsizing. Analytical relation between the operational parameters and the phenomena can be found, and for some are already known (e.g. stability reduction on the wave crest, roll, etc.). Yet, it is difficult to extrapolate those relations for a combination of various phenomena when they occur together or in a sequence. However, Fig.8 shows that there is a certain pattern of capsize events indicating a relationship between the operational conditions and the occurrence of capsizing.

4. One of the two main parameters of the polar diagram, V/T, represents the speed of a ship (V) relative to the wave velocity, expressed here by the wave period (T). Unfortunately, this parameter does not indicate the real speed of the ship, nor the size of the waves. For instance,

the low value of V/T could be achieved at a small speed in certain moderate waves, or at relatively high speed in larger waves. The parameter V/T will be the same in both cases, but the risk of capsizing will be significantly different. It is not only the range of V/T at which the most energy is transmitted in irregular waves at a certain sea state, but also the length of the main waves in the group in comparison with the ship length, which is essential to the resultant ship's response. It seems that the representation of wave length in relation to the ship's size (λ/L) should be incorporated into the polar diagram.

5. Almost all of the capsize events analyzed here lie below the dangerous zone proposed by Japan which were derived from the maximum energy concentration in following seas.

6. CONCLUSIONS

The results of the capsizing model tests and the considerations presented in this paper lead to the following general conclusions:

1. Stability safety of ships depends not only on the design stability but also on the way in which the ship is operated in encountered environmental conditions.

2. Operational parameters, such as loading condition, ship's speed and heading angle, affect the probability of capsizing through influencing or inducing some dangerous physical phenomena which contribute to capsizing.

3. The experimental results show a certain pattern of the operational parameters at which most capsizes occurred. This proves that there is a correlation between the operational parameters and the likelihood of capsizing. Concentration of the capsize events in the area of certain combination of ship's speed and heading angles provides the basis for the definition of the zone of the most dangerous combinations of these parameters. By avoiding operation at the speed and course direction within that zone, the risk of capsizing can be reduced.

4. Good inherent stability of a ship is of paramount importance to stability safety. Operational guidelines are only a complementary measure, and they would not provide a satisfactory safety level if the inherent stability is not sufficient. Any future guidance must emphasize the importance of good stability characteristics and request compliance with design stability standards.

5. Most capsizes of the tested ship are concentrated in the area confined to V/T = 0.8 - 1.6 and α = 20 - 35 deg. regardless of the loading conditions.

6. The relationship between the wave parameters and the ship size is extremely important. The experiments indicated that the wave length to ship's length ratio (λ/L) is one of the most significant factors. No capsize happened in waves smaller than 1.42L. Waves in the range λ/L = 1.5 - 3.0 were found to be the most dangerous. The influence of λ/L ratio should be included in the operational guidance.

7. The polar diagram, in its present form, is simple and convenient to use. However, the parameter V/T does not represent explicitly the factors determining safety or danger. The same value of V/T may be achieved by many different combinations of ship speed and wave period, from which some will represent extremely dangerous combinations while others very safe situations. This is because V/T does not combine the relative speed with the relative size of waves. This weakness would be removed if λ/L is incorporated into the criteria.

8. The polar diagram has an informative and advisory character only. If the ship's speed and course indicate that, in the actual wave conditions, the ship operates within the dangerous zone, it does not necessarily mean that it will capsize. Also, operation outside the dangerous zone does not mean that the ship is completely safe. The dangerous zone indicates only the largest probability of occurrence of various detrimental factors or dangerous phenomena which may cause the ship to capsize if stability in the actual conditions is not sufficient.

Table 1. Analysis of the model capsizing events. Cause of capsize.

Prefix - "R": regular wave test run
Prefix - "Ir": irregular wave test run

\+ - identified contribution

○ - main contributing factor

Run No:	Load. Cond.	Poor Stability	Wave Impact	Deck in Water	Water on Deck	Stab. Red. on a Wave	Riding on a Wave Crest	Broaching	Dynamic Rolling
R25	IA		+	○					
R27	IA		+	○					
R52	IB		+	+				○	+
R53	IB	+			+	○	+		
R54	IB	+	+	○					
R55	IB	○			+	+			
R56	IB	○		+	+	+	+		
R57	IB	+	+	○					
R58	IB	+		○	+	+			
R60	IB	+			+	+	○		
R63	IB		+	+				○	+
Ir68	IB	+	+	○				+	
Ir73	IB			+	+	○	+		
Ir74	IB		+	○				+	+
Ir77	IB		+	○					
Ir78	IB		+	+				○	+
Ir79	IB			+	+	○	+		
Ir80	IB		+	+				○	
R103	IIA				○	+			
R106A	IIA	+			○	+			
R106B	IIA			+	+	○			
R107	IIA	+			+	○	+		
R109	IIA		+	○	+				
R113	IIA				+	+	○		
R115	IIA			+	+	+	○		
R116	IIA				+	○			
R117	IIA			+			+	○	
Ir86	IIA	+			○	+			
Ir91	IIA	+	+	○	+				
Ir93	IIA		+	○		+			
Ir97	IIA		+	+				○	
Ir99	IIA	+			○				

Table 2. Capsize data.

Load.Cond.	Run. No.	H/λ	λ/L	α	V/T	Fn	Main Cause of Capsize
LA:	R 25	0.13	3.4	8.0	1.14	0.28	Deck in Water
	R 27	0.11	3.4	30.0	1.37	0.33	Deck in Water
IB:	R 52	0.14	1.99	32.5	1.02	0.19	Broaching
	R 53	0.11	1.99	22.6	1.03	0.19	Stab. reduction
	R 54	0.13	1.99	22.0	1.42	0.26	Deck in Water
	R 55	0.11	2.3	13.2	0.82	0.16	Poor stab.
	R 56	0.11	2.3	25.8	1.06	0.21	Poor stab.
	R 57	0.13	2.3	30.0	1.22	0.24	Deck in Water
	R 58	0.11	2.3	26.0	1.53	0.31	Deck in Water
	R 60	0.11	2.64	30.0	0.92	0.20	Riding on crest
	R 63	0.14	2.64	30.0	1.43	0.31	Broaching
	Ir 68	0.06	2.97	30.0	0.86	0.19	Deck in water
	Ir 73	0.06	2.4	30.0	1.58	0.32	Stab. reduction
	Ir 74	0.09	3.0	30.0	1.51	0.34	Deck in Water
	Ir 77	0.10	2.9	30.0	0.98	0.22	Deck in Water
	Ir 78	0.06	4.47	30.0	1.15	0.32	Broaching
	Ir 79	0.09	3.52	25.0	0.93	0.23	Stab. reduction
	Ir 80	0.05	5.03	12.2	0.97	0.29	Broaching
IIA:	R 103	0.11	1.42	20	0.88	0.14	Water on Deck
	R 106A	0.16	1.42	22.1	1.24	0.19	Water on Deck
	R 106B	0.17	1.42	42.6	0.62	0.10	Stab. reduction
	R 107	0.12	1.99	4.2	1.64	0.31	Stab. reduction
	R 109	0.12	2.3	34.2	0.97	0.19	Deck in water
	R 113	0.10	2.3	0	1.67	0.33	Riding on crest
	R 115	0.13	2.3	6.3	1.19	0.24	Riding on crest
	R 116	0.12	2.64	4.7	0.91	0.19	Stab. reduction
	R 117	0.12	2.64	28.1	1.3	0.28	Broaching
	Ir 86	0.08	2.54	20.0	0.73	0.15	Water on deck
	Ir 91	0.11	2.51	27.9	0.80	0.17	Deck in water
	Ir 93	0.10	3.12	20.0	0.94	0.22	Deck in water
	Ir 97	0.09	4.38	25.8	1.01	0.28	Broaching
	Ir 99	0.07	3.16	30.0	0.8	0.19	Water on deck

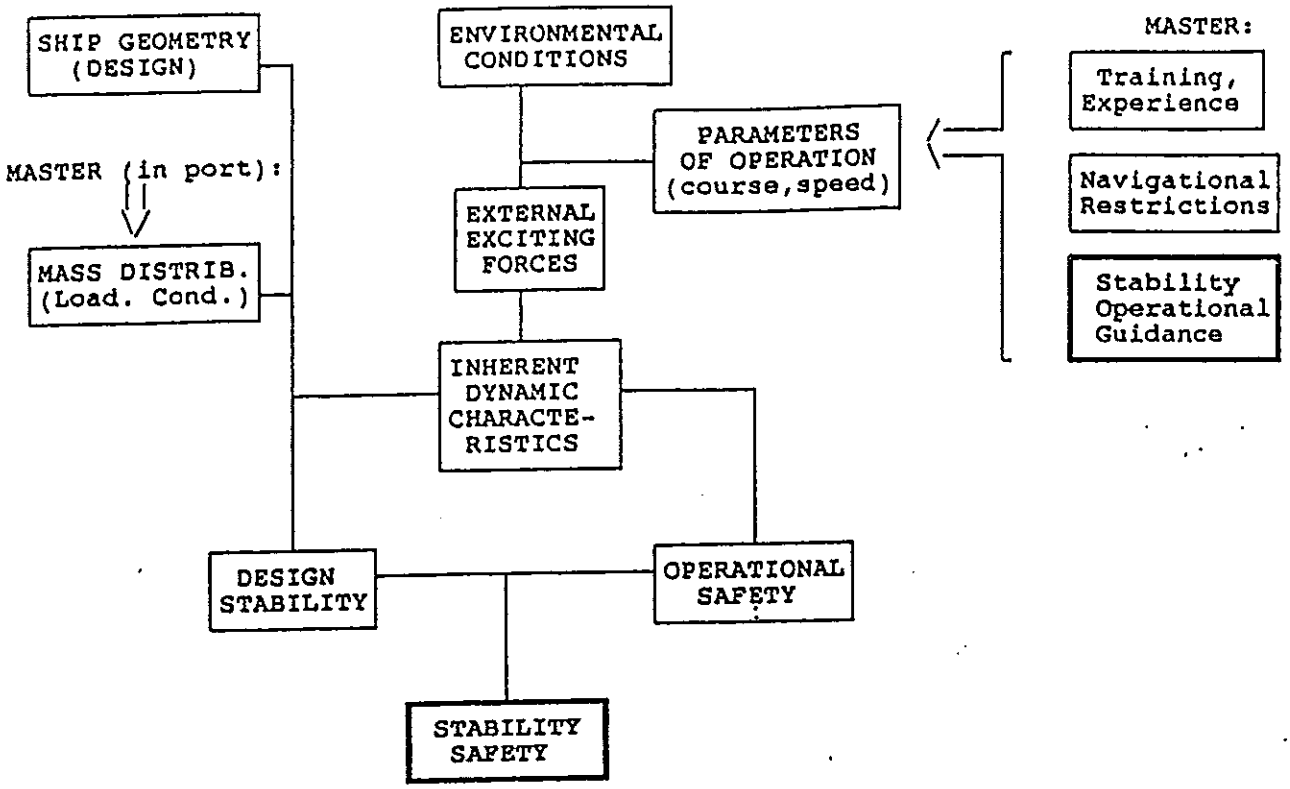

Fig. 1. Elements of stability safety.

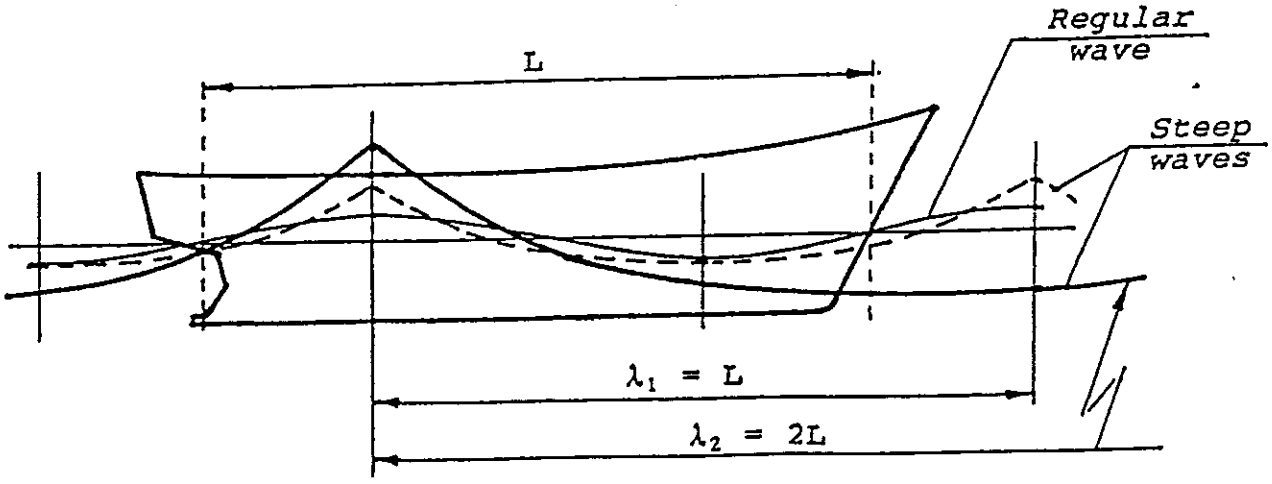

Fig. 2. Schematic representation of the immersed part of a ship in steep waves of various lengths.

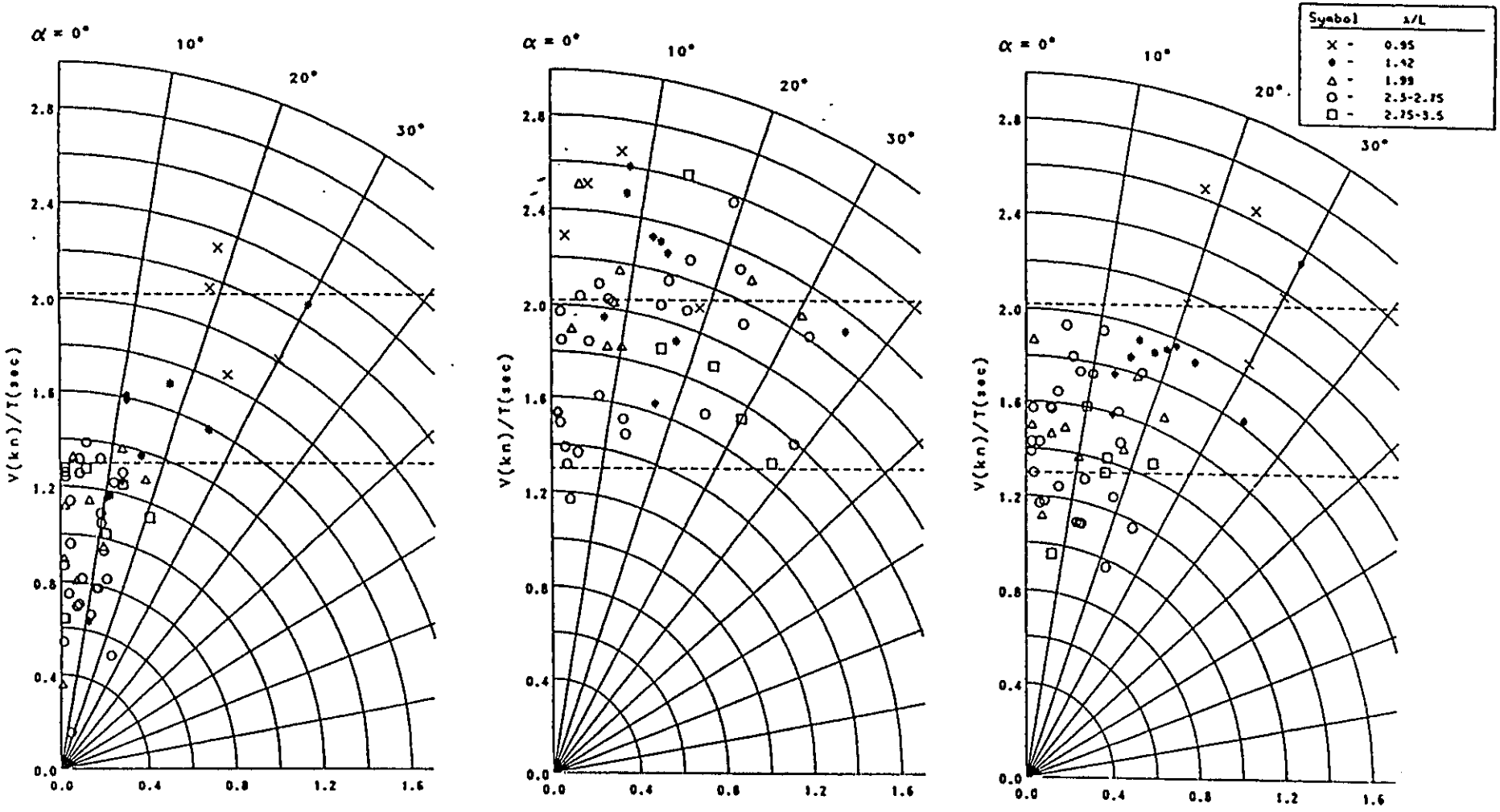

A)

Forward speed and heading angle defined as at the wave impact on the stern.

B)

Forward speed and heading angle defined as at the maximum speed during surf-riding.

C)

Forward speed taken as the average speed during one period before wave impact; heading angle as the average heading between the trough and the aft perpendicular.

Fig. 3. Surfing and riding on a wave crest.
Results of the model tests in extreme following and quartering waves.

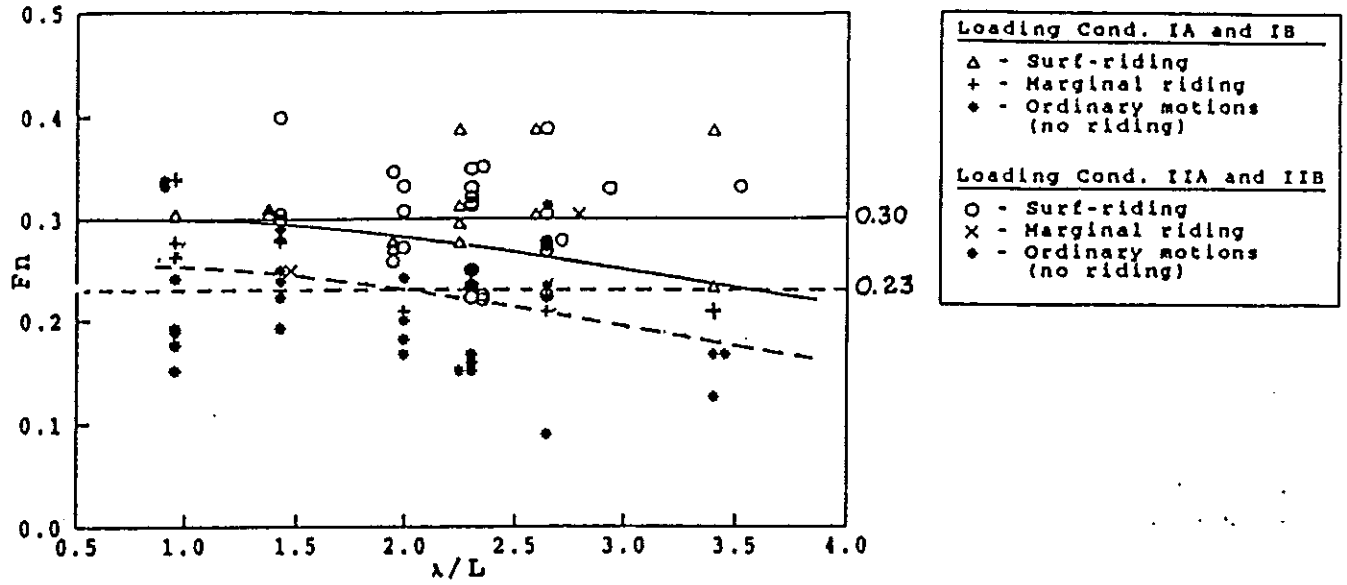

Fig. 4. Influence of the wave length to ship length ratio on surf-riding in extreme waves.

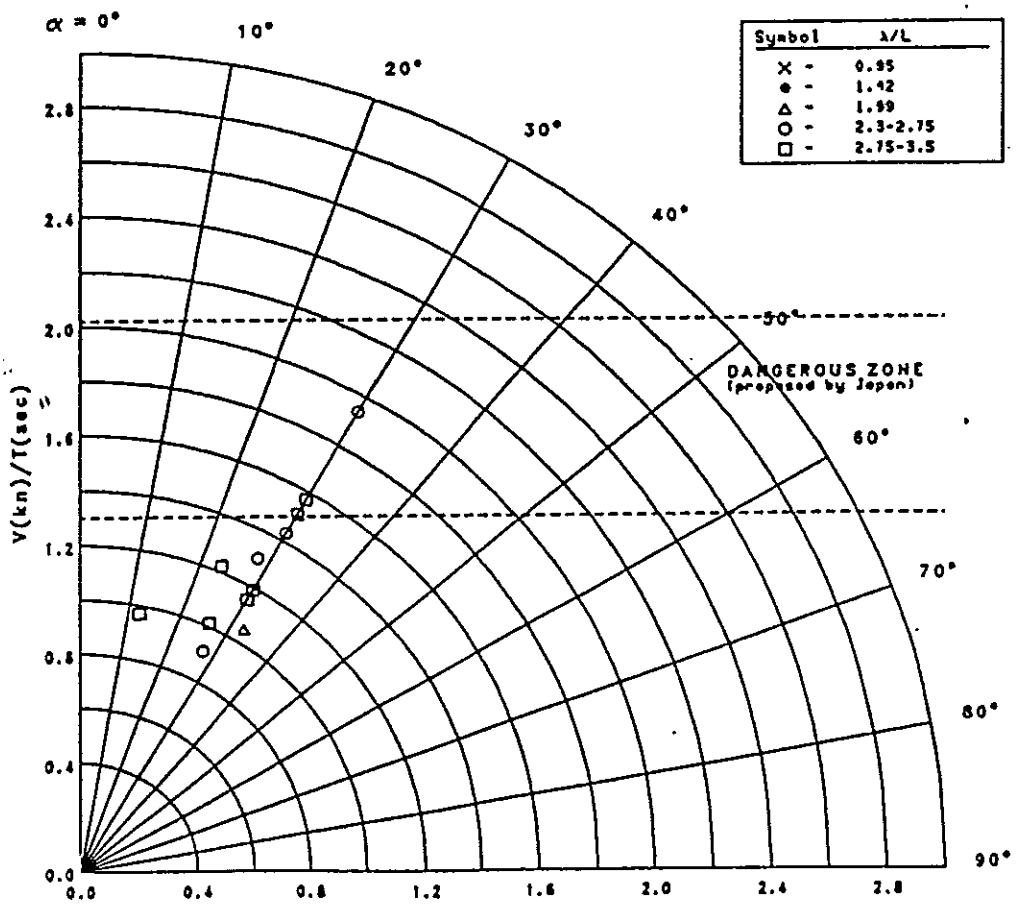

Fig. 5. Broaching in extreme following and quartering waves.

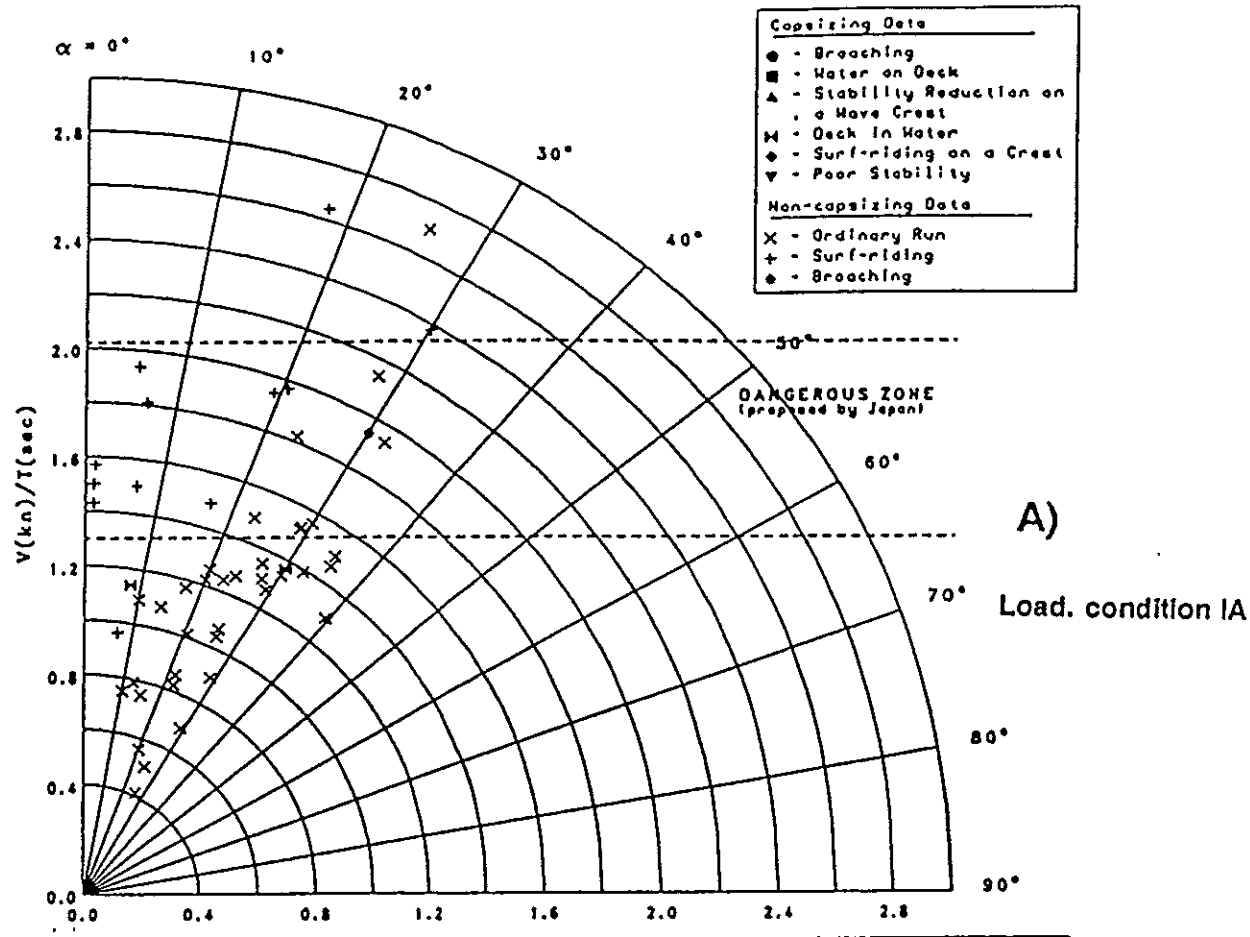

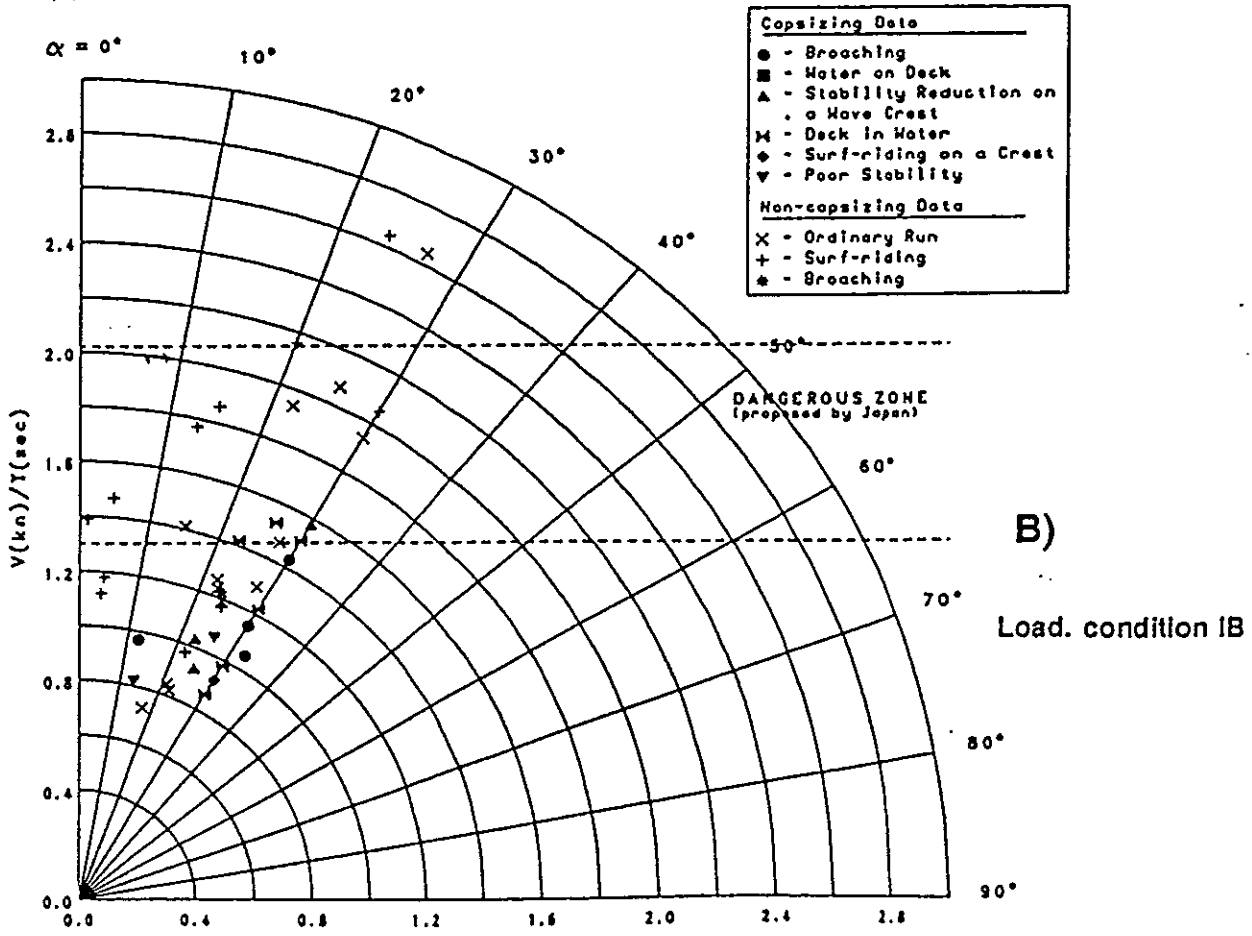

Fig. 6. Results of capsizing model tests of the fishing vessel in extreme following and quartering waves.

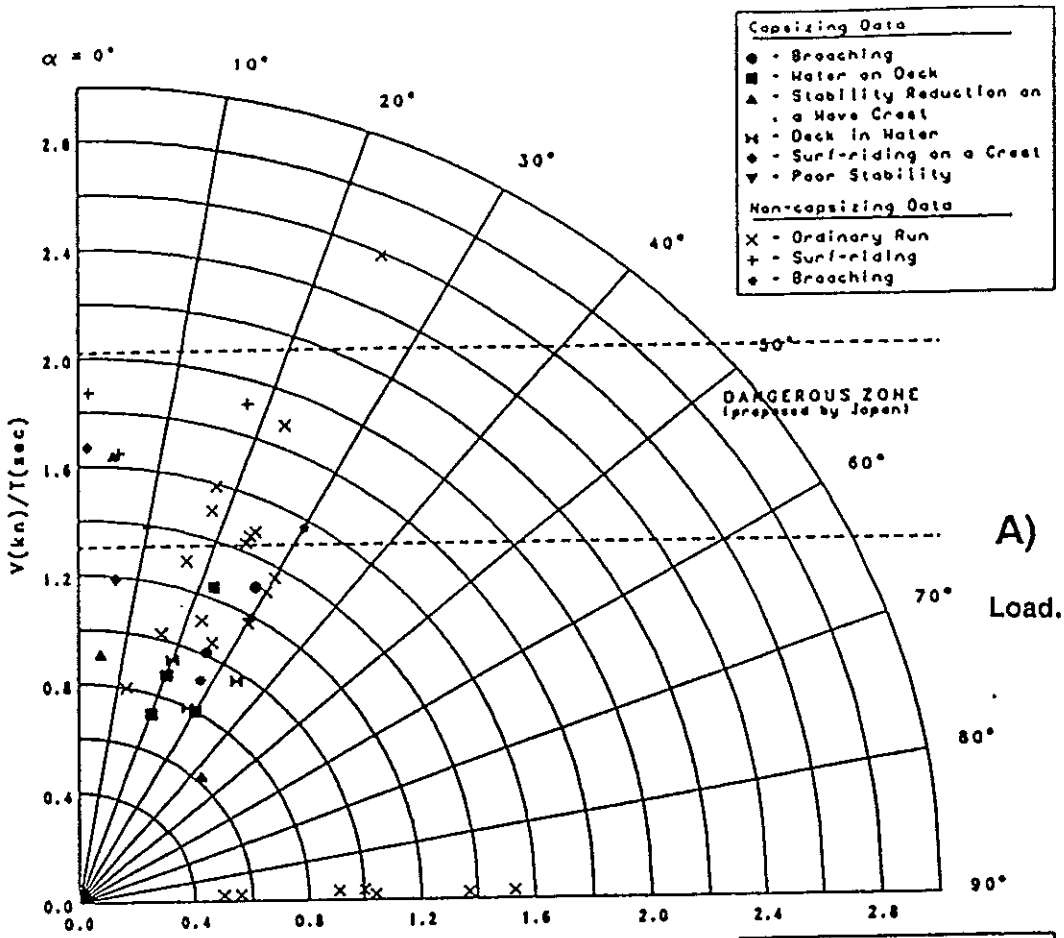

A)

Load. condition IIA

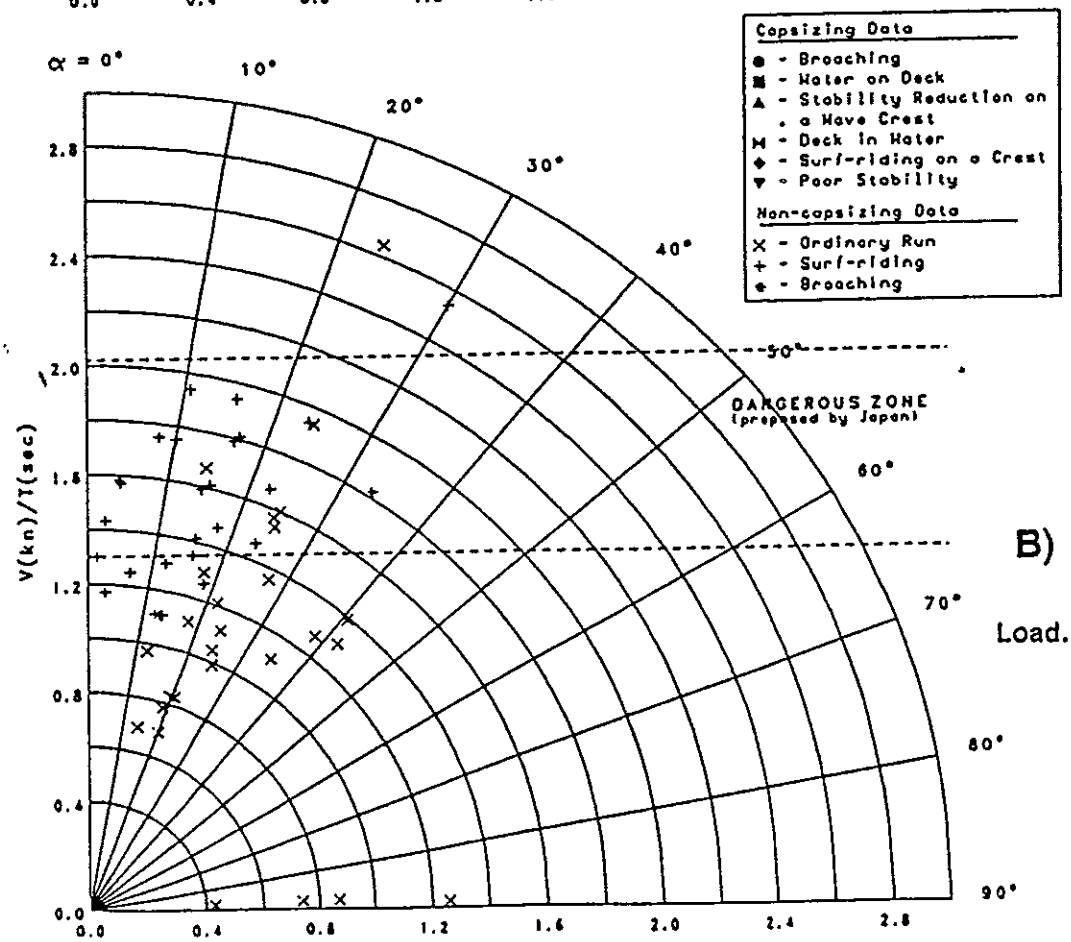

B)

Load. condition IIB

Fig. 7. Results of capsizing model tests of the fishing vessel in extreme following and quartering waves.

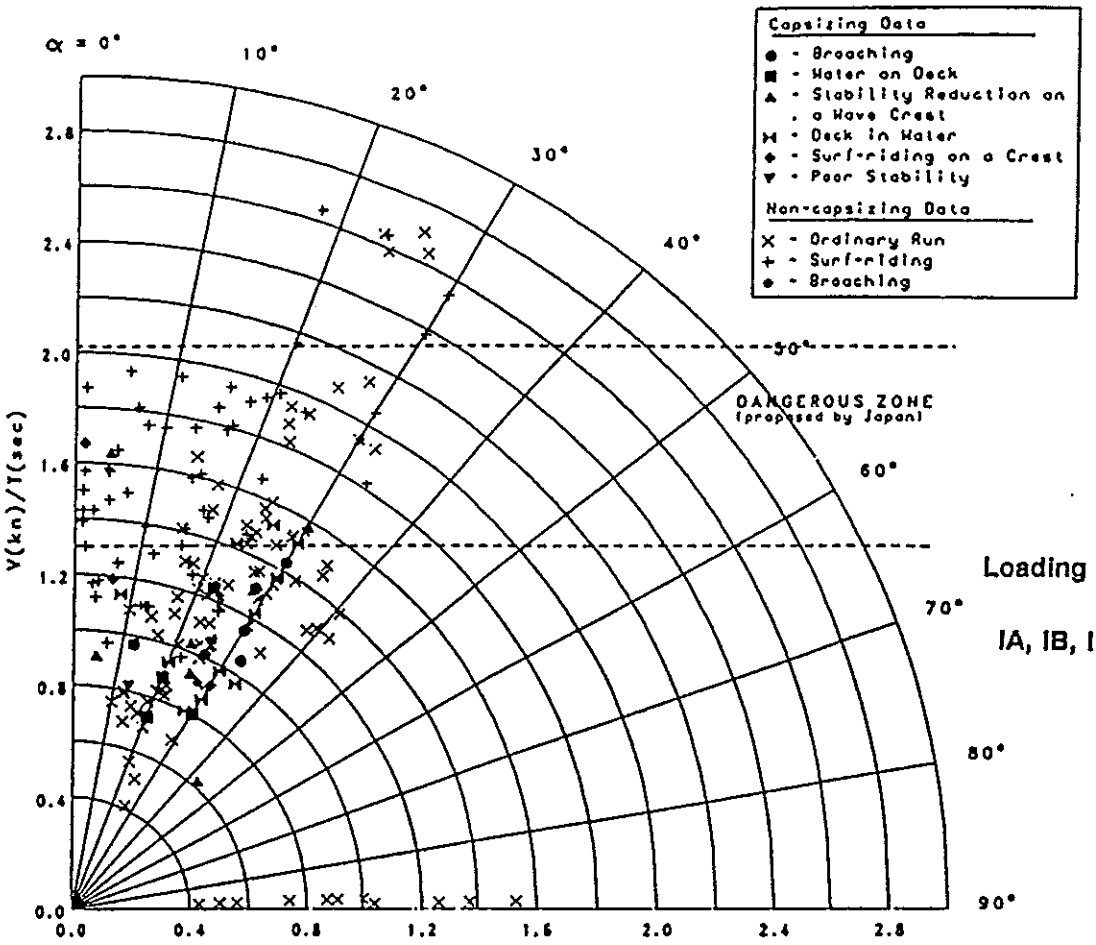

Fig. 8. Results of capsizing model tests of the fishing vessel in extreme following and quartering waves.

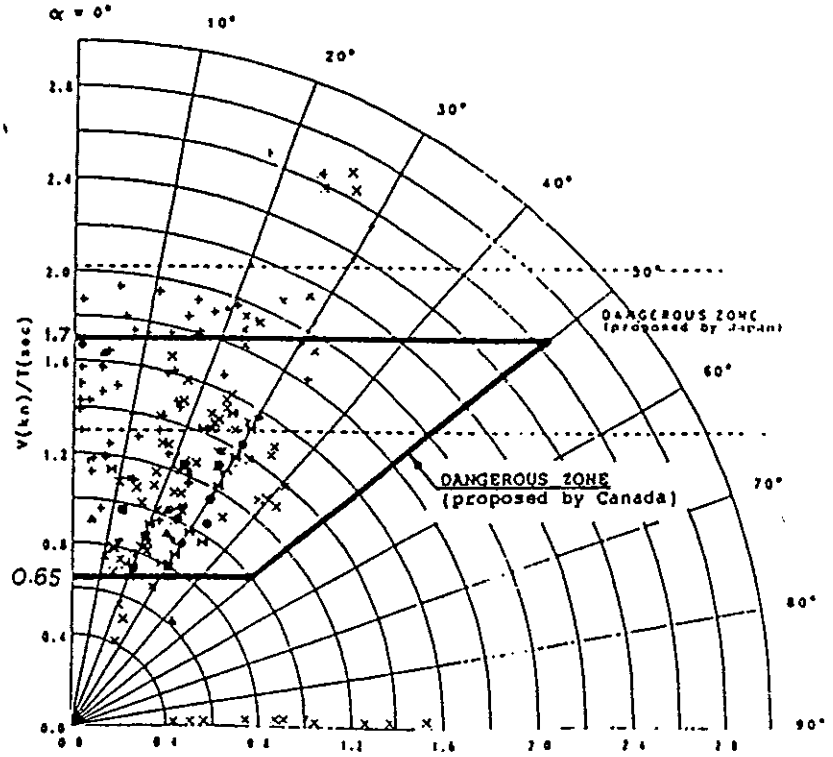

Fig. 9. Example of the definition of the dangerous zone.

Dynamic Stability of a Ship in Quartering Seas

by
M.Hamamoto
Osaka University,Japan
M.Fujino
University of Tokyo,Japan
and
Y.S.Kim
Samsung Heavy Industry,Korea

ABSTRACT

This paper is concerned with the combined motions of sway, roll and yaw of a ship in quartering seas. Such combined motions happen to be related to the dangerous situations leading up to capsize which is caused by the phenomena of pure loss of stability, parametric resonance and broaching–to. The problem here is the dynamic stability on the combined motions to obtain some guidance and insight into how to avoid the dangerous situations. The purpose of this paper is to analyze ship motion in dangerous situations. Equations of motion are derived for the analysis of the dynamic stability. The characteristic equation is presented for the dynamic stability with respect to the combined motions of sway, roll and yaw. The stable and unstable ranges of dynamic stability are computed and discussed for container ships. Finally numerical simulations are carried out to show unstable behaviors in limiting situation at zero frequency of encounter and in overtaking waves of low frequency of encounter for discussions.

INTRODUCTION

For a ship traveling in severe following and quartering seas, distinct modes leading up to capsizing are pointed out as follows:

Pure loss of intact stability

Parametric Resonance

Broaching–to

Surf–riding

Combination of these distinct modes

Although these modes are big problems to be investigated, the problem here is the dynamic stability of combined motions of sway,roll and yaw which is mainly related to broaching mode. The essential features of broaching are the breaking waves striking a ship in succession. As each wave strikes it,the ship is forced to yaw off course to such a situation that the steering rudder is unable to correct the heading in the time interval between waves. Such a loss of directional control makes it to swing through ninety degrees from a following sea course to beam seas. The ship is unable to regain it original course but remained in the beam sea condition even with the rudder hard over. Sometimes, the dynamic heeling moment resulting from the turn happens to combine to cause capsizing again at the wave crest amidships.

From the observation of model experiments, this problem seams to be related to the transverse stability and directional stability of a ship traveling in severe following and quartering seas. With respect to this problem, Wahab and Swaan[5] carried out a theoretical analysis of course-keeping of ship in following seas. Grim[4] pointed out that the metacentric height varies with the relative position of ship to waves. Paulling[3] indicated the loss of stability of ship in following seas. Motora et al. [8] pointed out that broaching-to is likely to occur under the conditions of $\lambda/L \simeq 2$, $\chi = 20° \sim 30°$ and $U\cos\chi \simeq c$. The problem here is the dynamic stability on the combined motions of sway, roll and yaw. Son [9] has originally treated this problem for his doctor's thesis in 1983 and carried out productive works. We are still now interested in this problem from the view point of how to avoid the dangerous situation leading up to capsizing. So that we shall again consider this problem in addition of something new. The purpose of this paper is to analyze the effects of following items :

1. Ship motion in limiting situation at zero frequency of encounter
2. Ship motion in overtaking waves of low frequency of encounter

on the dynamic stability by using linearized equations of the combined motions with sway, roll and yaw.

EQUATIONS OF MOTION BASED ON HORIZONTAL BODY AXES COORDINATE SYSTEM

Horizontal body axes coordinate system[10] as shown in Fig.1 is used for describing linearized equations of motion in a reasonable combination of manoeuvring motion and seakeeping motion.

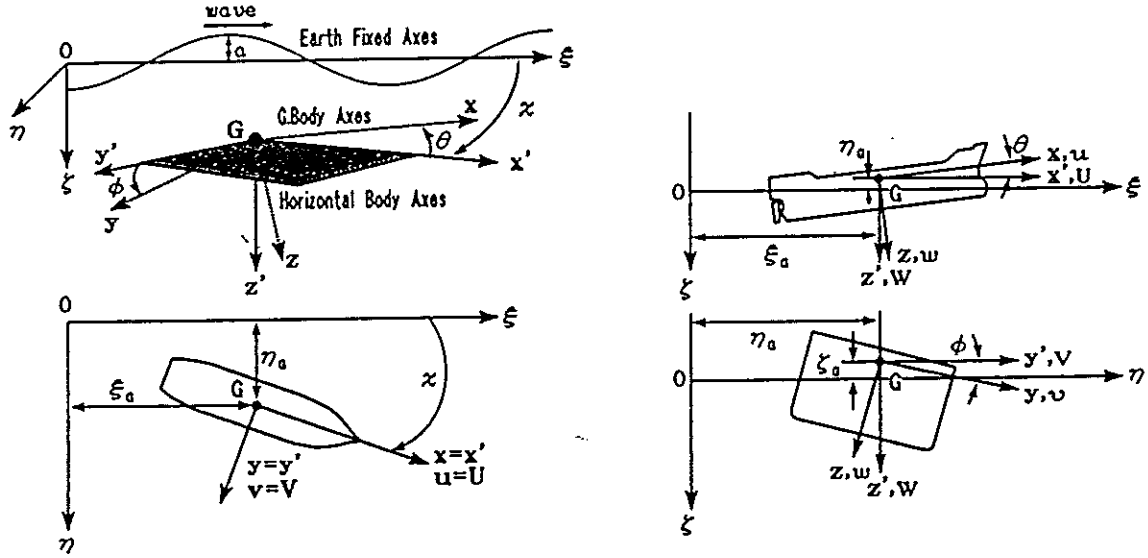

Fig.1 Coordinate systems

We shall first consider the momentums of ship motion including the fluid motion around the ship hull. The translational momentum L_G of a ship motion is described by taking the unit vectors i, j and k in the form.

$$\mathrm{L}_G = \mathrm{i}L_{x'} + \mathrm{j}L_{y'} + \mathrm{k}L_{z'} \tag{1}$$

and according to the equation of Euler-Lamb type, the components $L_{x'}$, $L_{y'}$ and $L_{z'}$ along the x', y' and z' axes are obtained as:

$$\begin{aligned} L_{x'} &= (\, m + m_x \,)U + m_x z_G \dot{\theta} \\ L_{y'} &= (\, m + m_y \,)V + m_y(\, x_G \dot{\psi} - z_G \dot{\phi} \,) \\ L_{z'} &= (\, m + m_z \,)W - m_z x_G \dot{\theta} \end{aligned} \tag{2}$$

where m is the mass of ship, m_x, m_y and m_z the added mass with respect to the x, y and z axes directions, x_G and z_G the displacement of added mass center with respect to the origin of the coordinate system fixed in the center of gravity of the ship, U, V and W the velocities along the x', y' and z' axes, and $\dot{\phi}$, $\dot{\theta}$ and $\dot{\psi}$ the angular velocities about the x', y' and z' axes.
The rate $\mathrm{d}\mathbf{L}_G/\mathrm{d}t$ of momentum is derived in the following form:

$$\begin{aligned} \frac{\mathrm{d}\mathbf{L}_G}{\mathrm{d}t} &= \mathrm{i}\dot{L}_{x'} + \mathrm{j}\dot{L}_{y'} + \mathrm{k}\dot{L}_{z'} + \frac{\mathrm{di}}{\mathrm{d}t}L_{x'} + \frac{\mathrm{dj}}{\mathrm{d}t}L_{y'} + \frac{\mathrm{dk}}{\mathrm{d}t}L_{z'} \\ &= \mathrm{i}(\dot{L}_{x'} - \dot{\psi}L_{y'}) + \mathrm{j}(\dot{L}_{y'} + \dot{\psi}L_{x'}) + \mathrm{k}\dot{L}_{z'} \end{aligned} \tag{3}$$

Here, Horizontal body axes coordinate system is defined to take a rotation about z' axis, and no rotation about y' and z' axes, but the ship can make a rotation about y' and z' axes, so that the time derivatives of the unit vectors have to be manipulated as:

$$\frac{\mathrm{di}}{\mathrm{d}t} = \mathrm{j}\dot{\psi}, \qquad \frac{\mathrm{dj}}{\mathrm{d}t} = -\mathrm{i}\dot{\psi}, \qquad \frac{\mathrm{dk}}{\mathrm{d}t} = 0 \tag{4}$$

Substituting Eq.(2) into Eq.(3), the equations of motion are translated into the following scalar form:

$$\begin{aligned} (m + m_x)\dot{U} - (m + m_y)V\dot{\psi} + m_x z_G \ddot{\theta} - m_y(x_G \dot{\psi}^2 - z_G \dot{\phi}\dot{\psi}) &= X' \\ (m + m_y)\dot{V} + (m + m_x)U\dot{\psi} + m_y(x_G \ddot{\psi} - z_G \ddot{\phi}) + m_x z_G \dot{\theta}\dot{\psi} &= Y' \\ (m + m_z)\dot{W} - m_z x_G \ddot{\theta} &= Z' + mg \end{aligned} \tag{5}$$

where X', Y' and Z' are the components of force along the x', y' and z' axes. In addition, the moment of momentum $\mathbf{H}_G$ is decomposed as:

$$\mathbf{H}_G = \mathrm{i}H_{x'} + \mathrm{j}H_{y'} + \mathrm{k}H_{z'} \tag{6}$$

and the components $H_{x'}$, $H_{y'}$ and $H_{z'}$ about x', y' and z' axes are described as:

$$\begin{aligned} H_{x'} &= (I_{xx} + J_{xx})\dot{\phi} - m_y z_G V + [(\, m + m_z \,)W - m_z x_G \dot{\theta}]V\Delta t \\ &\quad -[(m + m_y)V + m_y(x_G \dot{\psi} - z_G \dot{\phi})]W\Delta t \\ H_{y'} &= (I_{yy} + J_{yy})\dot{\theta} - m_z x_G W + m_x z_G U + [(m + m_x)U + m_x z_G \dot{\theta}]W\Delta t \\ &\quad -[(m + m_z)W - m_z x_G \dot{\theta}]U\Delta t \end{aligned} \tag{7}$$

$$H_{z'} = (I_{zz} + J_{zz})\dot{\psi} + m_y x_G V + [(m + m_y)V + m_y(x_G\dot{\psi} - z_G\dot{\phi})]U\Delta t$$
$$-[(m + m_x)U + m_x z_G\dot{\theta}]V\Delta t$$

where $I_{xx} + J_{xx}$, $I_{yy} + J_{yy}$ and $I_{zz} + J_{zz}$ are the moments of inertia plus added moments of inertia with respect to General body axes x, y and z.
The rate $\mathrm{d}\mathbf{H}_G/\mathrm{d}t$ of the moment of momentum is manipulated in the following way:

$$\frac{\mathrm{d}\mathbf{H}_G}{\mathrm{d}t} = \lim_{\Delta t \to 0}\left[\mathrm{i}\frac{\Delta H_{x'}}{\Delta t} + \mathrm{j}\frac{\Delta H_{y'}}{\Delta t} + \mathrm{k}\frac{\Delta H_{z'}}{\Delta t} + \frac{\Delta \mathrm{i}}{\Delta t}H_{x'} + \frac{\Delta \mathrm{j}}{\Delta t}H_{y'} + \frac{\Delta \mathrm{k}}{\Delta t}H_{z'} \right] \quad (8)$$

Substituting Eq.(7) into Eq.(8) and using Eq.(4), the scalar equations of motion with respect to the moments are:

$$(I_{xx} + J_{xx})\ddot{\phi} + m_y z_G(W\dot{\phi} - \dot{V}) - m_z x_G\dot{\theta}V - (m_y - m_z)WV$$
$$-(I_{yy} + J_{yy})\dot{\theta}\dot{\psi} - m_x z_G U\dot{\psi} - (m_y - m_z)x_G W\dot{\psi} = K'$$

$$(I_{yy} + J_{yy})\ddot{\theta} + m_x z_G(W\dot{\theta} + \dot{U}) + m_z x_G(U\dot{\theta} - \dot{W}) + (m_x - m_z)UW$$
$$+(I_{xx} + J_{xx})\dot{\phi}\dot{\psi} - m_y z_G V\dot{\psi} = M' \quad (9)$$

$$(I_{zz} + J_{zz})\ddot{\psi} + m_y x_G(U\dot{\psi} + \dot{V}) + (m_y - m_x)UV$$
$$-m_y z_G U\dot{\phi} - m_x z_G\dot{\theta}V = N'$$

where K', M' and N' are the components of moment due to external forces about the x', y' and z' axes. For linearizing the equations of motion in Eq.(5) and Eq.(9), we shall now make an assumption that the sway, heave velocities and all of the angular velocities are small enough to be negligible in the second order. According to this assumption, a linearized version of Eq.(5) and Eq.(9) is completely divided into two groups of the combined motions of sway, roll and yaw and the combined motions of surge , heave and pitch as follows:

Group I Linearized equations of combined motion of sway, roll and yaw

$$\begin{aligned} (m + m_y)\dot{V} + (m + m_x)U\dot{\psi} - m_y(z_G\ddot{\phi} - x_G\ddot{\psi}) &= Y' \\ (I_{xx} + J_{xx})\ddot{\phi} - m_y z_G\dot{V} - m_x z_G U\dot{\psi} &= K' \quad (10) \\ (I_{zz} + J_{zz})\ddot{\psi} + m_y x_G(\dot{V} + U\dot{\psi}) - m_y z_G U\dot{\phi} &= N' \end{aligned}$$

Group II Linearized equations of combined motion of surge, heave and pitch

$$(m+m_x)\dot{U}+m_x z_G\ddot{\theta}=X'$$

$$(m+m_z)\dot{W}-m_z x_G\ddot{\theta}=Z' \tag{11}$$

$$(\ I_{yy}+J_{yy}\ )\ddot{\theta}+(\ m_x-m_z\ )UW+m_x z_G\dot{U}-m_z x_G(\dot{W}-U\dot{\theta})=M'$$

where N' is the yaw moment including the so called Munk's moment $(m_y - m_x)UV$. Group I is linearized equations for stability and manoeuvrability, and Group II for seakeeping. We are now interested in the Group I for the stability and manoeuvrability of ship in following seas. So that the hydrodynamic force and moment on a ship with sway, roll and yaw motions are discussed in the next section.

LINEARLIZED EQUATIONS FOR COMBINED MOTION OF SWAY,ROLL AND YAW

In order to predict the force and moment on a ship, we can use here the workable results which have been developed in the both fields of the manoeuvrability and seakeeping because Horizontal body axes coordinate system is constructed to be compatible with General body axes to describe manoeuvring motion in still water and Earth fixed axes to describe the seakeeping motion in waves.
According to such a point of view, the force and moment here are divided into items of the hydrodynamic derivatives of manoeuvring and rolling motion, and wave excitation including Froude-Krylov force as follows.

$$\begin{aligned} Y' &= Y_S(V,\dot{\psi},\delta)+Y_W(\chi) \\ N' &= N_S(V,\dot{\psi},\delta)+N_W(\chi) \\ K' &= K_S(V,\dot{\psi},\dot{\phi},\delta)+K_W(\chi) \end{aligned} \tag{12}$$

Hydrodynamic derivatives of manoeuvring motion

Davidson and Schiff[1] in 1946 presented the side force Y_S and moment N_S in the following forms:

$$\begin{aligned} Y_S(V,\dot{\psi},\delta) &= -Y_V V+Y_{\dot{\psi}}\dot{\psi}-Y_\delta\delta \\ N_S(V,\dot{\psi},\delta) &= -N_V V-N_{\dot{\psi}}\dot{\psi}+N_\delta\delta \end{aligned} \tag{13}$$

where Y_V, N_V, $Y_{\dot{\psi}}$ and $N_{\dot{\psi}}$ are the hydrodynamic derivatives for the manoeuvring motion, Y_δ and N_δ the hydrodynamic derivatives for the rudder angle δ. According to Inoue's[7] practical formulae, these derivatives are described as:

$$
\begin{aligned}
Y_V &= \frac{1}{2}\rho L d U \left[\frac{\pi}{2}\left(\frac{2d}{L}\right) + 1.4 C_B \frac{B}{L} \right] \\
N_V &= \frac{1}{2}\rho L^2 d U \left(\frac{2d}{L}\right) \\
Y_{\dot{\psi}} &= \frac{1}{2}\rho L^2 d U \left[\frac{\pi}{4}\left(\frac{2d}{L}\right) \right] \\
N_{\dot{\psi}} &= \frac{1}{2}\rho L^3 d U \left[\frac{2d}{L}\left(0.54 - \frac{2d}{L}\right) \right]
\end{aligned}
\tag{14}
$$

where L is the length of ship, B the breadth, d the draft and C_B the block coefficient, U the ship speed, and ρ the density of water.
In addition, added mass m_y and added mass moment of inertia J_{zz} are evaluated as follows:

$$
\begin{aligned}
m_y &= \frac{\pi}{2}\rho \int_L d^2(x) C(x) \mathrm{d}x \\
J_{zz} &= \frac{\pi}{2}\rho \int_L x^2 d^2(x) C(\dot{x}) \mathrm{d}x \\
C(x) &= \frac{(1 - C_1)^2 + 3C_3^2}{(1 - C_1 + C_3)^2}
\end{aligned}
\tag{15}
$$

where C_1 and C_3 are the coefficients of Lewis form section.

Hydrodynamic moment for rolling motion

$$
K_S(V, \dot{\psi}, \dot{\phi}, \delta) = (Y_V V - Y_{\dot{\psi}}\dot{\psi}) z_G - K_{\dot{\phi}}\dot{\phi} + K_\delta \delta \tag{16}
$$

where Takahashi's[6] practical formula is available for roll damping coefficient $K_{\dot{\phi}}$

$$
\begin{aligned}
K_{\dot{\phi}} &= 2\alpha_e (I_{xx} + J_{xx})\{1 + 0.8(1 - e^{-10F_n})\} \\
\alpha_e &= \frac{2}{T_\phi} N_{20} \phi_m
\end{aligned}
\tag{17}
$$

where F_n is the Froude number of ship, T_ϕ the natural period of rolling, N_{20} the extinction coefficient and ϕ_m the mean rolling angle.

Froude – Krylov force

The hydrostatic pressure p including that of a sinusoidal waves ζ_w at any time t and at the position x', y' and z', and ζ_w are written in the following forms:

$$
p = \rho g(\zeta_G - x\theta + z) - \rho g a e^{-kd(x)} \cos k(\xi_G + x\cos\chi - y\sin\chi - ct) \tag{18}
$$

$$
\zeta_w = -\zeta_G + x\theta + a\cos k(\xi_G + x\cos\chi - y\sin\chi - ct) \tag{19}
$$

where g is the gravitational acceleration, χ the angle between prescribed course and direction of advance of waves, k the wave number, a the amplitude of waves, c the phase velocity of wave.
According to the hypothesis of Froude and Krylov, Froude–Krylov force and moments with respect to Horizontal body axes are evaluated as follows:

$$\begin{aligned} Y_{F.K} &\cong \rho g a k e^{-kz_s}(\sin\chi + \psi\cdot\cos\chi) \\ &\quad \times[\sin(k\xi_G - \omega t)\int_L A(x)\cos(kx\cos\chi)\mathrm{d}x \\ &\quad + \cos(k\xi_G - \omega t)\int_L A(x)\sin(kx\cos\chi)\mathrm{d}x] \end{aligned} \tag{20}$$

$$\begin{aligned} K_{F.K} &\cong -\rho g\nabla[GM + \Delta GM\cos(k\xi_G - \omega t)]\phi \\ &\quad -\rho g a k e^{-kz_s}(\sin\chi + \psi\cdot\cos\chi) \\ &\quad \times[\sin(k\xi_G - \omega t)\int_L A(x)z_s\cos(kx\cos\chi)\mathrm{d}x \\ &\quad + \cos(k\xi_G - \omega t)\int_L A(x)z_s\sin(kx\cos\chi)\mathrm{d}x] \end{aligned} \tag{21}$$

$$\begin{aligned} N_{F.K} &\cong \rho g a k e^{-kz_s}(\sin\chi + \psi\cdot\cos\chi) \\ &\quad \times[\sin(k\xi_G - \omega t)\int_L xA(x)\cos(kx\cos\chi)\mathrm{d}x \\ &\quad + \cos(k\xi_G - \omega t)\int_L xA(x)\sin(kx\cos\chi)\mathrm{d}x] \end{aligned} \tag{22}$$

where ψ is the yawing angle, ∇ the volume of a ship, ΔGM the change of metacentric height, $A(x)$ the area of section, $B(x)$ the breadth of section, and z_s subsurface of waves.
Substituting these results into Eq.(10), finally linearized equations of Group I are described in the following form:

Equations of combined motions of sway, roll and yaw

$$\begin{aligned} &(m+m_y)\dot{V} + Y_V V + m_y x_G\ddot{\psi} + [(m+m_x)U - Y_{\dot{\psi}}]\dot{\psi} \\ &\qquad + Y_\psi(\chi)\psi - m_y z_G\ddot{\phi} = Y(\chi) - Y_\delta\delta \\ &-m_y z_G\dot{V} - Y_V z_G V - (m_x z_G U - Y_{\dot{\psi}} z_G)\dot{\psi} + K_\psi(\chi)\psi \\ &\quad + (I_{xx} + J_{xx})\ddot{\phi} + K_{\dot{\phi}}\dot{\phi} + \rho g\nabla[GM + \Delta GM\cos(k\xi_G - \omega t)]\phi = K(\chi) + K_\delta\delta \\ &m_y x_G\dot{V} + N_V V + (I_{zz} + J_{zz})\ddot{\psi} + (N_{\dot{\psi}} + m_y x_G U)\dot{\psi} \\ &\qquad + N_\psi(\chi)\psi - m_y z_G U\dot{\phi} = N(\chi) + N_\delta\delta \end{aligned} \tag{23}$$

where $Y_\psi(\chi), K_\psi(\chi)$, and $N_\psi(\chi)$ are derivatives of perturbed yaw angle ψ in Eqs.(20), (21) and (22), $Y(\chi), K(\chi)$, and $N(\chi)$ are Froude–Krylov force and moments obtained from Eqs.(20), (21) and (22). In the wave exciting forces, only the Froude–Krylov force and moments are considered here since the diffraction force and moment are assumed to be negligible in comparison with Froude–Krylov force and moments.

DYNAMIC STABILITY

It is largely because of the reduction in frequency of encounter that course-keeping in following or quartering seas usually poses more difficulty than in head seas. For this reason most studies of combined motions of sway, roll and yaw in rough seas have been concerned with following and quartering seas. In quartering seas, the frequency of encounter ω_e between the ship and waves is

$$\omega_e = \frac{2\pi}{\lambda}(c - U\cos\chi) \tag{24}$$

The term $(c - U\cos\chi)$ can be very small and hence the frequency of encounter is low or down to zero for the ship in quartering waves of which length is comparable or longer than ship length. There are two possible situations in such a frequency range.

$c = U\cos\chi$: ship motion in limiting situation at zero frequency of encounter

$c > U\cos\chi$: ship motion in overtaking waves of low frequency of encounter

The first one is the situation for the ship remaining on the wave slope of a wave and travels with a wave. The second one is the situation for the ship in the waves overtaking the ship at low frequency of encounter. The ship motions are considered for two cases in this section.

Ship motion in limiting situation at zero frequency of encounter

Let us now derive the characteristic equation of combined motions to consider the dynamic stability of a ship in the limiting situation. When the ship is traveling with heading angle χ, the rudder force has to be balanced to the steady force and moment on the ship. So that, the right hand side of Eq.(23) is equal to zero. From Laplace transform of Eq.(23), the characteristic equation of dynamic stability is described as

$$\begin{vmatrix} & -m_y z_G s^2 & m_y x_G s^2 \\ (m+m_y)s & & +[(m+m_x)U - Y_{\dot{\psi}}]s \\ +Y_V & & +Y_\psi(\chi) \\ & (I_{xx}+J_{xx})s^2 & \\ -m_y z_G s & +K_{\dot{\phi}}\, s & -(m_x z_G U - Y_{\dot{\psi}} z_G)s \\ -Y_V z_G & +\rho g \nabla[GM + \Delta GM & +K_\psi(\chi) \\ & \times \cos(k\xi_G)] & \\ & & (I_{zz}+J_{zz})s^2 \\ m_y x_G s & -m_y z_G U s & +(N_{\dot{\psi}} + m_y x_G U)s \\ +N_V & & +N_\psi(\chi) \end{vmatrix} = 0 \qquad (25)$$

$$A_5 s^5 + A_4 s^4 + A_3 s^3 + A_2 s^2 + A_1 s + A_0 = 0 \qquad (26)$$

where the coefficients determinant polynomial consists of the hydrodynamic derivatives in Eq.(25). The characteristic roots of Eq.(27) are obtained as

$$s_k = a_k + i b_k \qquad k = 1,2,3,4,5 \qquad (27)$$

Thus, according to linear system theory, if the real parts of the root are negative, the ship is stable for the dynamic stability. And if one of them is positive, the ship is unstable.

Ship motion in overtaking waves of low frequency of encounter

For the ship traveling in overtaking waves of low frequency of encounter, it is necessary to control the heading deviation from the prescribed course. In this case, the rudder angle δ is controlled by the relation $\delta = \delta_0 + c_1\psi$ where δ_0 is the offset rudder angle balanced to the wave force keeping the ship in the heading angle χ and c_1 control gain constant. And then the numerical simulations are obtained from Eq.(23) replaced by the encounter frequency $\omega_e t$ in the place of $k\xi_G - \omega t$.

EXAMPLES OF NUMERICAL SIMULATION

According the ways mentioned above, we shall finally show some examples of numerical computation for discussions in detail. Fig.2 indicates the principal dimension and body plan of container ships used for computation. Fig.3 shows the GZ curves of the ship in still water, at wave crest and trough amidships and the GZ curves in waves are obtained from the hydrostatic force including Froude–Krylov force acting on the submerged hull surface of the inclined ship. The metacentric height which are obtained from the slope at the upright condition of the GZ curve with respect to the relative position of ship to waves in cases of $\lambda/L = 1.0, 1.5$ and 2.0.

Fig.4 is one example for the characteristic roots of dynamic stability in case of $\lambda/L = 1.0$. The real and imaginary parts of root are ploted in the abscisa and ordinate. The other cases are computed in the same way.

Fig.5 stands for the stable and unstable regions of unsteered ships in a wave of $\lambda/L = 1.0, 1.5$ and 2.0 for various wave directions. Here ξ_G/λ indicates the

relative position of ship to waves. The ship is at the wave trough amidships when ξ_G/λ equal to zero, at the up slope of a wave amidships when ξ_G/λ equal to 0.25, at the wave crest amidships when ξ_G/λ equal to 0.5, at the down slop of a wave amidships when ξ_G/λ equal to 0.75 and at the wave trough amidships again when ξ_G/λ equal to 1.0. The stability curve of the ship RR100 is relatively poor in comparison with that of the ship RR103 having rich one. The possibility of broaching–to seems to be not so much dependent on the poor or rich stability curve. But, when the heeling angle is developed at the wave crest amidships, it will be likely to play an important role because the intact stability is remarkably reduced. Both of the ships are unstable at the all down slope amidships. The unstable range become smaller at the up slope amidships when λ/L become larger.

Fig.6 indicates the time histories for combined motions of sway, roll and yaw of the ship in a wave of the stable and unstable regions for the heading angle $\chi = 30$ degrees. In this limiting case, the ship is traveling with a wave and the combined motions of sway , roll and yaw are computed from Eq.(23) under the unsteered condition. The combined motions are damped out in the stable region and rapidly developed up to capsize in the unstable region as show in Fig.5 Although the limiting case is of course idealized situation of ship, it will give us some suggestions to understand the mechanism leading up to capsize.

For the ship traveling in overtaking waves of low frequency of encounter, it is necessary to control the heading deviation from the prescribed course. So that we carry out the numerical simulations of ship motion by using an autopilot to keep the prescribed course. Finally, Fig.7 shows the time histories of ship motions in overtaking waves of low frequency of encounter for $U/c = 0.4$ and the heading angle $\chi = 30°, 60°$ and $90°$. It is necessary for the master to reduce the ship speed to less than half of the wave phase velocity.

Items		Ship	Model
Length	L(m)	150.0	2.5
Breadth	B(m)	27.2	0.453
Depth	D(m)	13.5	0.225
Draft	d_m(m)	8.50	0.142
Disp. Vol.	V(m^3)	23139.4	0.107
Block Coef.	C_b	0.667	0.667
Prismatic Coef.	C_p	0.678	0.678
Waterline Coef.	C_w	0.787	0.787
Model Scale	—	—	1/60

Items		Ship	Model
Length	L(m)	115.0	2.5
Breadth	B(m)	19.0	0.413
Depth	D(m)	8.4	0.183
Draft	d_m(m)	6.4	0.139
Disp. Vol.	V(m^3)	9841.9	0.101
Block Coef.	C_b	0.704	0.704
Prismatic Coef.	C_p	0.726	0.726
Waterline Coef.	C_w	0.814	0.814
Model Scale	—	—	1/46

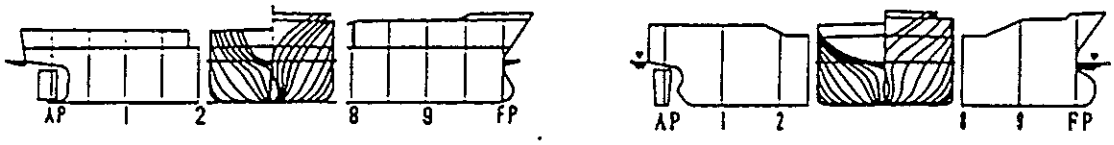

RR100 RR103

Fig.2 Body plans of RR100 and RR103

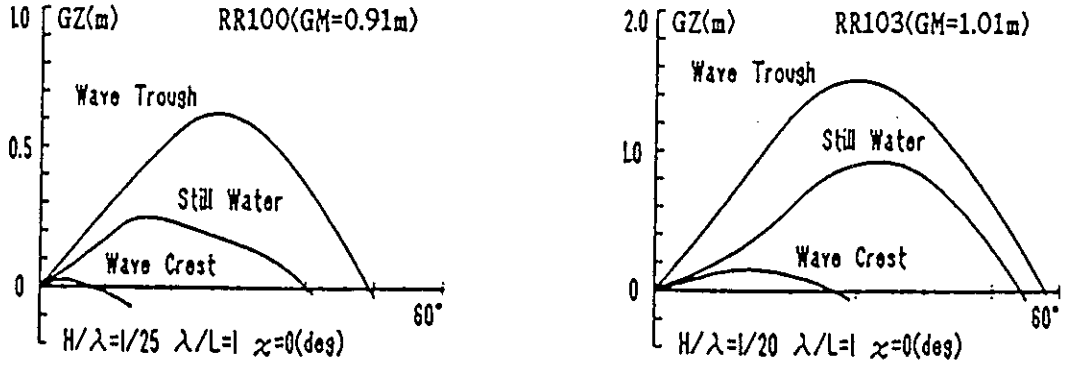

Fig.3 GZ curves of RR100 and RR103

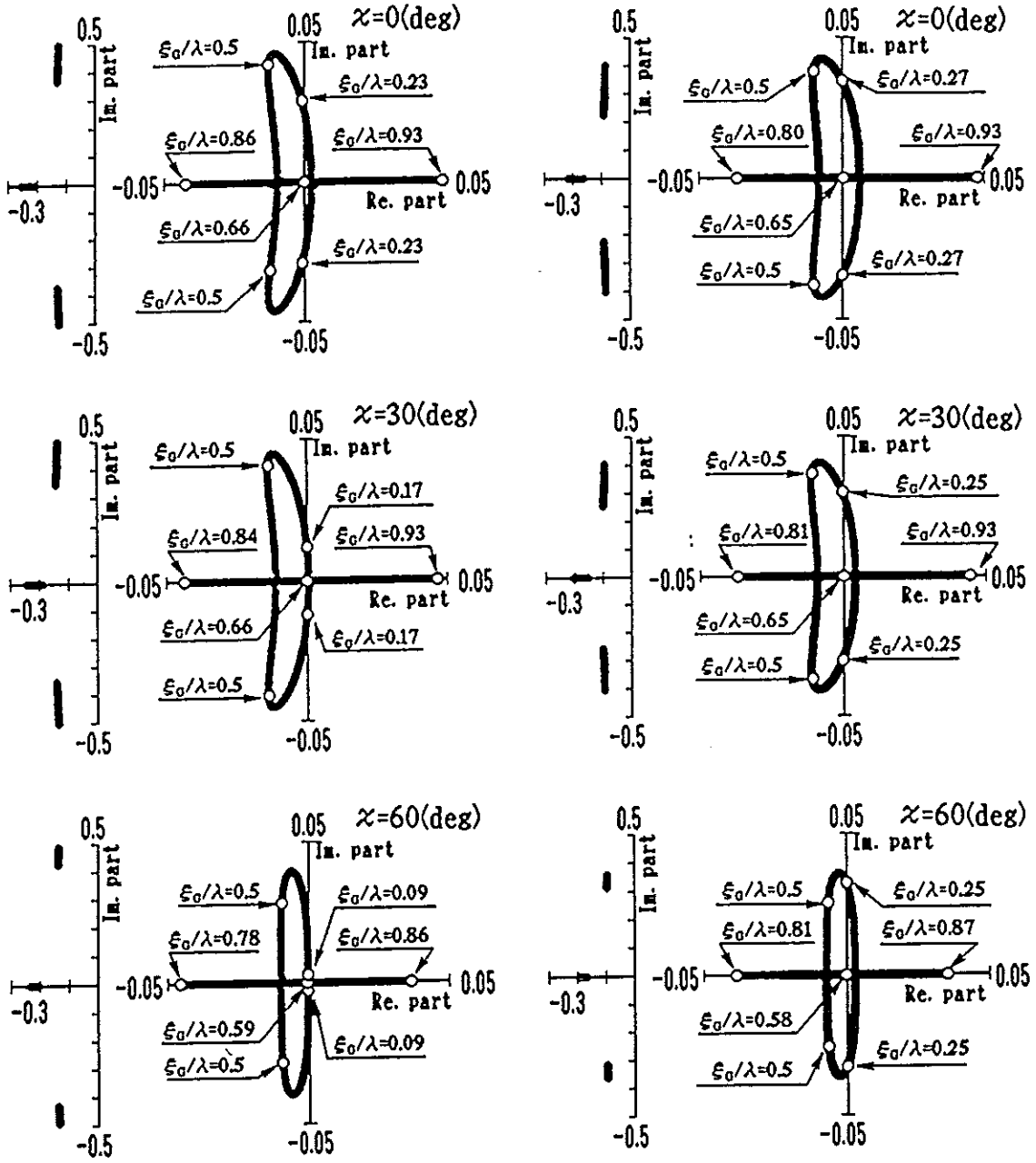

RR100 RR103

Fig.4 Characteristic roots for dynamic stability in case of $\lambda/L = 1.0$

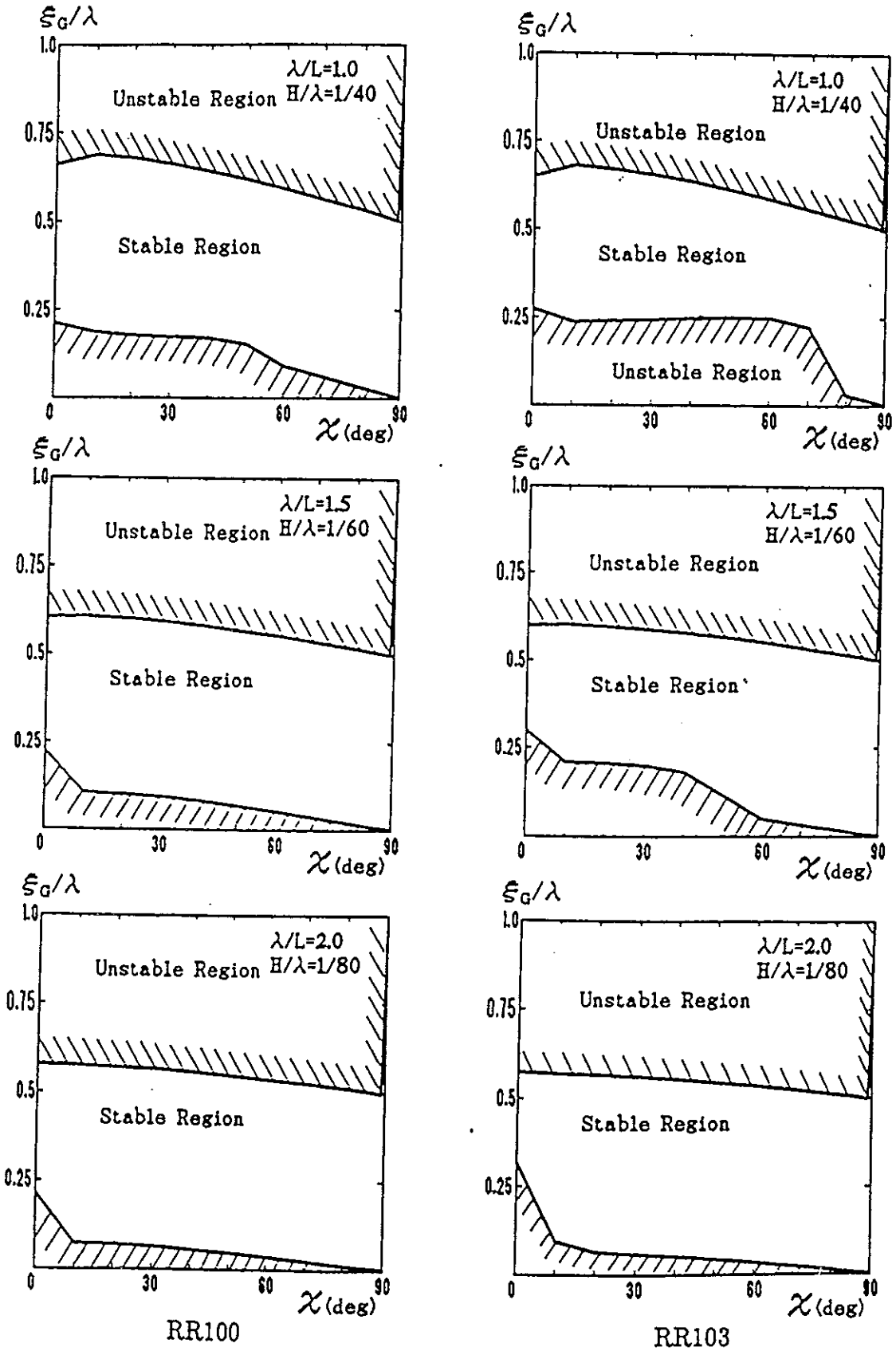

Fig.5 Stable and unstable regions of RR100 and RR103

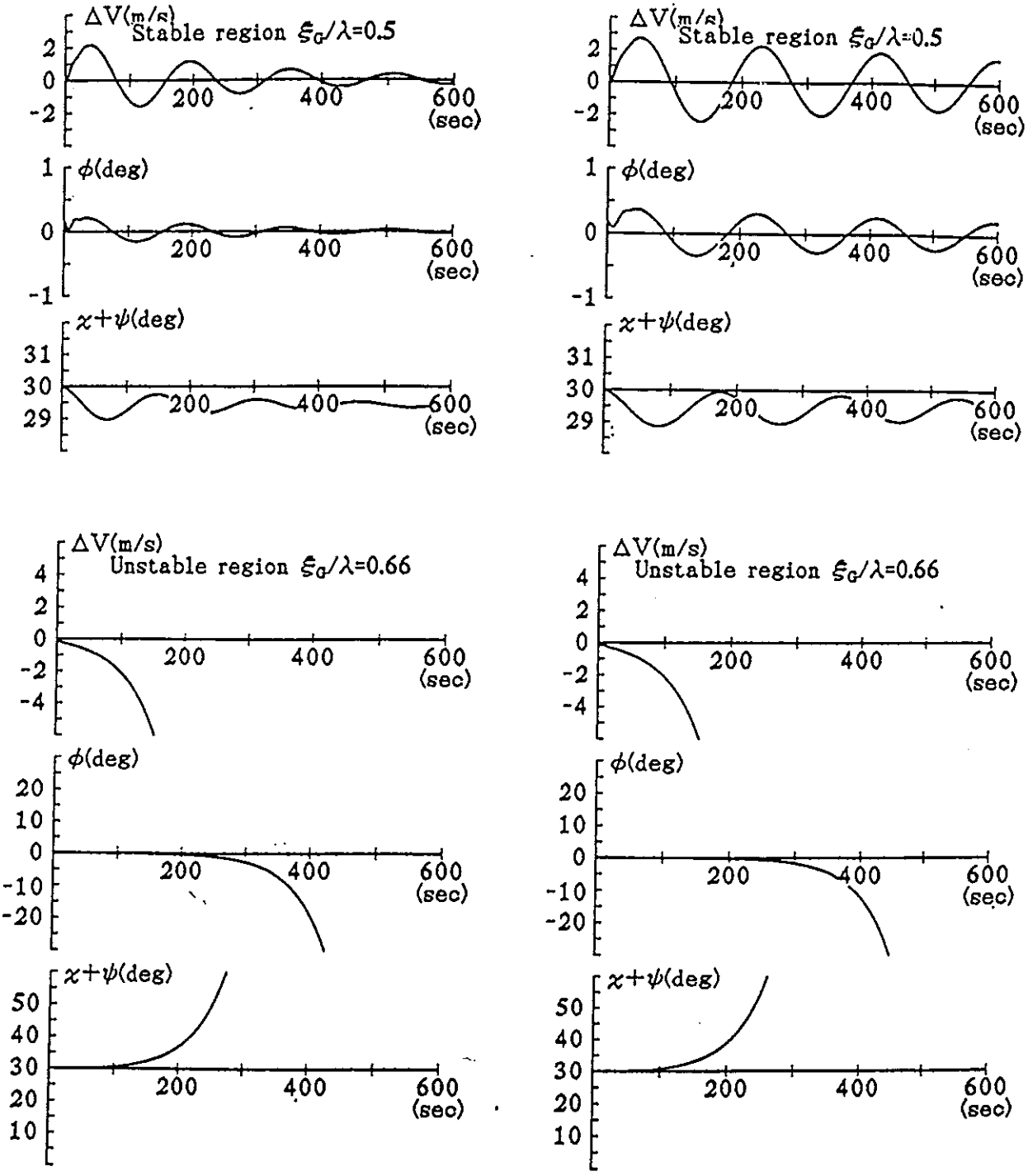

RR100 RR103

Fig.6 Time histories for combined motions of sway, roll and yaw of the ships of RR100 and RR103 in a wave of the stable region for the healing angle $\chi = 30°$

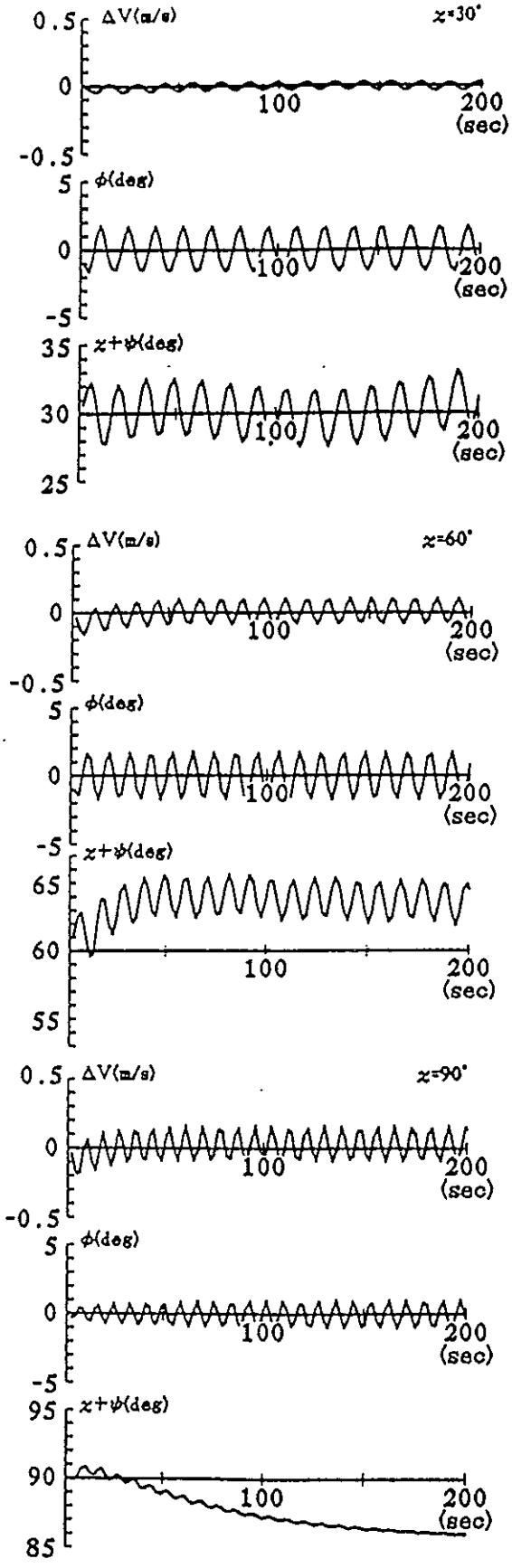

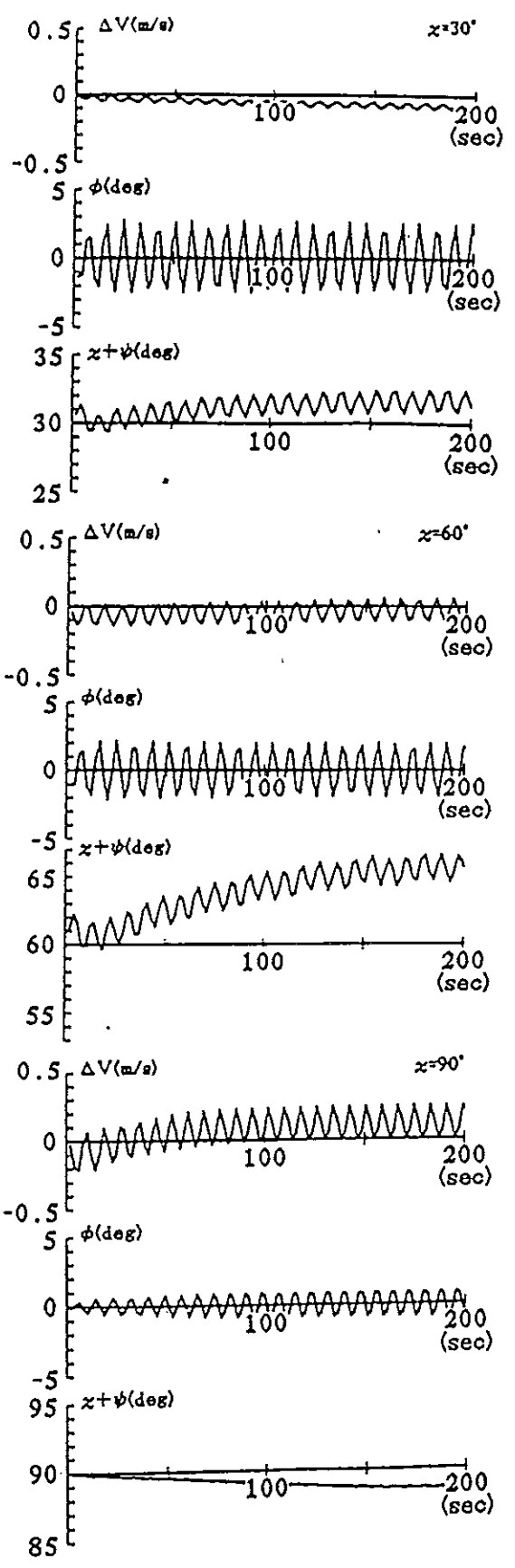

RR100 RR103

Fig.7 Time histories sway, roll and yaw of the ships of RR100 and RR103 in overtaking waves of low frequency of encounter for $U/c = 0.4$

CONCLUSIONS

A theoretical study was made to outline the dynamic stability of a ship in quartering seas. Based on the results of this study, the following conclusions are drawn.

(1) Linearized equations are developed for the combined motions of sway, roll and yaw to obtain the characteristic equation and to carry out numerical simulations of ship motion.

(2) The stable and unstable region of dynamic stability are specified for container ships in limiting situation at zero frequency of encounter. Two cases are considered about the possibility for broaching–to. First one is the case completely impossible to keep the prescribed course when the yawing moment due to the wave force is bigger than the moment due to the rudder force at the maximum angle. Second one is the case partially possible to keep the prescribed course from the up slop to the crest of a wave.

(3) Numerical simulations are carried out to show unstable behaviors in limiting situation at zero frequency of encounter and in overtaking waves of low frequency of encounter.

(4) For keeping the prescribed course, it seems to be the best way to reduce the ship speed to the range of overtaking wave.

REFERENCES

1. Davidson, K. and Schiff, L., "Turning and Course–Keeping Qualities of Ships", Trans. of Soc. of Naval Arch. and Marine Engineers, 1946.

2. Weinblum, G. and M. ST. Denis, "On the motions of ships at sea". Trans. of Soc. of Naval Arch. and Marine Engineers, 1950.

3. Paulling, J.R., "The Transverse Stability of a Ship in a Longitudinal Seaway", J. of Ship Research, SNAME, Vol.4, No.4, March, 1961.

4. Grim, O., "Beitrag zn dem Problem der Sicherheit des Schiffes in Seegang Von Dr–Ing.", Schiff unt Hafen 1961 Haft 6.

5. Wahab and Swaan, W.A., "Coursekeeping and Broaching of Ships in Following Seas.", I.S.P. Vol.7, no 4, April 1964.

6. Takahashi, T., "Mechanism of Rolling and Application", (in Japanese), Report of Mitsubishi Heavy Industry Nagasaki Technical Institute, No.2842, 1964, Unpublished

7. Inoue, S., Kijima, K. and Moriyama, F., "Presumption of Hydrodynamic Derivatives on Ship Manoeuvring in Trimmed Condition" Trans. of west–japan Society of Naval Architects. No.55, March 1978.

8. Motora, S., Fujino, M. and Fuwa, T., On the Mechanism of Broaching–to Phenomena, STABILITY '82, 1982.

9. Son, K.H., "Study on unstable behavior due to combined motion of manoeuvring on rolling", Dissertation thesis of Osaka University in 1983.

10. Hamamoto, M. and Kim, Y.S., "A New Coordinate System and the Equations Describing Manoeuvring Motion of a Ship in Waves", J. of Soc. of Naval Arch. Vol.173, 1993.

Fifth International Conference on
Stability of Ships and Ocean Vehicles
STAB'94
Melbourne, Florida, USA
7-11 November, 1994

SHIP'S STABILITY SAFETY in RESONANCE CASE

Witold BLOCKI
Faculty of Ocean Engineering & Ship Technology, Technical University of Gdansk, Poland

Abstract

The coupled, nonlinear and parametric system of equations for ship motions are introduced. Symulations of ship motions in regular, beam wave are caried out and a few symulations of ship's capsizing are presented. A new method for obtaining damping and added mass moments for large roll motions with immersing of the deck edge and taking into account the runing-off the water from the deck is used. The method of computing of the probability of ship's non-capsizing is presented. A relation of this method to the area of safe basin concept is discussed. The probability of ship's non-capsizing is recommended measure for ship's stability safety.

1. Introduction

The majority of traditional ship's stability criteria are based on the potential energy necessary for the capsizig of a ship. These criteria, in general, fulfil well their task in various non-resonance cases like gust of the wind or pure loss of stability. But they can be completely misleading in resonance cases. It may happen, that a reduction in the height of the centre of gravity (it is equivalent to improving of the ship's stability in non-resonance cases) could result in fact in worsening the ship's stability in resonance cases.

The paper presents a method for the assessment of the ship's stability safety in a resonance case. This method is based on the probability of occurrence the roll resonance, either the ordinary or parametric resonance. The parametric resonance is particularly dangerous. It is confirmed by model experiments and also by theoretical consideretions as well: Paulling and Rosenberg [1959], Blocki [1980] [1984], Tikka and Pauling [1990].

2. Coupled and unstable ship's motions leading to its capsizing in beam regular wave

It was assumed, that the following system of coupled differential equations describes sway, heave and roll motions of the ship (Blocki [1977]):

$$\begin{cases} \ddot{y}+2\delta_y\dot{y}=f_y\sin(\omega_e t+\lambda_y) \\ \ddot{z}+2\delta_z\dot{z}+\omega_z^2 z+Z_{\Phi\Phi}\Phi^2=f_z\sin(\omega_e t+\lambda_z) \\ \ddot{\Phi}+2\delta_\Phi(1+\frac{e_1}{\omega_\Phi^2}\dot{\Phi}^2+\ldots)\dot{\Phi}+d_W\dot{\Phi}^2\,sign\,\dot{\Phi}+ \\ +\omega_\Phi^2(1+\varepsilon_1\Phi^2+\ldots)+K_{\Phi z}\Phi z+w_a\cos\Phi=f_\Phi\sin(\omega_e t+\lambda_\Phi) \end{cases} \tag{2.1}$$

Factors $K_{\Phi z}$ and $Z_{\Phi\Phi}$ couple the heave and roll motions (Paulling and Rosenberg [1959], Blocki [1980]):

$$K_{\Phi z}=-\frac{\rho g(\frac{dI_T}{dz}-A_w b)}{I_X+m_\Phi} \tag{2.2}$$

$$Z_{\Phi\Phi}=\frac{\rho g A_w b}{2(I_X+m_\Phi)} \tag{2.3}$$

The factor $K_{\Phi z}$ makes it possible parametric resonance of the roll.

The nonlinear damping and nonlinear stiffness of the roll are presented in the form of polynomial expansions:

$$n(\dot{\Phi})=2\delta_\Phi(1+\frac{e_1}{\omega_\Phi^2}\dot{\Phi}^2+\ldots)\dot{\Phi} \tag{2.4}$$

$$k(\Phi)=\omega_\Phi^2(1+\varepsilon_1\Phi^2+\ldots)\Phi \tag{2.5}$$

The following coefficients of hydrodynamic forces and moments: $m_y, m_z, \delta_y, \delta_z, f_y, f_z$ and f_Φ were obtained from a computer program called Wares (Dudziak [1984]), which solves the radiation and dyfraction hydrodynamic problem.

The phase angle between responses and excitation forces (and moment) were obtained from the following formulae:

$$\lambda_y=arctg(-\frac{2\delta_y}{\omega_e}) \tag{2.6}$$

$$\lambda_z=arctg(\frac{2\delta_z\omega_e}{\omega_z^2-\omega_e^2}) \tag{2.7}$$

$$\lambda_\Phi=arctg(\frac{2\delta_\Phi\omega_e}{\omega_\Phi^2-\omega_e^2}) \tag{2.8}$$

The quantities: $(I_x + m_\Phi)$, δ_Φ and e_1 were obtained from model tests, the others like $K_{\Phi z}, Z_{\Phi\Phi}, \varepsilon_1$ were calculated. Factor d_W is a damping coefficient connected with the runing-off water from the immersed deck (see the next section):

$$d_W = \frac{I_3}{I_X + m_\Phi} \tag{2.9}$$

The initial conditions for sway and heave in simulations were taken from the linear model of motions in the following manner. The phase angles ε_y and ε_z between excitation forces and wave were obtained from quoted program Wares. The amplitudes y_a and z_a were obtained similarly. Then, the initial conditions for sway and heave were computed from the following formulae:

$$\begin{aligned} y_0 &= y_a \sin(\varepsilon_y + \lambda_y) \\ \dot{y}_0 &= y_a\, \omega_e \cos(\varepsilon_y + \lambda_y) \\ z_0 &= z_a \sin(\varepsilon_z + \lambda_z) \\ \dot{z}_0 &= z_a \omega_e \cos(\varepsilon_z + \lambda_y) \end{aligned} \tag{2.10}$$

The initial conditions for roll were assumed to be random (see section 5).

The computer simulations were carried out by the four order Runge-Kutta procedure with a predictor-corrector method, with initial step of integration taken as 0.001 s.

The model presented above can be expanded to six degree of freedom to simulate the motions in oblique wave.

3. Damping and added mass moment of the roll due to the running-off water from the deck

There are some hydrodynamic phenomena for large roll motions connected with immersing of the deck edge (Blocki [1993b]). These phenomena are schematically presented in Fig 1: the ship rolls in waves (a), at a certain moment the deck edge immerses into water and the water flows on to the deck (b); the shipbody reaches a maximum roll angle (c); the water runs-off from the deck during the return phase of motion (d). It is assumed that additional damping and added mass moment appear only in phase (d).

It was assumed that no additional moments act during phase (b), but situation radically changes after the moment corresponding to $\dot{\Phi} = 0$ (c). Running-off water from the deck in phase (d) separates on the deck edge and slows down the return roll motion. Substantial additional moments are connected with this phenomenon. Slowing down of such roll motion was observed in experiments (Blocki [1979]): a fragment of recorded roll motion is presented in Fig. 3 both in the time domain and on the phase plane.

An approximate calculation of the moments acting during running-off the water from deck is based on the principle of conservation of angular momentum. This is explained in Fig. 2.

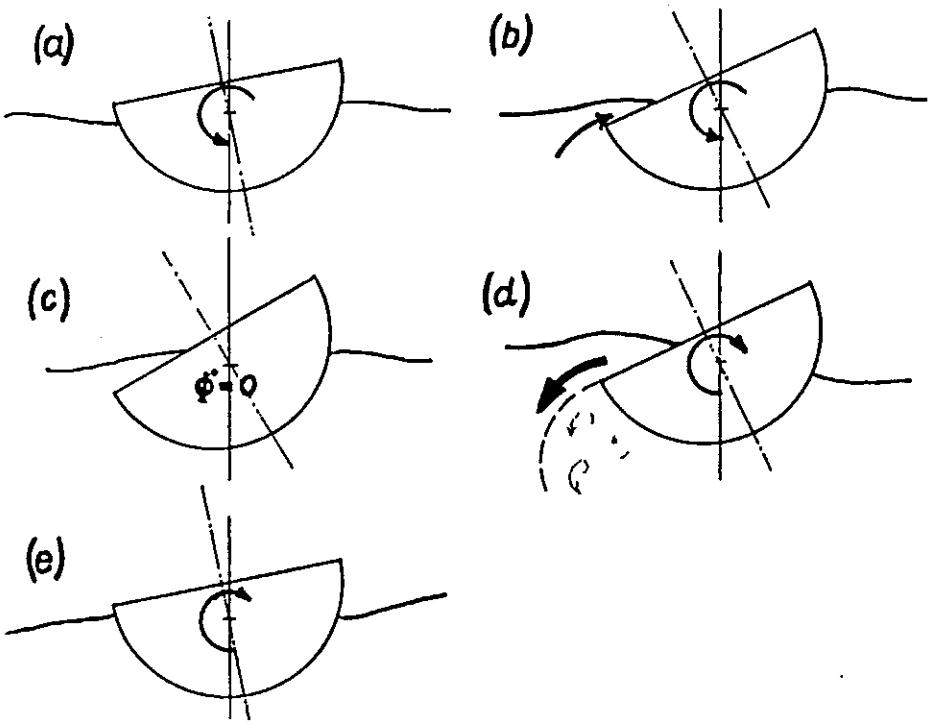

Fig.1. Phenomena connected with immersing of the deck edge.

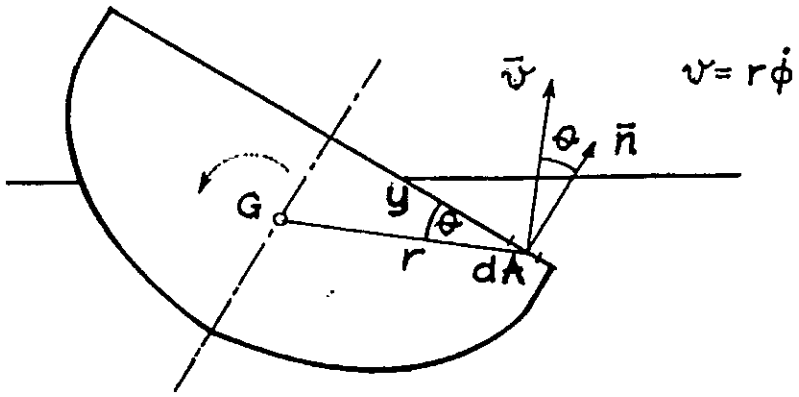

Fig. 2. Relations between the element of deck area dA, the normal vector to the deck $\overline{n}$ and the velocity $\overline{v}$ of the element of deck area.

The principle of conservation of angular momentum is aplied in the direction $\overline{n}$:

$$\frac{d}{dt}(m_n \upsilon_n) = R_n \tag{3.1}$$

or

$$\frac{dm_n}{dt}\upsilon_n + m_n\frac{d\upsilon_n}{dt} = R_n \tag{3.2}$$

From the equation of continuity we get:

$$\frac{dm_n}{dt} = \rho\,\upsilon_n\,dA \tag{3.3}$$

Taking into account that $\upsilon = r\dot{\Phi}$, $\upsilon_n = \upsilon\cos\Theta$, $\upsilon_n = r\dot{\Phi}\cos\Theta = y\dot{\Phi}$ and $\frac{d\upsilon_n}{dt} = y\ddot{\Phi}$ (Fig.2) equation (3.2) can be rewritten:

$$R_n = \rho\dot{\Phi}^2 y^2 dA + \rho\ddot{\Phi}\,y\,dV \tag{3.4}$$

or

$$dM = yR_n = \rho\dot{\Phi}^2 y^3 dA + \rho\ddot{\Phi}\,y^2 dV \tag{3.5}$$

The additional moment connected with the running-off water from the deck could be obtained after integration:

$$M = \dot{\Phi}^2\rho\int_A y^3 dA + \ddot{\Phi}\rho\int_V y^2 dV \tag{3.6}$$

where the integration is carried out with respect to the area of wetted deck A and volume of water on the deck V.

The approximate formula (3.6) is the sum of two parts: damping moment and added mass moment:

$$M = I_3\,\dot{\Phi}^2 + i_X\,\ddot{\Phi} \tag{3.7}$$

where $I_3 = \rho\int_A y^3 dA$, is the third order moment of area A and $i_X = \rho\int_V y^2 dV$ is the inertia mass moment of the water on the deck with respect to the central axis of the ship.

The mass of the ship increases by the mass of water on the deck:

$$m_a = \rho\int_V dV \tag{3.8}$$

and this mass is added to the total mass of the ship.

Fig. 3 shows a fragment of recorded run of roll motion during towing tank tests with immersing of the deck edge and with the running-off the water from the deck. Whereas Fig. 4 presents a numerical simulation of the moments acting during running-off the water from the deck based on the principle of conservation of angular momentum with similar conditions. Both runs show fairly good agreement between them.

ω_e =6.0 [1/s] ϕ_0 =0.03 [−]

ζ_{FA} =0.04 [m] α_0 =−0.87 [1/s]

δ_ϕ =0.03 [1/s]

ε_1 =−4.3 [−]

$K_{\phi z}$=−216 [1/ms²]

$Z_{\phi\phi}$=1.7 [m/s²]

e_1 = 9.5 [−]

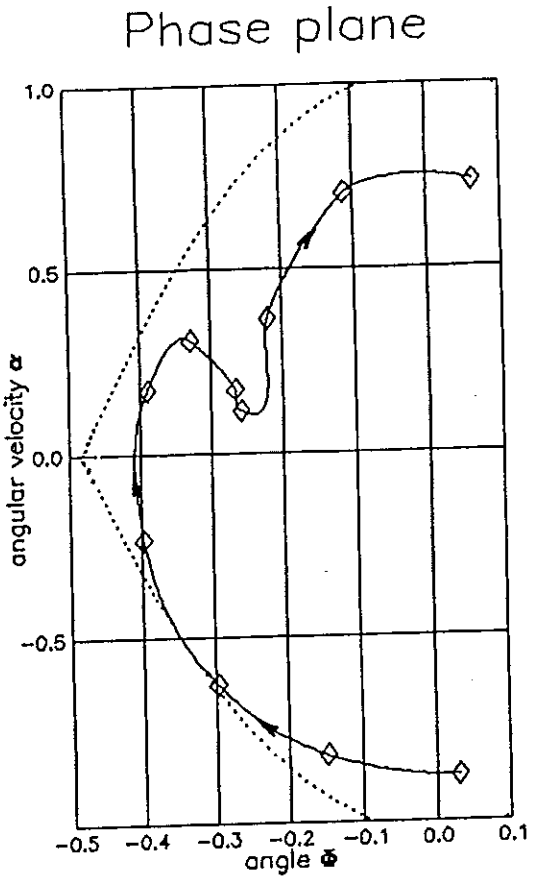

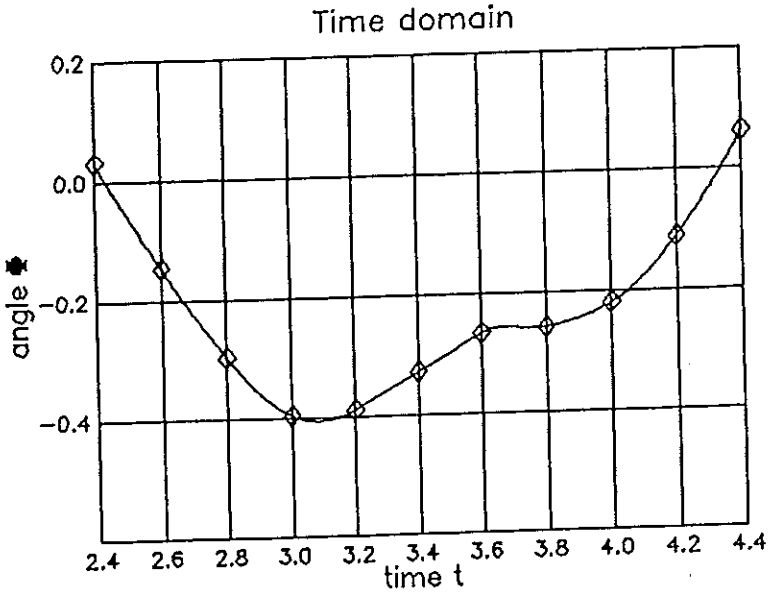

Fig. 3. A fragment of experimental run of cylindrical framelike ship's model with the slowing down roll motion connected with running-off the water from the deck (Blocki [1979]).

ω_e =6.0 [1/s] ϕ_0 =0.03 [−]

ξ_A =0.04 [m] α_0 =−0.7 [1/s]

δ_y =1.1 [1/s] δ_ϕ =0.03 [1/s]

f_y =0.9 [m/s^2] ε_1 =−4.3 [−]

λ_y =2.79 [−] f_ϕ =0.23 [1/s^2]

δ_z =2.37 [1/s] λ_ϕ =3.13 [−]

f_z =0.77 [m/s^2] $K_{\phi z}$ =−216 [1/ms^2]

λ_z =1.72 [−] $Z_{\phi\phi}$ =1.7 [m/s^2]

ω_z = 5.62 [1/s] e_1 = 9.5 [−]

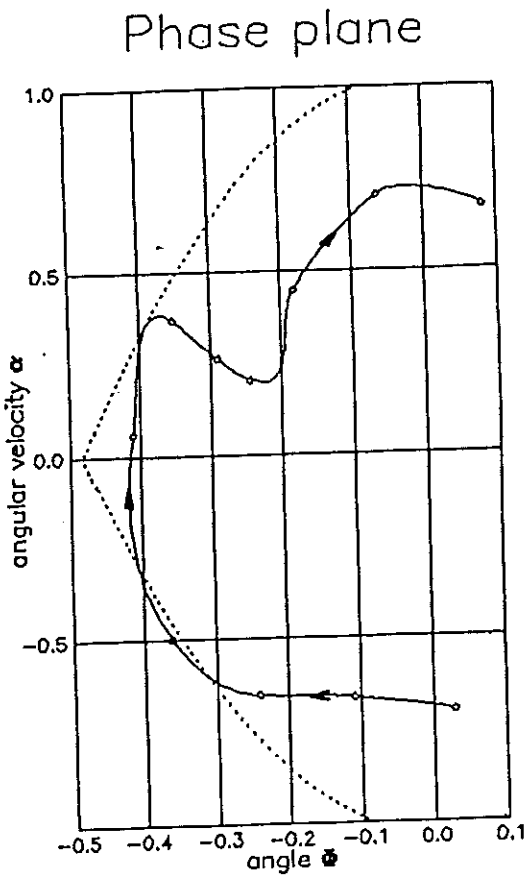

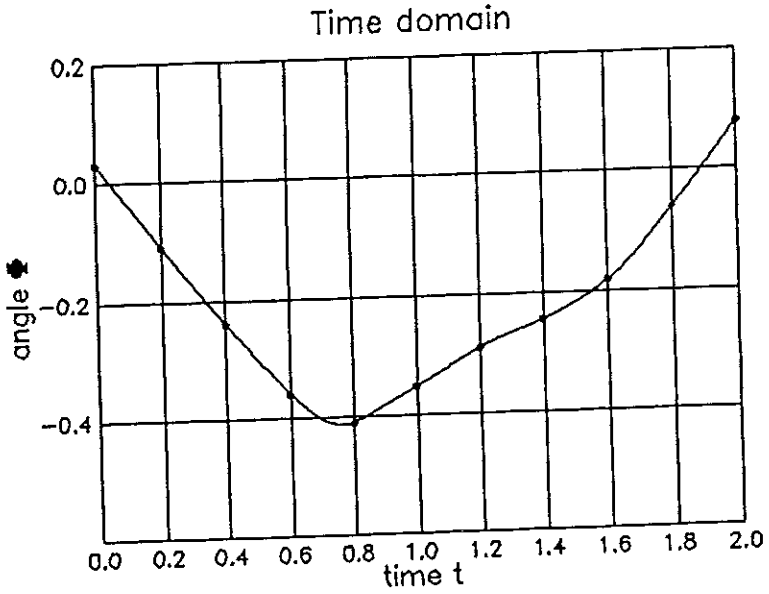

Fig. 4. A computer simulation of the run of cylindrical framelike ship's model with additional damping and added mass moments connected with runing-off the water from the deck.

4. Examples of unstable simulations

A few typical examples of the capsizing's simulations are presented in Figures 5 to 8. The simulations were carried out for a cylindrical framelike fishing ship's model in a parametric resonance. A convenient method for analysing of a motion is the Poincare phase plane (Blocki [1993a]), so the simulations in Figures 5 to 8 are presented on phase plane and in time domain.

5. Probability of non-capsizing of a ship as a measure of its safety

The randomness of ship's capsizing is caused by the fact that sea waves are stochastic and by the fact that the ship is a strong nonlinear mechanical object. The probability of noncapsizing of the ship is a convenient measure of ships' stability safety. This is a number from the interval [0,1]. The proposed method for the computation of this probability is based on the Goda's idea of high wave groups (Goda [1976], Ewing [1973]). This concept defines the probability distribution $P_1(j)$ of the length j of high wave groups:

$$P_1(j) = p^{j-1}(1-p) \tag{5.1}$$

and the mean distance between two subsequent wave groups:

$$E(j_2) = \frac{1}{p} + \frac{1}{1-p} \tag{5.2}$$

where p denotes the probability of exceeding of the level ρ by a single wave:

$$p = P(\xi_A \geq \rho) = \exp\left(-\frac{\rho^2}{2\sigma^2}\right) \tag{5.3}$$

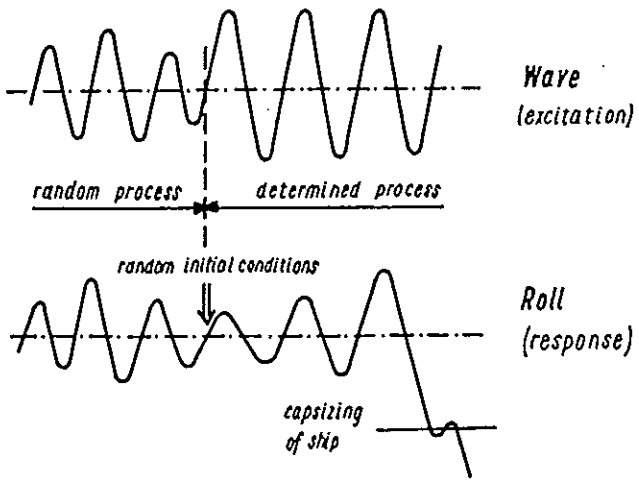

Fig. 9. Capsizing of a ship as a result of the wave group (Blocki [1980]).

ω_e =6.0 [1/s] ϕ_o =0 [-]

ξ_A =0.058 [m] α_o =0.2 [1/s]

δ_y =1.1 [1/s] δ_ϕ =0.03 [1/s]

f_y =0.9 [m/s^2] ε_1 =-4.3 [-]

λ_y =2.79 [-] f_ϕ =0 [1/s^2]

δ_z =2.37 [1/s] λ_ϕ =3.13 [-]

f_z =0.77 [m/s^2] $K_{\phi z}$=-216 [1/ms^2]

λ_z =1.72 [-] $Z_{\phi\phi}$=1.7 [m/s^2]

ω_z = 5.62 [1/s] e_1 = 9.5 [-]

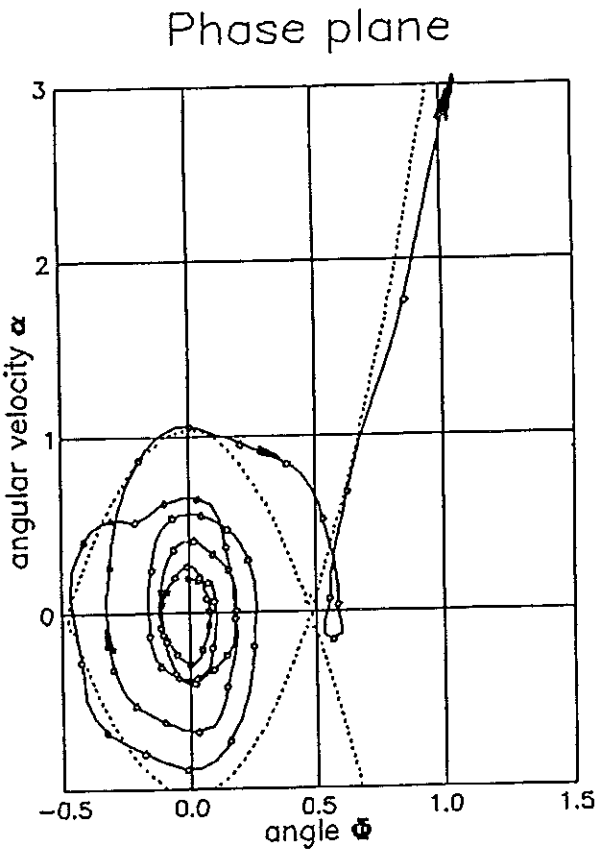

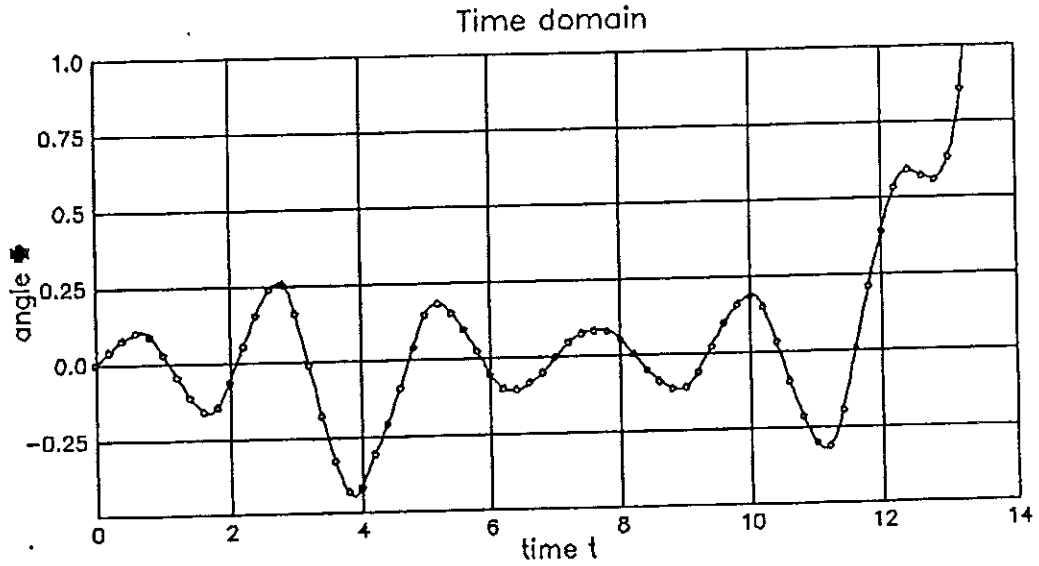

Fig. 5. A example of computer simulation of capsizing run in parametric resonance of the roll of cylindrical framelike ship's model.

ω_e =6.0 [1/s] ϕ_o =0 [-]

ζ_A =0.09 [m] α_o =0.3 [1/s]

δ_y =1.1 [1/s] δ_ϕ =0.03 [1/s]

f_y =0.9 [m/s^2] ε_1 =-4.3 [-]

λ_y =2.79 [-] f_ϕ =0.23 [1/s^2]

δ_z =2.37 [1/s] λ_ϕ =3.13 [-]

f_z =0.77 [m/s^2] $K_{\phi z}$ =-216 [1/ms^2]

λ_z =1.72 [-] $Z_{\phi\phi}$ =1.7 [m/s^2]

ω_z =5.62 [1/s] w_a =0.4 [1/s^2]

e_1 = 9.5 [-]

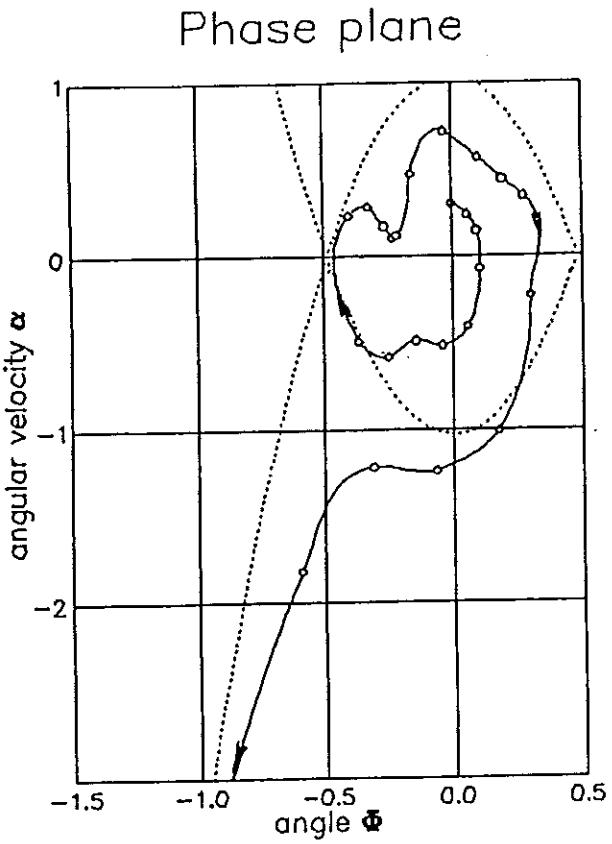

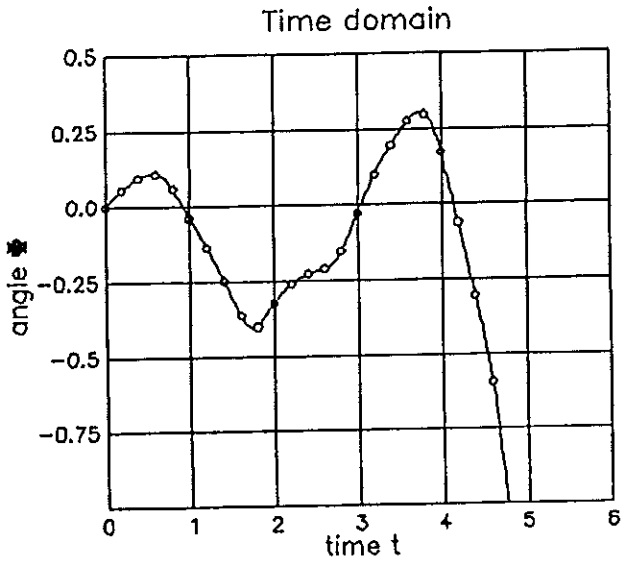

Fig. 6. A example of computer simulation of capsizing run in parametric resonance of the roll of cylindrical framelike ship's model.

ω_e =6.0 [1/s] ϕ_o =−0.35 [−]

ζ_A =0.09 [m] α_0 =0 [1/s]

δ_y =1.1 [1/s] δ_ϕ =0.03 [1/s]

f_y =0.9 [m/s²] ε_1 =−4.3 [−]

λ_y =2.79 [−] f_ϕ =0.23 [1/s²]

δ_z =2.37 [1/s] λ_ϕ =3.13 [−]

f_z =0.77 [m/s²] $K_{\phi z}$ =−216 [1/ms²]

λ_z =1.72 [−] $Z_{\phi\phi}$ =1.7 [m/s²]

ω_z = 5.62 [1/s] w_a =0.4 [1/s²]

e_1 = 9.5 [−]

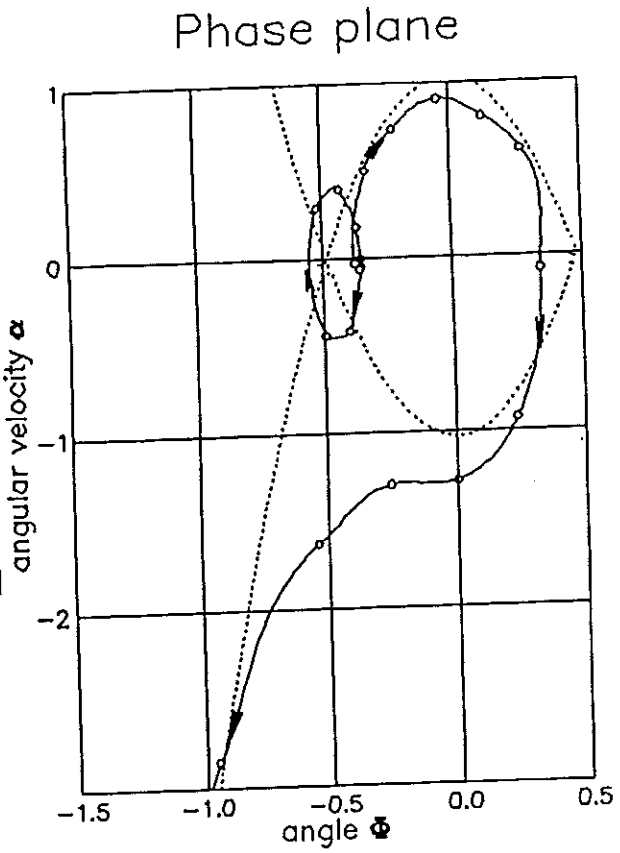

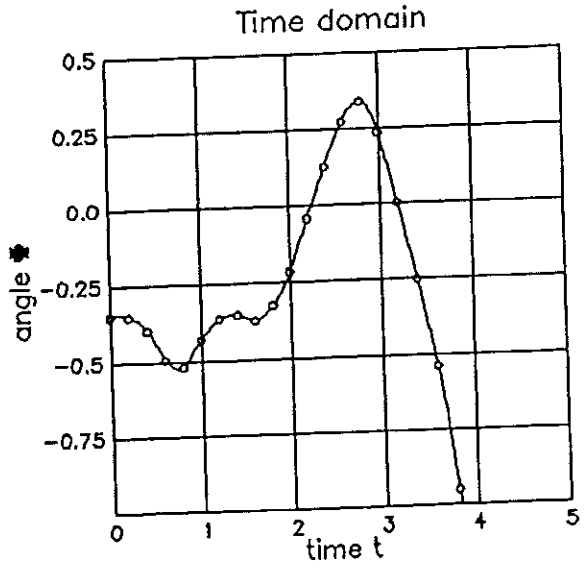

Fig. 7. A example of computer simulation of capsizing run in parametric resonance of the roll of cylindrical framelike ship's model.

ω_e =6.0 [1/s] ϕ_o =0.34 [−]

ξ_A =0.09 [m] α_o =0.16 [1/s]

δ_y =1.1 [1/s] δ_ϕ =0.03 [1/s]

f_y =0.9 [m/s^2] ε_1 =−4.3 [−]

λ_y =2.79 [−] f_ϕ =0.23 [1/s^2]

δ_z =2.37 [1/s] λ_ϕ =3.13 [−]

f_z =0.77 [m/s^2] $K_{\phi z}$ =−216 [1/ms^2]

λ_z =1.72 [−] $Z_{\phi\phi}$ =1.7 [m/s^2]

ω_z = 5.62 [1/s] W_a =0.4 [1/s^2]

e_1 = 9.5 [−]

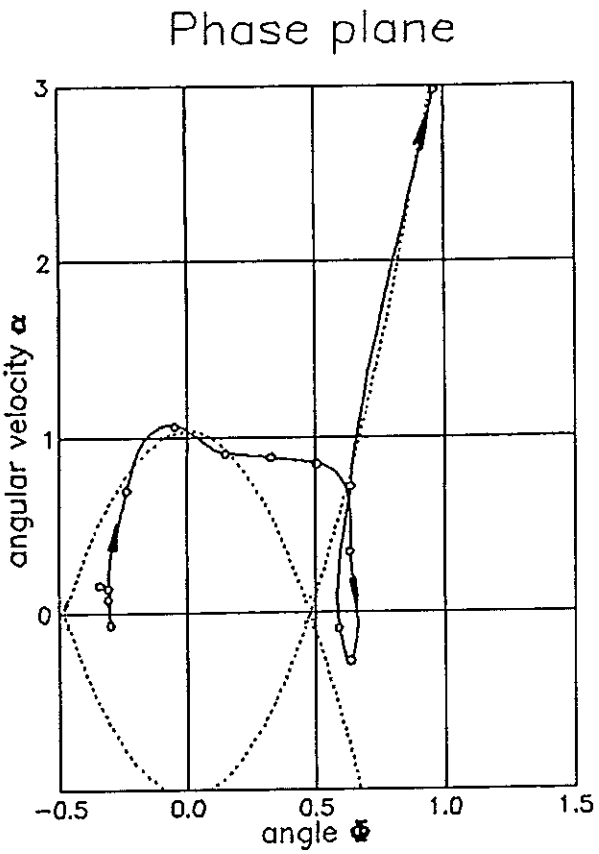

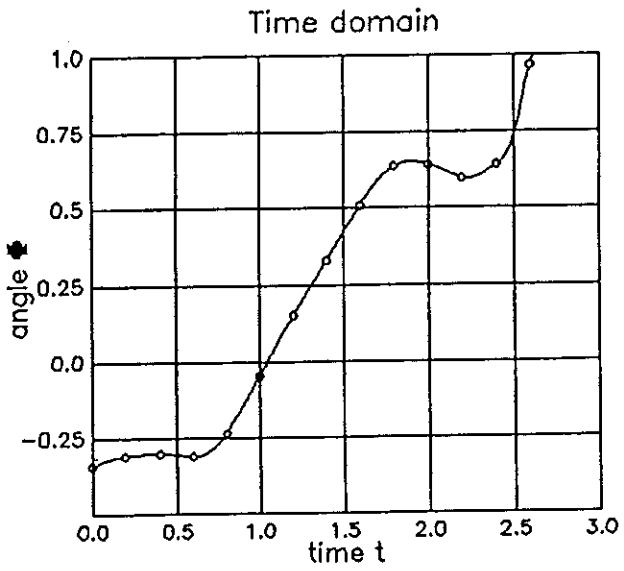

Fig. 8. A example of computer simulation of capsizing run in parametric resonance of the roll of cylindrical framelike ship's model.

Computation of the probability of ship's capsizing is based on the solution of the differential equations of ship motions for random initial conditions for the roll. It is assumed that the ship undergoes random oscilations until it meets wave group and then it undergoes determinate oscilations. At the moment of occurrence of the group of waves the roll angle Φ_0 and the roll angular velocity α_0 are random. It is assumed that the group of high waves can be approximated by means of a regular wave (Blocki [1980]). This is schematically shown in Fig. 9.

The probability of ship capsizing as a result of wave group of length j may be expressed by:

$$P(B_j) = \int_{G_j} p(\Phi, \alpha)\, d\Phi\, d\alpha \tag{5.4}$$

where B_j denotes a random event of ship's capsizing (as a result of wave group of length j), G_j means the initial value plane (Φ_0, α_0) of initial roll angle Φ_0 and initial roll angular velocity α_0 for which ship's casizing occurs, and $p(\Phi, \alpha)$ means the probability distribution of roll angle Φ and roll angular velocity α. The probability distribution $p(\Phi, \alpha)$ can be determined from the Fokker-Planck equation (Caughey [1963]):

$$p(\Phi, \alpha) = C \exp\left\{-\frac{8\delta_\Phi}{S_f(\omega_e)}\left[\frac{1}{2}\alpha^2 + \omega_\Phi^2\left(\frac{1}{2}\Phi^2 + \frac{\varepsilon_1}{4}\Phi^4 + \ldots\right)\right]\right\} \tag{5.5}$$

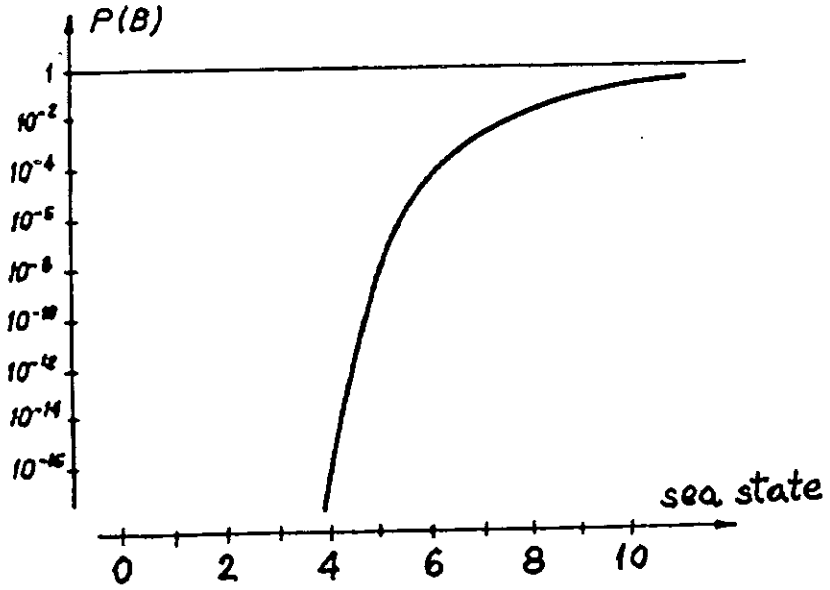

Fig. 10. The probability of capsizing of a small fishing vessel as a result of any single group of high waves (Blocki [1986]).

Constant C normalizes distribution $p(\Phi,\alpha)$ and has to fulfil the following condition:

$$\int_{-\infty}^{\infty}\int_{-\infty}^{\infty} p(\Phi,\alpha)\,d\Phi\,d\alpha = 1 \tag{5.6}$$

The probability of ship's capsizing as a result of any single group of high waves may be calculated as the entire probability by the following formula:

$$P(B) = \sum_{j} P_1(j)\,P(B_j) \tag{5.7}$$

The example of calculations of the probability of capsizing for a small fishing trawler is shown in Fig. 10 (Blocki [1986]).

The probability of ship's non-capsizing as a result of any single group of high waves can be simply calculated as follows:

$$P(A) = 1 - P(B) \tag{5.8}$$

Any group of waves is the trial which may cause either non-capsising of a ship (success) or capsizing of the ship (failure). The success occurs with the probability $P(A)$ and failure with probability $P(B)$. The probability of ship's non-capsizing for n trials (that is for n groups of waves) is given by:

$$P_n(A) = [P(A)]^n \tag{5.9}$$

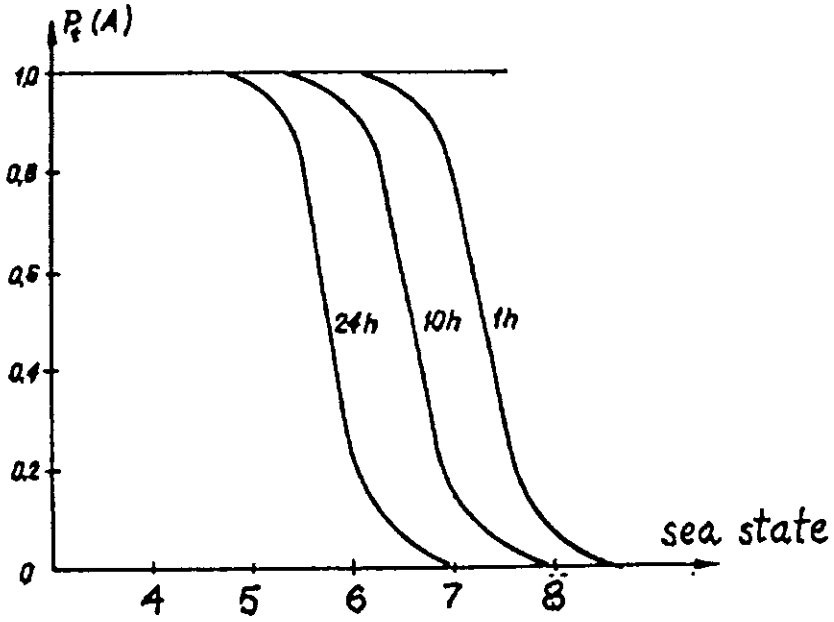

Fig. 11. The probability of non-capsizing of small fishing vessel during the period of time t (Blocki [1986]).

The relationship between four quantities: the number n of groups of high waves, the mean period of waves T_1, the mean distance $E(j_2)$ between the groups of waves and the period of time t of stay of the ship in definite conditions is given by the formula:

$$t = n\ T_1\ E(j_2) \tag{5.10}$$

Thus, the probability $P_t(A)$ of ship non-capsizing during a period of time t may be expressed by:

$$P_t(A) = [1 - P(B)]^{\frac{t}{T_1 E(j_2)}} \tag{5.11}$$

The example of calculations of non-capsizing during the period of time t for small fishing trawler is shown in Fig. 11 (Blocki [1986]).

It is proposed to take the probability $P_t(A)$ of non-capsizing of the ship as a measure of ship's stability safety.

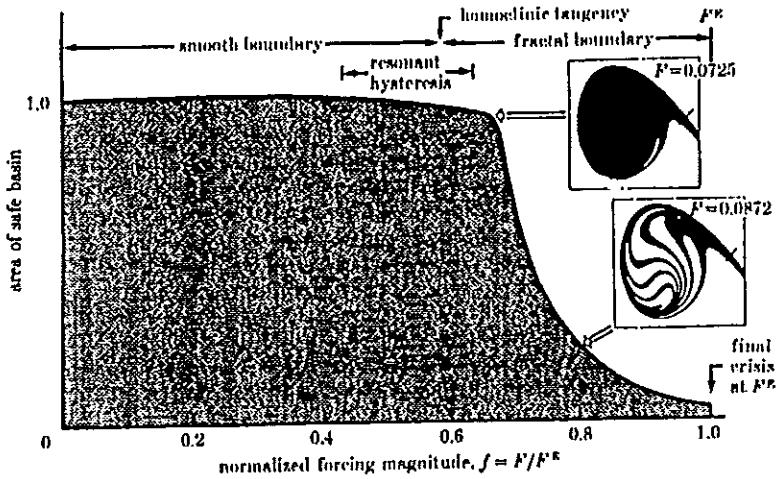

Fig. 12. The area of safe basin (after Thompson and Soliman [1990]).

6. Some comments regarding the proposal of the area of safe basin

Recently many chaotic responces of nonlinear mechanical objects, including ships, were investigated. A proposal regarding quantifying ship's stability safety by the area of safe basin was put forward by Thompson and Soliman [1990], Rainey, Thompson, Tam, and Noble [1990], Soliman [1990], Rainey and Thompson [1991], Kan and Taguchi [1991] - see Fig. 12. This concept, however assumes indirectly that the probability of initial conditions of roll is constant for the whole phase plane (Φ_0, α_0), wchich does not agree with reality. The distribution of initial conditions is definitly a modal one.

My suggestion is to replace the concept of safe basin area by the idea of probability of ship's noncapsizing. The area $G_j(\Phi_0, \alpha_0)$ of critical initial conditions of ship's capsizing can be taken as fractal safe basin space.

The idea of the probability $P_i(A)$ of noncapsizing of a ship as the measure of ship stability safety (instead of safe basin area) appears to be useful. This measure has strictly specified physical meaning and sound interpretation. This probability depends on the time of staying of a ship in constant sea conditions and this feature agrees with common sense. Long-lasting staying of a ship in heavy conditions obviously increases the risk of capsizing.

The presented probabilistic concept allows considering a ship in various particular dangerous situations such as beam wave, following sea, quartering wave, etc.

List of symbols

A	area of the deck
A	random event of noncapsizing of a ship
A_w	waterplane area
b	distance of the centre of gravity of a ship from waterplane
B	random event of capsizing of a ship
B_j	random event of capsizing of a ship as a result of wave group of length j
C	constant which normalises distribution $p(\Phi, \alpha)$
dA	element of area of the deck
d_W	relative additional moment connected with runnig-off the water from deck
e_1	coefficient of nonlinear part of damping moment of the roll
$E(j_2)$	mean value of the distance between two subsequent wave groups
f_y, f_z, f_Φ	relative exciting forces and moment for sway, heave and roll
$G_j(\Phi_0, \alpha_0)$	critical initial conditions of initial roll angle and initial roll angular velocity for which ship's capsizing occurs
i_X	inertia mass moment of the water on the deck with respect to the central axis of the ship
I_X	inertia mass moment of the ship with respect to the central axis
I_3	third order moment of wetted area of the deck
j	length of the high wave group
$k(\Phi)$	relative nonlinear restoring moment of the roll
$K_{\Phi z}$	coupling factor of the equations of heave and roll
m	mass of the ship
m_a	mass of the water on the deck
m_n	mass of water above the element of area dA
m_y, m_z	added masses for sway and heave
m_Φ	added inertia mass moment for roll

M	additional moment connected with the running-off water from the deck
n	number of groups of high waves
$\overline{n}$	normal vector to the deck
$n(\dot{\Phi})$	relative nonlinear damping moment of the roll
p	probability of exceeding of the level ρ by a single wave
$p(\Phi,\alpha)$	probability distribution of the roll angle and roll angular velocity
$P(A)$	probability of ship's non-capsizing as a result of any single group of high waves
$P(B)$	probability of ship's capsizing as a result of any single group of high wawes
$P(B_j)$	probability of ship's capsizing as a result of high waves group of length j
$P_1(j)$	probability of occurrence of the high waves group of length j
$P_n(A)$	probability of ship's non-capsizing for n groups of high waves
$P_t(A)$	probability of ship's non-capsizing during a period of time t
r	distance between element of deck area dA and centre of gravity of ship
R_n	reaction of the water on the element dA of the deck area
$S_f(\omega_e)$	value of spectral density of the excitation of roll for ω_e
t	time
T_1	mean period of waves
V	volume of water on the deck
w_a	coefficient of moment of wind pressure
y,z	sway and heave
y_a,z_a	amplitudes of sway and heave motions
y_0,z_0	initial position of the ship for sway and heave
$\dot{y}_0,\dot{z}_0$	initial velocity of sway and heave
$Z_{\Phi\Phi}$	coupling factor of equations of roll and heave
$\alpha=\dot{\Phi}$	angular velocity of the roll
α_0	initial angular velocity of the roll
$\delta_y,\delta_z,\delta_\Phi$	coefficients of damping moment for sway, heave and roll
ε_1	coefficient of nonlinear part of restoring moment of the roll
$\varepsilon_y,\varepsilon_z$	phase angles between excitation forces and wave for sway and heave
Θ	angle between two vectors: velocity $\overline{v}$ and direction $\overline{n}$ (Fig. 2)
$\lambda_y,\lambda_z,\lambda_\Phi$	phase angles between responses and excitation forces (and moment) for sway, heave and roll
ξ_A	amplitude of single wave
ρ	density of water

ρ	level of the exceeding by a single wave of amplitude ξ_A
σ^2	variance of waving
υ	velocity of the element of deck area dA
υ_n	projection of the velocity υ on the direction $\overline{n}$
$\Phi, \dot{\Phi}, \ddot{\Phi}$	angle, angular velocity and angular acceleration of the roll
Φ_0	initial angle of the roll
ω_e	encounter frequency
ω_z, ω_Φ	natural frequency of the roll and heave

References

Blocki, W. [1977]. The Stability Ship Safety in Connection with Parametric Resonance of the Roll. *Doctor's Thesis* (in Polish), *Faculty of Ocean Engineering and Ship Technolygy, The Technical University of Gdansk.*

Blocki, W. [1979]. Mechanism of ship's capsizing in group of high regular waves (in Polish). *Report of Faculty of Ocean Engineering and Ship Technology, Technical University of Gdansk,* nr 1245/MR-356/79, Gdansk.

Blocki, W. [1980]. Ship Safety in Cnnection with Parametric Resonance of the Roll. *International Shipbuilding Progress,* vol. 27, nr 306, Februar.

Blocki, W. [1984]. The Parametric Resonance of the Roll of Transport Barge (in Polish). *Report of Faculty of Ocean Engineering and Ship Technology, Technical University of Gdansk,* nr 1910/84, Gdansk.

Blocki, W. [1986]. Probability of Non-Capsizing of a Ship as a Measure of her Safety. *Third International Conference on Stability of Ships and Ocean Vehicles, STAB'86,* vol.2, pp.143-149, Gdansk, 22-26 September.

Blocki, W. [1993a]. The Phase Plane Method in Ships' Safety Dynamics. *The International Workshop on Physical and Mathematical Modelling of Vessel's Stabiliry in a Seaway,* Otradnoye'93, 17-22 May.

Blocki, W. [1993b]. Damping and added mass moments of the roll in simulations leading to ship's capsizing (in Polish). *X Conference of Ship's Hydrodynamics,* vol.2, pp. 5-22, Gdansk, 2-3 December.

Caughey, T.K. [1963]. Derivation and Application of the Fokker-Planck Equation to Discrete Nonlinear Dynamic Systems Subjected to White Random Excitation, *The Journal of the Acoustical Society of America,* vol. 35, nr 11, pp. 1683-1692, November.

Dudziak, J. [1984]. Prediction of dynamic preassures at hull of a ship in regular wave (in Polish). *Report of Center of Ship Technology,* nr B-029, Gdansk, April.

Ewing, J.A. [1973]. Mean Length of Runs of High Waves. *Journal of Geophysical Research,* vol. 78, nr 12, 20 April.

Goda, Y. [1976]. On Wave Groups. *An International Conference on Behaviour of Off-Shore Structures,* Norwegian Institute of Technology, Trondheim, Proceedings, vol. one, Boss'76.

Kan, M., and Taguchi, H.[1991]. Chaos and Fractal in Capsizing of a Ship. *International Symposium on Hydro- and Aerodynamics in Marine Engineering, HADMAR'91,* Varna, October.

Paulling, J.R. and Rosenberg, R.M. [1959]. On Unstable Ship Motions Resulting from Nonlinear Coupling. *Journal of Ship Research,* vol. 3, nr 1, June, pp. 36-46.

Rainey, R.C.T., Thompson, J.M.T., Tam, G.W. and Noble, P.G. [1990]. The Transient Capsize Diagram - A Route to Soundly-Based New Stability Regulations. *Fourth International Conference on Stability of Ships and Ocean Vehicles, STAB'90,* pp. 183-190, Naples, 24-28 September.

Rainey, R.C.T., Thompson, J.M.T. [1991]. The Transient Capsize Diagram - A New Method of Quantifying Stability in Waves. *Journal of Ship Research,* vol. 35, nr 1, pp. 58-62, March.

Soliman, M.S. [1990]. An Analysis of Ship Stability Based on Transient Motions. *Fourth International Conference on Stability of Ships and Ocean Vehicles, STAB'90,* pp. 183-190, Naples, 24-28 September.

Thompson, J.M.T. and Soliman, M.S. [1990]. Fractal Control Boundaries of Driven Oscilators and their Relevance to Safe Engineering Design. *Proceedings of the Royal Society of London,* vol. 428 A, pp. 1-13, 8 March.

Tikka, K.K. and Paulling, J.R. [1990]. Prediction of Critical Wave Conditions for Extreme Vessel Response in Random Seas. *Fourth International Conference on Stability of Ships and Ocean Vihicles, STAB' 90,* pp. 386-394, Naples, 24-28 Sept.

SECRETARIAT STAB 94

GENERAL CHAIRMAN	W. A. Cleary, Jr - Adjunct Professor O/E
OCEAN ENGINEERING PROGRAM CHAIRMAN	Professor A. Zborowski, Ph.D.
CENTRAL BAPTIST CHURCH - AUDITORIUM	Dr. Gary Fagan, Pastor
SPECIAL EVENTS - AUXILIARY SERVICES	Ms. Barbara Towers
OFFICE SERVICES - DIRECTOR	Mr. William Hamilton
OFFICE SERVICES - PUBLISHING	Ms. Rosary M. Pedreira
GLEASON AUDITORIUM COORDINATOR	Mr. Gary Allen
OCEAN ENGINEERING STAFF	Ms. Janet Carey Ms. Ann Bergonzoni Ms. Juanita Fennimore Mr. Daryl Slocum
OCEAN ENGINEERING STUDENTS	Ms. Jennifer Clark Mr. Michael Callahan Mr. Damian Hite Mr. Joe Blodgett Mr. Alejandro Gutierrez Mr. Mathew Craven
SOCIETY OF NAVAL ARCHITECTS AND MARINE ENGINEERS FLORIDA TECH STUDENT SECTION	Ms. Allison Link

AND

THE FLORIDA TECH STUDENT SUPPORTING TEAM

STAB 94 COMMITTEES

INTERNATIONAL PROGRAMME

Prof. C. Kuo, University of Strathclyde, Glasgow
Prof. M. Fujino, University of Tokyo
Prof. L. Kobylinski, Tech. Univeristy of Gdansk, Poland
Prof. P. Cassella, University of Naples, Italy
Prof. P. Bogdanov, Ship Hydrodynamics Center, Varna, Bulgaria
Dr. S. Grochowalski, National Research Council, Ottawa, Canada
Prof. P. Blume, Hamburg Ship Model Basin, Germany
Prof. D. Huang, Dalien University, Dalien, China
H. Hormann, Head Marine Safety Germanischer Lloyd
H. Vermeer, Netherlands Shipping Directorate
I. Manum, Norwegian Maritime Directorate
Prof. C. Guedes Soares, Instituto Superior Tech Libson, Portugal
Dr. I. Boroday, Krilov Ship Research Inst., St. Petersburg, Russia
Dr. N. Rachmanin, Krilov Ship Research Institute, Russia
Dr. R. Ozkan, Instanbul, Turkey
Chairman - W. A. Cleary Jr., Florida Institute of Technology

COMMITTEE of the AMERICAS

Prof. B. Adee, University of Washington, Seattle, WA USA
Prof. R. Battacharyya, Annapolis, MD USA
H. P. Cojeen, USCG Headquarters, Washington, DC USA
Prof. R. G. La torre, University of New Orleans, LA USA
Dr. M. A. S. Neves, COOPE/UFRJ, Rio de Janiero, Brazil
Prof. J. R. Paulling Jr., Richmand, CA USA
Prof. N. Perez, University of Chile, Valdiva, Chile
Prof. G. L. Petrie, Webb Institute, New York, NY USA
Prof. C. Sanguinetti, University of Chile, Valdiva, Chile
R. J. Sonnenschein, MARAD, Washington, DC USA
Dr. C. Spadavecchia, Prefectura Navale, Burnos Aires, Argentina
Prof. M. Santarelli, Buenos Aires, Argenina
Dr. J. S. Spencer, ABS AMERICAS, Huston, Texas USA
Prof. R. Yagle, University of Michigan, Ann Arbor, Michigan USA